# THE POTENTIAL ROLE OF STROMAL DERIVED FACTOR 1α IN REMOTE ISCHAEMIC CONDITIONING

**Thesis submitted by Daniel Ian Bromage**

**BSc (First class with Honours) MBChB (with Honours) MRCP (UK)**

**For the degree of Doctor of Philosophy**

**University College London, UK.**

Institute of Cardiovascular Science,

Hatter Cardiovascular Institute,

University College London,

67 Chenies Mews, London,

WC1E 6HX

28 October 2016

# DECLARATION

I, Daniel Ian Bromage, confirm that the work presented in this thesis is my own. Where information has been derived from other sources, I confirm that this has been indicated in the thesis. All technical assistance relevant to the results presented herein is duly acknowledged.

# ABSTRACT

## Background

Alleviating the injury associated with ST-elevation myocardial infarction is central to improving the global burden of coronary heart disease. The chemokine stromal cell-derived factor 1α (SDF-1α) and its receptor, CXCR4, have dual potential benefit in this regard: acutely protecting the heart from lethal ischaemia-reperfusion injury (IRI) whilst mitigating adverse ventricular remodelling by recruiting progenitor cells to the site of injury.

This project hypothesised that SDF-1α mediates the acute cardioprotection conferred by remote ischaemic conditioning (RIC), the phenomenon whereby brief cycles of non-lethal tissue ischaemia and reperfusion remote from the heart protects against myocardial IRI.

## Methods and Results

This thesis defines a paradigm for evidencing a role in RIC that includes induction of cardioprotection by exogenous administration of SDF-1α at the time of reperfusion, abolition of cardioprotection by specific antagonism of CXCR4, increased production of SDF-1α as a direct effect of RIC, and absence of cardioprotection in CXCR4-deficient mice. A murine *in vivo* model of myocardial IRI and a novel ELISA for *active* SDF-1α were established and used to investigate this paradigm.

This thesis provides the first description of cardioprotection against myocardial IRI as a result of exogenous SDF-1α administered prior to reperfusion. Moreover, AMD3100, a highly specific inhibitor of CXCR4, abolishes the beneficial effect of RIC *in vivo*. Next, SDF-1α cleavage and inactivation was unexpectedly demonstrated to increase after RIC, which may be attributable to up-regulation of dipeptidyl peptidase-4. Finally, inducible cardiomyocyte-specific CXCR4 deletion unexpectedly conferred protection against myocardial IRI. The protective mechanism was not

established and, furthermore, it prohibited the use of these mice in experiments to validate the role of CXCR4 signalling in RIC.

## Conclusions

The intrinsic role of SDF-1α in RIC remains equivocal. However, modulation of the SDF-1α-CXCR4 axis with other approaches, including exogenous SDF-1α, has potential utility in cardioprotection against myocardial IRI.

# ACKNOWLEDGEMENTS

My sincerest thanks go to my supervisors, Professor Yellon and Dr Davidson, for their constant support and expert guidance in both this thesis and my career. Specifically, I would like to thank Professor Yellon for giving me the opportunity to work at the Hatter Cardiovascular Institute and for his mentorship. My thanks also to Dr Davidson for teaching me with humour and patience. I am privileged to have trained under their direction and I will look back with immense fondness.

Thanks also to the research team at the Hatter Cardiovascular Institute, who have been a source of advice, support and respite. In particular I would like to thank Dr Hall for his enthusiasm and instruction. I also thank Ms Taferner, Mr Pillai and Dr Hamarneh for their substantial contributions. Dr He has been a dependable *in vivo* ally and I owe him special thanks for contributing data. Finally, my warmest thanks to Mr Pickard, Dr Rossello, Mr Burke and Dr Ziff for their involvement in the meta-analysis, among many other things. It has been a pleasure to work with the whole team and I have learnt important lessons from all of them.

I have profited enormously from our collaborators. In particular, thanks to Dr Dyson for his wide-ranging help, not least the *in vivo* model. Further acknowledgement is owed to Dr Pellet-Many, Professor Bernhagen and Dr Stoppe for their generous contributions. Finally, thanks to everyone in the Cruciform BSU, especially Mr Martin and Mr Lawson, for facilitating all of the animal work in this thesis.

My heartfelt thanks to my family who have provided tireless support and encouragement, especially my Mum for her meticulous proof-reading. I thank Kate for her unwavering belief in me and it was only through her dedication and selflessness that this thesis was finished. Special thanks to my beautiful daughters, Ada and Rosie, who make me laugh, and motivate and inspire me every day.

I was fortunate to be funded by a Medical Research Council Clinical Training Fellowship and I would like to thank them for this support.

# PUBLICATIONS

Below is a list of the publications and poster abstracts to date resulting from the work presented in this report.

## Primary research publications

Bromage DI*, Malik A*, He Z *et al.* Exogenous SDF-1α protects human myocardium from hypoxia-reoxygenation injury via CXCR4. Cardiovascular Drugs & Therapy 2015;29:589-592

## Review articles

Bromage DI, Davidson SM, Yellon DM. Stromal derived factor 1α: A chemokine that delivers a two-pronged defence of the myocardium. Pharmacology & Therapeutics 2014;143(3):305-315

## Poster abstracts

Bromage DI*, Pickard JMJ*, Rossello X, Ziff O, Burke N, Yellon DM, Davidson SM. Remote ischaemic conditioning reduces infarct size in animal in vivo models of ischaemia-reperfusion injury: a systematic review and meta-analysis. Frontiers in Cardiovascular Biology. Florence, Italy, 2016

Bromage DI, Pillai M, Davidson SM, Yellon DM. A novel antibody specific to full-length stromal derived factor-1 alpha reveals that remote conditioning induces its cleavage by endothelial dipeptidyl peptidase-4. Frontiers in Cardiovascular Biology. Florence, Italy, 2016

Davidson SM, He D, Bromage DI, Yellon DM. Supplemental oxygen has a major influence on cardioprotective strategies in mice. Ischaemic conditioning and targeting reperfusion injury: a 30 year voyage of discovery. Barcelona, Spain, 2016

Bromage DI, Pillai M, Davidson SM, Yellon DM. Remote ischaemic conditioning involves signalling via CXCR4 but does not increase circulating levels of its known ligands. Heart 2015;101 Suppl 6:A9

Yellon DM, Mailk A, Pickard JMJ, Bromage DI, Davidson S.M., Sivaraman V., He Z. Stromal Derived Factor 1 Alpha is a Mediator of Conditioning in Human and Rat Myocardium. Heart 2014;100 Suppl 3:A121-2.

Bromage DI, Yellon DM, Davidson SM. Characterising a novel antibody for full-length (active) stromal derived factor-1α(1-67). Heart 2014;100 Suppl 4:A13.

# CONTENTS

# FIGURES

# TABLES

# ABBREVIATIONS

Standard units of measurement are used throughout this report according to accepted conventions. A comprehensive list of non-standard abbreviations is provided below.

| | |
|---|---|
| AAR | Area at risk |
| ADP | Adenosine diphosphate |
| ADRC | Adipose-derived regenerative cell |
| AU | Arbitrary units |
| BCA | Bicinchoninic acid |
| BMSC | Bone marrow stem cell |
| BSA | Bovine serum albumin |
| BSU | Biological Services Unit |
| CABG | Coronary artery bypass graft |
| CHD | Coronary heart disease |
| CMR | Cardiac magnetic resonance |
| CSA | Cross-sectional area |
| Ct | Threshold cycle |
| CXCR4 | CXC Receptor 4 |
| Cyp-D | Cyclophilin-D |
| DPP4 | Dipeptidyl peptidase-4 |
| dsDNA | Double stranded deoxyribonucleic acid |
| ECSC | Endogenous cardiac stem cell |
| EDV | End diastolic volume |
| EF | Ejection fraction |
| ELISA | Enzyme-linked immunosorbent assay |
| eNOS | Endothelial nitric oxide synthase |
| EPC | Endothelial progenitor cell |
| Erk | Extracellular signal-regulated kinase |
| ES | Embryonic stem cells |
| FITC | Fluorescein isothiocyanate |
| FS | Fractional shortening |
| FSC | Forward light scatter |
| GAPDH | Glyceraldehyde 3-phosphate dehydrogenase |
| G-CSF | Granulocyte-colony stimulating factor |
| GLP-1 | Glucagon-like peptide-1 |
| GM-CSF | Granulocyte macrophage-colony stimulating factor |
| GPCR | G protein-coupled receptor |
| $H_2O_2$ | Hydrogen peroxide |
| HET | Heterozygote (+/-) |
| HGF | Hepatocyte-like growth factor |
| HIF-1α | Hypoxia inducible factor-1α |
| HPRT | Hypoxanthine guanine phosphoribosyl transferase |
| HS | Heparan sulfate |
| HUVEC | Human umbilical vein endothelial cell |
| IGF | Insulin-like growth factor |
| IL | Interleukin |
| IP3 | Inositol-1,4,5-triphosphate |
| IPostC | Ischaemic postconditioning |
| IPC | Ischaemic preconditioning |
| IRI | Ischaemia-reperfusion injury |
| IS | Infarct size |
| IU | International standard unit |
| IVSd | Interventricular septum in diastole |
| JAK | Janus kinase |

| | |
|---|---|
| KO | Knockout (-/-) |
| LAD | Left anterior descending coronary artery |
| LAS | Large area surface |
| LU | Luminescence unit |
| LV | Left ventricle |
| LVIDd | Left ventricular internal diameter in diastole |
| LVPWd | Left ventricular posterior wall in diastole |
| M-mode | Motion-mode |
| MAPK | Mitogen activated protein kinase |
| Mer | Mutant oestrogen receptor |
| MI | Myocardial infarction |
| MIF | Macrophage inhibitory factor |
| MMP | Metalloproteinase |
| MPTP | Mitochondrial permeability transition pore |
| MSC | Mesenchymal stem cell |
| MYH6 | α-cardiac myosin heavy chain |
| NO | Nitric oxide |
| OCT | Optimal cutting temperature |
| PAF | Platelet-activating factor |
| PAH | Pulmonary arterial hypertension |
| PAR | Protease-activated receptor |
| PBS | Phosphate buffered saline |
| PBS-T | Phosphate buffered saline-Tween® |
| PCR | Polymerase chain reaction |
| PE | Polyethylene |
| PE-Cy | Phycoerythrin-cyanine |
| PEEP | Positive end expiratory pressure |
| PFA | Paraformaldehyde |
| PFP | Platelet-free plasma |
| PI3K | Phosphoinositide 3-kinase |
| PKC | Protein kinase C |
| PPCI | Primary percutaneous coronary intervention |
| PVDF | Polyvinylidene difluoride |
| PW | Pulsed wave |
| QPCR | Quantitative polymerase chain reaction |
| rhSDF-1α | Recombinant human stromal derived factor-1α |
| RIC | Remote ischaemic conditioning |
| RISK | Reperfusion injury salvage kinase |
| RNases | Ribonucleases |
| ROS | Reactive oxygen species |
| RT | Room temperature |
| RV | Right ventricle |
| SAFE | Survivor activating factor enhancement |
| SCF | Stem cell factor |
| SDF-1α | Stromal derived factor-1α |
| SDS-PAGE | Sodium dodecyl sulphate-polyacrylamide gel electrophoresis |
| SMD | Standardised mean difference |
| STAT | Signal transducer and activator of transcription |
| STEMI | ST-elevation myocardial infarction |
| SV | Stroke volume |
| TBS | Tris-buffered saline |
| $T_m$ | Melting temperature |
| TRF | Transferrin |
| TTC | Triphenyltetrazolium chloride |
| TTE | Transthoracic echocardiography |
| VEGF | Vascular endothelial growth factor |
| VSD | Ventricular septal defect |

| | | | |
|---|---|---|---|
| VTI | Velocity-time integral | WT | Wild type (+/+) |
| WMD | Weighted mean difference | | |

# Chapter 1 General introduction

## 1.1 Introduction

Coronary heart disease (CHD) is the leading cause of death worldwide, accounting for an estimated 8.1 million deaths per year and strategies to mitigate the deleterious effects of ST-elevation myocardial infarction (STEMI) are therefore paramount.[1] Early reperfusion by primary percutaneous coronary intervention (PPCI) is the most effective strategy for reducing infarct size (IS) and improving clinical outcome.[2, 3] However, adverse sequelae persist: in a recent study, 30-day, 1-year, and 5-year all-cause (and cardiac) mortality rates following PPCI for STEMI were 7.9 % (7.3 %), 11.4 % (8.4 %), and 23.3 % (13.8 %), respectively.[4] Important therapeutic targets in this regard include platelet aggregation and adverse ventricular remodelling. Another potential target is the injury paradoxically inflicted by the therapeutic restoration of blood flow, known as reperfusion injury, which may account for up to 50% of final IS (Figure 1-1).[5, 6]

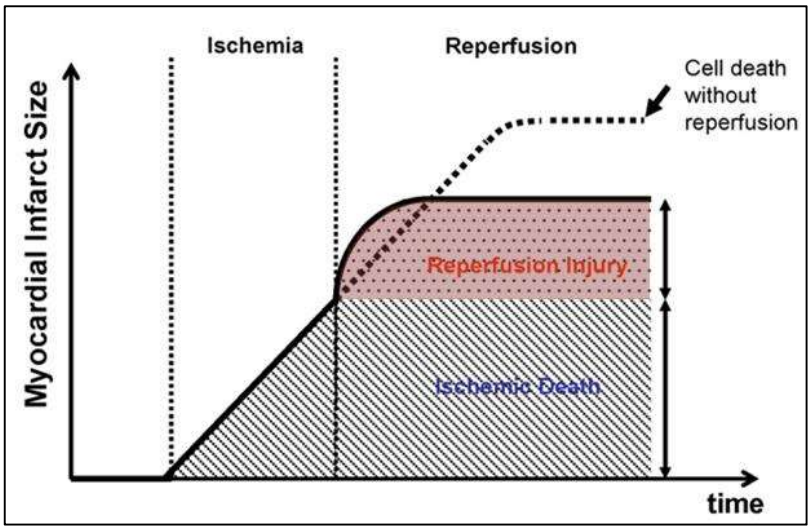


**Figure 1-1: Contribution of reperfusion injury to myocardial infarct size after therapeutic restoration of blood flow**

Reperfusion of an occluded epicardial artery is essential to limit cell death; however, reperfusion itself inflicts injury, known as reperfusion injury, which may account for up to 50% of final IS. Figure from [7].

Myocardial ischaemia-reperfusion injury (IRI) describes the deleterious consequences of several pathological processes and cardiac interventions. Most commonly, it is caused by thrombotic occlusion of the coronary artery in STEMI and subsequent reperfusion by PPCI, but may result from a range of elective and emergent causes of myocardial ischaemia, including cardiopulmonary bypass and spontaneous reperfusion of STEMI. The pathophysiology of IRI is not fully understood, but proposed mechanisms include oxidative stress,[8] deranged calcium metabolism,[9] rapid restoration of physiologic pH,[10] inflammation,[11] and deranged metabolism of glucose, insulin and potassium.[12, 13] Several potential mediators have been studied, however, manipulation of these mechanisms has largely failed to translate to benefit in clinical trials (reviewed by Hausenloy *et al.*, 2013[14]).

The chemokine stromal cell-derived factor 1α (SDF-1α) potentially delivers a 'two-pronged' defence of the myocardium with respect to IRI: acute protection from reperfusion injury and subsequent beneficial modulation of ventricular remodelling by recruiting progenitor cells to the site of injury.[15]

SDF-1α is known to play a central role in stem cell homing, retention, survival, proliferation, cardiomyocyte repair, angiogenesis and ventricular remodelling following myocardial infarction (MI).[16-19] It acts as a specific ligand for its receptor CXC Receptor 4 (CXCR4) and the SDF-1α-CXCR4 axis is activated in both experimental and clinical studies of MI.[17] SDF-1α-CXCR4 has been used to target stem cells to ischaemic tissue with consequent improvement of left ventricle (LV) dimensions and function.[20-23] Importantly, the SDF-1α-CXCR4 signalling axis exerts these effects via a Gα1 dependent mechanism and activation of phosphoinositide 3 kinase (PI3K), mitogen activated protein kinase (MAPK), and Janus kinase (JAK)-signal transducer and activator of transcription (STAT) signalling.

These signalling pathways are the same pathways that it is postulated are responsible for the protection against IRI conferred by all forms of conditioning such as pre-, post- and remote ischaemic conditioning (RIC).[24-26] The latter describes the phenomenon whereby non-lethal ischaemia and reperfusion applied to an organ or tissue remote

from the heart protects the myocardium from lethal reperfusion injury. The mechanism of cardioprotection conferred by RIC is so far unknown, but is thought to be due to a humoral factor that has been shown by biochemical fractionation studies to be a protein between 3.5 kDa and 15 kDa in size.[27, 28]

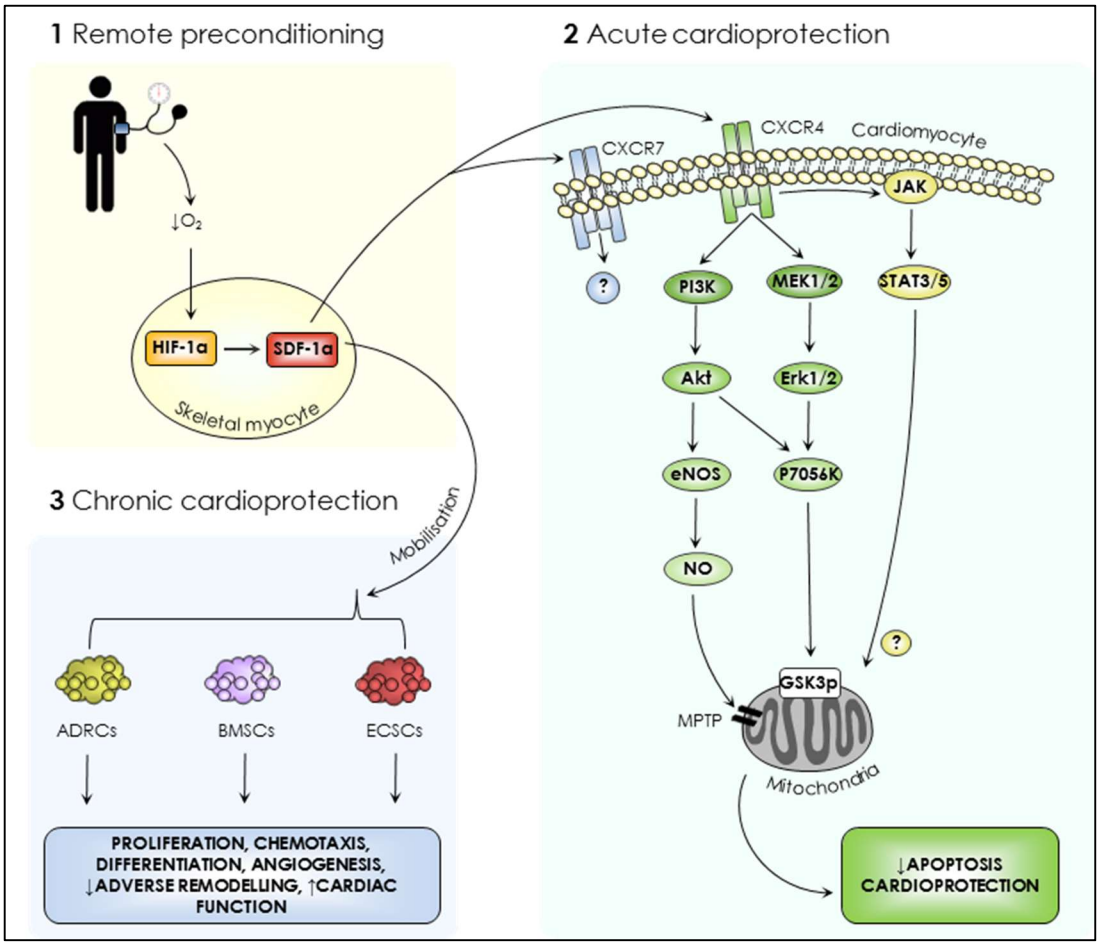


**Figure 1-2: The SDF-1α-CXCR4 signalling axis**

Remote preconditioning may enable both acute and chronic cardioprotective pathways (see text for details). SDF-1α, stromal derived factor-1α; HIF-1α, hypoxic inducible factor-1α; ADRCs, adipose tissue derived regenerative cells; BMSCs, bone marrow stem cells (including mesenchymal stem cells, haematopoietic stem cells and endothelial stem cells); ECSCs, endogenous cardiac stem cells; JAK, Janus kinase; STAT, signal transducer and activator of transcription; PI3K, phosphoinositide 3 kinase; MEK1/2, mitogen-activated protein kinase; Erk, extracellular signal-regulated kinases; eNOS, endothelial nitric oxide synthase; NO, nitric oxide; MPTP, mitochondrial permeability transition pore.

It is therefore hypothesised in this thesis that in addition to its chronic effects, SDF-1α has a direct role in the protection observed after RIC and a proposed paradigm for its roles is described in Figure 1-2.[15] Preliminary evidence for its role in RIC include a

demonstrable increase in circulating SDF-1α in animals subjected to RIC.[29-31] Furthermore, RIC, which was shown to significantly decrease IS and improve papillary muscle functional recovery in an *ex vivo* model, could be blocked by AMD3100, a highly specific inhibitor of CXCR4.[31, 32] This, together with the identification of SDF-1α as an 8 kDa peptide and its induction in response to hypoxia, has made it a prime candidate for a role in RIC.[33]

## 1.2 SDF-1α-CXCR4

Chemokines, or chemoattractant cytokines, play a critical role in the regulation and trafficking of leukocytes as well as haematopoietic and other progenitor cells.[18] They are also involved in a variety of other functions, including degranulation, mitogenesis, gene transcription, apoptosis, and angiogenesis.[34] There are over 50 human chemokines that are classified according to the position of two N-terminal cysteine residues as CXC, CCC, C or CX3C.[18] In myocardial ischaemia, several chemokines, including CXC and CC subtypes, have been shown to be upregulated in both experimental and clinical studies of MI.[18, 35, 36]

SDF-1 (also known as CXCL12) is a CXC chemokine, so-called because the two cysteines nearest the N-terminus are separated by a single amino acid.[37] It is a small (8 kDa), 89 amino acid peptide that is encoded by a gene originally cloned from murine bone marrow stromal cells, hence its name.[37] It is highly conserved (more than 92% similarity at the protein level) between species and has been shown to confer protection between species.[28, 38] Several isoforms of SDF-1, namely SDF-1 alpha (α) to zeta (ζ), arise from alternative splicing and have been identified by polymerase chain reaction (PCR).[18] All isoforms are agonists at CXCR4 but have distinct properties. For example, SDF-1β is more resistant than SDF-1α to proteolysis.[39] Interestingly, expression of SDF-1ɣ has recently been reported in non-vascular tissue that is susceptible to infarction, including the heart.[39] However, the predominant and best described isoform is SDF-1α,[40] which was the focus of this thesis. Note that many studies do not specify which isoform they are investigating and henceforth where this is the case the more general SDF-1 descriptor is adopted.

SDF-1α protein or mRNA expression has been reported in several organs, tissues and cells, including bone marrow, heart, liver, kidney, thymus, spleen, skeletal muscle, brain and, more recently, platelets,[18, 41-44] although it is likely that in some tissues this reflects expression in the vascular endothelium. In the heart, SDF-1α is expressed by endothelial cells, cardiac fibroblasts, vascular smooth muscle cells and cardiomyocytes.[45-47] It is a chemoattractant for a variety of cell types including T lymphocytes, bone marrow stem cells (BMSCs; including haematopoietic, endothelial and mesenchymal subtypes), adipose-derived regenerative cells (ADRCs) and c-kit$^{+}$ endogenous cardiac stem cells (eCSCs).[17, 48, 49] It also has a role in maintaining hematopoietic stem cell niches in bone marrow.[18]

SDF-1α is widely studied due to its pleiotropic biological processes, which are described in Figure 1-3. These functions have been investigated in a range of pre-clinical and clinical disciplines including, but not limited to, cardiology, neurology, oncology and haematology.


**Figure 1-3: The pleiotropic biological processes of SDF-1α**

The biological processes described in this figure are adapted from the Gene Ontology Consortium list of biological processes for SDF-1α.[50]

SDF-1α is cleaved by exopeptidases including dipeptidyl peptidase-4 (DPP4), matrix metalloproteinase (MMP)-2 and MMP-9 (albeit all acting at different positions),[51] although DPP4 predominates in this regard.[52] Injected SDF-1α has an estimated half-life *in vivo* by radiolabelling of 25.8±4.6 min.[53] However, it is unclear whether this represents full-length or cleaved SDF-1α, which are likely to have different kinetics. Similarly, all commercially available Enzyme-Linked Immunosorbent Assay (ELISA) kits measure both intact and cleaved SDF-1α and may therefore offer a skewed view of the role of SDF-1α in MI.

The best described receptor for SDF-1α is CXCR4. CXCR4 is a G protein-coupled receptor (GPCR) that, once activated, is thought to initiate a signalling cascade that regulates the functions described.[18, 54, 55] CXCR4 is expressed by a range of cell-types, and is known to be critical in embryogenesis, including cell migration and development of neuronal, cardiac, vascular, haematopoietic and craniofacial systems, which is reflected by its expression on a range of progenitor cells, including haematopoietic, endothelial and cardiac stem cells.[17, 18, 37] Importantly, CXCR4 is also known to be expressed by both platelets and endothelial cells.[44] Indeed, during angiogenesis, expression of CXCR4 on vessel endothelium correlates with areas of high SDF-1α expression.[56] In embryonic development transgenic homozygote mice lacking either CXCR4 or SDF-1α have abnormal B-lymphocyte development, as well as abnormal hepatic and cardiac development, including ventricular septal defects (VSD), and die in utero.[57] Similarly, in humans, CXCR4 mutation causes impaired mobilisation of neutrophils and B-cell lymphopaenia.[58]

More recently it has become apparent that CXCR7 plays a central role in regulation of SDF-1α. CXCR7 expression is known to be up-regulated in hypoxic conditions by HIF-1α and is thought to scavenge SDF-1α.[59] Hoffman *et al.* demonstrated rapid spontaneous internalisation of SDF-1α by CXCR7, unlike $G_{\beta\gamma}$ protein-coupling via CXCR4, resulting in rapid release of SDF-1α degradation products.[59] It has similarly been shown that serum SDF-1α is elevated in murine model in response to either genetic deletion or pharmacological inhibition of CXCR7.[60] As well as hypoxia, CXCR7 is thought to be upregulated in inflammation, cancer and autoimmune conditions.[61] It has been shown to improve the migration and paracrine function (angiogenesis and mitogenesis) of MSCs in mice subjected to renal IR, and consequently to reduce apoptosis and improve functional recovery.[62] However, the relative contribution and relationship of CXCR4 and CXCR7 is not fully elucidated and its contribution, if any, to cardioprotection is not yet known.[17] Furthermore, CXCR7 was not specifically investigated in this thesis and should be acknowledged as a potential confounding factor when considering the effects of SDF1α.

## 1.3 Chronic cardioprotection

### 1.3.1 SDF-1α-CXCR4 after acute myocardial infarction

In the cardiovascular field, most is known about the SDF-1α-CXCR4 axis in the context of myocardial repair after acute MI ('chronic cardioprotection'). In hypoxic conditions, the transcription factor hypoxia inducible factor-1α (HIF-1α) is upregulated and in turn up-regulates SDF-1α and CXCR4.[17, 18, 63] In this way SDF-1α acts as a diffusible 'homing beacon' directing CXCR4-expressing cells towards hypoxic tissue. In health, since the bone marrow is physiologically hypoxic, SDF-1α expression results in the retention of BMSCs.[17, 33] In response to MI, several clinical studies have demonstrated up-regulation of SDF-1α in infarct and peri-infarct zones, returning to baseline at 7 days,[46, 63-65] and in the serum.[66, 67] SDF-1α-CXCR4 signalling is also reportedly elevated in toxic liver damage, total body irradiation and after chemotherapy.[41] Thus, expression of SDF-1 in infarcted myocardium has been associated with recruitment, retention, survival and proliferation of ADRCs, eCSCs and BMSCs.[21, 49, 68-70] Conversely, decreased recruitment, angiogenesis and blood flow have been demonstrated when CXCR4 is blocked on infused progenitor cells or when SDF-1α is blocked in the recipient using neutralising antibodies.[17, 33]

Although a number of mechanisms can mobilize stem cells, including cytokines (granulocyte- and granulocyte macrophage-colony stimulating factor (G-CSF, GM-CSF), and stem cell factor (SCF)), interleukins (IL-7, IL-12, IL-3), chemokines (SDF-1α, IL-8), growth factors (vascular endothelial growth factor, hepatocyte- and insulin-like growth factor (VEGF, HGF, IGF)),[71] and chemotherapeutic agents like cyclophosphamide,[18] it is suggested that the SDF-1α-CXCR4 axis is the most potent and central to the process of mobilizing progenitor cells.[71, 72] For example, G-CSF, a cytokine known to increase the mobilisation of stem cells from bone marrow and widely used therapeutically, does so by disrupting the association of SDF-1 on bone marrow stromal cells, osteoblasts and reticulocytes with CXCR4 on BMSCs.[17, 71, 73] A similar mechanism may explain how AMD3100 increases circulating haematopoietic and endothelial progenitor cells.[69, 74]

Cardiomyocyte-expressed CXCR4 also seems to be important in ventricular remodelling after MI. This has been demonstrated in cardiomyocyte-specific CXCR4 null mice subjected to MI.[75] Wild type mice had better cell recruitment after BMSC engraftment and consequent improvements in ejection fraction (EF) and infarct size. Interestingly, this study identified a local paracrine effect of infused BMSCs, mediated by BMSC SDF-1α secretion. This study also identified a 33% reduction in SDF-1α expression in the infarct zone in cardiomyocyte-specific CXCR4-deficient mice. It is therefore apparent that in MI, transient increases in SDF-1α result in the gradient-guided homing of progenitor cells from the bone marrow, as well as adipose and cardiac tissue, to sites of injury and inflammation. These cells then exert advantageous effects via SDF-1α-mediated activation of local CXCR4, among other mechanisms. In support of this, it is suggested that SDF-1α and CXCR4 are up-regulated asynchronously after MI, with SDF-1α being increased as early as 1 h (to direct CXCR4-expressing cells towards injured tissue) and cardiomyocyte-specific CXCR4 being up-regulated some 36-48 h later,[68, 76] perhaps in readiness for the arrival of circulating progenitor cells that are estimated to peak around day 5.[77]

In both circulating cells and tissue-specific cells such as cardiomyocytes, SDF-1α-CXCR4 exerts its effects by activating intracellular signalling cascades. These include the MAPK p42/44 extracellular signal-regulated kinases (Erk1/2), PI3K-Akt, JAK-STAT and protein kinase C (PKC) signalling cascades, as well as inositol-1,4,5-triphosphate (IP3)-induced SR/ER calcium release.[78, 79]

### 1.3.2 Therapeutic application of SDF-1α-CXCR4 in chronic cardioprotection

Several pre-clinical studies have adopted a range of approaches to therapeutically manipulate the SDF-1α-CXCR4 pathway. Broadly, these centre on one or a combination of the following approaches: (1) increased mobilisation and recruitment of progenitor cells; (2) increasing SDF-1α to coincide with peak myocardial CXCR4 expression, including by inhibiting its breakdown; and (3) over-expression of CXCR4 to coincide with peak myocardial SDF-1α expression. Examples of each of these are given in turn and these approaches are discussed in more detail in the chapters that follow.

Firstly, with respect to increased mobilisation and recruitment of progenitor cells to facilitate over-expression of SDF-1α, approaches have included use of a PEGylated fibrin patch for SDF-1α over-expressing mesenchymal stem cell (MSC) transplantation,[68] intra-myocardial delivery of MSCs over-expressing SDF-1α,[80] MSCs over-expressing IGF-1 to activate SDF-1α,[79] and intra-cardiac injection of skeletal myoblasts over-expressing human SDF-1α.[81, 82] Abbott *et al.* found that stem cells delivered to the coronary artery following MI were only retained alongside adenovirus-mediated cardiac expression of SDF-1α, an effect that was abolished by AMD3100.[65] Finally, Misao *et al.* administered G-CSF or vehicle 3 days after IRI in rabbits and found increased BMSCs in the infarcted area, increased serum SDF-1α, reduced IS, improved EF and improved end-diastolic dimensions in the G-CSF group.[22] This was again abrogated by AMD3100.[22]

Secondly, with respect to increasing SDF-1α to coincide with peak myocardial CXCR4 expression, SDF-1α has been delivered by intra-cardiac injection after MI in mice and found to activate Akt in endothelial cells and cardiomyocytes, which was associated with improved cardiac function up to 28 days after infarction, increased VEGF, increased angiogenesis and reduced IS.[20, 23] Continued expression of active SDF-1α (peak at 7 days) has been achieved by expression from adenovirus injected in the myocardium after infarction, which resulted in smaller IS, improved LV parameters, less fibrosis and a greater density of cardiomyocytes and blood vessels in a rat model of STEMI.[21] Similar plasmid-based over-expression of SDF-1 has also been applied 1 month after MI, with similar results.[83] Askari *et al.* combined the injection of cardiac fibroblasts over-expressing SDF-1α into the infarcted myocardium of a rat with intraperitoneal G-CSF and found improved stem cell homing, angiogenesis and cardiac function.[76] Pre-clinical and clinical studies that have attempted to interfere with the degradation of SDF-1α are addressed in Chapter 7.

Thirdly, with respect to over-expression of CXCR4 to coincide with peak myocardial SDF-1α expression, this has likewise been achieved using viral vectors.[84] Cheng *et al.* delivered MSCs over-expressing CXCR4 intravenously to rats 24 h after IRI and found improved homing, better preservation of LV dimensions, reduced fibrosis and better

LV function, as assessed by echocardiography.[85] Similarly, injection of cultured stem cells with CXCR4 specifically upregulated by cultivation led to better angiogenesis.[86]

Interestingly, the mechanism whereby 3-hydroxy-3-methylglutaryl-coezyme A (HMG-CoA) reductase inhibitors (statins) mobilise endothelial progenitor cells (EPCs) and affect angiogenesis at sites of endothelial injury has been attributed to the SDF-1α-CXCR4 pathway.[87] Specifically, atorvastatin and rosuvastatin have been shown to up-regulate CXCR4 expression in circulating EPCs, improve their homing to ischaemic tissue in a mouse model of permanent femoral artery ligation, and increase capillary density and flow. The authors attributed this to endothelial nitric oxide synthase (eNOS) as it was not only significantly increased in EPCs treated with statins but up-regulation of CXCR4 was abrogated with the NO synthase inhibitor, L-NAME (NG-nitro-L-arginine methyl ester). The potential relationship between this hitherto unexplained function of statins and the SDF-1α-CXCR4 axis is interesting because statin treatment may confound attempts to therapeutically increase the expression of CXCR4 in patients with cardiovascular disease.

Despite these encouraging results, enthusiasm is tempered by (albeit limited) experimental data that indicate a deleterious role of SDF-1α-CXCR4 in MI. Chen *et al.* used adenovirus-mediated over-expression of CXCR4 injected into the rat heart 7 days prior to myocardial IRI and found significantly increased scar size, worse fractional shortening (FS), increased cardiomyocyte apoptosis and more LV hypertrophy at 24 h.[88] Most of the studies described above have up-regulated CXCR4 after MI and the over-expression of CXCR4 7 days *prior* to MI might be important in the study by Chen *et al.*, particularly with respect to inflammatory cell recruitment, and this is discussed further in Chapter 8. In another study, SDF-1α was injected into the peri-infarct zone of pigs 2 weeks after MI that, consistent with previous studies, resulted in increased vessel density.[89] However, there was no significant improvement in IS or myocardial perfusion compared to controls, and there was a significant deterioration in LV function in the SDF-1α-treated group.[89] This finding may have several explanations, including a requirement for combination therapy to both stimulate stem cell mobilisation from bone marrow niches and homing to sites

of injury. In addition, Koch *et al.* delivered only a single bolus of SDF-1, which could be expected to be rapidly proteolysed,[52] and administered SDF-1 at 14 days while there is evidence that intravenous MSCs are only effective when given within 4 days.[90]

Furthermore, it should not be forgotten that SDF-1α is involved in the mobilisation and recruitment of various progenitor cell types to hypoxic areas of tumours in addition to the other ischaemic tissues described, and can therefore support tumour proliferation, angiogenesis, metastasis and survival.[91] Similarly, stromal cell SDF-1α expression can induce leukaemia cell trafficking to the bone marrow, where malignant cells are provided with growth factors and protected from conventional chemotherapy.[92] To this end, AMD3100 (Plerixafor) has been shown in various malignancies, including leukaemia, non-Hodgkin's lymphoma and multiple myeloma, to increase drug responsiveness.[92] This paradox is a challenge for the wider field of cardioprotection, which aims to protect cells from apoptosis. Thus, care should be taken until more is known about what, if any, specific differences in signalling exist between ischaemic myocardium and tumours. It is reassuring to note that in the recent STOP-HF trial of SDF-1α treatment in ischaemic cardiomyopathy, patients with any history of cancer, with the exception of curable non-melanoma skin cancer or resection with no recurrence in 5 years, were excluded from the study.[93]

Likewise, SDF-1α may play a role in, atherosclerosis, a disease characterised by the recruitment of inflammatory cells to activated endothelium coupled with the migration and proliferation of smooth muscle cells in the intima. This is thought to be mediated by the expression of various chemokines, including SDF-1α.[94] In particular, SDF-1α has been shown to induce arterial smooth muscle cell proliferation and promote plaque formation.[95] Specific antagonism of chemokine receptors therefore presents a therapeutic opportunity with respect to atherosclerosis, although this has not been investigated with specific reference to SDF-1α-CXCR4. Furthermore, SDF-1α up-regulation was induced following smooth muscle cell-specific deletion of PTEN (phosphatase and tensin homolog), a lipid and protein phosphatase, in mice, resulting in pulmonary arterial hypertension (PAH) and pathological vascular

remodelling.[96] In other studies, pravastatin has been shown to mitigate hypoxia-induced PAH by suppressing SDF-1α in mice,[97] which was associated with fewer BMSCs in the pulmonary artery adventitia. This may represent a very specific contra-indication to the therapeutic application of SDF-1α-CXCR4 and should therefore be considered when targeting SDF-1α-CXCR4 clinically.

Finally, VEGF has been associated with SDF-1α-CXCR4-mediated recruitment of stem cells and subsequent myocardial repair.[98] Specifically, in a model of permanent LAD ligation in Sprague Dawley rats, Tang *et al.* administered VEGF-expressing MSCs and found increased myocardial expression of SDF-1α, improved BMSC mobilisation and homing, extensive angiomyogenesis, reduced infarct size and improved left ventricular function. In a similar study by Saxena *et al.*, described above, SDF-1α was delivered by intra-cardiac injection after MI in mice and found to increase VEGF and angiogenesis, and reduce IS.[20] VEGF, like SDF-1α, is up-regulated in response to HIF-1α and can promote angiogenesis in addition to many of the detrimental effects of SDF-1α described, including tumour growth and metastasis. Its similarity to SDF-1α in these respects, and apparent complex interaction of VEGF with SDF-1α, make it an intriguing alternative pathway for many of the processes described in this thesis and, despite not being specifically examined here, should be recognised. These are complicated issues for groups interested in utilising SDF-1α in the treatment of chronic ischaemic cardiomyopathy, and thus represent a confounding issue, but one which is not considered further in this thesis.

Despite these potentially detrimental effects of SDF-1α-CXCR4, and the potential importance of VEGF, research into the potential utility of SDF-1α in ischaemic cardiomyopathy has begun to be translated. For example, Theiss *et al.* have confirmed in humans that mRNA of HIF-1α and SDF-1 are significantly higher in explanted heart tissue of patients with ischaemic cardiomyopathy versus dilated cardiomyopathy.[99] The same group published a Phase I study of plasmid-based endomyocardial SDF-1 (pSDF-1) delivery to 17 patients with symptomatic ischaemic cardiomyopathy and found improvements in 6 min walk distance, New York Heart Association classification and quality of life after 12 months.[100] Although EF was not

significantly affected, and neither inflammation nor scar formation recorded, the primary safety end-point was met. They proceeded to a Phase II, double-blind, randomised, placebo-controlled trial called Stromal Cell-Derived Factor-1 Plasmid Treatment for Patients with Heart Failure (STOP-HF).[93] This was a safety and efficacy study of a single endomyocardial injection of pSDF-1 in patients with ischaemic cardiomyopathy. Ninety-three stable patients with mean LVEF 28±7% and on optimum medical therapy were included, 62 of whom received pSDF-1 with no adverse events. The primary endpoint of a composite of 6 min walk distance and quality of life, assessed at 4 months after injection, was not met. In a pre-specified subgroup analysis there was a significant 11% improvement in LVEF at twelve months in patients with the worst baseline EF (P=0.01). This finding may be related to the administration of a single dose of pSDF-1 or its timing (mean time since MI was 11±9 years).

## 1.4 Acute cardioprotection

### 1.4.1 Ischaemic preconditioning

The finding that the myocardium could be protected from lethal IRI by the application of multiple brief ischaemic episodes was first made by Murry *et al.*, who found a 25% reduction in IS in dogs subjected to four 5 min circumflex occlusions, each separated by 5 min of reperfusion, prior to sustained occlusion of the circumflex artery.[101] They termed this phenomenon ischaemic preconditioning (IPC).[101] It has been demonstrated in numerous pre-clinical studies, and confirmed in a recent meta-analysis,[102] that the myocardium can be protected from lethal IRI by IPC.

The mechanism of protection conferred by ischaemic conditioning, as it is currently understood, comprises extracellular autacoids acting on cardiomyocyte receptors in response to the conditioning stimulus and triggering protective intracellular signal transduction cascades.[103] These are thought to unite at the mitochondria, particularly the mitochondrial permeability transition pore (MPTP), to inhibit apoptosis and preserve cardiomyocyte viability (Figure 1-2).[104]

Several endogenous extracellular factors, such as adenosine and opioid peptides, are known to mitigate the deleterious effects of IRI and are thought to play a central role in ischaemic conditioning (reviewed by Yellon *et al.*, 2007[6]). They originate from a variety of sources including cardiomyocytes, endothelium, smooth muscle cells, nerve endings, inflammatory cells, mast cells and macrophages in response to the conditioning stimulus, and have been extensively investigated.[105-109] They are thought to have a number of actions, including reducing the activation of coronary vascular endothelium, reducing the production of pro-inflammatory cytokines and reactive oxygen species (ROS) and reducing adherence of neutrophils to the coronary artery, all of which contribute to ischaemic conditioning.[103, 110, 111] As described, these factors exert these effects by recruiting the same protein kinase signalling cascades that are thought to be activated by the SDF-1α-CXCR4 axis.[24, 26, 103] The best defined of these are the 'reperfusion injury salvage kinase' (RISK) and 'survivor activating factor enhancement' (SAFE) pathways.[25, 109, 112]

The RISK pathway was first described by Yellon's group in recognition of the activation of PI3K-Akt pathway and p42/p44 Erk1/2 MAPK by myocardial reperfusion.[12, 24, 113-115] Pharmacological activation of this pathway has been shown to reduce IS by 40-50% at the time of reperfusion.[103] Importantly, many of the known protective endogenous factors, including insulin, IGF-1, bradykinin and adenosine, have been shown to protect against IRI by recruiting the RISK pathway (reviewed by Hausenloy *et al.*[24]). IPC has also been shown to protect against lethal IRI by recruiting the RISK pathway.[116-118] Specifically, the Akt1 isoform appears to be essential to IPC as demonstrated in Akt1-deficient mice that were resistant to protection from IPC.[119] Further, it has been shown that the RISK pathway is recruited equally by IPC, ischaemic postconditioning (IPostC) and RIC, indicating that this signal transduction pathway may represent a common pathway in ischaemic conditioning.[120-123]

Lecour *et al.* described an alternative pathway, labelled the SAFE pathway, which activates JAK-STAT signalling.[112] In mice subjected to simulated ischaemia and reperfusion, IPostC reduced IS and increased phosphorylated (active) STAT3.[109] In this study, administration of a specific JAK-2 inhibitor (AG-490) reduced phosphorylated

STAT3 and abolished the beneficial effect of IPostC.[109] Likewise, cardiac-specific STAT3-deficient mice were not protected from IRI by IPostC.[109] Further, in a model of pharmacological preconditioning with tumour necrosis factor-α cardioprotection was not affected by inhibition of PI3K-Akt or Erk1/2 MAPK, but was abolished by inhibition of STAT3.[124] Likewise, the SAFE signalling pathway is also required for RIC.[123] The interplay between RISK and SAFE pathways is not fully defined, however it has been shown that in *ex vivo* mouse hearts functional protection conferred by IPostC was not only abolished by JAK-STAT inhibition, but also that STAT3 inhibition decreased both functional STAT3 and Akt, suggesting that these signalling cascades are not entirely independent.[125] What is known is that both pathways converge on the mitochondria, particularly the MPTP, to affect cardioprotection.

Many of the pathological processes thought to mediate IRI, including oxidative stress, deranged calcium metabolism and rapid recovery of physiologic pH, exert their effects at the mitochondria, resulting in cardiomyocyte death.[6] Specifically, the MPTP, a voltage- and calcium-dependent channel in the inner mitochondrial membrane, is implicated.[103] This is closed in ischaemia due to acidosis, a high mitochondrial membrane potential and high concentrations of $Mg^{2+}$ and adenosine diphosphate (ADP).[103, 126] However, in reperfusion, the MPTP opens in response to binding of cyclophilin D (Cyp-D), which is potentiated by depolarization, increased mitochondrial $Ca^{2+}$, inorganic phosphate and ROS, and restoration of normal pH.[103, 127-131] Once open, the mitochondrial membrane potential rapidly dissipates, respiration becomes uncoupled, further elevating ROS formation, which establishes a vicious cycle of further MPTP opening and consequent loss of cell viability.[103, 126] Importantly, it is known that IPC and IPostC antagonise MPTP opening and significantly limit IS in animal models of IR.[132-136] Furthermore, it is notable that several studies have associated activation of the RISK and SAFE pathways with inhibition of MPTP opening, indicating it may represent the final common effector of ischaemic conditioning.[136-140]

In pilot pre-clinical studies, specific chemical inhibitors of MPTP, including NIM811,[132] ciclosporin A,[127, 132, 133, 141] and N-methyl-4-valine ciclosporin A,[133] have been shown

to reduce MPTP opening, limit apoptosis, improve functional recovery and limit IS. Likewise, transgenic Cyp-D-deficient mice subjected to simulated IRI have been shown to have reduced IS.[142, 143] The improvement in functional recovery conferred by ciclosporin A, which prevents Cyp-D binding,[103] has also been demonstrated in human atrial tissue,[104] and successfully translated to a human pilot study of MI.[144] Despite this, a multi-centre, double-blind, randomised trial of 970 patients with STEMI who received IV ciclosporin prior to PPCI recently failed to meet its primary endpoint of a significant improvement in the composite of all-cause mortality, worsening in-hospital heart failure, rehospitalisation for heart failure or adverse LV remodelling at 1 year.[145] Interestingly, this result might have been predicted based on a systematic review and meta-analysis that showed that while, overall, ciclosporin reduced infarct size by a standardised mean difference (SMD) of -1.6 (95% CI -2.17 to -1.03), there was no demonstrable benefit in swine, which are considered the most representative of humans.[146]

### 1.4.2 SDF-1α and ischaemic conditioning

Given the role of SDF-1α-CXCR4 in myocardial repair and the involvement of signalling kinases known to be integral to IPC, namely the Erk1/2, PI3K-Akt, JAK-STAT and PKC signalling cascades,[82, 147] it has been hypothesised that SDF-1α may also be involved in the myocardial protection from IRI conferred by IPC. This is further supported by studies that have successfully used IPC to up-regulate SDF-1α and improve stem cell engraftment after MI. For example, Tang *et al.* applied IPC in a murine model of MI and demonstrated up-regulation of CXCR4 on cardiac progenitor cells, increased cardiac progenitor cell migration and recruitment, reduced IS and improved functional outcome, all of which were abolished by the addition of AMD3100.[148]

SDF-1α has been shown to be cardioprotective in the context of IRI in a number of different models.[46, 149, 150] As discussed in section 1.3.2, data from Yellon's group using *ex vivo* rat papillary muscle indicates that SDF-1α increases recovery of function of muscle subject to simulated IRI, which can be blocked by AMD3100 (this is discussed further in section 5.2.1).[31] Similarly, Huang *et al.* administered SDF-1 5 min before

ischaemia in isolated mouse hearts subject to ischaemia-reperfusion in a model of pharmacological preconditioning.[149] They found that SDF-1 significantly improved functional recovery, reduced markers of apoptosis and increased activation of STAT3, a central mediator of the SAFE pathway.[149] These effects were abolished by the addition of AMD3100.[149] Interestingly, they did not see any increase in Akt or Erk1/2 phosphorylation, and no attenuation of protection with LY294002, an inhibitor of the Akt pathway.[149] Jang *et al.* used an *ex vivo* Langendorff model of IRI to show that five different concentrations of SDF-1 (250 pM to 5 nM) infused from 10 min before reperfusion to 30 min afterwards reduced IS significantly more than that seen with IPC and IPostC.[150] They also saw an increase in Erk1/2 phosphorylation at 5 and 20 min after reperfusion, thereby implicating the RISK pathway in the mechanism.[150] Hu *et al.* demonstrated significantly increased SDF-1α release from isolated cardiomyocytes following hypoxia and reoxygenation.[46] In this study, 25 nmol/L exogenous SDF-1α administered to cultured myocytes for 10 min resulted in increased phosphorylation of both Erk1/2 and Akt, less lactate dehydrogenase release and less apoptosis, an effect abolished by pre-treatment with AMD3100. *In vivo*, they demonstrated pharmacological preconditioning with SDF-1α infused into the LV cavity significantly reduced IS, which was abrogated by AMD3100. Preliminary steps have been taken towards translating the beneficial effect of exogenous SDF-1α to humans. Specifically, SDF-1α has been shown to mimic the cardioprotection conferred by hypoxic preconditioning in a model of simulated IRI using isolated human atrial trabeculae muscle.[151]

The signalling cascades downstream of CXCR4 activation described above are inconsistent. CXCR4 is a GPCR that activates several signalling pathways, including both G protein-dependent and independent pathways.[152] With respect to cardioprotection, CXCR4 activates the RISK pathway via $G_{\beta\gamma}$ and the SAFE pathway in a G protein-independent manner.[153] Tong *et al.* related the cardioprotection conferred by IPC to $G_{\beta\gamma}$ by using a sequestering peptide in an isolated murine heart model of hypoxia and reoxygenation.[154] This supports the hypothesis that SDF-1α-CXCR4 is cardioprotective via the RISK pathway. CXCR7, on the other hand, phosphorylates MAPK pathway proteins, including Erk and p38, and signals via β-

arrestin, which inhibits G protein-mediated signalling and has also been implicated in cardioprotection.[155, 156] The relationship between these receptors is complex and remains poorly defined, especially in relation to cardioprotection.

### 1.4.3 Remote ischaemic conditioning

Despite promising experimental results for IPC, the translational potential of IPC is limited by the necessity to intervene before the index ischaemia, which is impossible to predict in STEMI. A potential solution is mechanical IPostC. Zhao *et al.* investigated repetitive ischaemia applied in early reperfusion of the left anterior descending (LAD) territory in a canine model, and found a 14% reduction in IS (compared to 15% in IPC in their model), a technique referred to as IPostC.[110] Several studies have investigated this approach in a clinical setting, with mixed results.[157-162] However, this mandates an invasive approach and risks associated procedural complications, including coronary artery dissection or perforation, access site complications, arrhythmias and stroke.

In response to these concerns RIC has emerged as a potentially cheap, non-invasive alternative that can be applied before, during or after the index ischaemia (remote pre-, per- or postconditioning, respectively). RIC was first shown to be protective by Przyklenk *et al.* in 1993, who applied four episodes of 5 min circumflex occlusion separated by 5 min of reperfusion, before 1 h of sustained LAD coronary artery (henceforth abbreviated to LAD) occlusion and reperfusion for 4.5 h in a canine model.[163] They found a 10% reduction in IS in the circumflex preconditioned dogs.[163] This has been developed by others who showed similar cardioprotective effects after applying a preconditioning stimulus to other remote organs and tissues, including the kidneys and skeletal muscle,[164, 165] and using remote IPostC.[166]

More recently it has been demonstrated that the application of brief cycles of ischaemia and reperfusion to a limb using a vascular occluder, tourniquet or blood pressure cuff has the same effect. Since the inception of limb RIC in 1997,[165] several pre-clinical studies have demonstrated its efficacy in myocardial IRI. It can be achieved non-invasively by tightening a tourniquet or inflating a blood pressure cuff

on the arm or thigh to above systolic pressure to induce brief ischaemia and then deflating it to allow reperfusion,[167] a finding which has greatly accelerated the rate of clinical trials.

Several proof-of-concept clinical studies have translated these findings to a variety of clinical settings, albeit frequently using cardiac enzymes and myocardial salvage as surrogate markers of outcome, including coronary artery bypass surgery (CABG),[168-171] elective percutaneous coronary intervention,[172] and in PPCI for STEMI.[173-175] For example, for patients suffering STEMI, Botker *et al.* randomised patients to receive PPCI with or without a pre-hospital RIC protocol. The primary endpoint of improved myocardial salvage index at 30 days, measured by myocardial perfusion imaging, was met.[173] Importantly, studies have demonstrated similar effects with RIC applied before,[168, 169, 176] during,[173] and after the index ischaemia,[166, 175] thereby improving its clinical utility and potential to mitigate IRI in patients.

A recent clinical study has also examined the combination of RIC with mechanical IPostC. The LIPSIA CONDITIONING trial was a prospective, controlled, single-centre study of 696 STEMI patients undergoing PPCI.[177] The primary endpoint was myocardial salvage index assessed by cardiac magnetic resonance (CMR) 3 days after MI, which was significantly greater in the combined RIC and IPostC group than in an unconditioned control group (P=0.02), although IPostC alone was no better than control. There was no difference in a combined clinical endpoint of death, re-infarction and new congestive heart failure at 6 months, although diverging lines on the Kaplan Meier curve suggest this might have been significant with longer follow-up. Interestingly, the authors did not include a RIC-only control group so it is unclear whether the benefit with RIC plus IPostC versus IPostC alone was entirely attributable to RIC or whether additive protection can be achieved with the combination.

Large clinical endpoint studies have so far only been published in the context of RIC in cardiac surgery. Hausenloy *et al*. found no difference in the primary end point of death from cardiovascular causes, nonfatal MI, coronary revascularization or stroke at 12 months between the sham and RIC arms of the Effect of Remote Ischemic

Preconditioning on Clinical Outcomes in Patients Undergoing Coronary Artery Bypass Surgery (ERICCA) study.[178] Similarly, Meybohm *et al*. found no difference between the sham and RIC arms with respect to the primary endpoint of death, nonfatal MI, stroke and acute renal failure up to 14 days in the Remote Ischaemic Preconditioning for Heart Surgery (RIP-HEART) study.[179] Furthermore, neither study identified any effect of RIC on troponin release as a secondary endpoint. Some potential reasons for the discrepancy between pre-clinical studies and these large randomised outcome studies are addressed in Chapter 3. Regarding STEMI, two randomised, multi-centre, controlled trials of RIC are currently recruiting, and the results are eagerly anticipated (ERIC-PPCI NCT02342522 and CONDI2 NCT01857414).[180]

It is suggested that the protective effect of RIC may be due to a humoral factor(s), which may be one, or a combination of, the factors described above, or a novel molecule(s), which is carried by the blood from the transiently ischaemic limb to the remote target organ where it activates endogenous pro-survival signalling pathways. Evidence for this comes from studies wherein the cardioprotective effect of RIC applied to the lower limb is abrogated by occlusion of the femoral vein.[181] Further, IS is significantly reduced when the effluent from an isolated perfused heart that is preconditioned is used to perfuse a second isolated heart prior to index ischaemia.[182, 183] The endogenous pro-survival signalling pathways in RIC remain poorly described and are assumed to be similar to those that mediate local IPC. The limited evidence to date has implicated PKC,[184, 185] the RISK pathway,[186-188] eNOS,[189] and HIF-1α,[190, 191] with sarcolemmal and mitochondrial $K_{ATP}$ channels their proposed targets.[174, 192, 193]

Interestingly, there also appears to be a neural component to RIC whereby severing the femoral and sciatic nerve in an *in vivo* mouse model of IRI abolishes the protection conferred by RIC, although the relationship between neural and humoral components of this phenomenon is debated.[181] It has recently been demonstrated that targeted inhibition of pre-ganglionic neurones in the dorsal motor nucleus of the vagus nerve, which generate parasympathetic tone, completely abolishes RIC.[194, 195] Furthermore, Mastitskaya and colleagues recently denervated various organs by sectioning specific branches of the vagus nerve, prior to RIC.[196] They found that RIC

was abolished by total subdiaphragmatic, gastric or posterior gastric vagotomy, but not coeliac, hepatic or anterior gastric branches, implicating a cardioprotective factor released from the stomach, proximal duodenum, jejenum or pancreas. Interestingly, studies have successfully used plasma dialysate from preconditioned animals to protect both isolated, denervated hearts and cardiomyocytes, suggesting that neuronal involvement may be limited to the release of the humoral factor(s) and not necessary for signal transduction or distant cardioprotection.[28, 197] The neural hypothesis is of considerable interest in the RIC field, but was not specifically examined in this thesis.

### 1.4.4 SDF-1α and remote ischaemic conditioning

The rationale for considering SDF-1α as part of this mechanism is fivefold. Firstly, the SDF-1α-CXCR4 axis has been implicated in RIC, albeit indirectly, using *ex vivo* models.[31] Secondly, SDF-1α is an 8 kDa peptide, therefore fulfilling size criteria for a role in RIC.[33] Thirdly, SDF-1α expression has been reported in several organs, tissues and cells, including bone marrow, liver, kidney, thymus, spleen, skeletal muscle, brain and, more recently, platelets.[18, 41-44] Although it is likely that organ expression, in part, reflects expression in the vascular endothelium, it is likely that SDF-1α can be upregulated in peripheral tissues following the application of non-injurious ischaemia and reperfusion. Fourthly, SDF-1α-CXCR4 expression is upregulated in response to tissue hypoxia, via up-regulation of the transcription factor HIF-1α.[17, 18, 63] This complements the hypothesis that the humoral factor involved in RIC is upregulated in response to cyclical, non-lethal, ischaemia (tissue hypoxia)-reperfusion, although it is unclear whether increased SDF-1α transcription via up-regulation of HIF-1α would be quick enough to explain RIC. Finally, SDF-1α is highly conserved (more than 92% similarity at the protein level) between species and has been shown to confer protection between species.[28, 38]

Despite this promise, an important drawback is the relatively short plasma half-life of SDF-1α, which might limit its therapeutic utility.[51, 198] An approach to translating the potential of SDF-1α relates to its possible manipulation by a new class of anti-diabetic drugs. DPP4 inhibitors such as Sitagliptin, Vildagliptin, Alogliptin and Saxagliptin, have

been designed to prevent the breakdown of the incretin glucagon-like peptide-1 (GLP-1) by inhibiting the protease DPP4 thereby increasing insulin and lowering glucose.[199] Active SDF-1α is also cleaved by DPP4 at its position 2 proline residue, and thus, similar to GLP-1, DPP4 inhibition increases the half-life of SDF-1α by preventing its degradation.[200, 201] This is discussed in more detail in Chapter 7.

## 1.5 Research Objectives

With this background in mind, the overall hypothesis of this project was that SDF-1α-CXCR4 mediates the mechanism of cardioprotection conferred by RIC. The principle objectives are outlined below and described in detail in the chapters that follow:

1. To perform a systematic review and meta-analysis of experimental variables in *in vivo* models of RIC. This objective is described in Chapter 3.
2. To establish and verify murine *in vivo* models of myocardial IRI and RIC. This objective was investigated in both rats and mice, and is described in Chapter 4.
3. To investigate the cardioprotective utility of exogenous SDF-1α. This objective was investigated in a mouse model of myocardial IRI, and is described in Chapter 5.
4. To investigate whether the SDF-1α receptor blocker AMD3100 abrogates the cardioprotective effect of RIC. This objective was investigated in a rat model of myocardial IRI, and is described in Chapter 6.
5. To investigate whether RIC increases the production of SDF-1α. This objective was investigated using an ELISA to the active (full-length) form of SDF-1α in a rat model of RIC, and is described in Chapter 7.
6. To investigate whether RIC remains effective in cardiomyocyte CXCR4 null mice. This objective was investigated in a mouse model of myocardial IRI, and is described in Chapter 8.

# Chapter 2 General research methods

This chapter describes the general methods used throughout this thesis, with specific experimental details described in the relevant chapters that follow. All chemicals were from Sigma-Aldrich (Dorset, UK) and all antibodies from Abcam (Kent, UK) unless specifically stated.

## 2.1 Experimental use of animals

All use of animals was in accordance with the United Kingdom (Scientific Procedures) Act of 1986 and Amendment Regulations 2012, and local guidelines. All experiments were performed under Project Licence (PPL) 70/7140 prior to 3rd August 2015 and 70/8556 thereafter. Animals were housed in 12 h light/dark cycles under pathogen-free conditions. Standard chow and water were provided *ad libitum* and the temperature was maintained at 21°C. All routine care was provided by the Biological Services Unit (BSU) at University College London (UCL, UK). Experiments were performed in line with best practice described in the Home Office Licensee Training Course Modules 1-4 with further reference made to Laboratory Animal Anaesthesia.[202] Each animal was inspected prior to use and any showing adverse features, including reduced weight gain, piloerection and hunching, were excluded from experiments.

## 2.2 Standard rat strains

Founder Sprague Dawley rats were purchased from Harlan Laboratories (Oxon, UK) and a colony subsequently maintained by the BSU (UCL, UK). Historically, Sprague Dawley is the strain of rat most commonly used for MI experiments,[203] and is the strain used here due to cost and experience within our laboratory. This is discussed further in section 4.3.4. Male rats weighing 200-250 g were used throughout.

## 2.3 Transgenic mouse lines

Transgenic mouse lines were necessary for this thesis and the general method of their use is given here.

### 2.3.1 Generation of transgenic mice

'Floxed' CXCR4 transgenic mice were generated externally by Dr Dan Littman, Columbia University, NY, USA using standard methods that are described elsewhere.[204-207] Briefly, a targeting vector that is complementary to CXCR4, containing two *loxP* sites and a neomycin cassette either side of CXCR4 exon 2 (*loxP* sites flank CXCR4 exon 2, which is therefore referred to as 'floxed'), was constructed. This was introduced into 129P2/OlaHsd-derived E14 embryonic stem cells (ES) causing homologous recombination and insertion of the targeted construct in place of the endogenous CXCR4 exon 2, which contains over 90% of the translated sequence.[207] The *loxP* sites are 34 base pair (bp) sequences that allow DNA modification by Cre recombinase enzyme (Cre; Figure 2-1). The specific orientation of *loxP* sites relative to each other dictates whether Cre catalyses excision, inversion or integration of the target gene.[208] In the present study, the *loxP* sites catalyse CXCR4 exon 2 excision. The neomycin cassette confers neomycin resistance, which is exploited by treating ES with neomycin to remove untargeted cells. Mutant cells are injected into wild type blastocysts to generate chimeric progeny that are used, in turn, to produce mice that are heterozygous for the floxed CXCR4 allele, and the subsequent $CXCR4^{flox/flox}$ colony. This strain was backcrossed 18 times to a C57BL/6N genetic background and a breeding pair was imported into our facility from The Jackson Laboratory (ME, USA).

Abbreviations used to describe genotypes throughout this thesis are as follows: wild type (WT, +/+); heterozygous (HET, +/-); knockout or mutant (KO, -/-); and homozygous *loxP* site insertion (flox/flox).

### 2.3.2 Cardiomyocyte-specific gene ablation

Transgenic mice expressing Cre recombinase were generated in a similar way to $CXCR4^{flox/flox}$ mice, described above. However, to investigate tissue-specific effects of CXCR4 deletion, Cre-driven recombination may be spatially regulated using upstream tissue-specific promoters.[208] Therefore, in this case the Cre transgene was designed with an upstream mouse cardiomyocyte-specific alpha-myosin heavy chain promoter

(MYH6), which limits Cre-induced recombination of *loxP*-flanked sequences to cardiomyocytes. The transgene was injected into FVB/N embryos and the resulting progeny used to generate mice that are heterozygous for the Cre allele.[209]

Furthermore, transgenic homozygote mice lacking CXCR4 die in utero,[57] so it is necessary to temporally regulate Cre expression. This can be achieved by fusing Cre with ligand-dependent proteins.[208] In this case, Cre is fused with two mutant murine oestrogen receptor (Mer) ligand-binding domains that are activated by the oestrogen-receptor antagonist tamoxifen but not by endogenous 17β-estradiol. Once activated, MerCreMer enters the cell nucleus from the cytoplasm to effect CXCR4 exon 2 excision,[210] which results in a cardiomyocyte-specific knockout mouse.

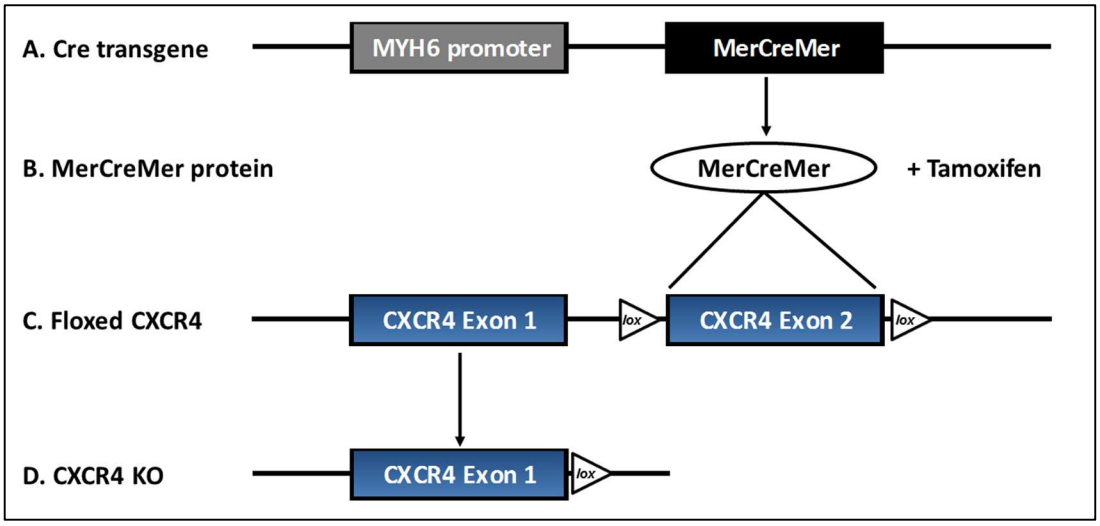


**Figure 2-1: Inducible cardiomyocyte-specific CXCR4 exon 2 deletion**

(A) MerCreMer gene product expression is spatially regulated by the MYH6 promoter; (B) Once bound to tamoxifen, MerCreMer protein migrates into the cell nucleus; (C) MerCreMer affects excision of CXCR4 exon 2, which is flanked by *loxP* sites; (D) This results in a cardiomyocyte-specific CXCR4 knockout strain.

MYH6-MerCreMer transgenic mice were backcrossed 15 times to a (B6 x 129/Sv)F1 background and >9 times onto a C57BL/6J background prior to being imported into our facility from The Jackson Laboratory (ME, USA). They have subsequently been backcrossed for several generations onto a C57BL/6 background in our laboratory. All backcrossing was completed by other members of our research group.

MYH6-MerCreMer mice were crossed with CXCR4 floxed mice, resulting in an inducible, cardiomyocyte-specific CXCR4 null bitransgenic strain.

### 2.3.3 Colony maintenance

First, $CXCR4^{flox/flox}$ mice were bred in a ratio of 1:1 with heterozygous MYH6-MerCreMer mice to yield $CXCR4^{flox/+}$, including 50% wild type and 50% heterozygous Cre mice. Then, $CXCR4^{flox/+}$ $Cre^{+/-}$ mice were bred with $CXCR4^{flox/+}$ $Cre^{+/+}$ mice to yield 25% $CXCR4^{flox/flox}$, 50% $CXCR4^{flox/+}$ and 25% $CXCR4^{+/+}$, 50% of which were $Cre^{+/-}$, as expected by Mendelian inheritance. The colony was then maintained as follows: all mice were $CXCR4^{flox/flox}$; heterozygous and wild type Cre transgenic mice were bred in a ratio of 1:1, to yield 50% wild type and 50% heterozygous Cre mice.

The Cre transgene is maintained as heterozygous for three reasons; firstly, it is difficult to distinguish heterozygosity from homozygosity by PCR as the precise insertion site of the transgene is unknown; secondly, as the Cre transgene can cause deletion of the gene into which it inserts, it is desirable to maintain a wild type allele; and thirdly, it is preferable that all mice express the minimal sufficient levels of Cre recombinase to avoid unwanted effects of over-expression, including cardiomyopathy.[211]

Breeding pairs were taken from different parents and females were allowed a maximum of five litters. All litters were weaned at 3-4 weeks old. The genotype of each animal was determined by PCR prior to experimentation as described below.

### 2.3.4 Genotyping

*Mouse biopsies:* Ear biopsies were taken from each mouse shortly after weaning (at approximately 3-4 weeks old) and labelled to facilitate matching of genotype to mouse. <u>All ear biopsies were taken by BSU technical staff.</u>

*Preparation of crude DNA lysates:* Ear biopsies were lysed within 1 h of collection to obtain template DNA. Ear biopsies were incubated in 150 µl Proteinase K (Qiagen, Lancs, UK) and DirectPCR Ear Lysis Reagent (Viagen Biotech, CA, USA) at a ratio of

1:10 at 50°C in a heating block overnight. Lysis was terminated by incubation at 85°C for 45 min to 1 h, to denature Proteinase K. Lysates were then mixed and stored at -20°C for a maximum of 1 week until their use for PCR and until the end of the study thereafter.

*Primer design:* The region of DNA to be amplified by PCR is defined using specific primers. For example, CXCR4 primers bind either side of the *loxP* site upstream of exon 2 to detect wild type or *loxP* inserted CXCR4.[207] Primers are short lengths of DNA that are complementary to the template DNA, bind following separation of the double-stranded (ds) DNA (denaturing), and serve as a starting point for replication and amplification, described below. The optimum DNA sequence and melting temperature ($T_m$) for primers used in genotyping were defined by The Jackson Laboratory (ME, USA) in the case of CXCR4 and were already established by our own laboratory in the case of MYH6-MerCreMer (described in Table 2-1). Primers were purchased from Eurofins Genomics (Ebersberg, Germany) and were diluted to 100 pmol/µl in autoclaved distilled water on arrival.

| **Primer** | **Sequence (5'→3')** | **Properties** | |
|---|---|---|---|
| | | **Length** | **$T_m$ (°C)** |
| CXCR4 *loxP* forward | CCACCCAGGACAGTGTGACTCTAA | 24 | 64.4 |
| CXCR4 *loxP* reverse | GATGGGATTTCTGTATGAGGATTAGC | 26 | 61.6 |
| MYH6-MerCreMer forward | ATCGGAAAAGAAAACGTTGA | 20 | 51.1 |
| MYH6-MerCreMer reverse | ATCCAGGTTACGGATATAGT | 20 | 53.2 |

**Table 2-1: PCR primer sequences**

PCR primer sequences, length and melting temperature ($T_m$).

*Amplification of DNA by PCR:* DNA was amplified by PCR to determine the genotype of each animal. A commercially available DNA polymerase kit (*Taq* DNA Polymerase Kit, Qiagen, Lancs, UK) was used for all reactions. In this kit, *Taq* DNA polymerase, a recombinant enzyme, catalyses the replication and amplification of a specific region of DNA by assembling deoxyribose nucleoside triphosphates (dNTPs).

| **Reagent** | **Volume per sample (µl)** | **Final concentration** |
|---|---|---|
| Qiagen 10X PCR Buffer | 2.0 | 1X |
| 10 mM dNTPs | 0.4 | 200 µM of each dNTP |
| Forward primer | 0.5 | 1.25 pM |
| Reverse primer | 0.5 | 1.25 pM |
| *Taq* DNA polymerase | 0.2 | - |
| Autoclaved distilled water | 15.4 | - |
| Template DNA | 1.0 | - |
| Total volume per sample (µl) | 20 | |

**Table 2-2: PCR reaction mix**

A master mix was prepared on ice according to Qiagen (Lancs, UK) guidelines and the composition given here. 1x Qiagen PCR buffer contains 1.5 mM $Mg^{2+}$.

Specifically, PCR reactions were performed by preparing a master mix of constituents from the *Taq* DNA Polymerase Kit (Qiagen, Lancs, UK). The same master mix composition, with the exception of different primers, was used in reactions for CXCR4 *loxP* and MYH6-MerCreMer. A fresh master mix was made for each experiment (see Table 2-2). The volume of master mix was enough for a negative control (without

template DNA) and accounted for 10% extra PCR assays than required. The PCR Buffer contains a red and orange marker dye that facilitated estimation of migration distance during electrophoresis. 1 µl of the template DNA was added to each PCR tube. A negative control, with autoclaved distilled water in place of template DNA, was included in all experiments to exclude DNA contamination.

After preparation, all PCR tubes were added to a thermal cycler with a heated lid (PTC 200 Thermal Cycler, MJ Research, Quebec, Canada) and the reaction run using a touchdown technique as described in Table 2-3. Touchdown PCR overcomes any uncertainty associated with calculating primer $T_m$ by beginning with an annealing temperature above the projected $T_m$ of the primer (see Table 2-1) and using successively lower temperatures with each cycle.[212] Ordinarily, it is possible to achieve highly specific binding of the primer to the DNA sequence of interest by annealing at a temperature just below the $T_m$ of the primer. Touchdown PCR facilitates this highly specific binding at the first permissive temperature, and subsequent cycles use incrementally lower annealing temperatures to increase the efficacy of the reaction. By doing so, any difference in $T_m$ between correct and incorrect annealing will create a fourfold advantage per $^{o}C$, thereby avoiding non-specific binding at lower annealing temperatures.[212] The sequences of interest out-compete non-specific sequences that might otherwise bind to the primer at these lower temperatures, resulting in increased specificity, sensitivity and yield without the need for primer optimisation.[212] Touchdown PCR was used for CXCR4 *loxP* and MYH6-MerCreMer PCR.

| PCR stage | Temperature and duration | Description |
|---|---|---|
| **5 cycles:** | | |
| 1 | 94$^{o}$C for 30 sec | DNA denaturing |
| 2 | 65$^{o}$C for 30 sec, decreasing by 1$^{o}$C per cycle until 61$^{o}$C | Primer annealing |
| 3 | 72$^{o}$C for 1 min | DNA synthesis |
| **Then 40 cycles:** | | |
| 16 | 94$^{o}$C for 30 sec | DNA denaturing |
| 17 | 60$^{o}$C for 30 sec | Primer annealing |
| 18 | 72$^{o}$C for 1 min | DNA synthesis |
| **Followed by 4$^{o}$C until collection** | | |

**Table 2-3: Touchdown PCR thermocycling protocol**

Touchdown PCR was performed using a thermal cycler (PTC 200 Thermal Cycler, MJ Research, Quebec, Canada).

*Visualisation of DNA products by gel electrophoresis:* PCR amplification produces products of a distinct size, defined in base pairs. This can be visualised by separating PCR products using agarose gel electrophoresis, whereby negatively charged products migrate through the gel upon the application of electrical charge and smaller products migrate further. In this case, 2% agarose gels were used to optimise separation. These were prepared using agarose (Thermo Fisher Scientific, MA, USA) in TAE buffer (Tris 40 mM, acetic acid 20 mM and EDTA 1mM). 0.001% Syto® 60 Red Fluorescent Nucleic Acid Stain (Thermo Fisher Scientific, MA, USA) was added to allow visualisation of DNA bands after fluorescent scanning. Gel electrophoresis was run in TAE buffer (constituted as above) in a Owl Easycast B2 Mini Gel Electrophoresis System (Thermo Fisher Scientific, MA, USA) set at 118 V for 40-50 min. The approximate migration distance was determined using the dyes contained within the

PCR Buffer, and electrophoresis was ceased when the leading edge reached approximately 75% of the available gel distance. Gels were subsequently scanned using the 700 nm laser of an Odyssey® Infrared Imaging System (LI-COR, Bad Homburg, Germany).

PCR product size was estimated by comparison to a standard GelPilot® 100 Base Pair Plus Molecular Weight Marker (Qiagen, Lancs, UK). The genotype of each animal was determined by comparing the PCR result with expected DNA bands for each genotype. Expected DNA product sizes for CXCR4 *loxP* and wild type mice were 550 bp and 481 bp, respectively. MYH6-MerCreMer$^{+/-}$ mice were expected to have a band of 650 bp, whilst wild types had no band. PCR products for all genotypes used in this thesis were reliably clear and easy to interpret using this protocol. Representative PCR results are shown in Figure 2-2.

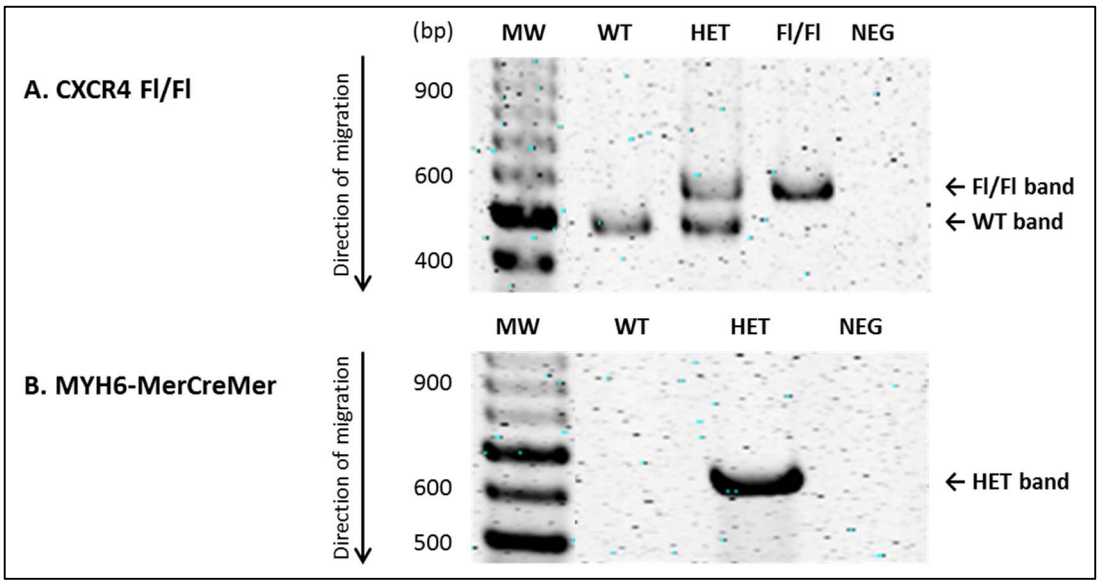


**Figure 2-2: Transgenic mouse colony representative genotyping results**

Each animal was genotyped based on the presence or absence of PCR products. (A) CXCR4 *loxP* wild type (WT) animals were expected to have a 481 bp band and mutant animals (flox/flox) a 550 bp band. Heterozygous (HET) animals were expected to have both; (B) MYH6-MerCreMer heterozygous (HET) animals were expected to have a 650 bp band and wild type (WT) animals no band.

### 2.3.5 Tamoxifen dosing

As discussed above, it is necessary to exploit the fusion of Cre with tamoxifen- or 4-hydroxytamoxifen-dependent proteins to temporally regulate Cre expression and avoid in utero death of mutated progeny. In the absence of tamoxifen or 4-hydroxytamoxifen, the Cre protein remains in the cytoplasm. Once activated, Cre translocates to the cell nucleus to effect *loxP*-mediated CXCR4 exon 2 excision.[210]

The tamoxifen administration protocol is well established within our laboratory, and is as follows. Tamoxifen was freshly prepared for each study by dissolution in 9 parts corn oil and 1 part 100% ethanol vehicle, to a final concentration of 5 mg/ml. This preparation was agitated at 37$^{o}$C for 1 h to ensure full dissolution, and stored at 4$^{o}$C between injections for a maximum of 5 days. Tamoxifen solution was administered as an intraperitoneal bolus daily for 5 consecutive days, at a dose of 20 mg/kg, in mice between 4 and 10 weeks old.[209, 213] All mice weighed approximately 25 g, indicating a final volume of 100 µl. Animals were monitored closely for 30 min afterwards due to an expected mortality rate of 10-20% due to acute tamoxifen toxicity. Tamoxifen-associated mortality was no higher in this thesis than expected (1/16, or 6.25%). Tamoxifen administration was performed at the same time each day to reduce confounding variables between groups. Mice were left for 3 weeks after completion of tamoxifen dosing prior to experimentation to ensure loss of protein.

### 2.3.6 Experimental groups

All offspring (CXCR4$^{flox/flox}$, Cre$^{+/+}$ and Cre$^{+/-}$) were injected with tamoxifen as described, resulting in 50% of animals with deleted CXCR4 and 50% wild type control littermates. This approach was intended to abrogate the reported confounding effects of tamoxifen administration, which are discussed further in section 8.4.4. Use of littermate controls also minimised potential confounding from genetic drift of in-bred colonies over time. All experiments were performed in male and female littermates aged 8-16 weeks old, unless specifically stated, with the upper limit imposed because of the susceptibility of the C57BL/6 background strain to develop

age-related obesity, type 2 diabetes and atherosclerosis.[214] Specific experimental groups used for each experiment are described in the relevant chapters.

## 2.4 *In vivo* non-recovery model of myocardial ischaemia-reperfusion injury

This thesis describes the validation and characterisation of rat and mouse *in vivo* non-recovery models of myocardial IRI. An overview of the method is given here, with detailed description of its characterisation and validation provided in sections 4.3 and 4.4, respectively.

### 2.4.1 Surgical protocol (rat)

Rats were anesthetised by left upper quadrant intraperitoneal injection of 100 mg/kg pentobarbitone sodium (Animalcare, Yorks, UK) at a concentration of 200 mg/ml, with a top-up dose of 25 mg/kg *pro re nata*. Surgery was started once pedal and tail reflexes were abolished, and depth of anaesthesia was monitored throughout the procedure.

After using tape to secure the animal in a supine position with limbs abducted, a loop of 5-0 suture (Ethicon, C of Edin, UK) was used around the upper incisors to secure the head in an extended position. Animals were subsequently intubated using cold light trans-illumination of the trachea (Photonic Optics PL2000, Oxon, UK), 200 mm angled dissecting forceps (all instruments from B. Braun (PA, USA) unless otherwise stated), and a modified 16G, 1.7 x 51 mm Abbocath-T intravenous cannula (Smiths Medical International Ltd, Kent, UK). Positive pressure ventilation was provided via connection to either a PhysioSuite (Kent Scientific, CT, USA) or Small Animal Ventilator (Harvard Apparatus, Kent, UK), supplemented with oxygen at a flow rate of 0.5 L/min. Correct intubation was confirmed by observation of chest expansion, appropriate airway pressure trace and tidal volume (PhysioSuite only), and the observation of gas bubbles from the ventilators' submerged expiratory tubing (Small Animal Ventilator only). Tidal volumes were calculated using the following allometric formula: tidal volume = 7.2 ml/kg.[215] The allometric formula for ventilation rate, provided by the ventilator manufacturer (Kent Scientific, CT, USA), is:

53.5 x (Body weight in kg)$^{-0.26}$

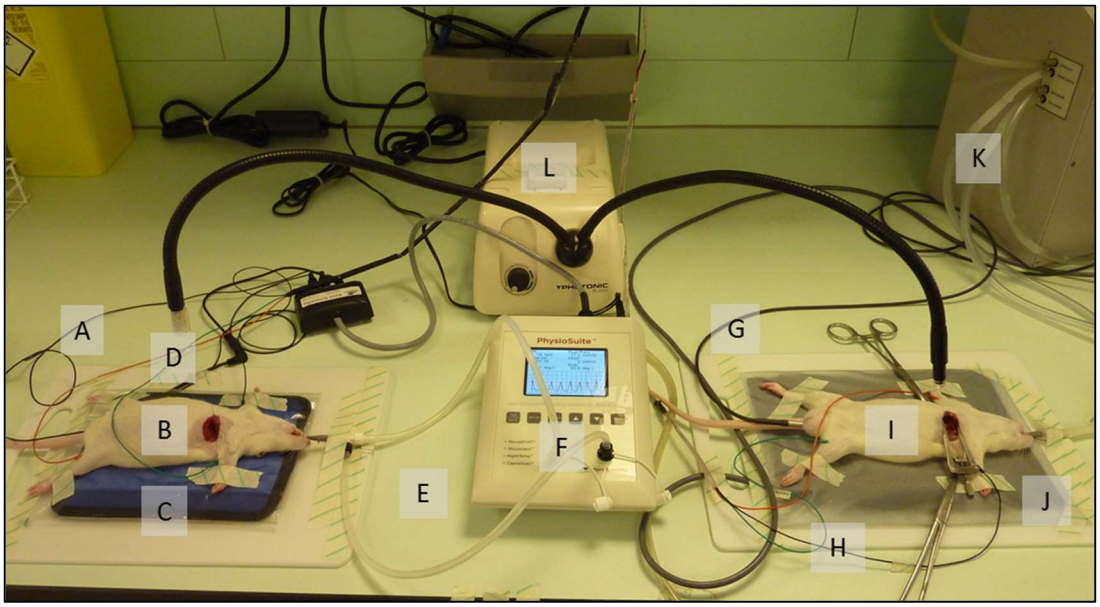


**Figure 2-3: Surgical setup for rat *in vivo* model of myocardial ischaemia-reperfusion injury**

Surgeries were conducted in tandem using the following arrangement (suppliers stated in the text): (A) Rectal temperature sensor to animal 1; (B) Animal 1; (C) Homeothermic heat mat 1; (D) Lead wires to Animal Bio Amp from animal 1; (E) Inspiratory and expiratory tubing to PhysioSuite; (F) PhysioSuite; (G) Rectal temperature sensor to animal 2; (H) Lead wires to Animal Bio Amp from animal 2; (I) Animal 2; (J) Homeothermic heat mat 2; (K) Inspiratory and expiratory tubing to Small Animal Ventilator; (L) Cold light source.

2 cm$H_2O$ of positive end expiratory pressure (PEEP) were added automatically (PhysioSuite) or by submersion of the expiratory tubing in water. This is important to prevent lung collapse during open chest surgery, and 1-5 cm$H_2O$ are recommended for small animals.[215] Surgeries were conducted in a controlled environment with regulated room temperature (19-21$^{o}$C). Core body temperature was monitored via a rectal temperature sensor and maintained at 37±0.5$^{o}$C by adjustment of a homeothermic heat mat (Kent Scientific, CT, USA or Harvard Apparatus, Kent, UK). ECG was recorded throughout using PowerLab 4/25 and Animal Bio Amp coupled to Chart 7 (AD Instruments, Oxon, UK; Figure 2-3 demonstrates the surgical setup).

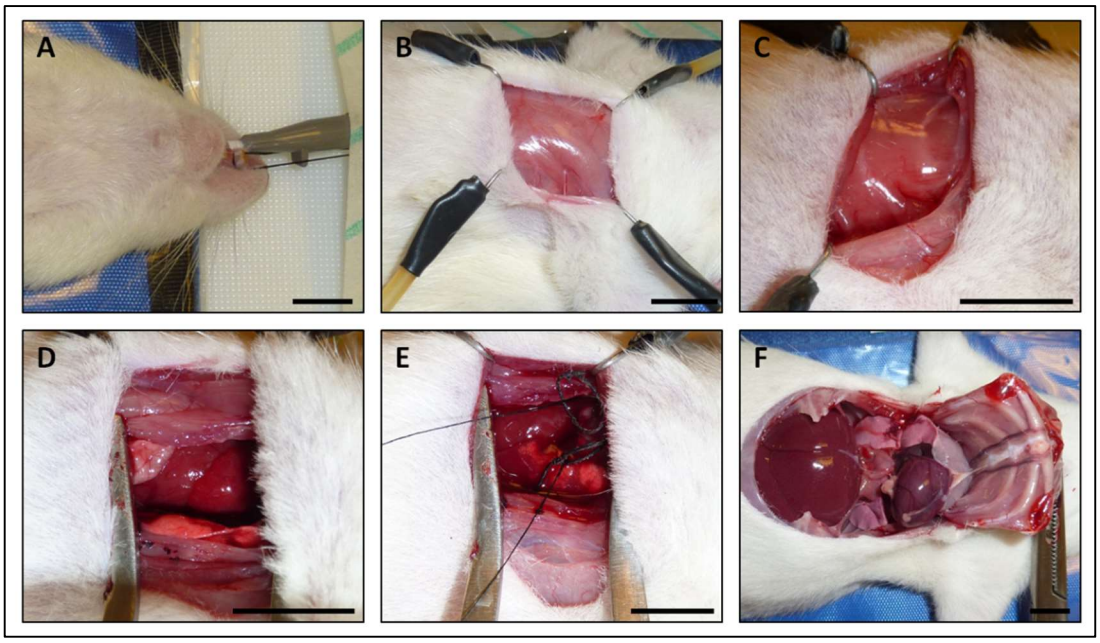


**Figure 2-4: Main stages of the rat *in vivo* myocardial ischaemia-reperfusion injury procedure**

The main procedural stages are: (A) Tracheal intubation and connection to a ventilator; (B) After shaving the left lateral hemithorax, skin incision and retraction reveals the pectoral muscles; (C) Sharp dissection of the pectoral muscles reveals the fourth intercostal space; (D) The intercostal space is opened by blunt thoracotomy and the ribs retracted; (E) After removal of the pericardium, the LAD is under-run with 6-0 suture with loops on either end to facilitate reperfusion. Once tightened the suture is secured with counterweights; (F) Following reperfusion the heart is eviscerated via a bilateral anterior (clamshell) thoracotomy. 1 cm scale bar.

The left thorax was shaved to facilitate surgery and a skin incision was made in the left lateral position, 1 cm below the forelimbs (Figure 2-4). Superficial muscles were sharp dissected. Blunt thoracotomy of the left fourth intercostal space was performed in order to gain access to the thoracic cavity. The pericardium was torn with splinter forceps. The LAD was under-run with a 6-0 braided silk non-absorbable suture with 9.3 mm, 3/8 curved needle (Ethicon, C of Edin, UK) positioned approximately 2 mm below the tip of the left atrium. After passing loops of 3-0 braided silk (Ethicon, C of Edin, UK) over each arm of the suture to facilitate reperfusion, ischaemia was initiated by occlusion of the ligating suture.

Successful ischaemia was confirmed by the occurrence of ST-segment elevation in the EGC trace (Figure 2-5), myocardial blanching and hypokinesia of the anterior wall

of the heart. Ischaemia, as indicated by ST-segment elevation, was maintained using surgical clamps as ballast on each end of the ligating suture. Following 30 min of ischaemia, reperfusion of the LAD territory was initiated by release of the occluding suture, which was left in place to facilitate subsequent analysis, and successful reperfusion confirmed by reversal of the ST-segment elevation and myocardial colour change. During ischaemia and reperfusion, the open wound was covered by a moistened swap to prevent desiccation and heat loss.

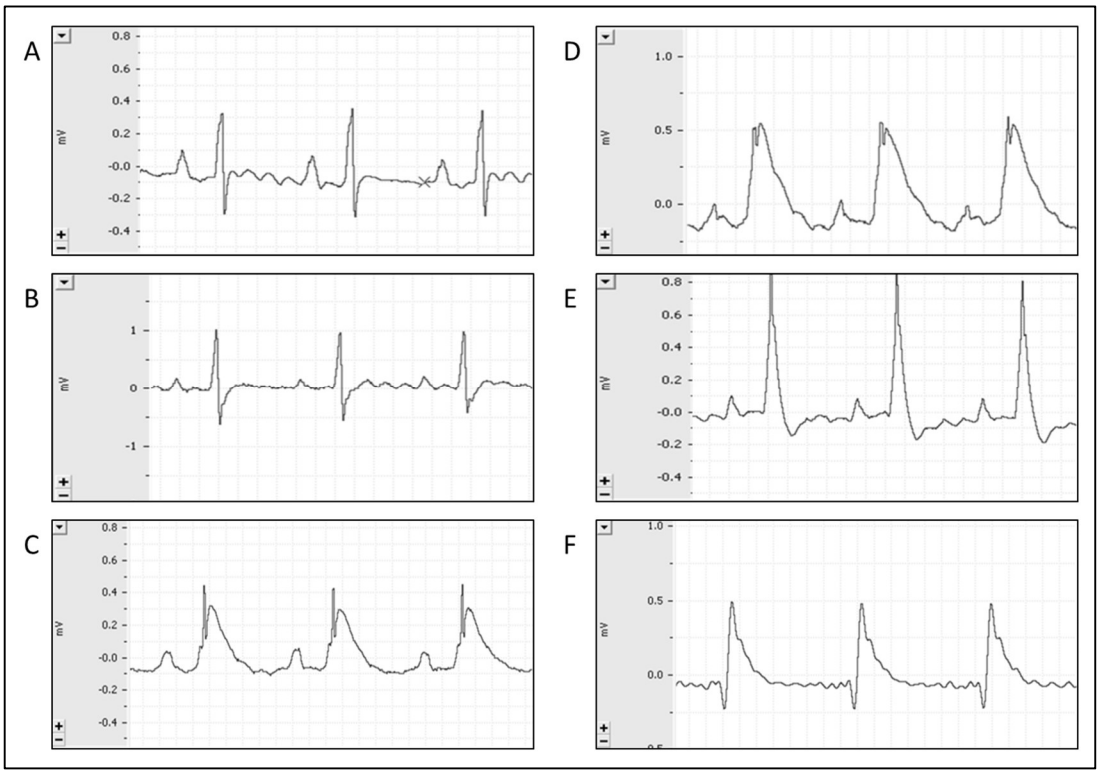


**Figure 2-5: Typical ECG changes seen during rat *in vivo* model of myocardial ischaemia-reperfusion injury**

The typical sequence of ECG changes includes: (A) Baseline; (B) ST segment depression; (C) ST segment elevation (moderate); (D) ST segment elevation (severe); (E) Broad QRS complexes in early reperfusion; (F) Q-wave formation.

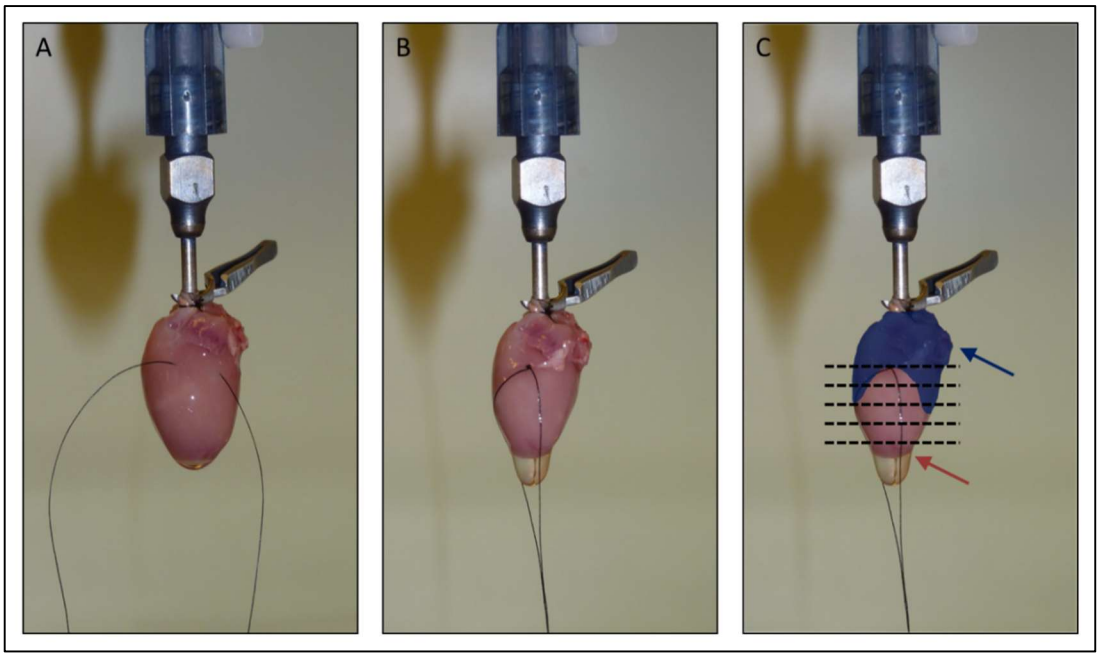


**Figure 2-6: Staining of a rat heart with Evans blue to define area at risk**

Each extracted heart was arrested in ice-cold Krebs-Henseleit buffer and subsequently rapidly mounted and secured onto a suspended cannula. Hearts were retrogradely perfused with Krebs-Henseleit buffer warmed to 37$^{o}$C (A) and the loosed LAD suture secured (B). Hearts were then retrogradely perfused with 0.5% Evans Blue to define the AAR (C). The area not at risk (Evans Blue area) is graphically represented in blue (blue arrow), whilst the remainder constitutes the AAR (pink arrow). After freezing, each heart was sliced into five transverse sections, indicated by the dashed lines.

Following 2 h of reperfusion animals were extubated and eviscerated. A clam-shell thoracotomy with cranial reflection of the anterior rib cage was performed, and pericardial adhesions removed (Figure 2-4). The aorta was transected at the level of the arch. The heart was arrested by submersion in cold Krebs-Henseleit buffer (NaCl 118.5 mM, $NaHCO_3$ 25.0 mM, KCl 4.8 mM, $MgSO_4$ 1.2 mM, $KH_2PO_4$ 1.2 mM, $CaCl_2$ 1.7 mM and glucose 11.0 mM). The heart was subsequently cannulated via the aorta, secured using 3-0 braided silk suture (Ethicon, C of Edin, UK) and retrogradely perfused with warm Krebs-Henseleit buffer in order to flush out any residual blood (Figure 2-6). The LAD suture was tied securely and approximately 500 µl 0.5% Evans Blue die retrogradely perfused through the same cannula to delineate an area at risk (AAR), whereby all areas of myocardium that were perfused during the index ischaemia are stained blue. Samples were labelled with a randomly-allocated four digit number to ensure operator blinding, and frozen for a minimum of 2 h at -20$^{o}$C.

IS was assessed within 5 days of freezing the sample, as described in section 2.4.4. The characterisation and validation of this model is described in detail in section 4.3.

### 2.4.2 Surgical protocol (mouse)

This model was based on the *in vivo* surgical protocol for rats, described in section 2.4.1, with relevant differences described here and further reference made to the description of this model by Fisher and Marber.[216]

Mice were anesthetised by intraperitoneal injection of 100 mg/kg pentobarbitone sodium (Animalcare, Yorks, UK) at a concentration of 20 mg/ml in 0.9% (w/v) saline, with a top-up dose of 17 mg/kg *pro re nata*. Surgery was started once pedal and tail reflexes were abolished and depth of anaesthesia was monitored throughout.

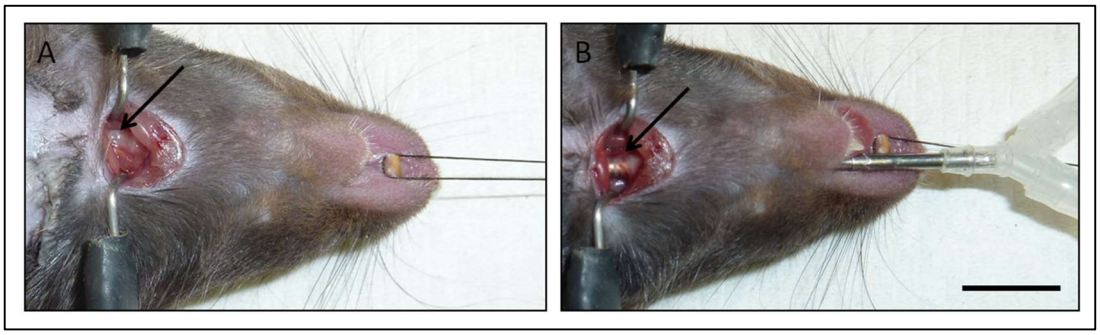


**Figure 2-7: Orotracheal intubation of mice was performed under direct visualisation**

(A) The salivary muscles were divided to expose the sternothyrohyoideus muscles overlying the trachea, which were subsequently blunt dissected in the midline to expose the trachea (arrowed); (B) A 19G cannula attached via a plastic Y-connector to the ventilator was passed down the trachea (arrowed) under direct visualisation. 1 cm scale bar.

All surgical procedures were performed using a standard binocular surgical microscope (EMX, Meiji Techno, Somerset, UK) at 5 times magnification. A midline skin incision was made over the anterior neck, and the salivary muscles were divided to expose the sternothyrohyoideus muscles overlying the trachea. These were bluntly dissected in the midline and retracted (Figure 2-7). A 19G cannula attached via a plastic Y-connector to the ventilator was passed, via the mouth, down the trachea under direct visualisation to prevent inadvertent oesophageal intubation. Positive

pressure ventilation was provided via connection to a PhysioSuite (Kent Scientific, CT, USA) without supplementary oxygen.

In mouse experiments, core body temperature was monitored using a rectal temperature probe (Hanna Instruments, Beds, UK) and maintained at 37±0.5$^{o}$C by adjustment of a heated veterinary operating mat (Peco Services, Cumbria, UK) Figure 2-8 demonstrates the surgical setup.

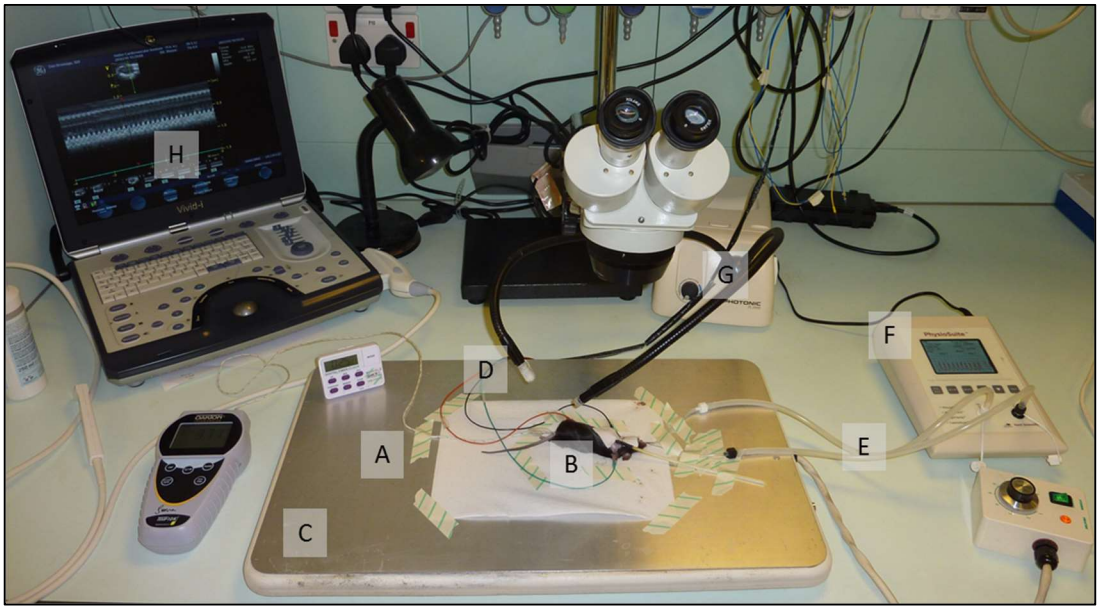


**Figure 2-8: Surgical setup for mouse *in vivo* model of myocardial ischaemia-reperfusion injury**

Surgeries were conducted on one mouse at a time using the following arrangement (suppliers stated in the text): (A) Rectal temperature sensor to animal; (B) Animal; (C) Homeothermic heat mat; (D) Lead wires to Animal Bio Amp from animal; (E) Inspiratory and expiratory tubing to PhysioSuite; (F) PhysioSuite; (G) Cold light source; (H) Vivid *i* ultrasound system.

Following intubation and stabilisation, hair was removed from the left thorax using a depilatory cream (Veet, Reckitt Benckiser, Berks, UK), to facilitate echocardiography and surgery. Mice were subjected to transthoracic echocardiography (TTE) assessment, as described in section 2.4.6. Then, to facilitate visualisation of the LAD, the left hind limb was adducted over the midline and secured. A left antero-lateral oblique skin incision was made using ligature scissors. The left major and minor pectoral muscles overlying the fourth intercostal space were blunt dissected and

retracted with blunt hook stays. Thoracotomy of the space, and cauterisation of any bleeding vessels, was performed with diathermy to the mid-clavicular line (Change-A-Tip cautery handle, Bovie Medical, NY, USA), taking care not to injure the underlying viscera. The wound was opened using hook stays. As in the rat model, the pericardium was torn with splinter forceps.

In the mouse model, the LAD was under-run with an 8-0 polypropylene non-absorbable monofilament suture with 6.5 mm, 3/8 curved needle (Ethicon, C of Edin, UK) positioned approximately 2 mm below the tip of the left atrium. The LAD was identified according to its anticipated position and bright orange appearance. A short piece of polyethylene tubing (PE-50, Deutsch and Neumann, Berlin, Germany) was secured to the end of the suture and used to assemble a snare system for reversible occlusion of the LAD. This was secured with further pieces of PE-50 tubing and a modified P200 pipette tip (Figure 2-9).

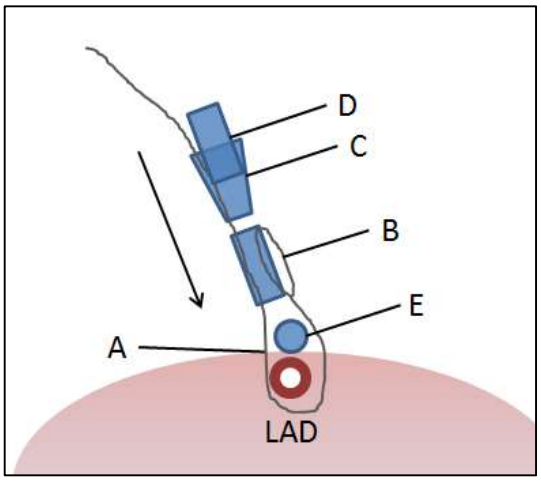


**Figure 2-9: Left anterior descending coronary artery snare system used for reversible occlusion in mice**

An 8-0 polypropylene suture (A) secured at one end to polyethylene tubing (B) and passed beneath the LAD. The suture was passed back through the tubing and through a modified pipette tip (C). It was secured using 'brake' tubing (D) and the whole construction advanced onto the LAD (indicated by the arrow) to induce ischaemia. A further piece of tubing was placed above the LAD to prevent slicing of the myocardium (E).

Ischaemia, as indicated by ST-segment elevation, was maintained for 40 min before reperfusion was induced by releasing the 'brake' tubing and disassembling the snare system. The suture was left in place to facilitate subsequent analysis. After 2 h of reperfusion, a repeat echocardiogram was performed and the heart was immediately removed. Hearts were prepared in the same way as described in section 2.4.1, with the exception that the aorta was secured on the cannula using a 5-0 braided silk suture (Ethicon, C of Edin, UK), 200 µl Evans blue dye was perfused under running

water, samples were frozen for 20 min at -80$^{o}$C, and staining for assessment of IS was performed on the same day (described in section 2.4.4).

The characterisation and validation of this model is described in detail in section 4.4.

### 2.4.3 Treatments and interventions

*Pharmacological treatment:* Pharmacological treatments were administered as a single bolus using either the left or right lateral tail vein. Injection was aided by ensuring the animal's tail was on the surgical heat mat beforehand and, in the case of mice, tightening a 5-0 braided silk suture (Ethicon, C of Edin, UK) tourniquet around the proximal tail, thereby causing venous dilatation and facilitating correct placement of the needle. Treatment was administered using a 25G x 5/8" Microlance needle (BD, Oxon, UK) for rats and the tip of a 27G x 1/22 needle (BD, Oxon, UK) mounted in 0.4 x 0.8 mm fine bore polythene tubing (Smiths Medical, Kent, UK). Successful venous puncture was confirmed by flash-back of venous blood, and successful delivery of the treatment was confirmed by washout of blood in the tail vein. Animals were excluded from the study if successful delivery of the treatment could not be confirmed. Saline (0.9%, Animalcare, Yorks, UK) was administered as a vehicle control to ensure the process of injection or administration of volume did not confound the results. The dose, volume and timing of pharmacological treatments is given in the relevant sections.

*Ischaemic preconditioning:* IPC describes cyclical non-injurious ischaemia and reperfusion in the same coronary distribution as the index, lethal IRI, and is a potent such strategy in all mammalian species.[102, 217] As IPC applied to the LAD is both effective and surgically feasible, it is an ideal positive control. After 5 min stabilisation, animals were subject to 5 min LAD occlusion and 5 min reperfusion prior to 30 min index ischaemia, which is a well-validated protocol for both rats and mice in our laboratory.[218, 219] Control animals were subjected to 15 min stabilisation to ensure equal anaesthetic times between groups (Figure 2-10).

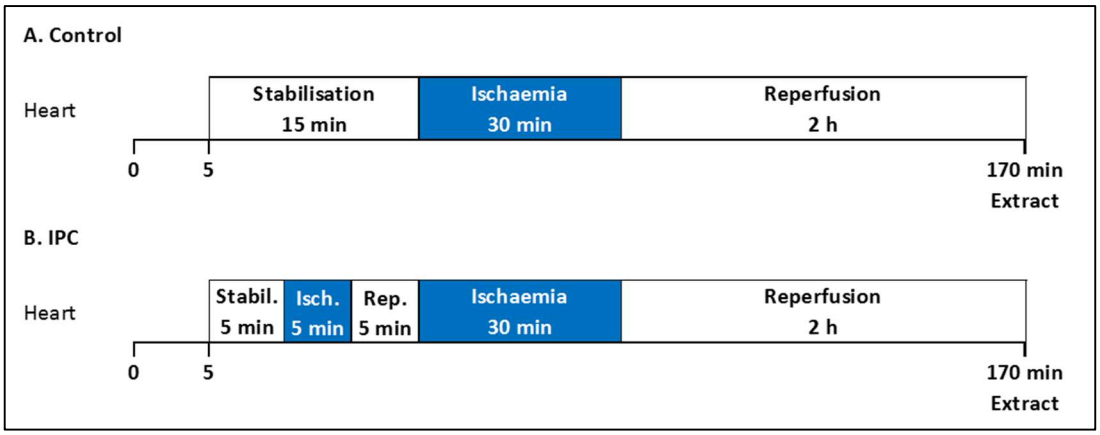


**Figure 2-10: Ischaemic preconditioning protocol**

(A) Control: 5 min stabilisation, 30 min ischaemia and 2 h reperfusion; (B) IPC: 5 min stabilisation, 1 cycle of 5 min ischaemia and 5 min reperfusion, 30 min ischaemia and 2 h reperfusion. Figure not to scale.

*Remote ischaemic conditioning:* In rats, RIC was applied using a modified human digital/penile cuff (1.6 x 9 cm cuff; Hokanson, WA, USA) around the right hind limb, which was inflated to 200 mmHg using a standard sphygmomanometer. Ischaemia was indicated by cyanosis of the right hind limb (arrowed in Figure 2-11). In mice, a 6 mm lumen custom vascular occluder (Kent Scientific, CT, USA) was similarly used around the right hind limb, but inflated to 250 mmHg with a standard sphygmomanometer.

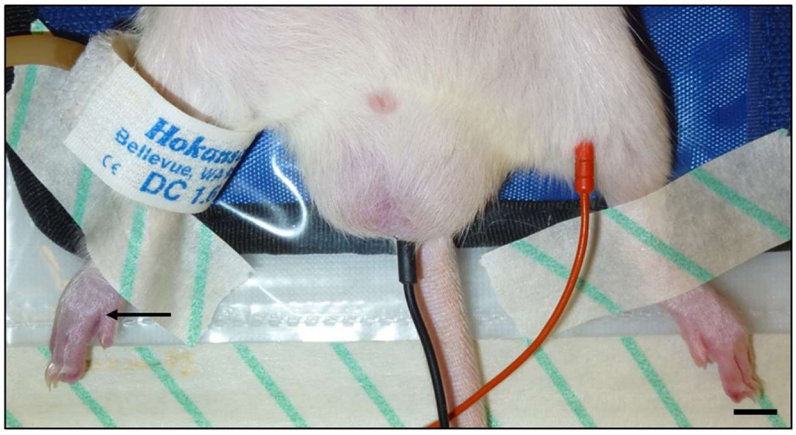

**Figure 2-11: Hind limb remote ischaemic conditioning in rats**

A human digital cuff was adapted for use on a rat hind limb. This figure shows the cuff inflated. Ischaemia is indicated by pedal cyanosis (black arrow) compared to the contralateral limb. 1 cm scale bar.

In both rats and mice, after 5 min stabilisation, three cycles of 5 min ischaemia and 5 min reperfusion was applied in the RIC group prior to 30 min index ischaemia and 2 h reperfusion. Control animals were subjected to 35 min stabilisation to ensure equal anaesthetic times between groups (Figure 2-12).

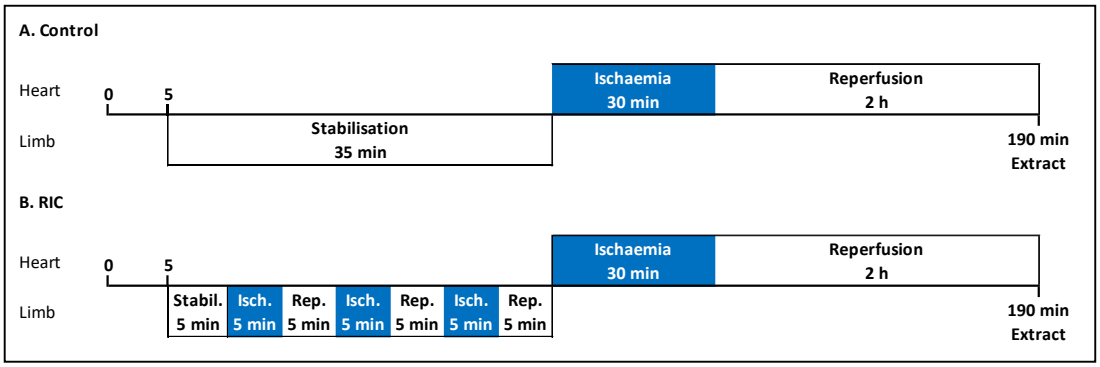


**Figure 2-12: Remote ischaemic conditioning protocol**

(A) Control: 35 min stabilisation, 30 min ischaemia and 2 h reperfusion; (B) RIC: 5 min stabilisation, three cycles of 5 min ischaemia and 5 min reperfusion, 30 min ischaemia and 2 h reperfusion. Figure not to scale.

### 2.4.4 Blood samples and preparation

Blood samples from mice and rats were collected on ice into tubes containing Sitagliptin to inhibit DPP4 and prevent degradation of full-length SDF-1α during sample preparation (equilibrium inhibition constant ($K_i$) 9 nM),[52, 220] to give a final concentration of 50 µM. Tubes were also pre-loaded with 1x citrate buffer to prevent coagulation. Aspiration of blood was performed by puncture of the right ventricle (RV) after thoracotomy using a wide-bore needle (19G x 1.5" Terumo needle (Surrey, UK) for rats, 21G x 5/8" Microlance needle (BD, Oxon, UK) for mice) to avoid platelet activation and subsequent release of SDF-1α (this is discussed further in section 7.6). Samples were immediately centrifuged at 1,600 g for 20 min then 10,000 g for 30 min to obtain platelet-free plasma (PFP), and frozen at -80$^{o}$C. Blood fractionation was performed according to previously published protocols without specific measurement of platelet numbers.[221] All experimental samples were defrosted at room temperature (RT) and used immediately.

### 2.4.5 Endpoint 1: Evaluation of infarct size

The primary endpoint of this *in vivo* model was myocardial IS. This is expressed as a percentage of the AAR (IS/AAR), that being the myocardial territory subject to ischaemia during LAD occlusion. The AAR was defined as described in section 2.4.1 and myocardial IS was established by staining of the *ex vivo* heart with triphenyltetrazolium chloride (TTC), a method that has been validated against histological assessment of necrosis in the early phase after MI.[222] After freezing, each heart was sliced into five 2 mm sections from the level of the LAD suture to the apex. These sections were incubated for 20 min in the dark in 10 ml phosphate buffer (2 parts 100 mM monobasic sodium phosphate and 8 parts 100 mM dibasic sodium phosphate) and 1% TTC. TTC is reduced by intracellular dehydrogenases in living cells to produce red formazan pigments. In areas of infarction TTC remains white, thereby allowing living and infarcted myocardium to be distinguished. Following incubation, the TTC solution was removed and sections were fixed in 10% formalin for 1-2 h at RT for rat sections and 24 h for mouse sections. This also has the effect of turning red blood cells brown, thereby facilitating their distinction from healthy myocardium. Sections were subsequently scanned for analysis using an Epson scanner (Epson Perfection V100 Photo, Epson, Herts, UK) at 1200 dpi, 48 bit colour and 50% brightness, and analysed by planimetry using ImageJ (version 1.45s, National Institutes of Health, MD, USA) (Figure 2-13). Mean AAR for each group is reported alongside the relevant experimental result, and all AAR and IS data are presented in scatter plots to clearly demonstrate any outliers.

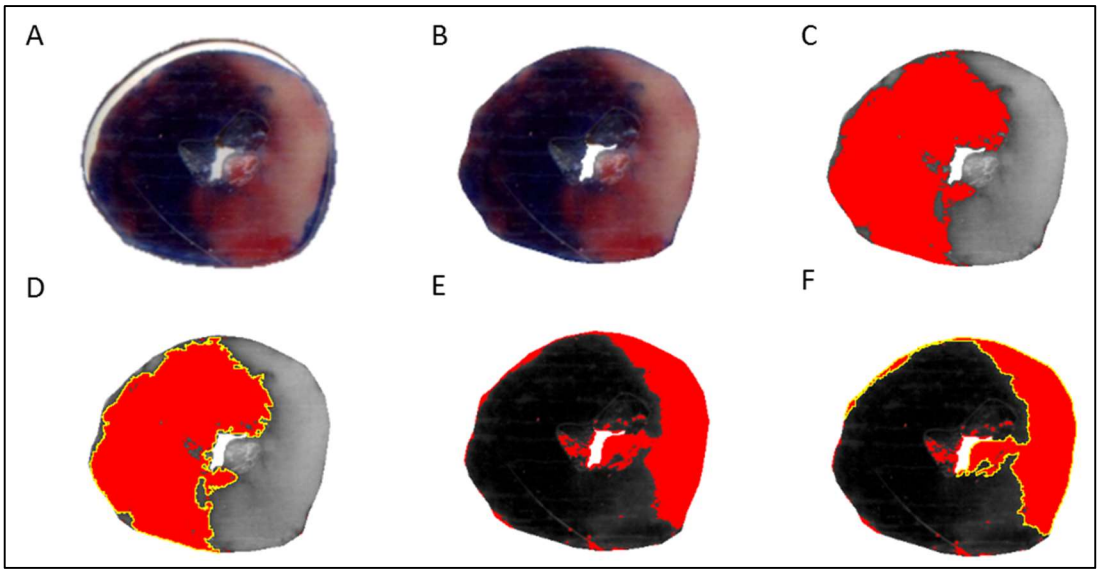


**Figure 2-13: Quantifying area at risk and infarct size in a mouse heart by planimetry**

(A) A scanned transverse heart section; (B) The background image was removed; (C) The Evans Blue area was measured by adjustment of the manual threshold of the green channel image to match the original image; (D) Quantification of Evans blue area by counting the number of pixels; (E) The IS was quantified by adjustment of the manual threshold of the red channel image to match the original image; (F) Quantification of IS by counting the number of pixels. Total myocardial area was calculated using the green channel image (not shown). AAR was calculated as (myocardial area – Evans Blue area) / myocardial area. IS was expressed as a percentage of AAR.

### 2.4.6 Endpoint 2: Echocardiographic assessment of left ventricular function

The secondary endpoint of this study was LV function assessed by TTE. TTE has been well validated as a non-invasive means of assessing cardiac function after MI in mice.[223] In mouse studies only, 2D TTE was performed on supine mice with hair removed, using a Vivid *i* ultrasound system with i12S-RS 11 MHz paediatric intra-operative phased-array transducer (GE Healthcare, Herts, UK) and ultrasound transmission gel (Skintact, Fannin, Gloucs, UK). An image depth of 1.5 cm was used throughout, and width and gain setting were carefully adjusted to maximise frame rates.

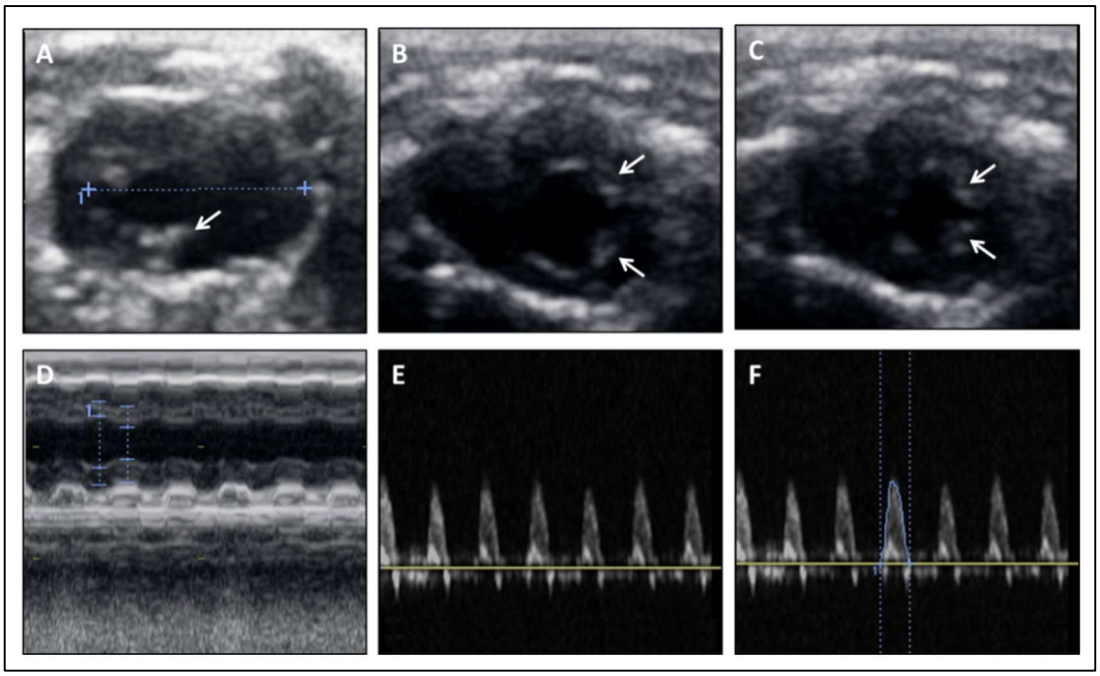


**Figure 2-14: Representative images from 2D trans-thoracic echocardiography of mice**

(A) Parasternal long axis view with measurement of the long axis end-diastolic dimension. A papillary muscle is arrowed; (B) Parasternal short axis view of the LV in diastole at papillary muscle (arrowed) level; (C) Parasternal short axis view of the LV in systole at papillary muscle (arrowed) level; (D) LV M-mode with measurement of LVIDd and LVIDs; (E) Aortic valve outflow, measured with CW Doppler; (F) demonstration of measurement of a VTI envelope.

First, a 2 sec cine loop was acquired in the parasternal long-axis view before interrogating the aortic root with pulsed wave (PW) Doppler in the same view. Observed peak velocities were within the Nyquist limit for PW Doppler and therefore not subject to aliasing. The possibility of aliasing was further reduced as the angle of incidence is approximately $15^{o}$ to the direction of flow in this view. This risks underestimating aortic root Doppler parameters but has previously been published and should not vary between experimental groups.[224, 225] Next, a 2 sec cine loop was acquired at papillary muscle level in the parasternal short-axis view and an M-mode trace recorded using the papillary muscles as a reference point. Representative images are provided in Figure 2-14. Frame rates for parasternal long axis, PW Doppler and M-mode images were 409.8 Hz, 129.9 Hz and 706.6 Hz, respectively. After surgery to induce IRI, a 6-0 braided silk non-absorbable suture (Ethicon, C of Edin, UK) was used to oppose the wound edges when necessary to facilitate echocardiography.

All measurements were made by a single observer and were the average of six consecutive cardiac cycles. Analysis was performed offline using EchoPAC (GE Healthcare, Herts, UK) according to the experiments' four-digit number to ensure operator blinding.

LV end-diastolic and end-systolic internal dimensions (LVIDd and LVIDs, respectively) were measured in Motion (M) mode (Figure 2-14, Panel D). M-mode echocardiography records motion along a single scan line (displayed on the y axis) over time (on the x axis). This narrow focus permits high frame rates (temporal resolution) and therefore accurate assessment of chamber dimensions. Temporal resolution was further improved using anatomical M-mode, which digitally derives M-mode analysis from 2D images and has the added advantage of allowing assessment along any line irrespective of transducer position, allowing the further optimisation of M-mode analysis.[226] LVIDd and LVIDs were used to derive fractional shortening (FS), which is a surrogate of LV function, according to the formula: FS = LVIDd – LVIDs / LVIDd x 100. End-diastole and end-systole were defined visually in the absence of integrated ECG recording.

LV end diastolic volume (EDV) was calculated according to the formula for a prolate spheroid, where volume = $4/3 \times \pi \times A^2 \times B$.[227] Here, 'A' represents the long axis end-diastolic dimension (Figure 2-14, Panel A), recorded in the parasternal long axis view, and 'B' represents LVIDd. Aortic root velocity-time integral (VTI) was measured using the PW Doppler trace (Figure 2-14, Panels E-F) and used to determine stroke volume (SV; µl), where SV = VTI x cross-sectional area (CSA). Mice of this weight have been shown from aortic casts to have an aortic root diameter of 1.2 mm and therefore CSA was assumed to be 1.1 $mm^2$ (according to $\pi r^2$) for all animals.[228] Cardiac output (ml/min) was calculated as a product of SV and heart rate, itself calculated by measuring the time between cardiac cycles in M-mode.

### 2.4.7 Experimental design

Animals were randomly assigned a four-digit number that was used to perform a blinded assessment of outcome, unless specifically stated. There was no formal randomisation to experimental group or blinded application of treatment protocols. Pre-defined exclusion criteria were applied to ensure consistency. Firstly, animals were excluded if their core body temperature deviated by more than 1$^{o}$C from the acceptable range of 37±0.5$^{o}$C, and this is discussed in detail in section 4.4. Secondly, if satisfactory ischaemia (indicated by ST-segment elevation in the EGC trace, myocardial blanching and hypokinesia of the anterior wall of the heart) was not achieved in ≤2 attempts at LAD ligation, the experiment was abandoned to exclude the potentially confounding effect of traumatic injury to the heart. Thirdly, animals were excluded if they failed to reperfuse satisfactorily, as indicated by reversal of the ST-segment elevation and myocardial colour change. Finally, hearts were excluded from analysis if the AAR was outside a pre-defined range of 35-70% in rats and 35-75% in mice.

## 2.5 Analysis of myocardial proteins by Western blot

### 2.5.1 Preparation of ventricular lysates

Mice were terminally anesthetised by intraperitoneal injection of 120 mg/kg pentobarbitone sodium (Animalcare, Yorks, UK) at a concentration of 20 mg/ml in 0.9% (w/v) saline, and 50 IU heparin. Once pedal and tail reflexes were abolished, hearts were extracted using clean tools as described in section 2.4.2, cannulated and manually perfused with ice-cold phosphate buffered saline (PBS) until the effluent ran clear. This was important to remove blood cells and platelets, which are known to express CXCR4.[44] Hearts were prepared as quickly as possible and in ice-cold conditions to prevent any protein modification. The atria were removed and the ventricles immediately homogenised in cold lysis buffer using a pestle and mortar. Lysis buffer was freshly made for each experiment, and consisted of Tris pH 6.8 (100 mM final concentration), NaCl (300 mM), NP4O (0.5%), cOmplete Mini protease inhibitor tablet (Roche, Sussex, UK), and Halt phosphatase inhibitor cocktail (Thermo

Fisher Scientific, MA, USA). The total volume was made up to 100 ml with distilled water and the pH adjusted to 7.4. 100 µl of lysis buffer was added per 10 mg heart tissue, which was homogenised on ice. After 10 min, samples were centrifuged for 10 min at 10,000 rpm at 4$^{o}$C. The supernatant was placed in a fresh tube on ice and immediately frozen at -20$^{o}$C pending further processing.

### 2.5.2 Preparation of isolated cardiomyocytes

Cardiomyocytes were isolated using a protocol established in the Hatter Cardiovascular Institute, UCL.[229] Briefly, sterile 6-well tissue culture plates (VWR, Leics, UK) were coated with 500 µl laminin/well, diluted in distilled water and left for at least 2 h before use. A stock perfusion buffer was prepared in distilled water as described in Table 2-4, adjusted to pH 7.4 and filter sterilised into a sterile bottle.

| Reagent | Quantity for 500ml (g) | Final concentration (mM) | Molecular weight (g/M) |
|---|---|---|---|
| Sodium chloride (NaCl) | 3.3 | 113 | 58.4 |
| Potassium chloride (KCl) | 0.175 | 4.7 | 74.6 |
| Potassium phosphate monobasic ($KH_2PO_4$) | 0.041 | 0.6 | 136 |
| Sodium phosphate dibasic ($Na_2HPO_4$) | 0.0425 | 0.6 | 142 |
| Magnesium sulfate heptahydrate ($MgSO_4$-$7H_2O$) | 0.15 | 1.2 | 246 |
| Sodium bicarbonate ($NaHCO_3$) | 0.505 | 12 | 84 |
| Potassium bicarbonate ($KHCO_3$) | 0.505 | 10 | 101 |
| HEPES Na Salt | 0.12 | 0.922 | 260 |
| Taurine | 1.875 | 30 | 125 |
| 2,3-Butanedione monoxime (BDM) | 0.5055 | 10 | 101.1 |
| Glucose | 0.4954 | 5.5 | 180 |

**Table 2-4: Stock perfusion buffer**

Stock perfusion buffer was prepared according to the composition given here. Components were added whilst stirring and the solution was adjusted to pH 7.4 before filter sterilising into a sterile bottle.

A Langendorff perfusion system was filled with perfusion buffer, with care taken to remove any air bubbles. Perfusion buffer was oxygenated by gently bubbling with oxygen throughout, and maintained at 37±0.5$^{o}$C using a heated water jacket. Mice were anaesthetised and eviscerated as described in section 2.5.1, with the exception that hearts were placed in, and flushed with, ice-cold stock perfusion buffer. The heart was mounted onto a 21G cannula that was attached to the Langendorff apparatus and perfused at 3 ml/min. After 5 min of perfusion to empty the ventricles and coronary vasculature, perfusion buffer was replaced with a digestion buffer consisting of stock perfusion buffer, 0.2 mg/ml Liberase™ (itself containing two collagenase isoforms) and 12.5 µM calcium chloride. The heart was perfused for a further 20 min or until appropriate loss of tissue integrity. Once fully digested, the heart was transferred to a single-well tissue culture dish (VWR, Leics, UK) containing digestion buffer where the ventricles were isolated, gently dissected and agitated with a Pasteur pipette to further degrade the tissue. 5 ml of stop buffer (stock perfusion buffer with 10% foetal bovine serum (Thermo Fisher Scientific, MA, USA)) was added in stages before filtering out any undigested tissue through sterile gauze. Cells were allowed to pellet for 10 min.

Next, calcium was gradually re-introduced by removing the supernatant and re-suspending the cells in stop buffer with consecutively higher concentrations of calcium chloride (112 µM, 300 µM, 710 µM and 1 mM). Between each stage, cells were allowed to pellet for 10 min. The pellet was then re-suspended with gentle inversions in warmed standard M199 tissue culture media supplemented with penicillin (100 IU/ml), streptomycin (100 IU/ml), blebbistatin (25 mM), L-carnitine (2 mM), creatine (5 mM) and taurine (5 mM).

Laminin was removed from the tissue culture plate wells, which were washed with supplemented M199. Two drops of cells were added per well or cover slip, with additional drops if 80% confluence was not achieved. Cells were placed in an incubator at 37$^{o}$C with 5% $CO_2$ for 1 h, after which the media was changed and the cells were ready for use in subsequent experiments.

### 2.5.3 Western blotting protocol

A bicinchoninic acid (BCA)-copper(II) sulphate ($CuSO_4$) colorimetric assay was performed to quantify the protein concentration of each sample, as per the manufacturer's instructions (Thermo Fisher Scientific, MA, USA). This assay relies on the reduction of $Cu^{2+}$ to $Cu^{+}$ by protein and the subsequent chelation of two BCA molecules to each $Cu^{+}$ ion. This causes BCA to change from green to purple, with an intensity proportional to the concentration of protein in the sample. Briefly, whole heart or cell lysates were diluted 1:100 in 50:1 BCA:$CuSO_4$ solution and incubated at 37$^{o}$C for 15 min with agitation, and colour intensity was subsequently measured using a FLUOstar Omega microplate reader (BMG Labtech, Bucks, UK). Sample protein concentrations were interpolated using a standard curve of known concentrations of bovine serum albumin (BSA) in lysis buffer.

Samples were subsequently prepared for standard sodium dodecyl sulphate-polyacrylamide gel electrophoresis (SDS-PAGE) to separate proteins according to their size. Specifically, 40 µg of protein per sample was diluted in lysis buffer (described in section 2.5.1) so all samples occupied the same volume. 4X NuPAGE® LDS Sample Buffer (Thermo Fisher Scientific, MA, USA) mixed with 5% β-mercaptoethanol was added and further diluted with lysis buffer to achieve a 1X solution. Samples were boiled at 80$^{o}$C for 10 min to reduce the disulphide bonds and denature the proteins. Prepared samples were either run immediately or stored at -20$^{o}$C until use.

NuPAGE SDS-PAGE 10% polyacrylamide pre-cast gels (Thermo Fisher Scientific, MA, USA) were mounted in a Criterion™ Vertical Electrophoresis Cell (Bio-Rad, Herts, UK) filled with running buffer (50 mM MOPS (3-(N-morpholino)propanesulfonic acid), 50 mM Tris Base, 0.1% SDS, 1 mM EDTA, pH 7.7). The first lane of each gel was loaded with 6µl molecular weight marker (Precision Plus Protein™ Dual Colour Standards, Bio-Rad, Herts, UK) and the remaining lanes were loaded with equal concentrations of protein, as described above. The chamber was kept on ice and the gel was run at 60 V for 10-15 min followed by 100 V for 2 h.

After electrophoresis, wet transfer was performed to capture all of the separated proteins on a membrane to permit interrogation of proteins of interest with antibodies. An Immobilon®-FL polyvinylidene difluoride (PVDF) transfer membrane (Merck, Darmstadt, Germany) was activated with 100% methanol for 1 min and rinsed with transfer buffer (25 mM Tris base, 200 mM glycine, 20% methanol, pH 8.3) prior to use. Transfer of proteins was performed by mounting a standard stack in a Mini Trans-Blot® Electrophoretic Transfer Cell (Bio-Rad, Herts, UK) filled with transfer buffer under gentle stirring. Caution was taken to remove all air bubbles during this process to ensure smooth protein transfer. The transfer was run at 100 V and 0.35 mA for 1 h and confirmed by either protein ladder transfer or staining with 0.1% Ponceau S Solution.

Membranes were blocked by incubation in 5% BSA/PBS supplemented with 0.05% Tween® 20 (BSA/PBS-T; 'blocking buffer') for 1 h at RT with gentle rocking. This was then replaced with the relevant primary antibody diluted in blocking buffer. Details of specific antibodies and their concentrations for each experiment are given in the relevant chapters. Primary antibodies were incubated with gentle rocking at 4$^{o}$C overnight.

After overnight incubation, the primary antibody was removed and replaced with an anti-alpha Tubulin antibody as a loading control, diluted 1:5000 in BSA/PBS-T and added for 1 h at RT with gentle rocking. Non-specifically bound and unbound antibody was removed with six 10 min washes with 0.05% PBS-T followed by addition of the appropriate secondary antibody at 1:5000 dilution in 50% PBS and 50% Odyssey® blocking buffer (LI-COR, Cambs, UK) for 1 h at RT with gentle rocking. Details of specific secondary antibodies used for each experiment are given in the relevant chapters, with green fluorescent secondary antibodies being used preferentially.

Finally, five 10 min washes in PBS-T were performed, followed by one wash in PBS. Membranes were imaged using the Odyssey® Infrared Imaging System (84 μm resolution, medium quality, red intensity 3.0, green intensity 6.0). Protein level was

analysed by densitometry using Image Studio™ version 5.0 for Windows (LI-COR, Cambs, UK), with the index protein being normalised to the loading control for each sample and expressed as arbitrary units (AU). All values are presented as mean AU±SEM.

## 2.6 Analysis of myocardial proteins by immunofluorescence

### 2.6.1 Preparation of frozen sections for immunofluorescence (IF-F)

Mouse hearts were extracted and manually perfused as described in section 2.5.1. The ventricles were isolated whilst submerged in ice-cold PBS and an approximately 2 $mm^3$ section dissected for further processing. This was placed in a Shandon™ Peel-A-Way disposable embedding mould, covered with optimal cutting temperature (OCT) cryoembedding matrix (both from Thermo Fisher Scientific, MA, USA) and flash frozen by submersion in isopentane (to avoid OCT cracking) in a liquid nitrogen bath. Frozen sections were stored at -80$^{o}$C until use.

Samples were then cut into 8 µm sections at −20°C in a microtome-cryostat (OTF 5030, Bright Instruments, Beds, UK; Figure 2-15). Specifically, OCT was used to mount samples on a sample stub and samples were then allowed to equilibrate to the cryostat chamber temperature. A microtome blade was mounted, and the height and angle adjusted to the sample. Samples were obtained by rotating a wheel mounted outside the chamber causing the mounted sample to pass over the microtome blade. Sections were kept flat using an anti-roll plate and subsequently transferred onto a glass microscope slide (VWR, Leics, UK).

Sections were immediately fixed with HistoChoice® for 20 min at RT followed by a single wash with ice-cold PBS. To keep reagents localised, a circle was drawn around each sample using a hydrophobic barrier pen (Vector Laboratories, Cambs, UK) and slides were either stored at -20$^{o}$C or immediately prepared for immunofluorescence, described in section 2.6.3.

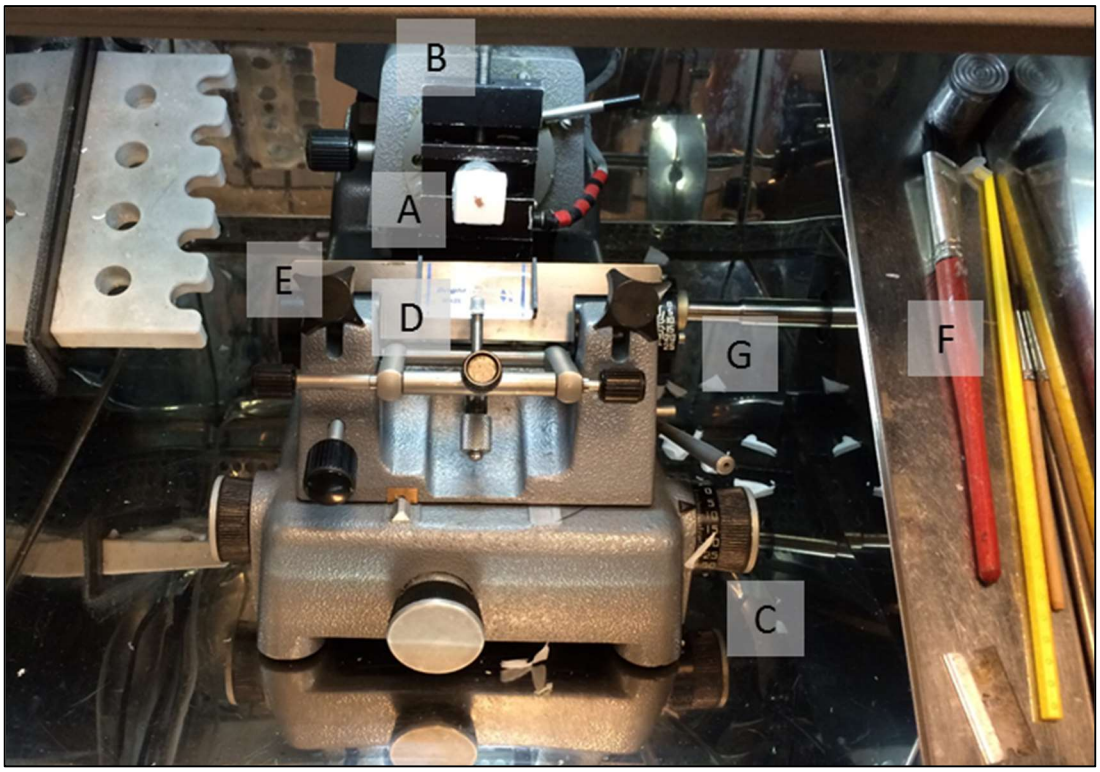


**Figure 2-15: Microtome-cryostat configuration**

Essential components of the microtome-cryostat are: (A) Tissue mounted in OCT and adhered to sample stub; (B) Screw to hold stub in place; (C) Section thickness control; (D) Anti-roll plate; (E) Screws to hold blade in place; (F) Tools kept in chamber to avoid melting samples; (G) Knife angle control.

Human right atrial appendage samples were collected by Dr A. Hamarneh (Hatter Cardiovascular Institute, UCL, UK) from patients with chronic stable angina undergoing cannulation for cardiopulmonary bypass for CABG. Patients with diabetes, impaired renal or ventricular function, dilated left atria, unstable angina, or a history of arrhythmias or on rhythm stabilising medications were excluded. After harvest, atrial appendage samples were placed in ice-cold, oxygenated modified Tyrode's buffer (NaCl 118.5 mM, KCL 4.8 mM, $NaHCO_3$ 24.8 mM, $KH_2PO_4$ 1.2 mM, $MgSO_4.7H_2O$ 1.44 mM, $CaCl_2.2H_2O$ 1.8 mM, glucose 10.0 mM, pyruvic acid 10 mM, pH 7.4) and transferred promptly to the Hatter Cardiovascular Institute. Atrial trabeculae measuring ≤1.2 mm in diameter and ≥2.0 mm in length were carefully dissected whilst submerged in ice-cold modified Tyrode's buffer by Dr D. He (Hatter Cardiovascular Institute, UCL, UK) and subsequently prepared as described above.

### 2.6.2 Preparation of isolated cardiomyocytes for immunofluorescence (IF-C)

Cardiomyocytes were isolated as described in section 2.5.2 and subsequently prepared for immunofluorescence. Briefly, 22 mm cover slips (VWR, Leics, UK) were placed in sterile 6-well tissue culture plate wells and coated with 200 µl laminin/well. Reagents were applied to each well in a volume of 500 µl. After 1 h incubation, cells were fixed with HistoChoice® for 20 min at RT, then given three 5 min washes with ice-cold PBS. Cells were permeablised with 0.3% Triton non-ionic surfactant on ice for 10 min and subsequently analysed by immunofluorescence, described in section 2.6.3.

### 2.6.3 Immunofluorescence protocol

5 min washes with PBS were applied between every step of this immunofluorescence protocol. First, non-specific antibody binding was blocked by the addition of 5% BSA in PBS (BSA/PBS) for 1 h at RT. Samples were then incubated in primary antibody diluted in 1% BSA at 4°C overnight. Pre-adsorbed anti-rabbit secondary antibodies conjugated to Alexa Fluor 488 or 555 were diluted in 1% BSA/PBS and added to samples for 1 h at RT. 0.1 µg/ml Hoechst nuclear stain (Life Technologies, Renf, UK) was added with the secondary antibodies to all sections. Cover slips were mounted on glass microscope slides using fluorescence mounting medium (Dako, Cambs, UK). Samples were allowed to dry in the dark overnight.

Preparation of control sections was as described above, with incubation in either 1% BSA/PBS only (unstained control) or with the relevant secondary antibody in the absence of any primary antibody. Control experiments were performed to confirm the absence of fluorescence bleed-through or non-specific staining with secondary antibodies alone. After drying, fluorescence was imaged using a 40× oil immersion objective by sequential scanning using the 405 nm, 488 nm, 543 nm and/or 633 nm lines of a Leica SP5 confocal microscope, as appropriate, and by collecting emitted light at 410-470 nm, 500-530 nm, 580-650 nm and 640-710 nm, respectively.

## 2.7 Analysis of myocardial messenger RNA levels

### 2.7.1 Extraction of RNA

Care was taken throughout to avoid contamination of samples with ribonucleases (RNases). All tools and pipettes were cleaned prior to use and between samples, and gloves, sterile filter tips and disposable plasticware were used throughout. The whole procedure was performed at RT and as quickly as possible to prevent degradation of RNA.

RNA was extracted using a dedicated kit according to the manufacturer's instructions (RNeasy, Qiagen, Lancs, UK). Briefly, hearts were extracted as described in section 2.5.1, and a 20-30 mg section of the LV promptly isolated, washed and immersed in 600 µl RLT buffer with 1% β-mercaptoethanol. RLT buffer contains guanidine thiocyanate to denature RNases and β-mercaptoethanol reduces protein disulphide bonds. Samples were simultaneously disrupted and homogenised by sonication for 10 sec (130 W, 20 kHz, Vibra-Cell, Sonics and Materials, CT, USA) and the lysate was subsequently centrifuged for 3 min at 20,800 g to remove any undigested tissue. The supernatant was removed and mixed with a matching volume of 70% ethanol to facilitate selective membrane binding. Samples were transferred to a RNeasy spin column containing a silica-based membrane that binds the RNA in the sample prior to washing and elution into water. The protocol is outlined in Table 2-5.

RNA was quantified, and its purity measured, using an Lvis reader in a FLUOstar Omega plate reader (BMG Labtech, Germany), where 1 unit of absorbance at 260 nm corresponds to 44 µg/ml of RNA. The purity of each sample with respect to protein contamination was measured using the $OD_{260/280}$ ratio and found to be 1.97±0.01 for all samples, where a ratio of 1.8-2.0 indicates good quality RNA.[230] Purified RNA was either immediately subject to reverse transcriptase PCR (described below) or stored at -20$^{o}$C until use.

| Buffer | Centrifugation speed and duration | Description |
|---|---|---|
| RLT | 10,000 g for 15 s, discard flow-through | Denature RNases |
| RW1 700 µl | 10,000 g for 15 s, discard flow-through | Wash |
| RPE 500 µl | 10,000 g for 15 s, discard flow-through | Wash |
| RPE 500 µl | 10,000 g for 2 min, discard flow-through | Wash |
| Change collection micro-centrifuge tube | | |
| RNAase-free water 50 µl | 10,000 g for 1 min, keep flow-through | Elute |
| RNAase-free water 50 µl | 10,000 g for 1 min, keep flow-through | Elute |

**Table 2-5: RNA extraction protocol**

RNA extraction was performed using a RNeasy kit (Qiagen, Lancs, UK) according to the protocol provided here.

### 2.7.2 Reverse transcriptase polymerase chain reaction protocol

250 ng RNA was converted to first-strand cDNA using the AffinityScript cDNA Synthesis kit (Agilent Technologies, Ches, UK), as per the manufacturer's instructions. A master-mix was prepared in a micro-centrifuge tube, as per Table 2-6.

| Reagent | Volume per sample (µl) |
|---|---|
| RNase-free water | 20 |
| cDNA synthesis master mix (2X) | 10 |
| Oligo(dT) primer | 3 |
| AffinityScript reverse transcriptase/RNase block | 1 |
| Template mRNA | Variable |
| Total volume per sample (µl) | 34 + template mRNA volume |

**Table 2-6: cDNA synthesis reaction mix**

A master mix was prepared on ice according to Agilent Technologies' (Ches, UK) guidelines and in the composition and order given here. The volume of master mix accounting for 10% extra PCR assays than required and a negative control (without template DNA) was made for each experiment. Template mRNA was added to each PCR tube prior to placement in a thermal cycler. The cDNA synthesis master mix contains $MgCl_2$ and dNTPs.

First strand cDNA synthesis PCR was subsequently performed using a thermal cycler (PTC 200 Thermal Cycler, MJ Research, Quebec, Canada) according to the protocol given in Table 2-7.

| PCR stage | Temperature and duration | Description |
|---|---|---|
| 1 | 25$^{o}$C for 5 min | Primer annealing |
| 2 | 45$^{o}$C for 25 min | cDNA synthesis |
| 3 | 95$^{o}$C for 5 min | Terminate reaction |

**Table 2-7: cDNA synthesis PCR thermocycling protocol**

cDNA synthesis PCR was performed using a thermal cycler (PTC 200 Thermal Cycler, MJ Research, Quebec, Canada).

Completed reactions were then placed on ice or frozen at -20$^{o}$C prior to quantitative polymerase chain reaction (QPCR).

### 2.7.3 Quantitative polymerase chain reaction

QPCR allows real-time quantification of PCR product using a dye that fluoresces when non-specifically bound to the minor groove of double stranded DNA (dsDNA). During the annealing phase of PCR, primers bind to the target sequence and elongate to produce dsDNA, to which SYBR® Green is able to bind and fluoresce. As cDNA is amplified over successive cycles the signal intensity increases accordingly to a maximum dictated by the amount of template cDNA in the sample.

The QPCR reaction was prepared according to guidelines from Agilent Technologies (Ches, UK). Specifically, 12.5 µl of 2X Brilliant II SYBR® Green QPCR Master Mix, which contains *Taq* DNA polymerase and 2.5 mM (at 1X concentration) $MgCl_2$, was mixed with 1 µl each of forward and reverse primer, 8 µl nuclease-free water and 2.5 µl template cDNA per reaction (in that order and on ice). The specific primer sequences used in these experiments were obtained from the literature in the case of CXCR4,[231] and were already established by our own laboratory in the case of glyceraldehyde 3-phosphate dehydrogenase (GAPDH) and hypoxanthine guanine phosphoribosyl transferase (HPRT). Primers were purchased from Eurofins Genomics (Ebersberg, Germany) (described in Table 2-8) and were diluted to 2 pmol/µl in autoclaved distilled water on arrival. GAPDH and HPRT were included as constitutively expressed genes that served as a positive control in QPCR experiments.

| Primer | Sequence (5'→3') | Properties | |
|---|---|---|---|
| | | Length | $T_m$ ($^oC$) |
| GAPDH forward | AGGTCGGTGTGAACGGATTTG | 21 | 59.8 |
| GAPDH reverse | TGTAGACCATGTAGTTGAGGTCA | 23 | 58.9 |
| HPRT forward | TCAGTCAACGGGGGACATAAA | 21 | 57.9 |
| HPRT reverse | GGGGCTGTACTGCTTAACCAG | 21 | 61.8 |
| CXCR4 forward | TCAGTGGCTGACCTCCTCTT | 20 | 59.4 |
| CXCR4 reverse | CTTGGCCTTTGACTGTTGGT | 20 | 57.3 |

**Table 2-8: QPCR primer sequences**

PCR primer sequences, length and melting temperature ($T_m$).

After gentle mixing and brief centrifugation, samples were placed in a spectrofluorometric thermal cycler (CFX Connect™ Real-Time PCR Detection System, Bio-Rad, Herts, UK) and run according to the two-step protocol given in Table 2-9.

A representative amplification plot, showing increasing fluorescence over time, is given in Figure 2-16, Panel A. The quantity of template cDNA can be ascertained according to a threshold cycle (Ct), defined automatically as the PCR cycle number where SYBR® Green fluorescence is significantly higher than background, and is inversely proportional to the log of the initial number of cDNA copies.[232] Therefore, the higher the amount of template cDNA in the sample, the quicker the threshold cycle will be reached. Results were normalised to two reference genes (GAPDH and HPRT) as internal controls using double delta Ct analysis.[233] Double delta Ct analysis calculates the difference between reference and experimental cDNA Ct values for experimental and control samples. As the quantity of cDNA doubles with consecutive cycles, expression fold change is calculated according to $2^{-\Delta\Delta Ct}$.

| PCR stage | Temperature and duration | Description |
|---|---|---|
| 1 | 95$^{o}$C for 10 min | Hot start |
| **Then 40 cycles:** | | |
| 2 | 95$^{o}$C for 30 sec | DNA denaturing |
| 3 | 60$^{o}$C for 1 min | Primer annealing |
| 4 | 72$^{o}$C for 30 sec | DNA synthesis |
| **Followed by:** | | |
| 5 | 65$^{o}$C for 5 sec increasing at 0.2$^{o}$C/sec to a maximum of 95$^{o}$C | Melt curve |
| **Followed by 4$^{o}$C until collection** | | |

**Table 2-9: QPCR thermocycling protocol**

QPCR was performed using a CFX Connect™ Real-Time PCR Detection System (Bio-Rad, Herts, UK). The initial incubation ('hot start') activates *Taq* DNA polymerase.

To confirm that observed signal was due to template cDNA accumulation rather than non-specific dsDNA (from contamination or primer dimers, for example) a dissociation (melt) curve was generated for all reactions (demonstrated in Figure 2-16, Panel B). Based on the premise that non-specific dsDNA products have a lower $T_m$, samples were gradually heated to 95$^{o}$C and loss of fluorescence due to SYBR® Green dissociation was plotted against temperature. Signal from primer dimers could then be identified by comparison to a control reaction lacking template cDNA.

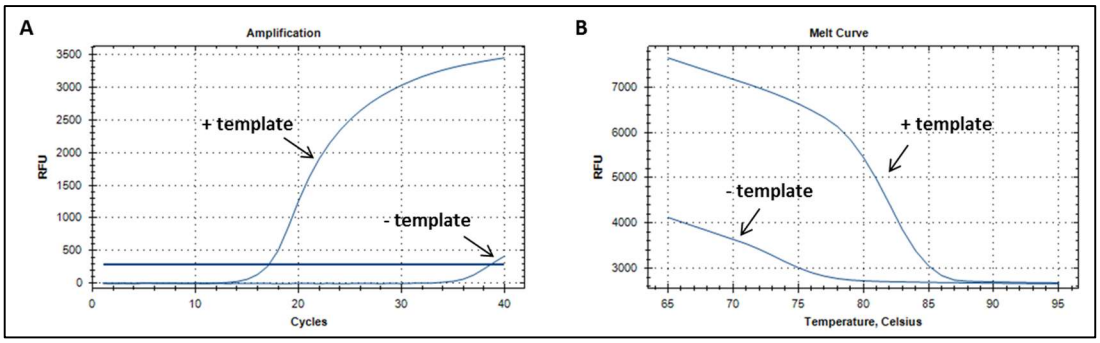


**Figure 2-16: Representative QPCR amplification plot (Panel A) and dissociation curve (Panel B)**

Panel A demonstrates a representative amplification plot, showing relative fluorescence units (RFU) against cycle number. Here, a sample including template cDNA reaches the threshold cycle after approximately 17 cycles whilst a sample without template cDNA takes approximately 38 cycles. Panel B demonstrates a representative melt curve, whereby fluorescence is lost at a lower $T_m$ in a sample without template.

Upon completion of the reaction, the PRC products were separated using 2% agarose gel electrophoresis, as described in section 2.3. This verified that a single product was created for each reaction (with no amplification of non-specific dsDNA), that the band size was correct and that the relative band intensity correlated with the Ct value obtained from QPCR. A representative image is given in Figure 2-17. During this process, every effort was made to prevent cross-contamination of pre-amplification samples with amplified cDNA.

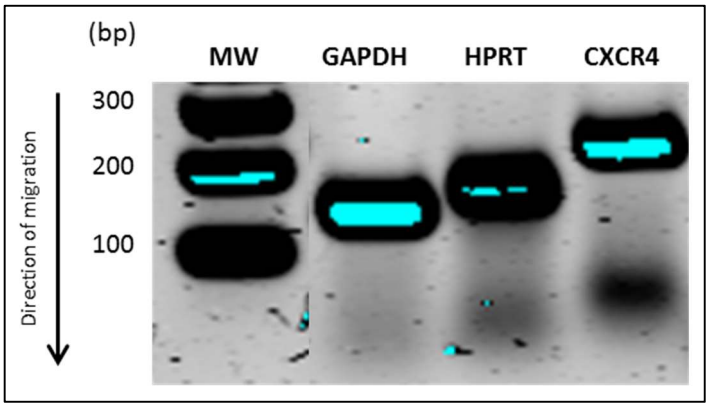


**Figure 2-17: Representative gel electrophoresis showing products of QPCR**

RNA was extracted from WT C57BL/6N mice and converted to cDNA as described. QPCR was performed using primers for GAPDH, HPRT and CXCR4 messenger RNA, which were confirmed to have product sizes of 123 bp, 148 bp and 203 bp, respectively.

## 2.8 Analysis of SDF-1α by ELISA

The characterisation and validation of this ELISA is described in detail in section 7.3. Briefly, blood samples were collected and prepared as described in section 2.4.4. Flat bottom, clear, 96-well plates (R&D Systems, Oxon, UK) were coated with either 5 µg/ml human IgG bivalent anti-SDF-1α mini-antibodies to detect full-length SDF-1α (HCI.SDF1α, AbD Serotec, Oxon, UK), or 9 µg/ml of a commercially available monoclonal mouse IgG against mouse and human SDF-1α (MAB350, R&D Systems, Oxon, UK) in 0.2M anhydrous sodium carbonate-sodium bicarbonate buffer at 4$^{o}$C overnight. Wells were washed three times for 5 min with 0.05% PBS-T before blocking with 5% BSA/PBS-T for 1 h at RT. After three further 5 min washes with PBS-T, 100 µl of sample was added to each well and allowed to incubate for 2 h at RT. Standard samples were prepared using known concentrations of recombinant human (rh)-SDF-1α (R&D Systems, Oxon, UK), starting at 10,000 pg/ml with twofold dilution steps (range 156-10,000 pg/ml) in a diluent augmented with mammalian serum proteins (BUF037A, AbD Serotec, Oxon, UK). All standards and samples were measured in triplicate. Samples and standards were incubated for 2 h at RT. After three 5 min washes with PBS-T, 0.4 µg/ml of biotinylated polyclonal goat IgG against human and mouse SDF-1α (BAF310, R&D Systems, Oxon, UK) was added to each well for a further 1 h at RT. Following incubation, wells were washed a further three 5 min with PBS-T. The biotin tag was detected with 1:200 of streptavidin conjugated to horseradish peroxidise (streptavidin-HRP; R&D Systems, Oxon, UK) in Hispec buffer (AbD Serotec, Oxon, UK), which was incubated with the detection antibody for 20 min in the dark at RT. After five 5 min washes with PBS-T, 100 µl of Substrate Solution, composed of a 1:1 mix of hydrogen peroxide ($H_2O_2$) and tetramethylbenzidine (R&D Systems, Oxon, UK), was added and incubated for a further 20 min, in the dark at RT. Without further washes, 50 µl of 2N sulfuric acid (Sigma-Aldrich, Dorset, UK) was added per well to halt the oxidation reaction, and turn the solution yellow. Colour intensity was measured using a FLUOstar Omega microplate reader set to 450 nm and 20 flashes per well.

## 2.9 Experiments in humans

Human studies received Local Research Ethics Committee approval (12/0448) and were carried out at the Hatter Cardiovascular Institute (UCL, UK) in accordance with the University College Hospitals London Hospitals NHS Trust guidelines. All experiments were performed on healthy volunteers, all of whom were provided with a Patient Information Sheet and a verbal explanation of the study, in line with Good Clinical Practice guidelines. All patients provided written informed consent and were free to withdraw from the study at any time.

### 2.9.1 Remote ischaemic conditioning

In humans, RIC consisting of three cycles of 5 min right upper limb ischaemia and 5 min reperfusion was applied by inflation of a manual sphygmomanometer to a pressure of 200 mmHg. Ischaemia was confirmed by the absence of a pulse, pallor and paraesthesia. Blood samples were collected into citrated tubes at baseline and after the final 5 min of reperfusion via ipsilateral antecubital fossa venepuncture using a 21G x 1.5" Microlance needle and Vacutainer™ system (BD, Oxon, UK). Samples were collected into citrated tubes (BD, Oxon, UK) on ice and immediately supplemented with Sitagliptin to inhibit DPP4 and prevent degradation of full-length SDF-1α during sample preparation,[52] to give a final concentration of 50 µM. Samples were immediately prepared as described in section 2.4.4.

### 2.9.2 Analysis of platelet-expressed SDF-1α by flow cytometry

Blood was collected as described above and fixed immediately by diluting 1:20 in PBS containing 0.1% BSA and 1% paraformaldehyde (PFA) for 10 min at RT. A 10 µl aliquot of each sample was added to 500 µl PBS/0.1% BSA and incubated with 1:100 primary antibody (HCI.SDF1α) overnight, rotating at 4$^{o}$C. Control samples were prepared in the same way but without the addition of HCI.SDF1α. Samples were washed (x3) by spinning at 10,000 g for 10 min to aggregate platelets, removing the supernatant and re-suspending in 500 µl PBS/0.1% BSA. Samples were subsequently incubated for 2 h at RT with 1:1000 phycoerythrin-cyanine dye (PE-Cy5) mouse anti-human CD41 (BD Pharmingen, Oxon, UK) to identify platelets and 1:400 goat anti-human IgG Fab-

fluorescein isothiocyanate (FITC, AbD Serotec, Oxon, UK) to detect HCI.SDF1α. Control samples were incubated with PE-Cy5 mouse anti-human CD41 and goat anti-human IgG Fab-FITC alone and in combination, or with no secondary antibody. A further sample was incubated in HCI.SDF1α as described and subsequently stained with PE-Cy5 mouse anti-human CD41 only to exclude cross-reactivity.

Blood platelet count ($x10^9$/L) was determined by flow cytometry using double-gated events according to forward light scatter (height; FSC-H), with a trigger threshold of 25,000 to exclude debris, and PE-Cy5 fluorescence (FL3 channel, >670 nm), as per published protocols (BD Accuri™ C6 Flow Cytometer, BD Biosciences, Oxon, UK).[234] Positive PE-Cy5 fluorescence was set at 5000 AU, based on precedent in our laboratory. The count was multiplied by 1000 to account for the final dilution of the blood sample, and all samples were measured in duplicate. Platelets expressing SDF-1α were quantified by selecting the platelet population as described here, and further gating them according to FITC fluorescence (FL1 channel, 533/30 nm). Positive FITC fluorescence was set at 5000 AU.

## 2.10 Statistics

All analyses were performed using GraphPad Prism® version 5.00 for Windows (CA, USA). The specific statistical test used is reported next to each result.

**Comparison of means:** The statistical test used to compare group means was contingent on the nature of the data being analysed. An unpaired t-test was used for two independent groups of continuous variables and a one-way analysis of variance (ANOVA) with Tukey's multiple comparison test for three or more independent groups. For dependent observations, a paired t-test was used in the case of two groups and a two-way ANOVA with Bonferroni correction for multiple comparisons in the case of three or more.

Data is presented as mean ± standard error of the mean (SEM). Statistical significance was reported if $P<0.05$ using the following nomenclature: *$P<0.05$, **$P<0.01$ and

***P<0.001. Results where P>0.05 were reported as non-significant (NS). Statistical significance is presented alongside all statistical analyses.

**Regression:** For both SDF-1α and macrophage inhibitory factor (MIF) assays, sample and standard values were baseline corrected and transformed to a logarithmic scale (X=log[X]). Full-length SDF-1α assay values were interpolated from linear regression of the standard curve. All other standard curves were evaluated with nonlinear regression using log(agonist) versus response. Results were transformed according to $X=10^X$ and the data interpreted as described above.

**Sample size:** Sample size calculations were used to estimate the minimum necessary sample size for *in vivo* experiments, except where specifically indicated. The assumptions regarding effect size upon which these calculations are based are outlined in the relevant sections. For all power calculations a Gaussian distribution was assumed, as discussed below, and a significance level of 5% (α=0.05) and 80% power (β=0.2) were used. Sample sizes are presented alongside all statistical analyses in the graph bars and/or the figure legend.

**Normality:** The (parametric) statistical tests described above assume the data come from a Gaussian (normal) distribution. However, confirming this with statistical tests of normality (the D'Agostino-Pearson omnibus test, for example) is precluded by the small sample sizes. If a parametric test is applied to non-Gaussian data, the results are meaningless, especially when the sample size is small.[235] However, non-parametric statistical tests have significantly lower power and require much larger sample sizes. This is problematic in the context of a reductionist approach to animal experimentation. Therefore, data were assumed to be normally distributed throughout this thesis. This is discussed further in section 6.3.

# Chapter 3 Remote ischaemic conditioning in *in vivo* models of ischaemia-reperfusion injury: A systematic review and meta-analysis

This chapter is derived from a manuscript that was jointly first authored with Mr J. Pickard. The statistical method was co-designed with Dr X. Rossello and executed in its entirety by him. Mr N. Burke and Dr O. Ziff collected the data for analysis of study quality. The study was conceived and the manuscript written by Dr D. Bromage. All contributors were from the Hatter Cardiovascular Institute (UCL, UK).

## 3.1 Introduction

To investigate RIC it is first necessary to establish a valid experimental model. As will be discussed in Chapter 4, this requires a model that provides the best chance of demonstrating protection (reduction of IS) by RIC. To achieve this requires a critical evaluation of the literature and, in particular, what experimental factors might influence the generation of a reproducible IS and demonstrable cardioprotection with RIC.

Furthermore, as discussed in 0, the efficacy of RIC at ameliorating myocardial IRI in patients has been called into question by the neutral results of ERICCA and RIP-HEART. As a result of the recent neutral clinical trials discussed in 0, there is renewed interest in the pre-clinical evidence base and potential impediments to successful translation.[236, 237] The difficulty in translating RIC to the clinic may be attributed to several factors: (1) the animal models used in basic studies may not reflect the complex risk factor and comorbidity profile of humans with cardiovascular disease.[238, 239] Indeed, several such comorbidities have been shown to abrogate the beneficial effect of RIC, including age and diabetes;[240] (2) adjunctive medication and techniques administered to patients during cardiac surgery or treatment for MI (nitrites, volatile anaesthetics, cardioplegia, anticoagulants and opioids, for example) may confer cardioprotection such that RIC has no added potential,[241-247] or interfere with RIC development;[248] (3) the degree of IRI may be too small in cardiac surgery (or even STEMI) to be conducible to benefit from RIC or would require an enormous sample size to be proven; (4) unlike direct ischaemic conditioning, systematic pre-

clinical characterisation of the optimal RIC stimulus is lacking.[249] Consequently, optimal clinical study design is complicated by inconsistent experimental conditions used in basic *in vivo* RIC studies in animals. For example, in direct ischaemic conditioning, the number of cycles and the interval between the conditioning stimulus and index ischaemia are demonstrably important,[102] but only a limited number of studies have investigated these factors in RIC; and (5) study quality and small study publication bias have also been shown to result in over-estimation of effect size and are consequently implicated as confounders in the translation of interventions that are cardioprotective in pre-clinical studies.[237, 250]

This chapter therefore aims to describe an analysis of the existing literature relating to RIC to both inform the development of an *in vivo* model of RIC and investigate potential reasons for the neutral results of large outcome studies.

## 3.2 Research aims and objectives

The main objective of this chapter was to perform a systematic review and meta-analysis of experimental variables in *in vivo* models of RIC. The research aims for this objective were:

1. Perform a systematic review of studies of RIC in *in vivo* models of myocardial IRI;
2. Perform a meta-analysis of studies of RIC in *in vivo* models of myocardial IRI.

## 3.3 Aim 1: Perform a systematic review of studies of remote ischaemic conditioning in *in vivo* models of myocardial ischaemia-reperfusion injury

### 3.3.1 Background

Systematic reviews are indispensable tools for collating existing literature on a topic in a reproducible and accountable way. They are defined as an attempt to summarise all the empirical evidence according to pre-specified eligibility criteria to address a specific question, and can provide the basis for meta-analysis and facilitate conclusions that can inform clinical study design and practice.[251] Despite this, systematic reviews are frequently poorly performed and reported, to which end the

Preferred Reporting Items for Systematic reviews and Meta-Analyses (PRISMA) guidelines have been developed.[251] These guidelines encourage the use of unambiguous (systematic) methods that minimise the risk of bias and support firm conclusions. These guidelines are used here to scrutinise pre-clinical studies of RIC in *in vivo* animal models of myocardial IRI.

### 3.3.2 Methods

A systematic review was performed, and is reported here, in accordance with PRISMA guidelines and all data sources, eligibility criteria, data extraction and data synthesis methods were pre-defined.[251] A literature search was conducted on 21st August, 2015. Keywords and MeSH terms were used to search Medline and Embase (via OVID) between 1997 and present, and further studies were identified by consultation with experts in the field.

The search strategy was defined in an iterative manner, using previously published guidelines,[252-254] and peer reviewed by members of the Hatter Cardiovascular Institute research group. The following search strategy was used, incorporating keywords and MeSH terms, for MEDLINE:

1. (remote adj2 $condition$).mp.
2. (remote adj isch$emic).mp.
3. remote precondition$.mp.
4. remote postcondition$.mp.
5. remote percondition$.mp.
6. limb $condition$.mp.
7. ripc.mp.
8. limb isch$emi$.mp.
9. $condition$.mp.
10. 8 and 9
11. 1 or 2 or 3 or 4 or 5 or 6 or 7 or 10
12. exp Reperfusion Injury/
13. exp Myocardial Ischemia/
14. Myocardial Infarction/
15. infarct size.mp.
16. ("infarct size" or "size of infarct*").mp.

17. cardioprotection.mp.
18. 12 or 13 or 14 or 15 or 16 or 17
19. 11 and 18
20. Limit 19 to animal
21. Limit 20 to (english language and yr="1997-Current")
22. Limit 21 to review articles
23. 21 not 22

Differences in the search strategy between Medline and Embase are described in Table 3-1.

| **Search term** | **Database** | |
|---|---|---|
| | **Medline** | **Embase** |
| Cardioprotection | cardioprotection.mp. (keyword) | heart protection/(MeSH term) |
| Search review articles | limit 21 to review articles | limit 21 to "reviews (maximizes sensitivity)" |

**Table 3-1: Differences in search strategy between databases**

A combination of keywords and MeSH terms were used to search Medline and Embase (via OVID) between 1997 and present with differences in search terms given here.

Study eligibility criteria were defined using the PICOS (Population, Intervention, Comparison, Outcome, Study design) approach.[255] *In vivo* animal studies were included and were eligible if they investigated the effect of limb RIC (pre-, per- or post-) versus a control (sham procedure or no treatment) on myocardial IS, as measured by TTC,[256] in any mammalian species, regardless of study design. Transient infra-renal aortic occlusion was considered as bilateral hind limb ischaemia.

Studies were excluded if they did not include or report absolute myocardial IS as a percentage of AAR, defined as the myocardial tissue within the vascular territory distal to the occluded artery that, if not reperfused, is at risk of irreversible ischaemic

death.[257] The AAR varies depending on the exact position of the LAD suture and variable LAD anatomy. IS has a strong positive correlation with AAR and therefore, without correction, a small AAR could create false-positive results for cardioprotection, and vice versa.[258] Furthermore, studies were excluded if they specifically investigated only the 'second window' of cardioprotection (RIC to infarction interval >1 h),[259-261] if the animals had co-morbidities, if IS was only measured using a method other than TTC, or if they were investigating the impact of RIC in the context of heart transplant. Groups in which RIC was administered in combination with another conditioning protocol (local conditioning, for example), or with pharmacological treatments known to have cardioprotective effects, were excluded.

The search was limited to reports available in English due to limited time and financial resources for translation, and a publication date restriction of 1997-present was imposed in view of the first publication of the efficacy of RIC in the limb.[165] Review articles, unpublished material and ongoing studies were excluded.

Duplicate reports were excluded using Endnote for Windows (Thomas Reuters, PA, USA). Retrieved records were initially screened for eligibility using their title and abstract. Eligibility assessment was performed in an un-blinded, standardised manner by two assessors. To ensure reliability and improve the objectivity of screening, the assessors independently screened a randomly selected 10% sample of the search results. The exercise was repeated until 90% agreement was achieved, before screening all search results. During the title and abstract screening calibration exercise inter-rater agreement was 94%. Disagreements between reviewers were resolved by examining the full text of the article or by consensus in all cases.

Next, the full text of all eligible records was retrieved and subjected to a second stage of eligibility screening in an independent, un-blinded, standardised way by two assessors. Overall, inter-rater agreement was 87%. The 13% of references upon which the assessors disagreed were accounted for by screening errors rather than

fundamental disagreement about the features of the study and disagreements were resolved by consensus in all cases.

| Category | Data item |
|---|---|
| **Study details** | First author, senior author, date, report format (abstract/full), country of origin |
| **Populations/subjects (P)** | Species, strain, age/weight |
| **Interventions (I)** | Pre-/per-/post-conditioning, RIC cycle time, RIC number of cycles, number of limbs, RIC technique (cuff/clamp), time to index ischaemia, index ischaemic duration, coronary territory occluded, reperfusion duration, non-recovery versus recovery, anaesthetic type, anaesthetic dose (mg/kg), other peri-operative medication, use of anti-coagulant, type of anti-coagulant, intubated/ventilated, supplementary oxygen |
| **Outcomes (O)** | IS as primary endpoint, mean IS (%AAR), mean AAR, AAR technique, standard deviation, SEM, other reported statistical analyses (pertinent to infarct) |
| **Study design (S)** | Sample size |

**Table 3-2: Data items used for data extraction were developed using the PICOS approach**

Data items were selected according to their recognised effect on myocardial IRI, or their reported or potential impact on the efficacy of RIC.

Experimental variables for which data were sought were developed using the PICOS approach.[255] Data items were chosen if they had an evidence-based effect on myocardial IRI, or a reported or potential impact on the efficacy of RIC. These

included species and strain, gender, choice of anaesthetic and duration of ischaemia and reperfusion. A full list of data items is given in Table 3-2. Prior to formal data extraction, the following assumptions were made:

- When a report described 'femoral artery occlusion' it was assumed to be with a vascular clamp. Likewise, where hind limb occlusion was reported, the use of an external cuff or tourniquet was assumed. A cuff was defined as an external inflatable device, while a tourniquet described any other kind of external compression. In all cases it was assumed that the cuff was inflated to an appropriate pressure.
- Any reperfusion duration ≤4 h was assumed to be non-recovery and anything over that to be a recovery model.
- An interval >1hr from the last RIC cycle to the onset of index ischaemia was defined as the 'second window' of protection. This study was concerned with the acute cardioprotective potential of RIC, thus these studies were excluded from the analysis.
- Descriptions of the LAD and left coronary artery were assumed to be interchangeable in rodents.
- If the study did not mention whether supplementary oxygen was used, it was assumed the animal was ventilated with room air.

A data extraction sheet was developed based on the Cochrane Consumers and Communications Review Group's data extraction template,[262] which was pilot-tested on ten randomly-selected included studies, and refined accordingly. Data was independently extracted by two reviewers using predefined data fields, including study quality indicators. To ensure reliability and improve subjectivity of data extraction, a similar calibration exercise as described above was performed. Disagreements were resolved by consensus in all cases.

Following data extraction, searches were conducted according to first and senior author name, sample size and size of outcome to identify double counting. These parameters were chosen due to expected high completeness and based on recommendations in the PRISMA statement.[251] If multiple reports for the same study were identified they were compared for logical inconsistencies, which were subsequently accounted for by contacting the report author by e-mail. Attempts were made to acquire key missing information in the same way.

Study quality was assessed using a component approach based on the study report, using the ARRIVE guidelines and a 12-item quality score.[263-265] This approach is based on a recent meta-analysis of ciclosporin.[146] The 12-item quality score was adapted from a 10-item quality score developed by Macleod *et al.* in response to a perceived failure of translation of promising neuro-protective agents in stroke,[263-265] by removing two and adding four items (described in Table 3-3), resulting in a custom 12-item quality score that was applied to all full studies in the meta-analysis. Abstracts were not subject to quality assessment due to their brevity. Study quality was assessed independently from data extraction and between assessors in an un-blinded, standardised manner by two reviewers. Disagreements were resolved by consensus in all cases. It was assumed in this analysis that, if the monitoring of ST segments or rhythm was reported, heart rate monitoring was available.

| **Added to Cochrane study quality score** | **Removed from Cochrane study quality score** |
|---|---|
| Statement of measurement of $P_aO_2$ and $S_aO_2$ | Use of animals with co-morbidities |
| Statement of recording of ECG | Blinded induction of ischaemia |
| Statement of measurement of blood pressure | |
| Blinded application of conditioning protocol | |

**Table 3-3: Items removed and added from the Cochrane study quality score to make the adapted score used in the study**

A published quality score was adapted to be appropriate for *in vivo* studies of cardioprotection by RIC against myocardial IRI.

### 3.3.3 Results

The systematic review returned 539 records, including 169 duplicate reports. 370 reports underwent title and abstract screening, which resulted in 256 exclusions. The remaining 114 reports were retrieved for detailed full text evaluation. 71 articles

were excluded, 57 due to failing to meet the inclusion criteria, 12 were duplicate reports of identical studies published in separate journals, and two were not retrievable. Of the remaining 43 reports (studies), nine were missing data on one or more important experimental variables that we were unable to retrieve by contacting the study authors, and were consequently excluded. The remaining 34 studies were included in the quantitative synthesis (Figure 3-1).

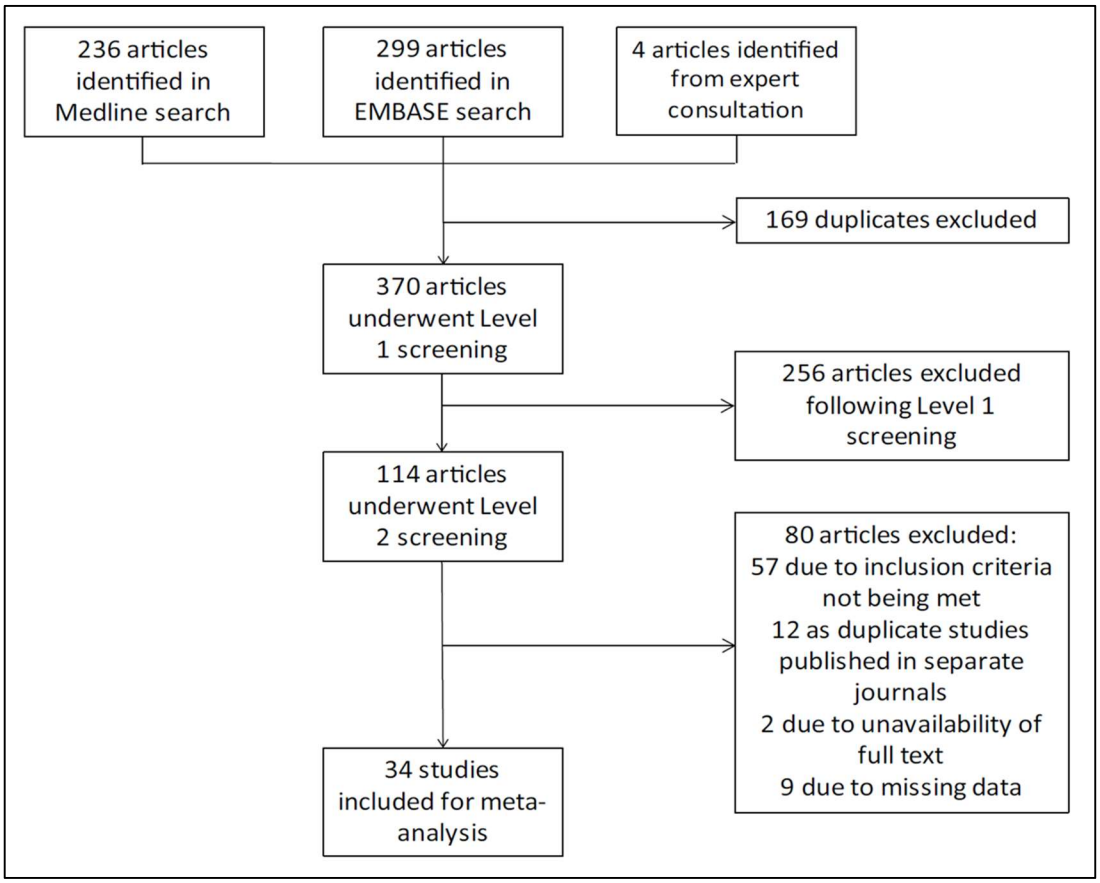


**Figure 3-1: Flow chart of the study selection process**

A systematic review yielded 539 reports. After removal of duplicates and the application of inclusion and exclusion criteria, 34 studies were included in the meta-analysis.

All included studies and their main characteristics are described in Table 3-4.

| Study reference | Species | Gender | Age or weight | Conditioning protocol | RIC cycle duration (min) | RIC reperfusion duration (min) | Number of cycles | Number of limbs | Total RIC ischaemia duration (min) | RIC occlusion technique | RIC-index ischaemia interval (min) | Index ischaemia duration (min) | Coronary artery occluded | Reperfusion duration (min) | Recovery or non-recovery | Supplementary oxygen | Induction anaesthetic | Anticoagulants | Measure of variance | Control group sample size | Control group mean IS/AAR | Control group variance (IS/AAR) | Conditioning group sample size | Conditioning group mean IS/AAR | Conditioning group variance (IS/AAR) |
|---|---|---|---|---|---|---|---|---|---|---|---|---|---|---|---|---|---|---|---|---|---|---|---|---|---|
| [266] | Pig | M | 25-30kg | Per | 5 | 5 | 4 | 1 | 20 | Clamp | N/A | 40 | LAD | 120 | NR | Y | Propofol, fentanyl | N | SEM | 10 | 59.2 | 3.17 | 7 | 36.5 | 4.7 |
| [166] | Pig | M/F | 18-22kg | Post | 5 | 5 | 4 | 1 | 20 | Cuff | N/A | 90 | LAD | 4320 | R | Y | Ketamine | Heparin | SEM | 12 | 48.4 | 5.2 | 12 | 23 | 2.4 |
| [267] | Rat | M | N/R | Pre | 15 | 10 | 1 | 2 | 30 | Clamp | 10 | 30 | LAD | 120 | NR | N | Pentobarbitone | N | SD | 8 | 46 | 7 | 10 | 19 | 5 |
| | Rat | M | N/R | Per | 15 | N/A | 1 | 2 | 30 | Clamp | N/A | 30 | LAD | 120 | NR | N | Pentobarbitone | N | SD | | | | 10 | 21 | 7 |
| [268] | Rat | M | Adult | Pre | 15 | N/A | 1 | 2 | 30 | Clamp | 10 | 30 | LAD | 120 | NR | N | Pentobarbitone | N | SEM | 8 | 41 | 2 | 12 | 19 | 1 |
| | Rat | M | Adult | Per | 15 | N/A | 1 | 2 | 30 | Clamp | N/A | 30 | LAD | 120 | NR | N | Pentobarbitone | N | SEM | | | | 10 | 18 | 1 |
| | Rat | M | Adult | Per | 15 | N/A | 1 | 2 | 30 | Clamp | N/A | 30 | LAD | 120 | NR | N | Pentobarbitone | N | SEM | | | | 10 | 18 | 2 |
| | Rat | M | Adult | Post | 15 | N/A | 1 | 2 | 30 | Clamp | N/A | 30 | LAD | 120 | NR | N | Pentobarbitone | N | SEM | | | | 10 | 21 | 1 |
| | Rat | M | Adult | Post | 15 | N/A | 1 | 2 | 30 | Clamp | N/A | 30 | LAD | 120 | NR | N | Pentobarbitone | N | SEM | | | | 10 | 43 | 3 |
| [269] | Rat | M | Adult | Pre | 5 | 5 | 4 | 1 | 20 | Clamp | 5 | 40 | LAD | 120 | NR | N | Pentobarbitone | N | SEM | 6 | 66.5 | 5.5 | 6 | 48.2 | 5.2 |
| [270] | Rat | M | 8-10 weeks | Per | 10 | 10 | 1 | 1 | 10 | Tourniquet | N/A | 40 | LAD | 120 | NR | N | Pentobarbitone | N | SEM | 6 | 54.9 | 6.01 | 6 | 21.9 | 4.0 |
| [188] | Pig | M | 27-35kg | Pre | 5 | 5 | 4 | 1 | 20 | Clamp | 5 | 60 | LAD | 180 | NR | Y | Propofol, pancuronium, fentanyl | Heparin | SEM | 5 | 48.8 | 4.2 | 5 | 13.3 | 2.2 |
| | Pig | M | 27-35kg | Per | 5 | 5 | 4 | 1 | 20 | Clamp | N/A | 60 | LAD | 180 | NR | Y | Propofol, pancuronium, fentanyl | Heparin | SEM | | | | 6 | 18.2 | 2 |
| [271] | Rat | M | Adult | Pre | 5 | 5 | 4 | 2 | 40 | Cuff | 10 | 35 | LAD | 120 | NR | Y | Pentobarbitone | N | SD | 10 | 76 | 14 | 10 | 54 | 15 |
| [272] | Rat | M | 8-10 weeks | Pre | 10 | 10 | 1 | 1 | 10 | Clamp | 10 | 40 | LAD | 120 | NR | N | Pentobarbitone | N | SEM | 9 | 64.9 | 2.6 | 11 | 52.2 | 3.7 |
| [273] | Rat | M | 288+/-9kg | Per | 10 | 10 | 1 | 1 | 10 | Tourniquet | N/A | 40 | LAD | 120 | NR | N | Pentobarbitone | N | SEM | 6 | 54.6 | 4.7 | 6 | 24.4 | 5.9 |
| [274] | Rat | M | Adult | Pre | 5 | 5 | 4 | 1 | 20 | Clamp | 5 | 40 | LAD | 120 | NR | N | Pentobarbitone | N | SEM | 7 | 65.3 | 2.9 | 6 | 47.3 | 2.2 |
| [190] | Mouse | M | N/R | Pre | 5 | 5 | 4 | 1 | 20 | Clamp | 5 | 30 | LAD | 120 | NR | N | Pentobarbitone | N | SEM | 9 | 40.6 | 3.6 | 6 | 24.1 | 2.8 |

| | | | | | | | | | | | | | | | | | | | | | | | | | |
|---|---|---|---|---|---|---|---|---|---|---|---|---|---|---|---|---|---|---|---|---|---|---|---|---|---|
| | Rat | M | 2-3 months | Pre | 5 | 5 | 4 | 1 | 20 | Clamp | 5 | 40 | LAD | 120 | NR | N | Pentobarbitone | N | SEM | 7 | 65.1 | 2.7 | 6 | 47.3 | 2.1 |
| [167] | Pig | N/R | 15kg | Pre | 5 | 5 | 4 | 1 | 20 | Tourniquet | 5 | 40 | LAD | 120 | NR | Y | Midazolam, pentobarbitone | Heparin | SEM | 8 | 53 | 8 | 9 | 26 | 9 |
| [275] | Rat | M | N/R | Per | 15 | N/A | 1 | 2 | 30 | Clamp | N/A | 30 | LAD | 120 | NR | N | Pentobarbitone | N | SEM | 10 | 69 | 2 | 10 | 43.4 | 3.8 |
| | Rat | M | N/R | Per | 15 | N/A | 1 | 2 | 30 | Clamp | N/A | 30 | LAD | 120 | NR | N | Pentobarbitone | N | SEM | 6 | 68.6 | 0.8 | 6 | 46.4 | 4 |
| [276] | Rabbit | M/F | 2.5-3kg | Per | 5 | 1 | 1 | 1 | 5 | Clamp | N/A | 30 | LAD | 180 | NR | Y | Pentobarbitone | Heparin | SD | 10 | 31.5 | 1.3 | 10 | 17.1 | 1.7 |
| [181] | Mouse | M | 10-12 weeks | Pre | 5 | 5 | 3 | 1 | 15 | Clamp | 5 | 30 | LAD | 120 | NR | Y | Ketamine, xylazine, atropine | N | SEM | 10 | 56.7 | 3.2 | 9 | 21.6 | 1.6 |
| [277] | Rat | M | 280-300g | Pre | 5 | 5 | 1 | 1 | 5 | Clamp | 5 | 30 | LAD | 120 | NR | N | Pentobarbitone | N | SD | 6 | 54.7 | 6 | 6 | 28.3 | 4.9 |
| | Rat | M | 280-300g | Pre | 5 | 5 | 3 | 1 | 15 | Clamp | 5 | 30 | LAD | 120 | NR | N | Pentobarbitone | N | SD | | | | 6 | 51.1 | 7.4 |
| [194] | Rat | M | Adult | Pre | 15 | 10 | 1 | 2 | 30 | Clamp | 10 | 30 | LAD | 120 | NR | N | Pentobarbitone | N | SEM | 7 | 54.6 | 3.1 | 8 | 36.6 | 3 |
| [278] | Rat | M | 250-300g | Pre | 15 | 10 | 1 | 2 | 30 | Clamp | 10 | 30 | LAD | 120 | NR | N | Pentobarbitone | N | SEM | 7 | 42 | 3 | 7 | 28 | 4 |
| [279] | Rat | F | 200-250g | Per | 5 | 5 | 4 | 2 | 40 | Clamp | N/A | 45 | LAD | 120 | NR | N | Ketamine, xylazine | N | SEM | 22 | 48.7 | 3.4 | 22 | 42.2 | 3.9 |
| [174] | Pig | N/R | 20kg | Per | 5 | 5 | 4 | 1 | 20 | Tourniquet | N/A | 40 | LAD | 120 | NR | Y | Midazolam, pentobarbitone | Heparin | SEM | 10 | 60 | 5 | 10 | 38 | 5 |
| [280] | Pig | M/F | Newborn | Pre | 5 | 5 | 4 | 1 | 20 | Tourniquet | 5 | 40 | LAD | 120 | NR | N | Midazolam, azaperone, etomidate | Heparin | SD | 8 | 16.5 | 3.6 | 8 | 19.4 | 1.7 |
| [281] | Rat | M | Adult | Pre | 15 | 10 | 1 | 2 | 30 | Clamp | 10 | 30 | LAD | 120 | NR | N | Urethane | N | SEM | 6 | 55.5 | 3.1 | 6 | 21.5 | 3.5 |
| [123] | Rat | M | 8-10 weeks | Per | 10 | 10 | 1 | 1 | 10 | Tourniquet | N/A | 40 | LAD | 120 | NR | N | Pentobarbitone | N | SEM | 6 | 54.9 | 6.5 | 6 | 24.7 | 6.0 |
| [189] | Mouse | M | 12±3 weeks | Pre | 5 | 5 | 4 | 1 | 20 | Cuff | 5 | 30 | LAD | 1440 | R | Y | Ketamine, xylazine | N | SD | 5 | 37 | 4 | 5 | 17 | 3 |
| [282] | Rat | M | 250-280g | Per | 5 | 5 | 4 | 1 | 20 | Tourniquet | N/A | 45 | LAD | 4320 | R | N | Pentobarbitone | Heparin | SD | 8 | 50.5 | 4.1 | 8 | 35.6 | 4.2 |
| [283] | Rat | M | 250-350g | Pre | 15 | 0 | 1 | 2 | 30 | Clamp | 0 | 30 | LAD | 120 | NR | Y | Pentobarbitone | N | SEM | 6 | 62 | 5 | 6 | 52 | 4 |
| | Rat | M | 250-350g | Pre | 5 | 10 | 1 | 2 | 10 | Clamp | 10 | 30 | LAD | 120 | NR | Y | Pentobarbitone | N | SEM | | | | 6 | 42 | 2 |
| | Rat | M | 250-350g | Pre | 10 | 10 | 1 | 2 | 20 | Clamp | 10 | 30 | LAD | 120 | NR | Y | Pentobarbitone | N | SEM | | | | 6 | 37 | 8 |
| | Rat | M | 250-350g | Pre | 15 | 10 | 1 | 2 | 30 | Clamp | 10 | 30 | LAD | 120 | NR | Y | Pentobarbitone | N | SEM | | | | 8 | 18 | 3 |
| [284] | Rat | M | 300±25g | Pre | 5 | 5 | 3 | 1 | 15 | Clamp | 5 | 30 | LAD | 120 | NR | N | Pentobabitone | N | SD | 6 | 52.8 | 5.9 | 6 | 29.6 | 5.8 |
| [285] | Rat | M | 8 week | Per | 5 | 5 | 4 | 1 | 20 | Cuff | N/A | 45 | LAD | 120 | NR | N | Pentobabitone | Heparin | SD | 8 | 48.9 | 6.66 | 8 | 33.5 | 5.8 |
| [286] | Rat | M | 8-9 weeks | Per | 10 | N/A | 1 | 2 | 20 | Tourniquet | N/A | 30 | LAD | 180 | NR | Y | Pentobarbitone | N | SD | 9 | 60 | 3 | 9 | 48 | 1 |
| [287] | Rat | M | 250-300g | Per | 5 | 5 | 3 | 1 | 15 | Clamp | N/A | 45 | LAD | 180 | NR | N | Pentobarbitone | Heparin | SEM | 12 | 55.8 | 2.2 | 12 | 31.3 | 1.9 |
| [288] | Rat | M | 8 weeks | Per | 10 | N/A | 1 | 2 | 20 | Tourniquet | N/A | 30 | LAD | 120 | NR | Y | Pentobarbitone | N | SD | 20 | 71.6 | 8.7 | 20 | 56.9 | 8.8 |
| [289] | Rat | M | 230-260g | Pre | 5 | 5 | 3 | 1 | 15 | Clamp | 5 | 30 | LAD | 120 | NR | Y | Chloral hydrate | N | SD | 6 | 51 | 6 | 6 | 20.3 | 2.4 |

| | | | | | | | | | | | | | | | | | | | | | | | | | | |
|---|---|---|---|---|---|---|---|---|---|---|---|---|---|---|---|---|---|---|---|---|---|---|---|---|---|---|
| [290] | Rat | M | Adult | Pre | 5 | 5 | 3 | 2 | 30 | Tourniquet | 5 | 30 | LAD | 180 | NR | N | Chloral hydrate | | Heparin | SEM | 12 | 34.7 | 5.9 | 12 | 14.5 | 3.5 |
| | Rat | M | Adult | Per | 5 | 5 | 3 | 2 | 30 | Tourniquet | N/A | 30 | LAD | 180 | NR | N | Chloral hydrate | | Heparin | SEM | | | | 12 | 15.3 | 5.2 |
| | Rat | M | Adult | Post | 5 | 5 | 3 | 2 | 30 | Tourniquet | N/A | 30 | LAD | 180 | NR | N | Chloral hydrate | | Heparin | SEM | | | | 12 | 19.8 | 5.9 |

**Table 3-4: Main characteristics of included studies**

The time between RIC and index ischaemia is included for studies of preconditioning only. N/R, not recorded; N/A, not applicable; LAD, left anterior descending; R, recovery; NR, non-recovery; SEM, standard error of the mean; SD, standard deviation.

32 full studies were subject to quality assessment and a full breakdown of their score according to the ARRIVE guidelines is given in Table 3-5.

| Reference | 1 | 2 | 3 | 4 | 5 | 6 | 7 | 8 | 9 | 10 | 11 | 12 | 13 | 14 | 15 | 16 | 17 | 18 | 19 | 20 | Quality score |
|---|---|---|---|---|---|---|---|---|---|---|---|---|---|---|---|---|---|---|---|---|---|
| [266] | 1 | 1 | 1 | 1 | 1 | 0 | 0 | 1 | 0 | 0 | 0 | 1 | 0 | 1 | 1 | 1 | 0 | 1 | 1 | 1 | 13 |
| [166] | 1 | 1 | 1 | 1 | 1 | 1 | 0 | 1 | 0 | 0 | 0 | 1 | 0 | 0 | 1 | 1 | 0 | 1 | 1 | 1 | 13 |
| [268] | 1 | 1 | 1 | 1 | 1 | 0 | 0 | 1 | 0 | 0 | 0 | 0 | 0 | 0 | 1 | 1 | 0 | 0 | 1 | 1 | 10 |
| [269] | 0 | 1 | 1 | 0 | 1 | 0 | 0 | 1 | 0 | 0 | 0 | 1 | 0 | 0 | 1 | 1 | 0 | 1 | 0 | 0 | 8 |
| [270] | 1 | 1 | 1 | 1 | 1 | 1 | 1 | 1 | 0 | 0 | 0 | 0 | 0 | 0 | 1 | 1 | 0 | 1 | 1 | 1 | 13 |
| [188] | 1 | 1 | 1 | 1 | 1 | 1 | 0 | 1 | 0 | 0 | 0 | 0 | 0 | 1 | 1 | 1 | 1 | 1 | 1 | 1 | 14 |
| [271] | 1 | 1 | 1 | 1 | 1 | 1 | 0 | 1 | 0 | 0 | 0 | 0 | 1 | 1 | 0 | 1 | 0 | 1 | 1 | 0 | 12 |
| [272] | 1 | 1 | 1 | 1 | 1 | 1 | 0 | 1 | 0 | 0 | 0 | 1 | 1 | 0 | 1 | 1 | 0 | 1 | 1 | 1 | 14 |
| [273] | 0 | 1 | 1 | 1 | 1 | 1 | 0 | 1 | 0 | 0 | 0 | 0 | 0 | 0 | 1 | 1 | 0 | 1 | 1 | 1 | 11 |
| [274] | 1 | 1 | 1 | 1 | 1 | 1 | 0 | 1 | 0 | 0 | 0 | 0 | 1 | 0 | 1 | 1 | 0 | 1 | 1 | 1 | 13 |
| [190] | 1 | 1 | 1 | 1 | 1 | 1 | 1 | 1 | 0 | 0 | 0 | 0 | 1 | 0 | 1 | 1 | 1 | 1 | 1 | 1 | 15 |
| [167] | 1 | 1 | 1 | 1 | 1 | 1 | 0 | 1 | 0 | 0 | 1 | 1 | 1 | 1 | 1 | 1 | 0 | 0 | 1 | 1 | 15 |
| [275] | 1 | 1 | 1 | 1 | 1 | 1 | 0 | 1 | 0 | 0 | 1 | 0 | 0 | 1 | 1 | 1 | 0 | 1 | 1 | 1 | 14 |
| [276] | 1 | 1 | 1 | 1 | 1 | 1 | 0 | 1 | 0 | 0 | 0 | 0 | 0 | 1 | 1 | 1 | 0 | 1 | 1 | 1 | 13 |

| | | | | | | | | | | | | | | | | | | | | | |
|---|---|---|---|---|---|---|---|---|---|---|---|---|---|---|---|---|---|---|---|---|---|
| 181 | 1 | 1 | 1 | 1 | 1 | 1 | 0 | 1 | 0 | 0 | 1 | 0 | 0 | 1 | 1 | 1 | 0 | 1 | 1 | 1 | 14 |
| 277 | 1 | 1 | 1 | 1 | 1 | 1 | 0 | 1 | 0 | 0 | 0 | 0 | 0 | 1 | 1 | 1 | 1 | 1 | 1 | 1 | 14 |
| 194 | 1 | 1 | 1 | 1 | 1 | 0 | 1 | 1 | 0 | 0 | 0 | 0 | 0 | 0 | 1 | 1 | 0 | 0 | 1 | 1 | 11 |
| 279 | 1 | 1 | 1 | 1 | 1 | 1 | 0 | 1 | 0 | 1 | 0 | 1 | 0 | 1 | 1 | 1 | 1 | 1 | 0 | 1 | 15 |
| 174 | 1 | 1 | 1 | 1 | 1 | 1 | 1 | 1 | 0 | 1 | 1 | 0 | 1 | 1 | 1 | 1 | 1 | 1 | 1 | 1 | 18 |
| 280 | 1 | 1 | 1 | 1 | 1 | 1 | 0 | 0 | 0 | 0 | 0 | 0 | 1 | 1 | 1 | 1 | 1 | 1 | 1 | 1 | 14 |
| 281 | 1 | 1 | 1 | 1 | 1 | 1 | 0 | 1 | 1 | 0 | 0 | 0 | 0 | 1 | 1 | 1 | 1 | 1 | 0 | 1 | 14 |
| 123 | 1 | 1 | 1 | 1 | 1 | 1 | 1 | 1 | 0 | 0 | 1 | 0 | 0 | 0 | 1 | 1 | 0 | 1 | 1 | 1 | 14 |
| 189 | 1 | 1 | 1 | 1 | 0 | 0 | 0 | 0 | 1 | 0 | 0 | 0 | 0 | 1 | 1 | 1 | 0 | 1 | 1 | 1 | 11 |
| 282 | 1 | 1 | 1 | 1 | 1 | 1 | 1 | 1 | 1 | 0 | 0 | 0 | 0 | 0 | 1 | 1 | 0 | 1 | 1 | 1 | 14 |
| 283 | 1 | 1 | 1 | 1 | 1 | 0 | 0 | 1 | 0 | 0 | 0 | 0 | 0 | 1 | 1 | 1 | 1 | 0 | 1 | 1 | 12 |
| 284 | 1 | 0 | 1 | 1 | 1 | 0 | 0 | 1 | 1 | 1 | 0 | 1 | 0 | 1 | 1 | 1 | 1 | 1 | 0 | 1 | 14 |
| 285 | 1 | 1 | 1 | 1 | 1 | 1 | 1 | 1 | 0 | 0 | 0 | 0 | 0 | 1 | 1 | 1 | 0 | 1 | 1 | 1 | 14 |
| 286 | 1 | 1 | 1 | 1 | 1 | 1 | 1 | 1 | 0 | 1 | 1 | 0 | 1 | 1 | 1 | 1 | 0 | 1 | 1 | 1 | 17 |
| 287 | 1 | 1 | 1 | 1 | 1 | 1 | 1 | 1 | 1 | 0 | 0 | 0 | 0 | 1 | 1 | 1 | 0 | 0 | 1 | 1 | 14 |
| 288 | 1 | 1 | 1 | 1 | 1 | 1 | 1 | 1 | 1 | 1 | 1 | 0 | 1 | 1 | 1 | 1 | 0 | 1 | 1 | 1 | 18 |
| 289 | 1 | 1 | 1 | 1 | 1 | 0 | 0 | 1 | 0 | 0 | 0 | 0 | 0 | 1 | 1 | 1 | 0 | 0 | 0 | 1 | 10 |
| 290 | 1 | 1 | 1 | 1 | 1 | 1 | 1 | 1 | 0 | 0 | 0 | 0 | 0 | 1 | 1 | 1 | 1 | 1 | 1 | 1 | 15 |

**Table 3-5: Study quality based on ARRIVE guidelines**

Study quality items are: (1) Title; (2) Abstract; (3) Background; (4) Objectives; (5) Ethical statement; (6) Study design; (7) Experimental procedures; (8) Experimental animals; (9) Housing and husbandry; (10) Sample size; (11) Allocating animals to experimental group; (12) Experimental outcomes; (13) Statistical methods; (14) Baseline data; (15) Numbers analysed; (16) Outcomes and estimation; (17) Adverse events; (18) Interpretation/scientific implications; (19) Generalizability/translation; (20) Funding.

A full breakdown of study quality score according to a 12-item quality score is given in Table 3-6.

| Reference | 1 | 2 | 3 | 4 | 5 | 6 | 7 | 8 | 9 | 10 | 11 | 12 | Quality score |
|---|---|---|---|---|---|---|---|---|---|---|---|---|---|
| [266] | 1 | 0 | 0 | 1 | 0 | 1 | 1 | 1 | 0 | 0 | 0 | 1 | 6 |
| [166] | 1 | 1 | 1 | 1 | 1 | 1 | 1 | 0 | 0 | 0 | 0 | 1 | 8 |
| [268] | 1 | 0 | 0 | 1 | 1 | 1 | 1 | 1 | 1 | 0 | 0 | 0 | 7 |
| [269] | 1 | 0 | 0 | 1 | 1 | 1 | 0 | 0 | 0 | 0 | 0 | 0 | 4 |
| [270] | 1 | 1 | 0 | 1 | 1 | 1 | 0 | 0 | 0 | 0 | 0 | 1 | 6 |
| [188] | 1 | 1 | 0 | 1 | 0 | 0 | 1 | 1 | 1 | 0 | 0 | 1 | 7 |
| [271] | 1 | 1 | 0 | 1 | 1 | 1 | 1 | 0 | 1 | 0 | 0 | 0 | 7 |
| [272] | 1 | 1 | 0 | 1 | 1 | 1 | 0 | 0 | 0 | 0 | 0 | 1 | 6 |
| [273] | 1 | 1 | 0 | 1 | 1 | 1 | 0 | 0 | 0 | 0 | 0 | 1 | 6 |
| [274] | 1 | 1 | 1 | 1 | 1 | 1 | 0 | 0 | 0 | 0 | 0 | 1 | 7 |
| [190] | 1 | 1 | 1 | 1 | 1 | 1 | 0 | 0 | 0 | 0 | 0 | 1 | 7 |
| [167] | 1 | 1 | 1 | 1 | 1 | 1 | 1 | 1 | 1 | 0 | 1 | 0 | 10 |
| [275] | 1 | 1 | 0 | 1 | 1 | 1 | 1 | 0 | 1 | 0 | 0 | 1 | 8 |
| [276] | 1 | 1 | 0 | 1 | 1 | 1 | 1 | 0 | 1 | 0 | 0 | 0 | 7 |
| [181] | 1 | 1 | 0 | 1 | 1 | 1 | 1 | 0 | 1 | 0 | 0 | 0 | 7 |
| [277] | 1 | 1 | 0 | 1 | 1 | 1 | 1 | 0 | 1 | 0 | 0 | 0 | 7 |
| [194] | 1 | 0 | 0 | 1 | 1 | 1 | 1 | 1 | 1 | 0 | 0 | 1 | 8 |
| [279] | 1 | 1 | 0 | 1 | 0 | 1 | 1 | 0 | 0 | 0 | 0 | 1 | 6 |
| [174] | 1 | 1 | 1 | 1 | 1 | 1 | 1 | 1 | 1 | 1 | 1 | 0 | 11 |
| [280] | 1 | 1 | 1 | 1 | 1 | 1 | 1 | 0 | 1 | 0 | 0 | 1 | 9 |
| [281] | 1 | 1 | 1 | 1 | 1 | 1 | 1 | 1 | 1 | 0 | 0 | 0 | 9 |
| [123] | 1 | 1 | 1 | 1 | 1 | 1 | 0 | 0 | 0 | 0 | 0 | 1 | 7 |
| [189] | 1 | 0 | 0 | 1 | 0 | 0 | 0 | 0 | 0 | 0 | 0 | 1 | 3 |
| [282] | 1 | 1 | 1 | 1 | 1 | 0 | 1 | 0 | 0 | 0 | 0 | 1 | 7 |
| [283] | 1 | 0 | 0 | 1 | 1 | 1 | 1 | 1 | 1 | 0 | 0 | 0 | 7 |
| [284] | 1 | 0 | 0 | 1 | 1 | 1 | 1 | 0 | 1 | 1 | 0 | 1 | 8 |
| [285] | 1 | 0 | 1 | 1 | 1 | 1 | 1 | 0 | 1 | 0 | 0 | 1 | 8 |
| [286] | 1 | 1 | 1 | 1 | 1 | 1 | 1 | 1 | 1 | 1 | 1 | 1 | 12 |
| [287] | 1 | 1 | 0 | 1 | 0 | 0 | 1 | 0 | 1 | 0 | 0 | 0 | 5 |
| [288] | 1 | 1 | 1 | 1 | 0 | 1 | 1 | 1 | 1 | 1 | 0 | 0 | 9 |
| [289] | 1 | 0 | 0 | 1 | 1 | 1 | 1 | 0 | 1 | 0 | 0 | 0 | 6 |
| [290] | 1 | 1 | 1 | 1 | 1 | 0 | 1 | 0 | 0 | 0 | 0 | 1 | 7 |

**Table 3-6: Study quality based on a 12-item quality score**

Study quality items are: (1) Publication in a peer-reviewed journal; (2) Randomization to either control or conditioning treatment with RIC or placebo control; (3) Blinded assessment of outcome; (4) Statement of compliance with regulatory requirement; (5) Method of confirmation of ischaemia; (6) Statement of control of temperature; (7) Statement of recording ECG; (8) Statement of measuring PaO2 or SaO2; (9) Statement of measurement of BP; (10) Sample size calculation; (11) Blinded application of conditioning protocol; (12) Statement of conflict of interest.

### 3.3.4 Discussion

Experimental variables for which data were sought were chosen according to their evidence-based effect on myocardial IRI or on the efficacy of RIC. Further data items were discretionary and chosen according to their potential to impact on the efficacy of RIC. Although some data items have not been investigated in the literature in the setting of cardioprotection, this project aimed to address a broad range of experimental variables in order to obtain a clear picture of how the efficacy of RIC may be influenced *in vivo*. A separate systematic review to develop these data items was not performed, but all potentially relevant and recordable methodological variables are believed to have been included. The rationale for the main data items is briefly described below.

Firstly, the choice of animal is central to any *in vivo* experimental model. For example, dogs have extensive collateral circulation which is known to afford cardioprotection; therefore, species with extensive collateral circulation have smaller IS after IRI relative to rabbits, pigs, rats and mice.[258, 291] This is important because the confounding effect of a collateral circulation must be quantified, increasing the time, complexity and cost associated with the model. Conversely, rabbits, pigs, rats and mice have virtually absent collateral flow.[258] These species therefore suffer a large enough insult after IRI to facilitate the demonstration of statistically significant cardioprotection with various experimental interventions, including IPC and RIC. Despite their smaller size and faster heart rates, murine models have the added advantages of relative low cost, speed and ease of breeding.[292] It should be acknowledged, however, that although the paucity of a collateral circulation is desirable in an experimental model, it does not necessarily reflect the anatomy of

many patients who have extensive collateral circulations as a consequence of chronic CHD.

Furthermore, although Sprague-Dawley is the strain of rat most commonly used for MI experiments,[203] it has been demonstrated that Sprague Dawley rats have the most marked variability in IS and cardiac dysfunction after IRI owing to the least consistent LAD branching pattern of six strains tested.[203] These factors may additionally impact on the efficacy of RIC.

Similarly, in a recent meta-analysis, Lim *et al.* demonstrated that ciclosporin was not effective at limiting myocardial IS in pig models of IRI, compared to small animal models.[146] This may be species-specific or related to species size more generally.[146] It may also be a consequence of variable plasma concentrations of ciclosporin according to species, despite the administration of similar weight-adjusted doses.[146] For example, it has been demonstrated that swine have a lower blood concentration of ciclosporin than humans despite the same dosing regime.[146] This reinforces the requirement to investigate species as an important experimental variable.

Regarding gender, IRI experiments conventionally use male subjects. This is justified by reference to the cardioprotection conferred by oestrogen and potential temporal variability in cardioprotection as a result of the oestrous cycle of female rats,[293-295] and is therefore an important variable to include in a systematic review and meta-analysis of cardioprotection.

Pentobarbitone is a commonly used anaesthetic agent for non-recovery experiments. Pentobarbitone is comparable in its haemodynamic effects to two other commonly used regimens: isoflurane and ketamine/xylazine.[296] However, all of these agents adversely affect cardiovascular functional indices, which include heart rate, cardiac output, blood pressure and LV dimensions, compared to tiletamine/zolazepam.[296] Furthermore, it has been suggested that propofol interferes with the development of RIC,[248, 297] and it has been implicated as a potential reason for the apparent lack of

translation of RIC.[298] For these reasons, it is an important variable in the context of this study.

The duration of ischaemia and reperfusion are also important variables as increased ischaemic duration,[299] and possibly reperfusion duration,[300] have been reported to increase IS and may consequently impact upon the efficacy of RIC. For example, there is evidence that the degree of cardioprotection conferred by RIC is proportional to the duration of index ischaemia. Specifically, Kleinbongard *et al.* demonstrated longer cross-clamp (ischaemic) times to be associated with a greater efficacy of RIC in a study of patients undergoing CABG.[301]

Furthermore, it has been hypothesised that the interval between the conditioning stimulus and the onset of index ischaemia might be an important determinant of the efficacy of remote preconditioning.[249]

Finally, there is interest regarding the precise conditioning protocol, including number and duration of cycles. Johnsen *et al.* recently reported that four and six, but not eight, cycles of RIC were protective in mice subject to *in vivo* RIC prior to heart extraction and simulated IRI on a Langendorff apparatus.[302] Similarly they found that 2 and 5 min, in contrast to 10 min, cycles were beneficial in mice. These are all, therefore, important facets to synthesise as part of any systematic review and meta-analysis of *in vivo* studies of myocardial IRI.

## 3.4 Aim 2: Perform a meta-analysis of studies of remote ischaemic conditioning in *in vivo* models of myocardial ischaemia-reperfusion injury.

### 3.4.1 Background

Meta-analysis describes the quantitative synthesis of data from independent studies.[251] In the context of pre-clinical *in vivo* studies of RIC in myocardial IRI, meta-analysis facilitates calculation of the overall effect size compared to control (sham procedure or no treatment). It is likewise possible to investigate whether the heterogeneity of experimental conditions used between studies, including variables such as RIC protocol and use of supplementary oxygen, impacts on outcome and

might confound attempts at clinical translation, which is a further aim of this section. Finally, poor methodological quality and publication bias can result in over-estimation of effect size.[303-305] In turn, this can engender enthusiasm about the benefit of a treatment where, in fact, none exists. It is therefore essential to examine the impact of study quality on size of effect, which was a further aim of this section.

### 3.4.2 Methods

The primary outcome was pre-specified and defined as the weighted (unstandardised) mean difference (WMD) between IS in the RIC and control groups in *in vivo* models of myocardial IRI. WMD was used as all data were presented in the same units and it gives a biologically relevant value. In each publication, all independent comparisons of IS/AAR in RIC versus control groups were identified. Where a study made multiple comparisons to the same control group, the size of the control group was corrected for the number of comparisons made (n/number of comparisons).[306] In studies that included additional groups that were, for example, subjected to RIC in addition to another conditioning protocol or to pharmacological treatments known to have cardioprotective effects, only the RIC and control groups (as per our eligibility criteria) were included in the analysis.

For each independent comparison the effect size was calculated as a raw difference in IS/AAR means (the mean of the control groups minus the mean of the experimental group) and the corresponding 95% confidence interval (CI). To account for anticipated heterogeneity effect sizes were pooled using random-effects meta-analysis, which considers the within-study and between-study variability and weights each study accordingly. Heterogeneity was quantified using $I^2$ and $T^2$ statistics.[306, 307] Studies with missing data on any of the pre-defined experimental variables were excluded from the meta-analysis.

The secondary outcome was the effect of eight pre-defined experimental variables, which were considered most likely to impact on the efficacy of RIC, on WMD. These were defined as:

1. *Species:* Studies that used either mice or rats were grouped as 'small animals', and those using rabbits or pigs were grouped as 'large animals'.
2. *Protocol:* The retrieved studies contained several definitions of pre-, per- and post-conditioning. For clarity, despite the terminology used in the report, preconditioning was defined as any stimulus where the last cycle of ischaemia had been completed by the time of index ischaemia; perconditioning as any ischaemic stimulus that overlapped in full or in part with the index ischaemia; and postconditioning as any stimulus that began at or after the time of myocardial reperfusion.
3. *Cycle duration:* The reported duration of ischaemia applied to the limb in each cycle. In the analysis, studies were grouped as 5, 10 or 15 min of limb ischaemia.
4. *Number of cycles:* The number of times this ischaemic episode was applied in succession to the limb. Studies were grouped as using one, three or four cycles of ischaemia.
5. *Number of limbs:* The RIC protocol reported by each study was either applied to one or both (bilateral) limbs. Conditioning by infra-renal aortic occlusion was classed as bilateral hind limb ischaemia, whereas studies using supra-renal aortic occlusion were excluded.
6. *Oxygen:* Each study was given a binary score according to its reported use of supplementary oxygen in their ventilation protocol.
7. *Technique of occlusion:* Whether the study reported use of a cuff/tourniquet or femoral artery clamp to induce hind limb ischaemia.
8. *Heparin:* A binary measure of whether the study reported the use of heparin as part of their *in vivo* protocol.

Subgroup analyses were performed using univariate meta-regressions to explore which experimental factors and study quality indicators contributed to any observed heterogeneity. The percentage of between-study variance explained by variables of interest was assessed using the $T^2$ and adjusted $R^2$ statistics. The significance level was adjusted according to the number of comparisons using the Holm-Bonferroni method.[308]

Sensitivity analysis was performed to assess the robustness of our findings by performing an additional analysis for both the primary and the secondary endpoints using the SMD (the mean of the control group minus the mean of the RIC group, divided by the pooled SD of the two groups). We performed a stratified meta-analysis by subgroup to validate the results obtained by meta-regression.

Potential publication bias was assessed by visual inspection of a funnel plot for asymmetry, and Egger's regression analysis for small study effects. No protocols were available with which to examine for selective reporting, however, the methods and results sections of all included studies were carefully compared for inconsistencies.

All analyses were pre-specified and performed using STATA/SE version 13.1 (StataCorp, College Station, TX, USA); GraphPad Prism version 5.00 for Windows (CA, USA) was used in the production of figures.

### 3.4.3 Results

From the 34 included reports, we extracted data on 48 controlled comparisons of RIC in models of myocardial IRI. In total, our analysis includes data from 305 control animals and 418 animals undergoing RIC. Overall, RIC reduced IS/AAR by 20.9% (95% CI 18.2-23.7%), when compared to untreated controls (n=48 comparisons, P<0.001, Figure 3-2). Interestingly, significant heterogeneity in effect size was observed ($T^2$=92.9 and $I^2$=99.4%, P<0.001).

Potential experimental sources of the observed heterogeneity were investigated using meta-regression analysis with IS/AAR as the dependent variable. However, there were no significant associations of experimental variables with efficacy of RIC (Figure 3-3).

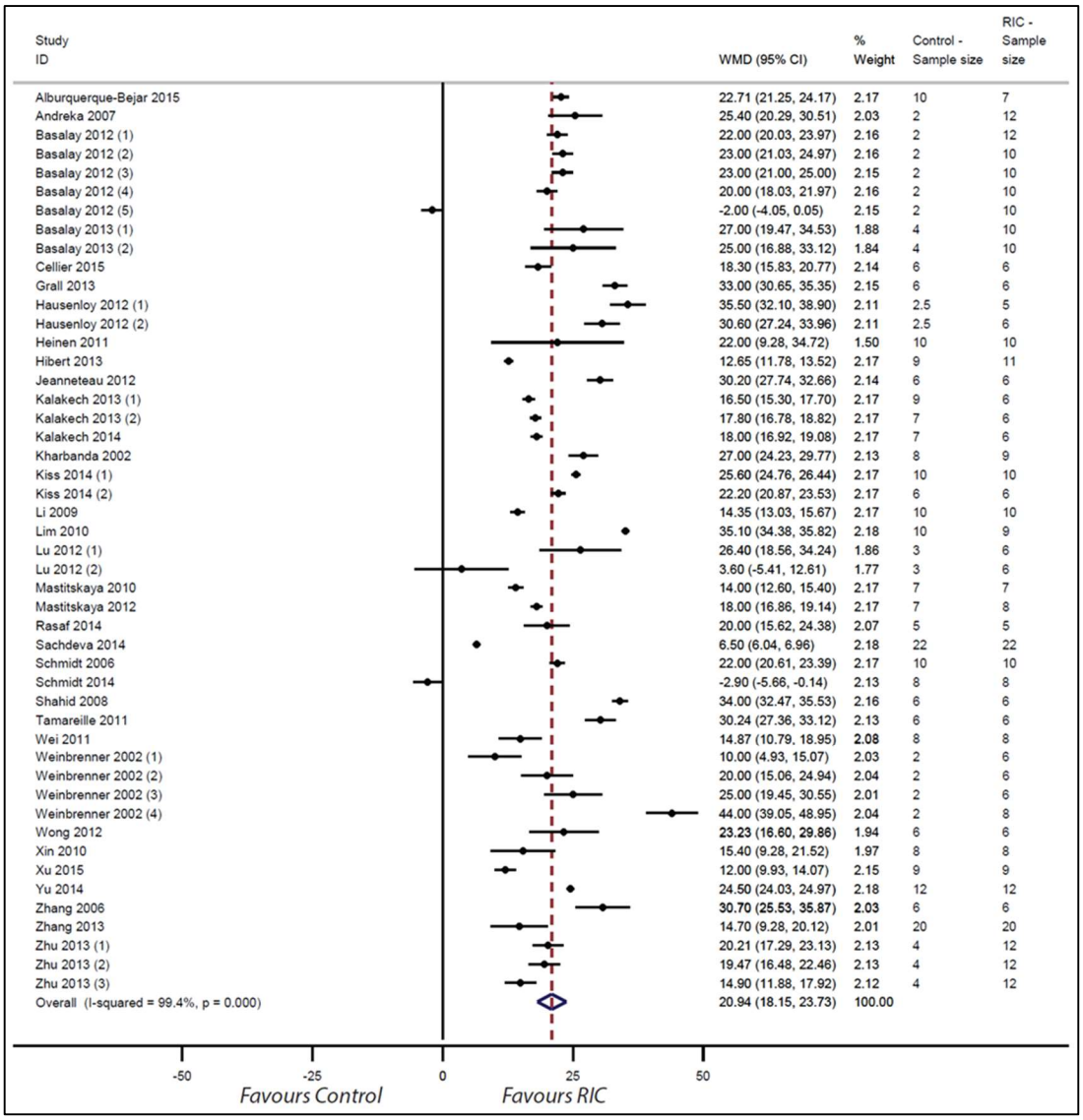


**Figure 3-2: Forest plot of meta-analysis of conditioning efficacy**

A forest plot of the effect of RIC on IS/AAR, pooled using random-effects meta-analysis. 48 controlled comparisons were included, amounting to data from 305 control animals and 418 animals undergoing RIC.

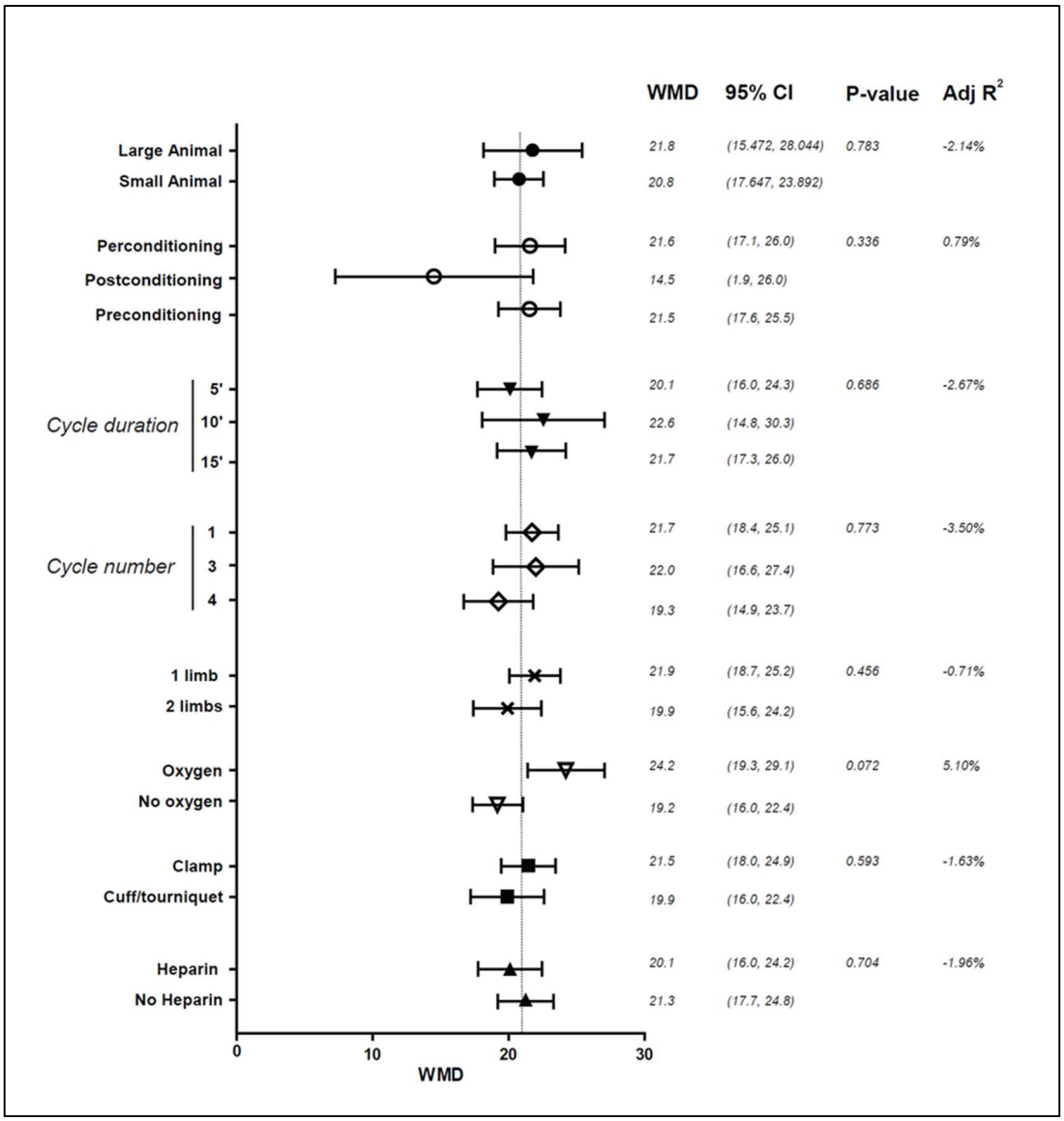


**Figure 3-3: Impact of experimental factors on the efficacy of remote ischaemic conditioning**

WMD and the corresponding 95% CI for each variable were obtained by subgroup stratification. However, the reported P-value was obtained by meta-regression to reduce false-positive findings. Studies that used either mice or rats were grouped as 'small animals', and those using rabbits or pigs were grouped as 'large animals'.

Furthermore, the reduction in IS/AAR after RIC was not statistically contingent upon the duration of index ischaemia. However, there was a pattern of increasing efficacy of RIC at longer index ischaemic durations that appears to diminish at the longest durations, especially in small animals, but this should only be considered exploratory. In the group of studies in which RIC was applied before the index ischaemia (preconditioning), the interval between the conditioning stimulus and the onset of

index ischaemia did not affect the efficacy of RIC. Results of both of these analyses are provided in Table 3-7.

| Experimental variables | WMD | (95% CI) | % Weight | P-value | Adj R-squared |
|---|---|---|---|---|---|
| **Interval between RIC and index ischaemia** | | | | 0.387 | -1.35% |
| 0-5 min | 20.1 | (14.5, 25.6) | 60.5 | | |
| 10 min | 23.7 | (18.2, 29.2) | 39.6 | | |
| **Duration of index ischaemia (small animals)** | | | | 0.569 | -1.88% |
| 30 | 21.0 | (17.5, 24.5) | 69.9 | | |
| 35 | 22.0 | (9.3, 34.7) | 1.8 | | |
| 40 | 22.8 | (17.9, 27.6) | 18.1 | | |
| 45 | 15.3 | (2.9, 27.7) | 10.1 | | |
| **Duration of index ischaemia (large animals)** | | | | 0.271 | 6.80% |
| 30 | 14.4 | (13.0, 15.7) | 12.8 | | |
| 40 | 17.2 | (7.6, 26.9) | 50.6 | | |
| 60 | 33.0 | (28.2, 37.8) | 24.8 | | |
| 90 | 25.4 | (20.3, 30.5) | 11.8 | | |

**Table 3-7: Meta-analysis evaluating the effect of experimental variables on WMD**

Analysis of the effect of the interval between the last cycle of RIC and index ischaemia on WMD included only studies of remote preconditioning (n=25 comparisons). Analysis of the impact of index ischaemia duration on WMD in studies using small animals (rat or mouse) included n=40 comparisons; the 35 min group included only 1 comparison. In large animals (rabbit or pig) there were n=8 comparisons; the 30 and 90 min groups included only 1 comparison.

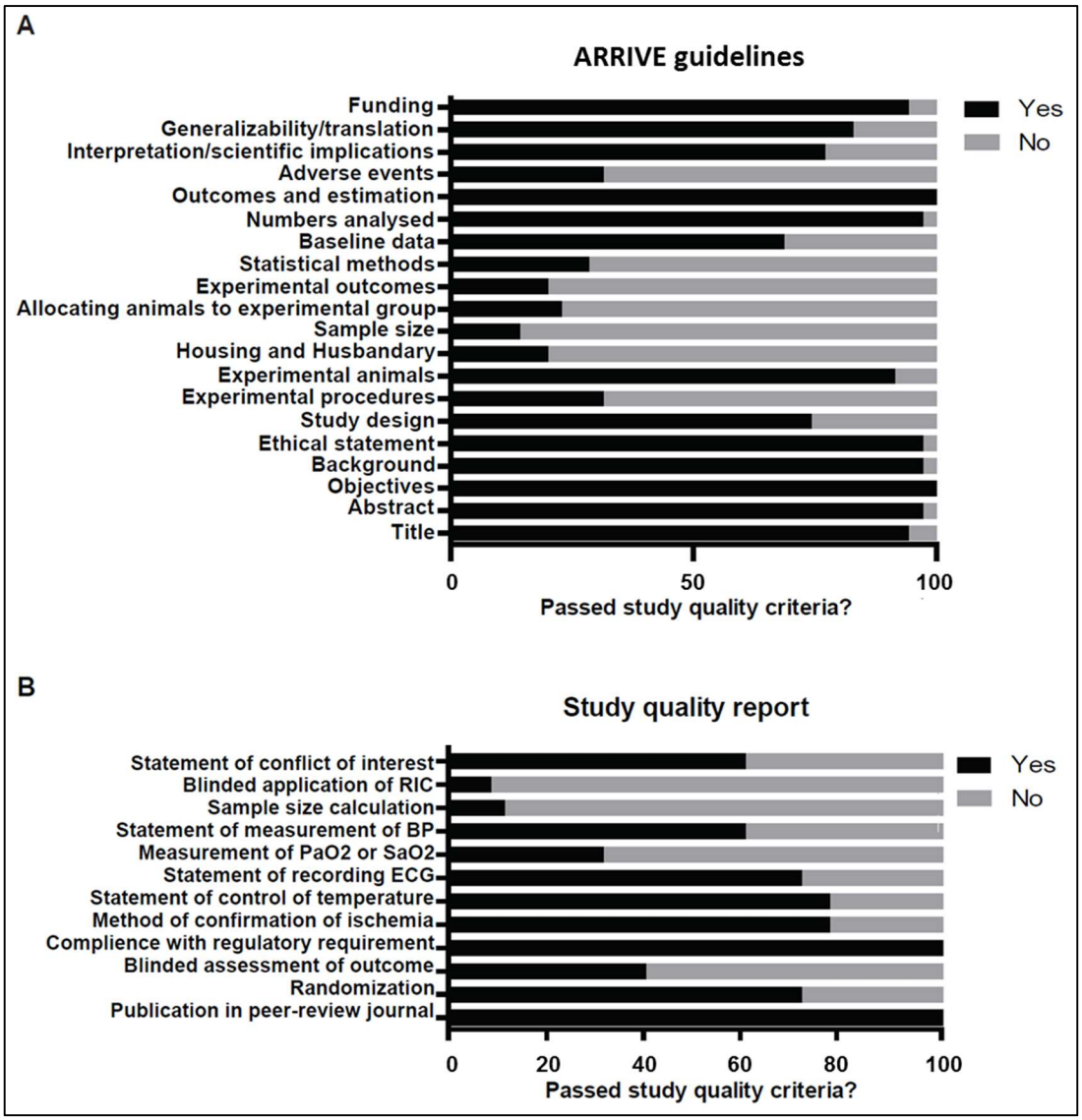


**Figure 3-4: Reporting of study quality indicators**

Study quality was assessed using the ARRIVE guidelines on reporting *in vivo* experiments (A) and a 12-item quality score (B). Values are expressed as the percentage of studies reporting each quality indicator.

Meta-regression indicated that study quality according to the ARRIVE guidelines score and a 12-item quality score was not associated with the overall effect (P=0.663 and P=0.557, respectively). Reports achieved a median ARRIVE guidelines score of 14 (IQR 12-14) and a median 12-item quality score of 7 (IQR 6-8). Figure 3-4 demonstrates graphically the reporting of study quality indicators.

The impact of publication bias on the overall effect was assessed by visual analysis of the funnel plot, which suggested that small and negative studies might be under-represented (Figure 3-5). In Egger's regression test the null-hypothesis of no small-study effect was not rejected at P=0.392 (estimated bias coefficient 2.45±2.83 SE).

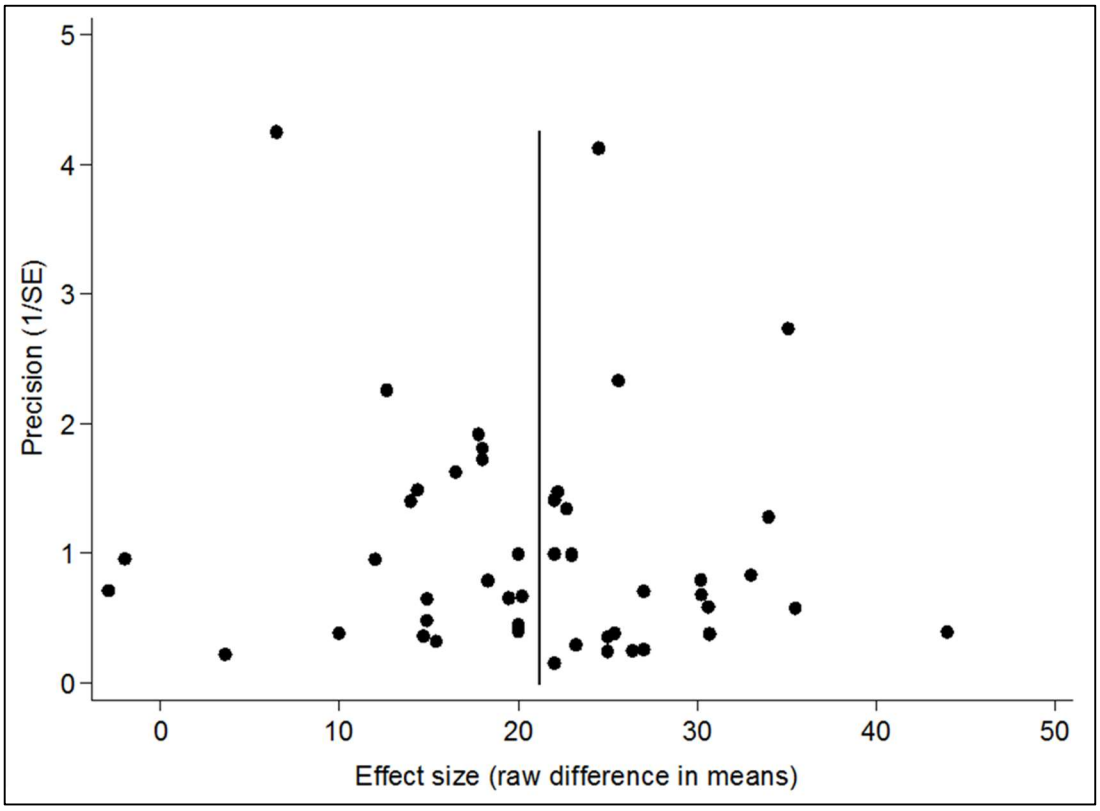


**Figure 3-5: Assessment of publication bias**

A funnel plot comparing treatment effect to a measure of study size (precision of the effect estimate). The vertical line represents the mean effect size. This plot was assessed visually, with further analysis of publication bias performed using Egger's regression test.

When the analysis was re-run using the SMD, all results were similar to those found using the WMD. There was a highly significant overall effect (SMD of 10.49, 95% CI 8.93-12.05, P<0.001), as well as a similar level of heterogeneity ($I^2$=92.9%). None of the experimental variables were significant after correction by multiple comparison.

### 3.4.4 Discussion

Clinical trials investigating the efficacy of RIC in myocardial IRI have had mixed results.[173, 178] This meta-analysis of pre-clinical *in vivo* studies of myocardial IRI is the

first to confirm an overall large beneficial effect of RIC on IS, based on data from 34 studies and over 700 animals. This is an important finding in the context of recent pessimism regarding RIC as a genuine cardioprotective phenomenon.[309, 310] Interestingly, there was high heterogeneity between studies and resolving this may be the key to understanding the mixed results in clinical studies.

To facilitate the investigation of any factors that might impair clinical translation and to be as clinically relevant as possible, only *in vivo* models were included in this study. The impact of experimental variables on effect size is important as any over-estimation of effect size might justify recent neutral clinical studies of RIC. This approach has been successfully applied to several promising pre-clinical interventions to date.[102, 146] For example, the finding that ciclosporin was less effective in large compared to small animal models might be important in the context of a subsequent neutral clinical study of ciclosporin before reperfusion in patients with STEMI.[311] In their meta-analysis, Lim *et al.* point to the similarity between swine and human hearts in terms of coronary anatomy, collateralisation and myocardial mass. Therefore, finding the parameters responsible for heterogeneity can guide pre-clinical and clinical study design.

However, the meta-regression analyses did not identify any cause for the observed heterogeneity. Unlike the meta-analysis of ciclosporin described above, RIC was well conserved between species. Interestingly, there was no difference in effect size according to the number and duration of cycles. This is consistent with the description from Johnsen *et al.* described in section 3.3.4, who reported that four and six, but not eight, cycles of RIC were protective in mice, notwithstanding their application of *ex vivo* IRI,[302] as studies using eight cycles were not represented in the present sample. Similarly, this analysis supports their finding of no association with the number of limbs conditioned. Johnsen *et al.* further reported that 2 and 5 min, in contrast to 10 min, cycles were beneficial in mice.[302] This analysis demonstrated 10 min cycles to be equally effective, albeit only in larger species as no studies included in the meta-regression used 10 min cycles in mice. Pre-, per- and post-conditioning

were also statistically equally effective (WMD 21.5, 21.6 and 14.5, respectively) despite observing an apparently smaller effect in studies of postconditioning.

The use of supplementary oxygen in acute MI is controversial,[312] but the potential role of supplementary oxygen in RIC has not been investigated. If RIC is driven by cellular hypoxia in the conditioned limb, the role of supplementary oxygen could be central to the efficacy of the stimulus. However, this meta-analysis found conditioning of animals with and without oxygen to be equally effective. Similarly, there was not a difference between limbs occluded by femoral artery (or aortic) clamping versus external compression via a cuff, which was considered potentially important due to the possible involvement of limb collaterals and in relation to the putative effect of shear stress in RIC,[189] which might be greater with direct arterial clamping compared to external cuff inflation. Finally, RIC was equally effective in animals treated with and without heparin, which was included as a variable in light of reports that heparin is cardioprotective in the context of IRI.[242-246]

In studies of preconditioning only, there was no relationship between effect size and the interval between the preconditioning stimulus and index ischaemia, although the included range of intervals was small (0-10 min) and studies with an interval ≥1 h were excluded as the so-called second window of cardioprotection is believed to have a different mechanism.[313]

In an exploratory analysis of the effect of index ischaemia duration, comparisons were stratified according to species as identical durations of index ischaemia can return dissimilar IS/AAR in different species due to, for example, variable collateralisation. There was no statistical effect of index ischaemic time; however, there was a pattern of increased efficacy of RIC at longer ischaemic durations that appeared to weaken at the longest durations, especially in small animals. This might suggest an important role for the timing of intervention, but should be interpreted with caution in view of the limited number of comparisons available after stratification.

There were several experimental variables that were of considerable interest but that lacked sufficient power for statistical analysis. For example, the potential importance of anaesthetic agent was discussed in section 3.3.4. In particular, the potential of propofol to abrogate RIC is highly topical.[298] Interestingly, we observed studies where propofol (together with either opioid analgesia ± pancuronium) was administered to have effect sizes above the mean, although no trends were observed with other anaesthetic agents. Furthermore, studies reporting the use of either female or mixed gender experimental groups reported apparently smaller effect sizes. These qualitative data require further testing in formal, well-designed studies.

No statistical relationship was found between study quality and effect size using meta-regression. However, there were some interesting observations. In particular, it is noteworthy that there was generally poor observation of the ARRIVE guidelines, particularly in relationship to blinding and statistics. These facets are clearly essential to ensure good quality research and increase the likelihood of successful clinical translation, and were a central tenet of a recent position paper on improving the pre-clinical assessment of novel cardioprotective therapies.[237] However, aspects of the report relating to the experimental procedure, including control of temperature and recording of the ECG, were generally well reported. Each quality criterion was not analysed independently to avoid false positive findings due to multiple comparisons.

Finally, an assessment of publication bias by visual analysis of the funnel plot suggested that small, neutral studies may be under-represented; however, this did not statistically impact on the overall effect size, which is reassuring.

Meta-analysis has several limitations. The validity of this meta-analysis is contingent upon the quality of reporting of the included studies. Unpublished studies and those with missing data could not be included in the meta-analysis, and others did not meet important quality criteria including poor information regarding statistical analysis and blinding. However, the absence of a statistical impact from study quality or publication bias is reassuring in this regard. Being unable to consider manuscripts not available in English was a further limitation and it is acknowledged that a systematic

review of the literature to determine which experimental variables to include in the meta-regressions was not performed, which might therefore be subject to selection bias. A relatively small number of studies were included in the meta-analysis, thereby limiting the power of the study, which was further affected by multiple comparisons within individual studies; however, all comparisons were included to avoid selection bias. Meta-regression is inherently limited; however, to ensure this was as robust as possible a stratified meta-analysis by subgroup was performed and yielded similar results including a highly significant overall effect of RIC, significant heterogeneity, and no effect of any of the experimental variables included in the model.

## 3.5 Summary

This systematic review and meta-analysis of pre-clinical *in vivo* studies of myocardial IRI demonstrates a significant and highly reproducible beneficial effect of RIC, which is encouraging. This effect was highly heterogeneous, which could not be explained by any of the experimental variables tested. This heterogeneity may be due to un-measurable, multifactorial differences between individual experimenters and laboratories. However, importantly, *in vivo* studies to date suggest the optimal RIC stimulus has not yet been identified. Therefore, this meta-analysis provides little guidance regarding the establishment of an *in vivo* IRI protocol, but does reinforce the importance of adhering to the ARRIVE guidelines.

It also does not explain the neutral findings of ERICCA and RIP-HEART in CABG patients. The results suggest that the discrepancy between RIC in *in vivo* animal experiments and large outcome studies of RIC in CABG surgery might be better explained by failure of translation to humans rather than a type I error in pre-clinical studies. Furthermore, it is possible that RIC in animals more accurately models STEMI. While pilot trials in this setting have been promising, a large randomised outcome study is only now underway.[180] If this is positive, it might be explained by a difference between STEMI and CABG patients with respect to the extent of ischaemia reperfusion injury, co-morbidities, or by adjunctive medications and techniques.

# Chapter 4 Establishment and verification of murine *in vivo* models of myocardial ischaemia-reperfusion injury

## 4.1 Introduction

Following STEMI, early reperfusion by PPCI or pharmacological thrombolysis is a priority for reducing IS and improving clinical outcome.[2, 3] Nonetheless, despite the widespread uptake of PPCI as the default strategy for STEMI in the UK (60% of centres offered 24/7 PPCI for STEMI in 2014 compared to 5% in 2004) there remains a significant burden of heart failure following MI.[314] For example, in 2010, heart failure hospitalisations within 1 year of MI reached 14.2%, with unadjusted 1-year mortality of 45.5%.[315] It is recognised that outcome following STEMI is related to IS,[316] and as lethal IRI contributes to final IS it constitutes an important, and thus far unfulfilled, potential target for conferring better outcomes to these patients.[5, 6, 9, 157]

Investigating IRI in human patients is complicated by the difficulty in measuring the AAR, that is, the portion of myocardium that is rendered ischaemic by an obstructed epicardial coronary artery and stands to be salvaged by reducing IRI. AAR can be calculated from angiographic jeopardy scores, including the Alberta Provincial PRoject for Outcome Assessment in Coronary Heart disease (APPROACH) score.[317] However, although such scores have been prospectively validated, they require invasive angiography with its associated cost and procedural risk. CMR techniques using $T_2$-weighted imaging of myocardial oedema have been validated as a measure of AAR by comparison to histology in animals, angiographic jeopardy scores, myocardial single photon emission CT (SPECT) and, recently, hybrid positron emission tomography and magnetic resonance (PET-MR).[318]

However, although the use of CMR to evaluate AAR and IS has been described and validated in rodents,[319] it is limited by financial constraints. Therefore, an experimental model of IRI that permits the direct measurement of injury is required. Several are available, including simulated IRI (hypoxia-reoxygenation) of *in vitro* cultured cells, *ex vivo* isolated cardiomyocytes, *ex vivo* hearts on a Langendorff apparatus, and *ex vivo* human atrial trabeculae. However, an *in vivo* model of

myocardial IRI is preferred here as this project aims to investigate cardioprotective mechanisms that are remote from the heart and therefore require intact organ systems.

Myocardial IRI in humans most commonly occurs as a result of atheromatous plaque rupture, thrombus formation and subsequent mechanical or pharmacological reperfusion. To replicate this in an animal model is time-consuming, expensive and unpredictable, and therefore alternative approaches are necessary. Surgical induction of myocardial ischaemia has the advantages of being under the spatial and temporal control of the experimenter.[292] A surgical model of IRI was first described in dogs in 1967, in a study of the haemodynamic effects of isoproterenol, but was complicated by high mortality due to ventricular tachycardias and small IS due to collateral circulation.[320] Rats and mice lack an extensive collateral circulation, and although rodent hearts are less similar to human hearts than those of large animals, they are cheaper, easier to breed and less time-consuming than large animal models.[292]

This chapter therefore aims to describe the establishment of an *in vivo* model of myocardial IRI in both rats and mice.

## 4.2 Research aims and objectives

The main objective of this chapter was to establish a murine *in vivo* model of myocardial IRI. The research aims for this objective were:

1. Establish and verify a rat *in vivo* model of myocardial IRI;
2. Establish and verify a mouse *in vivo* model of myocardial IRI.

## 4.3 Aim 1: Establish and verify a rat *in vivo* model of myocardial ischaemia-reperfusion injury

### 4.3.1 Background

The first rat model of permanent left coronary artery occlusion was described in 1979.[321] Since then, the rat model of myocardial IRI has been established and widely

used in our laboratory and others to investigate potential therapeutic interventions and has been extensively described in the literature (reviewed by Klocke *et al.*).[292] This includes confirmation of its suitability for demonstrating cardioprotection by IPC and RIC (validation).[283, 322] Once established by any individual researcher, it is necessary to verify the model. This requires demonstrating that the application of a valid method is effective. Here, this mandates demonstrating a reduction of IS in response to known cardioprotective interventions. Furthermore, the model should be reliable, meaning it produces consistent results. This is important as good reliability (low variance) reduces the sample size necessary to demonstrate a statistically significant effect, which is an important reductionist concept. Therefore, it is necessary to develop a model that is reproducible enough to permit the detection of cardioprotection (reduction of IS) upon application of an established cardioprotective intervention.

As discussed in 0, several cardioprotective interventions are available, including both pharmacological and mechanical strategies. IPC has been confirmed in a large meta-analysis to substantially (mean difference of 24.6% in this particular study) reduce IS in pre-clinical models,[102] and is therefore a suitable cardioprotective intervention to verify this model. It is equally important to demonstrate cardioprotection by RIC, as the subject of this project. Cardioprotection by RIC in an *in vivo* rat model of IRI is less well described and, in studies published to date, has been shown to confer less marked (WMD 20.9%) and more variable protection, as demonstrated by the significant heterogeneity in the meta-analysis described in Chapter 2 ($I^2$ 99.4% compared to 94.7% in the meta-analysis of IPC, described above).[102] Nonetheless, in order to investigate the mechanism it is essential to first successfully reduce IS using RIC, which is the main aim of this section.

### 4.3.2 Methods

Rats were randomly assigned to control, IPC or RIC groups. To confirm the cessation of blood flow during cuff inflation, non-invasive, two-dimensional blood flow assessment was undertaken using a high resolution laser Doppler imager (Moor Instruments, Devon, UK). Briefly, an infra-red (785 nm) laser was used to sequentially

scan the whole hind limb. The incident beam undergoes Doppler shift when it is reflected by moving erythrocytes, and the magnitude and frequency of the backscattered signal is converted by photodiodes to an electrical signal representing the number and velocity of erythrocytes.[323, 324] These signals are digitally transformed into a colour-coded map indicating the spatial distribution of flow in the hind limb, whereby low or absent flow is blue and areas of highest flow are red. A Sprague Dawley rat was anaesthetised and subjected to the RIC protocol described in section 2.4.3. Laser Doppler images were taken at baseline, during ischaemia and during reperfusion.

In addition, in an exploratory analysis, skeletal muscle oxygen tension ($tPO_2$) was measured during cuff inflation. This relied on a 650 µm diameter large-area-surface (LAS) sensor connected to an OxyLite dissolved oxygen monitor (Oxford Optronix, Oxon, UK). Oxygenation is measured along the shaft of the LAS sensor, resulting in a sampling area of 8 $mm^2$, which allows averaging of local $tPO_2$ fluctuations caused by placement and movement. Measurements are accurate in the physiological range and oxygen is not consumed during recording.[325]

To insert the probe, a skin incision was made over the left lateral thigh. A 10 mm deep puncture was made in the vastus intermedius muscle with a 21G x 5/8" Microlance needle (BD, Oxon, UK), and the LAS sensor was immediately passed into the track. The probe was withdrawn by 1 mm prior to recording to negate the confounding effect of local haematoma. $tPO_2$ measurements were continuously recorded using PowerLab 4/25 coupled to Chart 7 (AD Instruments, Oxon, UK).

Sample size was not calculated *a priori* for any experiments in rats, in which six animals per group were used in line with convention.

### 4.3.3 Results

During the establishment of this *in vivo* rat model of myocardial IRI, a number of problems were identified that largely resulted from surgical inexperience. The major challenges were: (1) successful intubation; (2) surgically-induced haemorrhage; and

(3) inadequate staining with Evans blue. These were mainly resolved by experiential learning, but some specific refinements are considered here. Firstly, initial attempts to intubate were complicated by an inadequate view of the vocal cords and trans-illuminated trachea, caused by failure to move the epiglottis out of the line of vision. Failed intubation typically causes respiratory arrest, usually resulting in death. The intubation technique was modified by using angled dissecting forceps with a longer blade (200 mm; B. Braun, PA, USA) to ensure apposition of the epiglottis to the posterior tongue and an unobstructed view of the vocal cords. Secondly, it was apparent that myocardial puncture in order to under-run the LAD caused significant surgical bleeding, which was another major cause of animal loss. To rectify this, the needle shape was changed from 1/2 circle to 3/8 circle, and its size from 13 mm to 9.3 mm. This facilitated more precise placement of the LAD suture, resulted in less surgical trauma, and consequently less haemorrhage and animal loss.

Early results are not described here due to the variability in IS, survival and surgical technique. However, subsequent experiments were conducted after completion of this process, to maximise their validity. During this experiment, reasons for experiment failure were documented, audited and discussed with experienced operators, and a training log was maintained throughout. A summary is given in Figure 4-1. Whenever possible, hearts were removed from animals that died prematurely to check correct placement of the LAD suture by Evans blue staining to guide future technical refinement.

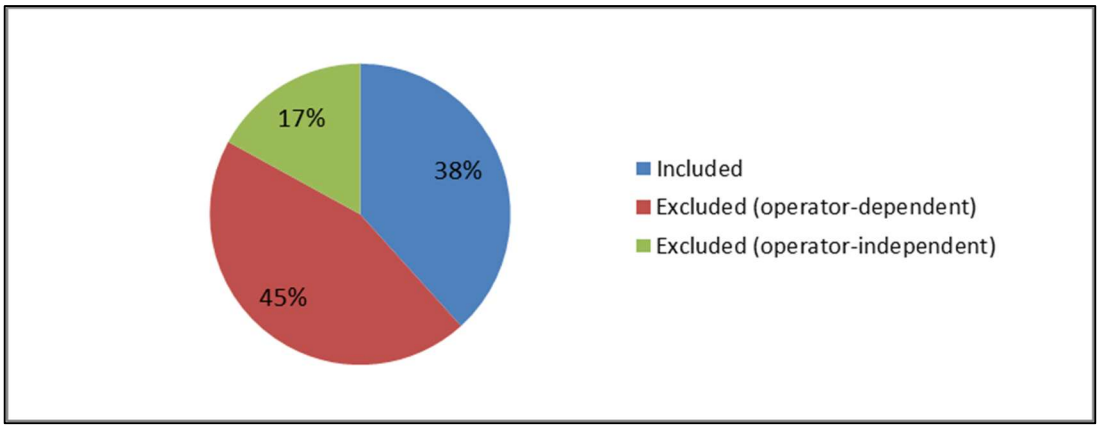


**Figure 4-1: Experimental success during establishment of a rat *in vivo* model of myocardial ischaemia-reperfusion injury**

47 animals were used during the course of the experiment. 18 were included in the analysis (38%). Excluded animals were defined as operator-dependent (72% of exclusions) or operator-independent (28%). The former related to surgical inexperience and most frequently included haemorrhage and inadequate staining with Evans blue. The latter were predominantly due to unexplained mortality or due to their AAR falling outside the pre-defined range.

Doppler images of the lower limb demonstrated cessations of blood flow during cuff inflation to 200 mmHg and return of blood flow to the distal tissues upon cuff deflation. Representative images are shown in Figure 4-2.

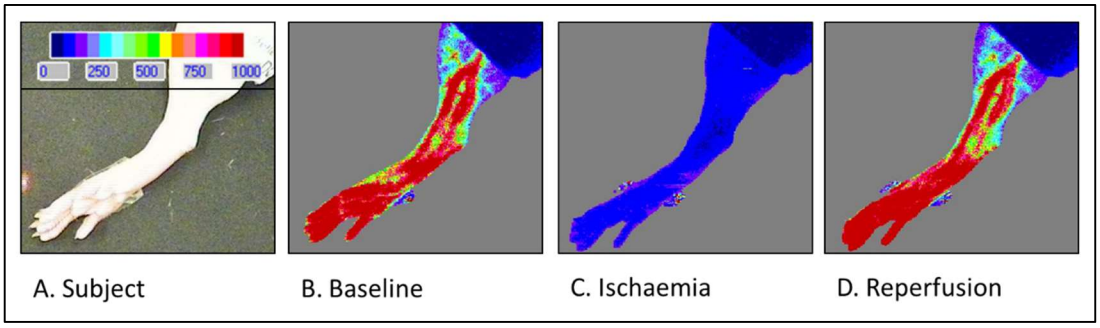


**Figure 4-2: Laser Doppler blood flow assessment demonstrating rat hind limb ischaemia during remote ischaemic conditioning**

A rat was anaesthetised and subjected to three cycles of 5 min hind limb ischaemia and 5 min reperfusion. A representative image from each step is shown here, alongside a plain photograph of the subject (A). Low or absent flow is blue and areas of highest flow are red (scale bar shown in Panel A).

Skeletal muscle $tPO_2$ measurement confirmed reduced oxygen tension, but interestingly showed that the rate of decline is longer in animals anaesthetised with supplementary oxygen (Figure 4-3). Consequently, oxygenated animals spend less of the RIC cycle with $tPO_2$ at hypoxic levels. This will be discussed in more detail in section 4.4.1.

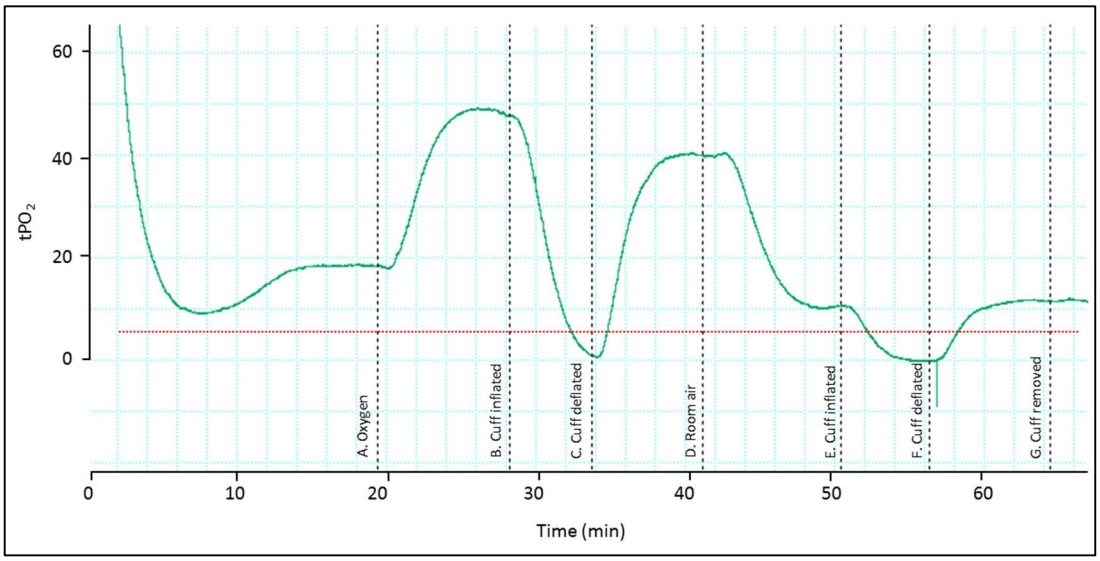


**Figure 4-3: Representative rat skeletal muscle $tPO_2$ assessment during remote ischaemic conditioning with and without supplementary oxygen**

Sprague Dawley rats were anaesthetised and stabilised without supplementary oxygen prior to the following interventions: (A) Supplementary oxygen started; (B) Hind limb cuff inflated to 200 mmHg; (C) Cuff deflated; (D) Supplementary oxygen stopped; (E) Cuff inflated; (F) Cuff deflated; (G) Cuff removed. The dashed red line gives an approximate 'hypoxic' $tPO_2$ (6 mmHg). During RIC on supplementary oxygen, skeletal muscle $tPO_2$ spends less time below this line than during RIC without supplementary oxygen.

This experiment measured IS as a proportion of AAR in Sprague Dawley rats following *in vivo* IRI. Six animals were included per group and analysis of their respective areas at risk, to ensure surgical consistency, revealed no significant differences (control 45.0±3.6% vs. IPC 38.9±1.0% vs. RIC 47.1±2.9%, n=6, P=NS, Figure 4-4).

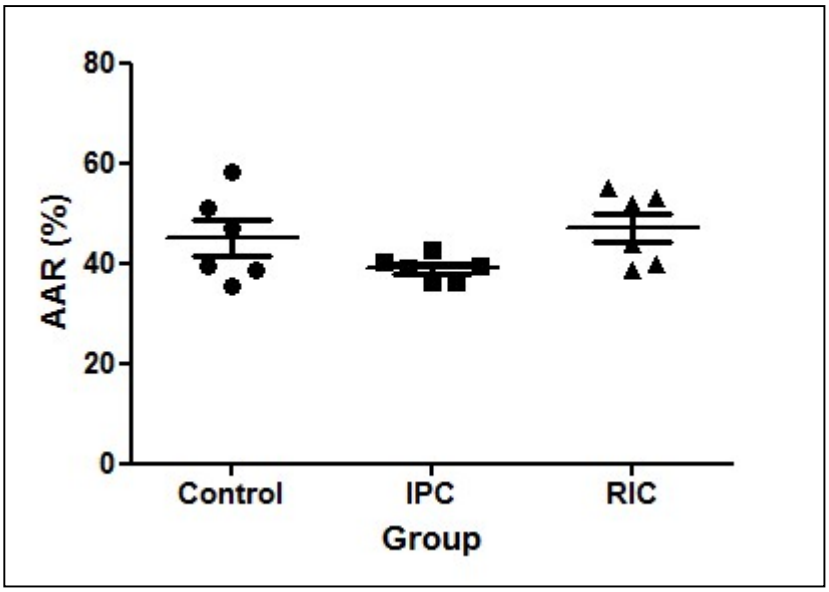


**Figure 4-4: Comparison of area at risk between control, ischaemic preconditioning and remote ischaemic conditioning groups**

Sprague Dawley rats were anaesthetised and treated with either IPC (5 min LAD occlusion and 5 min reperfusion) or RIC (three cycles of 5 min hind limb ischaemia and 5 min reperfusion) prior to 30 min ischaemia and 2 h reperfusion *in vivo*. Analysis of their respective areas at risk, to ensure surgical consistency, revealed no statistically significant differences. Statistical significance was assessed using one-way ANOVA and Tukey's multiple comparison test, n=6, P=NS for all comparisons. Data presented as mean ± SEM.

Subsequent analysis of IS as a proportion of AAR revealed that the application of IRI, as described, resulted in an IS of 51.1±4.0 (Figure 4-5), which is broadly consistent with IS described in Chapter 2. As expected, IPC significantly reduced IS/AAR (17.9±1.5%, n=6, P<0.001 vs. control). IS were smaller after the application of RIC, although this effect was less marked and more variable than IPC, as predicted (37.6±4.2%, n=6, P<0.05 vs. control). Representative transverse heart sections are shown in Figure 4-5. This study confirms that it is feasible to investigate IRI and RIC in this rat *in vivo* model of IRI.

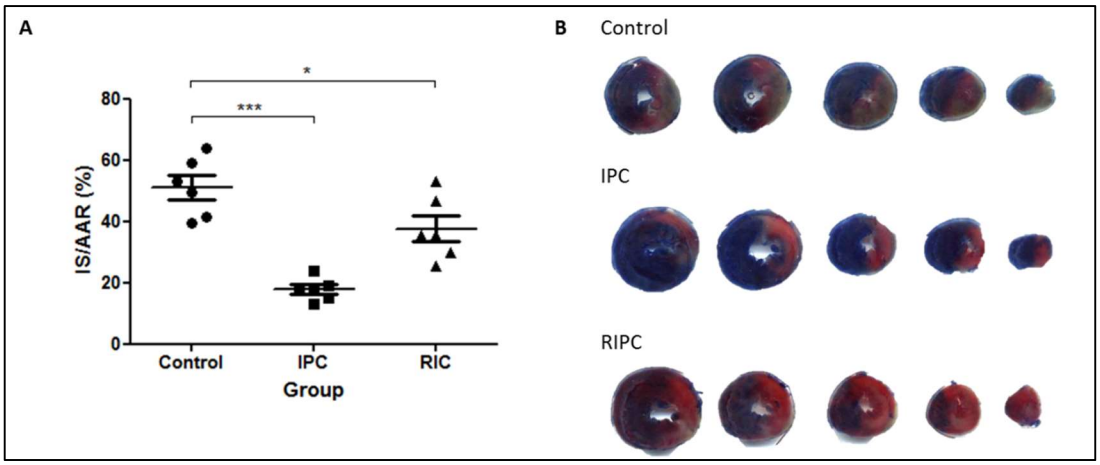


**Figure 4-5: Infarct size following ischaemic preconditioning and remote ischaemic conditioning prior to myocardial ischaemia-reperfusion injury *in vivo***

Sprague Dawley rats were anaesthetised and treated with either IPC (5 min LAD occlusion and 5 min reperfusion) or RIC (three cycles of 5 min hind limb ischaemia and 5 min reperfusion) prior to 30 min ischaemia and 2 h reperfusion *in vivo.* IS as a proportion of AAR was analysed using Evans Blue and TTC staining. (A) Both IPC and RIC significantly reduced IS compared to control. Statistical significance was assessed using one-way ANOVA and Tukey's multiple comparison test, n=6, ***P<0.001, *P<0.05. Data presented as mean ± SEM; (B) Representative scanned transverse heart sections demonstrating Evans Blue area (blue), area at risk (pink) and infarct (white).

### 4.3.4 Discussion

Initial surgical experiments were complicated by a range of issues, as described in section 4.3.3. However, by making the refinements outlined above, it was possible to develop a robust and reproducible *in vivo* model of myocardial IRI.

The protocol described here, which is used as standard in our laboratory, applies 30 min of ischaemia followed by 2 h of reperfusion. This generated an IS of approximately 50%, which was broadly similar to the IS described in Chapter 2. Furthermore, the mean IS and SEM in this group were sufficient to be amenable to cardioprotection from known cardioprotective interventions, namely IPC and RIC, without being large enough to cause premature complications and death.

Previous studies have examined the impact of time of surgery on IS, and found significantly larger infarcts on animals undergoing surgery in the early morning.[326] This is of particular interest with reference to SDF-1α, which is known to exhibit

circadian rhythm in its expression in bone marrow.[327] To control for this potentially confounding effect, control and intervention groups were distributed evenly between morning and afternoon operating sessions, and no surgeries were conducted out of hours.

Furthermore, AAR exclusion criteria are a potential confounder as AAR is variable depending upon the exact position of the LAD suture and variable LAD anatomy, especially in Sprague Dawley rats that are reported to have variable IS and cardiac dysfunction after IRI due to variable LAD branching.[203] As discussed in section 3.3.2, IS has a strong positive correlation with AAR and, therefore, it is essential to evaluate both the AAR and absolute IS. Only then can IS be interpreted in context, as a percentage of AAR. This corrects, in part, for subtle variations in the position of the LAD suture and murine cardiac vessel anatomy. However, at the extremes of AAR the linear relationship with IS fails.[216, 258] This can confound results and, for this reason, hearts were excluded from analysis if the AAR was outside a pre-defined range (based on precedent within the laboratory) of 35-70%. The present study found no significant difference in AAR between the groups, and exclusions were evenly distributed between groups.

While MI clearly affects, thereby mandating basic research in, both genders, this was not specifically examined in experiments involving rats, which used male animals throughout. This experimental variable is discussed in more detail in section 4.4.4. All rats were anesthetised with pentobarbitone in view of our laboratory's experience with this agent, and the well-described cardioprotective effects of volatile anaesthetics such as isoflurane.[241] Furthermore, no impact of pentobarbitone on effect size was identified in Chapter 2. As discussed in 0, it is hypothesised that SDF-1α affects cardioprotection by activating the RISK pathway at the time of reperfusion. A remote ischaemic *pre*-conditioning protocol was applied here, and throughout this thesis, to allow sufficient time for circulating SDF-1α levels to reach their peak. This is discussed in more detail in section 7.4. Finally, all rats were ventilated with supplementary oxygen. Despite finding no difference between ventilation with room

air and supplementary oxygen in Chapter 2, the use of supplementary oxygen is routine in our laboratory. This is discussed in more detail in section 4.4.1.

## 4.4 Aim 2: Establish and verify a mouse *in vivo* model of myocardial ischaemia-reperfusion injury

Dr D. Bromage conceived and co-designed the oxygenation experiments described in this section. The experiments were performed by Dr D. He from the Hatter Cardiovascular Institute (UCL,UK).

### 4.4.1 Background

This non-recovery mouse model of myocardial IRI was first described in 1995.[328] It has since been used to investigate myriad interventions including IPC and RIC, both of which are well validated in this model.[181, 329] Prior to instituting this technique, it is necessary to consider important experimental variables. Although none apparently affected efficacy in the meta-analysis described in Chapter 2, there is interesting recent data from our laboratory that is apposite in this context.

Firstly, while the analysis in Chapter 2 found no significant difference in the efficacy of RIC in animals ventilated with oxygen versus those with room air, this may still be important in view of the finding of slower skeletal muscle de-oxygenation during RIC in the limbs of rats ventilated with supplementary oxygen in section 4.3.3. Therefore, a comparison of the efficacy of RIC in oxygenated versus un-oxygenated animals was performed in our laboratory by Dr D. He. This demonstrated a reduction in control IS in mice ventilated with oxygen and, importantly, cardioprotection by RIC was abrogated in these mice (Figure 4-6). To investigate whether this was a function of limb oxygenation or the lower control IS, further mice were treated with vehicle or 40 µg/kg bradykinin (a pharmacological cardioprotective agent), in addition to supplementary oxygen, prior to IRI.[218] Bradykinin conferred cardioprotection in these mice, despite oxygenation, suggesting that the development of IPC and RIC might be related to limb oxygenation.

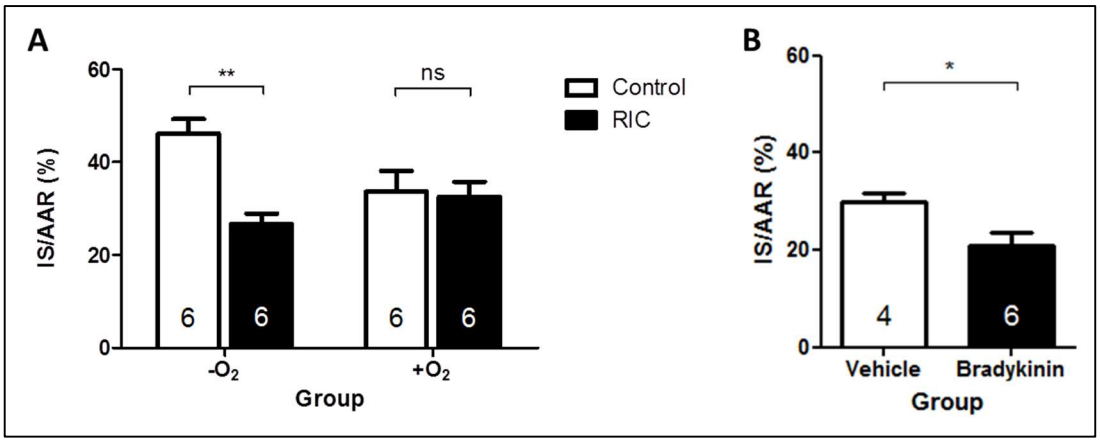


**Figure 4-6: Infarct size following remote ischaemic conditioning with and without supplementary oxygen *in vivo***

(A) Comparison of IS/AAR in C57BL/6 mice subjected to IRI with and without preceding RIC (three cycles of 5 min hind limb ischaemia and 5 min reperfusion) in animals ventilated with and without supplementary oxygen. RIC significantly reduced IS compared to control in mice ventilated with room air, but not in mice ventilated with 100% oxygen. Statistical significance was assessed using a two-way ANOVA with Bonferroni correction, n=6, **P<0.01; (B) In a separate experiment, bradykinin significantly reduced IS/AAR in mice ventilated with oxygen. Statistical significance was assessed using an unpaired t-test, n=4-6, *P<0.05. Data obtained by Dr D. He.

An alternative explanation might be that bradykinin is simply a more powerful cardioprotective intervention than RIC and, therefore, is able to protect over and above the diminished IS in oxygenated animals. Furthermore, oxygen clearly did not abrogate RIC in rats, due to the findings discussed in section 4.3.3. Nonetheless, based on the finding described here, mice used in this section were ventilated without supplementary oxygen.

Dr D. He also performed a similar assessment of blood flow during cuff inflation using high resolution laser Doppler imaging to that described in section 4.3.2. Interestingly, this demonstrated incomplete cessation of blood flow at a cuff pressure of 200 mmHg that was rectified by inflating the cuff to 250 mmHg (Figure 4-7). Therefore, a higher pressure of 250 mmHg was used specifically for the mouse *in vivo* model of RIC described in this thesis. Finally, in his further characterisation, Dr D. He found 30 min of ischaemia to be insufficient in the generation of a control IS amenable to cardioprotection, and instead applied 40 min of ischaemia (data not shown). This was

applied to the mouse *in vivo* model of IRI described in this thesis without further enquiry.

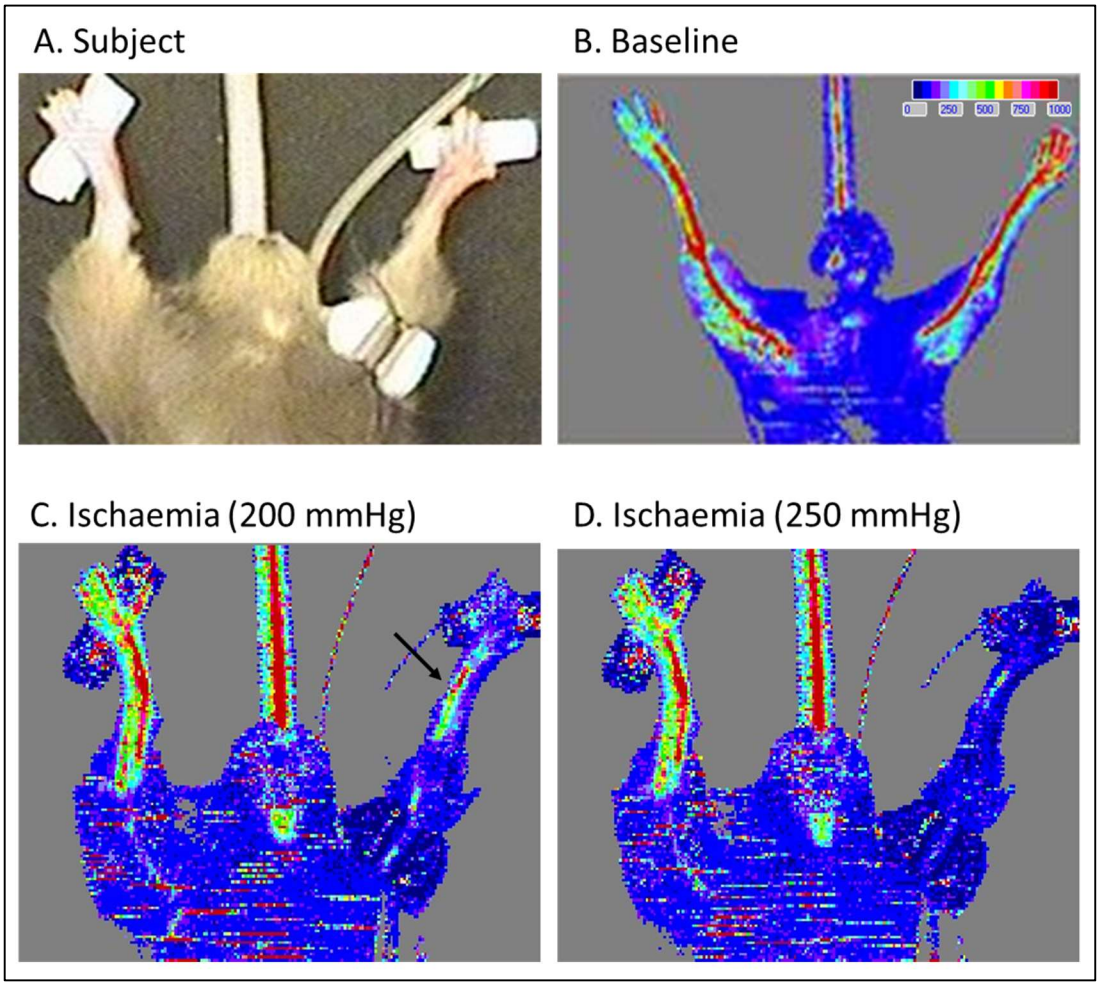


**Figure 4-7: Laser Doppler blood flow assessment demonstrating hind limb ischaemia during cuff inflation**

A mouse was anaesthetised and subjected to RIC (three cycles of 5 min hind limb ischaemia and 5 min reperfusion). A representative image from each step is shown here, alongside a plain photograph of the subject (A). During cuff inflation to 200 mmHg residual flow was apparent (Panel C, arrowed) compared to baseline (Panel B). This was abrogated by cuff inflation to 250 mmHg (Panel D). Data obtained by Dr D. He.

It was then necessary to both verify the ability of this model to demonstrate cardioprotection following the application of known cardioprotective interventions, and to confirm its reliability. In these experiments in mice, cardioprotection was validated using hypothermia and RIC.

### 4.4.2 Methods

Excess CXCR4$^{flox/flox}$ Cre$^{+/+}$, un-injected mice (wild type) were used in this experiment. *LoxP* sites were not expected to interfere with the generation of MI, and this is discussed further in section 4.4.4. All mice underwent 5 min of stabilisation, 30 min of (index) LAD ischaemia and 2 h of reperfusion, as described above. Heart sections were fixed in formalin for 24 h compared to 2 h in rats, as this was found to improve demarcation of infarcted and viable myocardium without significantly impacting on mean AAR or IS. This is discussed further in section 5.2.3.

During the characterisation of the model, it became apparent that the temperature probe was not calibrated and was overestimating core body temperature by 2$^{o}$C. Consequently, the homeothermic heat mat (Kent Scientific, CT, USA) was not hot enough, resulting in hypothermic animals (approximately 35±0.5$^{o}$C) for the duration of the experiment. Temperature regulation was subsequently managed manually using a rectal temperature probe, which was calibrated prior to each experiment, and adjustment of a heated veterinary operating mat.

Heart rate was recorded throughout using PowerLab 4/25 and Animal Bio Amp coupled to Chart 7 (AD Instruments, Oxon, UK). Mean heart rate over 5 min was specifically documented at the following time points: (1) baseline; (2) after the onset of ischaemia; (3) after the onset of reperfusion; (4) after 1 h reperfusion; and (5) prior to extraction of the heart.

Mice were subsequently randomly assigned to control or RIC groups and RIC was applied as described in section 2.4.3. The necessary sample size for the evaluation of RIC was calculated using a two-sided test for the comparison of two means. A 20% estimate of effect size was applied, based on the meta-analysis described in Chapter 3 and the following assumptions made: a control IS of 60%, a SD of 10%, a significance level of 5% ($\alpha$=0.05) and 80% power ($\beta$=0.2). This required a minimum sample size of four animals per group.

### 4.4.3 Results

During this experiment, reasons for failure were documented, audited and discussed with experienced operators, and a training log was maintained throughout. A summary is given in Figure 4-8.

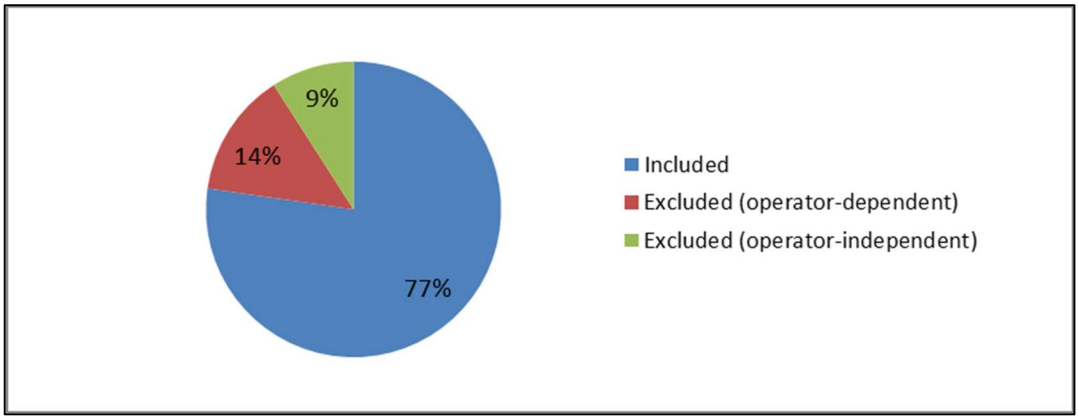


**Figure 4-8: Experimental success during characterisations of a mouse *in vivo* model of myocardial IRI**

22 animals were used during the course of the experiment. 17 were included in the analysis (77%). Excluded animals were defined as operator-dependent (60% of exclusions) or operator-independent (40%). The former related to surgical inexperience and included trauma to the LAD and inadequate staining with Evans blue. The latter were due to unexplained mortality, anaesthetic complications or due to their AAR falling outside the pre-defined range.

Overall, the treatment group (control, hypothermia or RIC) had a significant effect on heart rate throughout the experiment (n=4-7, P for effect of heart rate <0.05, Figure 4-9). Interestingly, mice treated with RIC had significantly lower heart rates at baseline compared to control animals (P<0.05), although hypothermic animals were generally more bradycardic throughout.

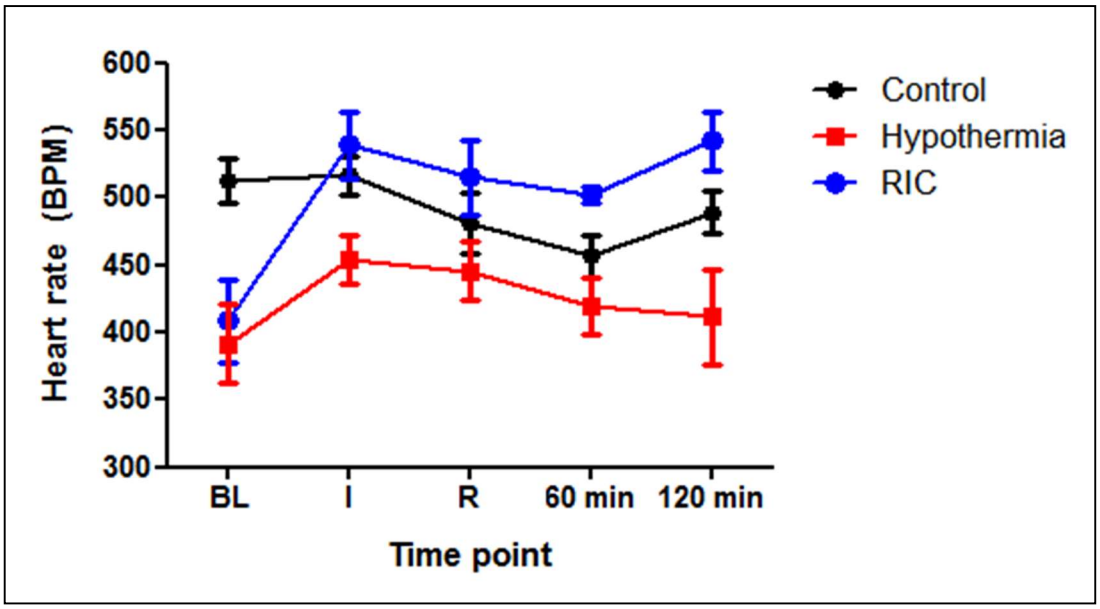


**Figure 4-9: Comparison of heart rate according to treatment group in mice**

C57BL/6 mice were anaesthetised and treated with either RIC (three cycles of 5 min hind limb ischaemia and 5 min reperfusion) or hypothermia prior to 40 min ischaemia and 2 h reperfusion *in vivo*. Mean heart rate was recorded over 5 min at each of the following time points: Baseline (BL); Immediately after the onset of ischaemia (I); Immediately following reperfusion (R) and at 60 and 120 min into reperfusion. Hypothermic animals had significantly lower heart rates than either normothermic (control) or RIC groups. Statistical significance was assessed using repeated measures ANOVA and Tukey's multiple comparison test, n=4-7, $P<0.05$.

This experiment measured IS as a proportion of AAR in mice following *in vivo* IRI. Six animals were included in the control group, four in the RIC group and seven in the hypothermia group. Analysis of their respective areas at risk revealed no significant differences (control 56±6% vs. RIC 59±5 vs. hypothermia 58±4%, n=6, P=NS, Figure 4-10).

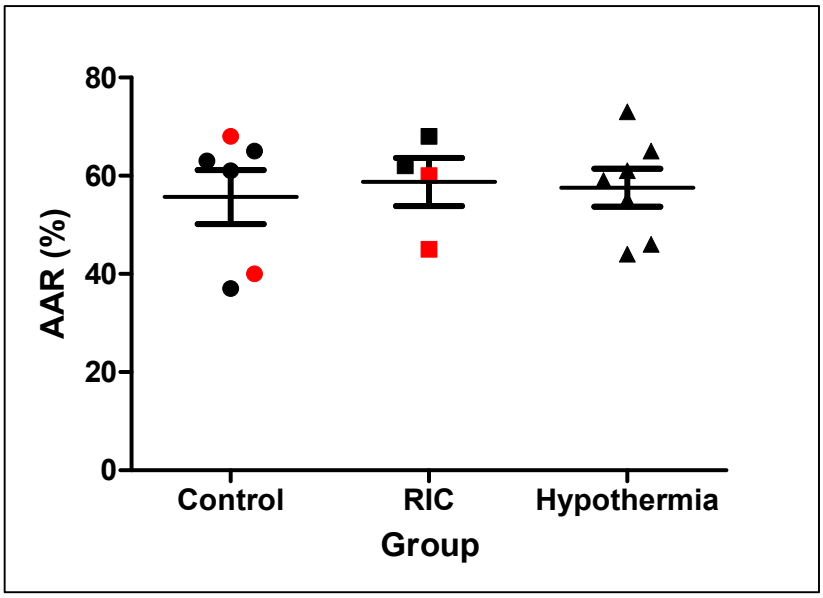


**Figure 4-10: Comparison of area at risk between control (normothermia), remote ischaemic conditioning and hypothermia groups**

C57BL/6 mice were anaesthetised and treated with either RIC (three cycles of 5 min hind limb ischaemia and 5 min reperfusion) or hypothermia prior to 40 min ischaemia and 2 h reperfusion *in vivo*. Analysis of their respective areas at risk, to ensure surgical consistency, revealed no statistically significant differences. Black points indicate male mice and red points indicate female mice. Statistical significance was assessed using one-way ANOVA and Tukey's multiple comparison test, n=4-7, P=NS for all comparisons. Data presented as mean ± SEM.

Subsequent analysis of IS as a proportion of AAR revealed that the application of IRI, as described, resulted in an IS of 43±3% (n=6, Figure 4-11), which is consistent with IS generated using standard protocols within our laboratory (data not shown). RIC significantly reduced IS/AAR compared to control (23±4%, n=4, P<0.0001 vs. control). Furthermore, hypothermia reduced IS/AAR compared to control to an even greater degree (14±1%, n=7, P<0.0001 vs. control, P<0.05 vs. RIC). Representative transverse heart sections are shown in Figure 4-11. This study confirms that it is feasible to investigate cardioprotection in this mouse *in vivo* model of IRI.

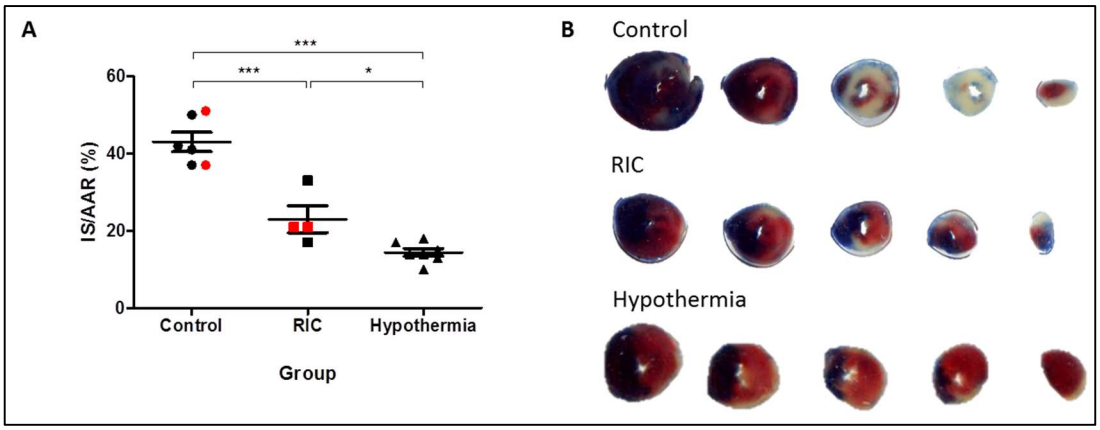


**Figure 4-11: Infarct size following remote ischaemic conditioning and hypothermia *in vivo***

C57BL/6 mice were anaesthetised and treated with either RIC (three cycles of 5 min hind limb ischaemia and 5 min reperfusion) or hypothermia prior to 40 min ischaemia and 2 h reperfusion *in vivo.* IS as a proportion of AAR was analysed using Evans Blue and TTC staining. (A) Both RIC and hypothermia significantly reduced IS compared to control. Black points indicate male mice and red points indicate female mice. Statistical significance was assessed using one-way ANOVA and Tukey's multiple comparison test, n=4-7, ***P<0.0001, *P<0.05. Data presented as mean ± SEM; (B) Representative scanned transverse heart sections demonstrating Evans Blue area (blue), area at risk (pink) and infarct (white).

Echocardiogram measurements were successfully obtained in 100% of control and RIC animals, and 74% of hypothermic animals, with the remainder attributable to poor image quality. Echocardiography revealed a pattern of reduced fractional shortening, stroke volume and cardiac output between scans performed before and after IRI, which reached significance with respect to stroke volume (P<0.001). Importantly, however, there was no discernible difference in any parameter between treatment groups (Figure 4-12).

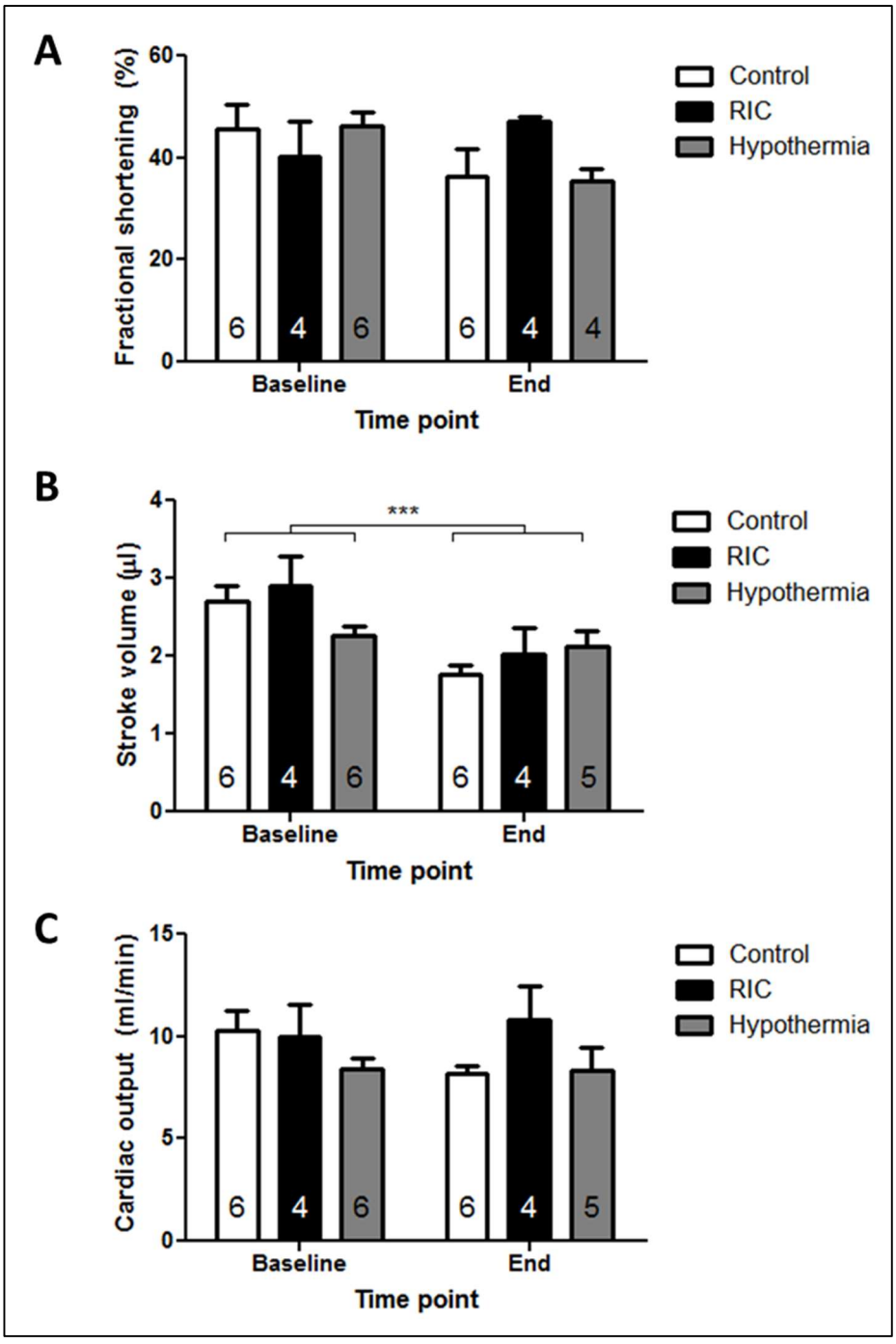


**Figure 4-12: A comparison of echocardiographic parameters according to treatment group**

C57BL/6 mice were anaesthetised and treated with either RIC (three cycles of 5 min hind limb ischaemia and 5 min reperfusion) or hypothermia prior to 40 min ischaemia and 2 h reperfusion *in vivo.* Echocardiography was performed prior to the onset of ischaemia (baseline) and prior to heart extraction (end). Stroke volume, but not fractional shortening or cardiac output, was significantly reduced after IRI. Treatment group (control, RIC and hypothermia) made no detectable difference to any of these parameters, either at baseline or after IRI. Statistical significance was assessed using two-way ANOVA and Bonferroni correction for multiple comparisons, n=4-6, ***P<0.001 between baseline and end.

As discussed in section 2.4.5, mouse heart sections were fixed in formalin for 24 h, in contrast to 1 h for rat heart sections. To exclude this as a source of bias, comparison was made between sections fixed for 1h and the same sections fixed for 24 h using the control group described above. Analysis of the areas at risk revealed no significant differences (1 h 56±4% vs. 24 h 56±6%, n=6, P=NS, Figure 4-13). IS as a proportion of AAR similarly revealed no significant difference (1 h 42±4% vs. 24 h 43±3%, n=6, P=NS, Figure 4-13).

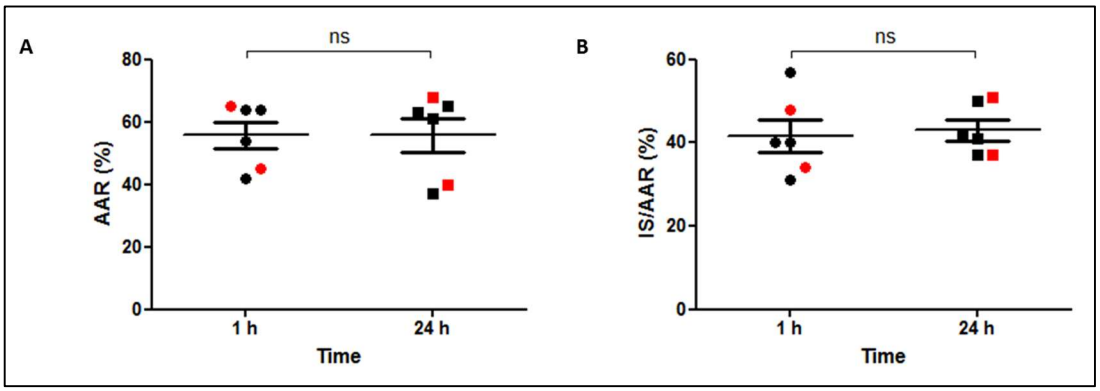


**Figure 4-13: Comparison of 1 h versus 24 h fixation time on area at risk and infarct size as a proportion of area at risk**

C57BL/6 mice were anaesthetised and subjected to 40 min ischaemia and 2 h reperfusion *in vivo.* IS as a proportion of AAR was analysed using Evans Blue and TTC staining, before either 1 h or 24 h fixation in formalin. Neither AAR (A) or IS/AAR (B) were significantly altered by a longer duration of fixation. Black points indicate male mice and red points indicate female mice. Statistical significance was assessed using paired t-tests, n=6, P=NS. Data presented as mean ± SEM.

To further investigate the effect of duration of fixation in formalin, a single sample was scanned daily for analysis of the AAR and IS (Figure 4-14). AAR remained stable up to day 9 while IS/AAR seemed to enlarge beyond 5 days of fixation. Representative images are given in Figure 4-14.

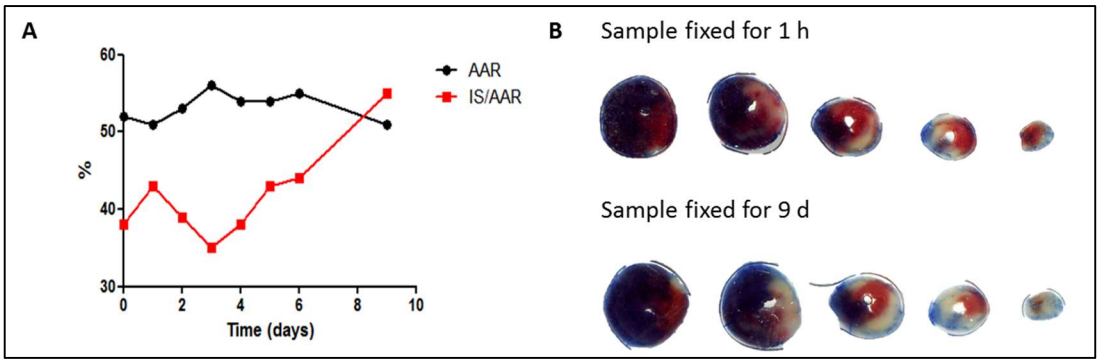


**Figure 4-14: Effect of formalin fixation time on area at risk and infarct size as a proportion of area at risk**

C57BL/6 mice were anaesthetised and subjected to 40 min ischaemia and 2 h reperfusion *in vivo.* IS as a proportion of AAR was analysed using Evans Blue and TTC staining, before fixation in formalin and daily analysis until day 9. (A) Effect of fixation in formalin on AAR (black line) and IS/AAR (red line); (B) Representative transverse heart sections scanned at 1 h and 9 days demonstrating Evans Blue area (blue), area at risk (pink) and infarct (white).

### 4.4.4 Discussion

This protocol conferred an IS of approximately 40%, which was consistent with the IS described in Chapter 3. Furthermore, this *in vivo* model of myocardial IRI was robust and reproducible; specifically, the mean IS and SEM in this group was sufficient to be amenable to cardioprotection from known cardioprotective interventions, namely RIC and hypothermia.

The C57BL/6 background strain was used throughout. This is the most widely investigated inbred general purpose strain and has the advantage of breeding well. C57BL/6 mice also tolerate the generation of most transgenic strains and are the background strain to the $CXCR4^{flox/flox}$ mice described above and used for this experiment. Specifically, all mice used here were un-injected, $CXCR4^{flox/flox}$ $Cre^{+/+}$ mice. As *LoxP* sites do not alter gene expression *per se*, they were not expected to affect IS or the ability to confer cardioprotection.

Mice of both genders were used in this study for several reasons: (1) both male and female humans suffer MI and it is therefore important that this is reflected in pre-clinical studies; (2) using both gender animals avoids animal wastage and is an important reductionist concept; and (3) no difference in the efficacy of RIC or IPC

according to gender was observed in the meta-analysis described in Chapter 3 or the study by Wever *et al.*, respectively.[102] While the numbers of each gender included in each group in the present study were too small for statistical comparison, there were no obvious trends and both male and female mice were included in mouse *in vivo* infarction studies throughout this thesis.

Mice were anaesthetised with pentobarbitone in view of our laboratory's experience with this agent, the lack of effect on WMD seen in Chapter 2, and the well-described cardioprotective effects of volatile anaesthetics such as isoflurane.[241] Similar studies have used a combination of ketamine, xylazine and atropine.[330] Although this reportedly has comparable haemodynamic effects to isoflurane and pentobarbitone,[296] all these agents adversely affect cardiovascular functional indices compared to tiletamine and zolazepam.[296] Nonetheless, in the absence of any experience in our laboratory of tiletamine and zolazepam, and to be consistent with the rat model, pentobarbitone was used throughout.

As discussed, mice were ventilated without supplementary oxygen. This factor was not specifically examined in this thesis, but it would be fascinating to investigate further as the effect of oxygenation on the development of RIC might have important implications for both pre-clinical and clinical study design.

In the present study, 40 min of ischaemia and 2 h of reperfusion were applied, and these durations were closely controlled. All experiments were distributed evenly between morning and afternoon operating sessions, and no surgeries were conducted out of hours. To correct for variations in the position of the LAD suture and murine cardiac vessel anatomy, IS was expressed as a percentage of AAR. To avoid confounding by areas at risk at either extreme, hearts were excluded from analysis if the AAR was outside a pre-defined range of 35-75%. This varied from the exclusion criteria used in rats due to different precedents in our laboratory. However, provided the exclusion criteria are applied consistently to all groups, this should not impact on experimental outcomes. The present results found no significant

difference in AAR between the groups, and exclusions were equally distributed between groups.

Although the initial intention was not to investigate hypothermia, it was decided to exploit the experiments in which mice were maintained at a lower temperature and examine its effects. Mild hypothermia is known to significantly reduce myocardial IS. For example, Hamamoto *et al.* demonstrated cardioprotection in sheep subjected to myocardial IRI after systemic cooling to 35.5$^{o}$C for the duration of ischaemia and reperfusion (IS/AAR 21.7±2.2% vs. 49.4±1.4% at 37.5$^{o}$C, P<0.05).[331] A similar effect has been demonstrated in several species, including 60-80 kg pigs, using several techniques, including endovascular, topical and intracoronary cooling.[332-337] These studies have applied hypothermia at various time-points during the ischaemia-reperfusion protocol, although Kanemoto *et al.* reported the temperature at reperfusion to correlate most strongly with reduction in IS.[333] All studies reduced core temperature between 2-5$^{o}$C and one study, by Chien *et al.*, reported a reduction in IS of approximately 10% for each 1$^{o}$C reduction in core body temperature.[338] This is broadly consistent with the present data that demonstrated a 25% reduction in IS with a 2$^{o}$C reduction in core body temperature (Figure 4-11).

The mechanism of hypothermia-induced cardioprotection has been less well investigated, but has been attributed to moderation of oxidative stress,[335] attenuation of the no-reflow phenomenon (whereby coronary microvasculature disruption during ischaemia impedes successful reperfusion),[339] inhibition of p53-mediated apoptosis and up-regulation of Akt,[340] increased NO synthesis and PKC activation.[341]

Interestingly, hypothermia apparently synergises with preconditioning, suggesting the mechanisms of protection are distinct. Van den Doel *et al.* reported that the combination of IPC and hypothermia applied in the setting of IRI in the *in vivo* rat heart reduced IS more than either intervention alone,[342] and a similar phenomenon has been demonstrated in rabbits.[334] However, this was not tested in the present study.

This study found a significantly reduced mean heart rate in hypothermic mice, which is caused by a non-vagal reduction in spontaneous sinoatrial node depolarisation. However, the advantages of hypothermia in IRI described above are apparently independent of this bradycardia (and consequent reduced myocardial oxygen demand and preservation of aerobic metabolism), as evidenced by studies that have maintained heart rate during hypothermia by electrical pacing and still observed a benefit with hypothermia.[337, 338]

Based on this pre-clinical evidence, there is significant interest regarding the potential benefit of therapeutic hypothermia in STEMI, and there have been several randomised controlled trials to date. These were recently subject to systematic review and meta-analysis which demonstrated that, despite being safe with regard to bleeding, ventricular arrhythmias and bradycardia, therapeutic hypothermia in STEMI did not benefit any clinical end-points.[343] The only significant benefit was seen with regard to IS, as measured by CMR or SPECT, in patients with anterior wall involvement. Interestingly, this is precisely the scenario in the present study where hypothermia mitigated IS in mice subject to LAD territory (anterior wall) IRI. Therefore, it is unclear how generally applicable the present results are.

In the RIC group there was significant bradycardia at baseline, measured prior to the onset of ischaemia and during the last cycle of RIC. This is interesting in the context of studies investigating the role of vagus nerve activation during RIC (reviewed by Gourine *et al.*[195]). Increased parasympathetic tone as a result of RIC may be responsible for the observed relative bradycardia. However, in a retrospective analysis of heart rates in the rat characterisation experiment described in section 4.3 there was no difference between control and RIC groups (P=NS, data not shown). Furthermore, a study investigating humoral and neural mechanisms of RIC likewise reported no effect of either pathway on heart rate.[181] This finding may therefore represent a chance statistical finding and was not pursued further.

Regarding the echocardiographic assessment of mice, it is known that the degree of LV impairment is directly proportional to IS,[223, 321] and the use of echocardiographic

parameters might therefore increase the reliability and validity of the results. The present study demonstrated a fractional shortening at baseline of 45.7±4.8%, which is consistent with published values that range from 34-45% for C57BL/6 mice of a similar age and weight.[223, 225, 344] However, cardiac output at baseline was 10.3±1.0 ml/min, which is lower than estimates in the literature of 14-21 ml/min, depending on the method used.[225] This is most likely to be attributable to underestimation of aortic root Doppler parameters due to an angle of incidence >15$^{o}$ or error associated with calculating the aortic root CSA.[224, 225] However, any error should not vary between experimental groups.

The broad pattern of deteriorating echocardiographic parameters over the course of the experiment, which reached significance with respect to stroke volume, might be attributable to infarction. However, in view of the lack of difference between injured and protected experimental groups, it seems more likely that this was a consequence of prolonged anaesthesia. As discussed, pentobarbitone adversely affects cardiovascular functional indices, which include heart rate, cardiac output, blood pressure and LV dimensions, compared to tiletamine/zolazepam.[296] This may explain the present results, although the relationship between duration of anaesthesia and LV impairment is unknown. Nonetheless, all groups were anaesthetised with pentobarbitone so, despite its negative inotropic and chronotropic effects, comparisons between experimental groups should remain valid.

Furthermore, the absence of any measurable difference in echocardiographic parameters between infarcted and protected groups is consistent with previously published reports that differences are only apparent after *at least* 1 week. Gao *et al.* subjected C57 mice to coronary artery ligation and only identified significant differences in LVIDd, LVIDs and FS after 3 weeks.[223]

## 4.5 Summary

This chapter describes the development and refinement of rat and mouse *in vivo* models of myocardial IRI. *In vivo* models of myocardial IRI have some important limitations. Firstly, as described above, several animals died prematurely in these

studies. It was not appropriate to measure IS in these animals due to the confounding effects of cardiopulmonary arrest. However, it is possible that this introduced bias towards animals with smaller infarcts and better survival. Nonetheless, survival was not different between experimental groups. Secondly, the application of IRI in an open-chest model has important differences to MI in humans. These include surgical trauma, including a profound inflammatory response, and the effect of anaesthesia on IS and autonomic tone, all of which can affect IS.[345] To this end, several groups have developed closed-chest, conscious, unrestrained models of *in vivo* IRI (reviewed by Lujan *et al*).[345] Thirdly, although staining with TTC is considered the gold standard for histological assessment of IS, its utility is impaired by: (1) difficulty in distinguishing cell types, including red blood cells in haemorrhagic infarcts; (2) subjectivity in defining infarct and AAR by planimetry; (3) 'stunning' of living cells, impairing their ability to reduce TTC; and (4) difficulty in identifying cells in the ischaemic penumbra that will die, particularly after short periods of reperfusion. Fourthly, it is important to acknowledge that ligating the LAD of young, healthy, drug naive animals does not necessarily reflect clinical experience with MI patients, and thereby limits the translational utility of this model.[238, 239]

Nonetheless, the key findings are that the IS conferred by IRI is consistent with previous data from our laboratory, and IS and variability were amenable to cardioprotection. The models were subsequently verified by demonstrating significant cardioprotection with the application of cardioprotective interventions, and are suitable for ongoing use in this thesis.

# Chapter 5 Is exogenous SDF-1α cardioprotective?

## 5.1 Introduction

The Working Group of Cellular Biology of the Heart of the European Society of Cardiology published criteria that must be satisfied to define a molecule as an endogenous mediator of IPostC.[103] These criteria apply equally to the characterisation of a molecule as an endogenous mediator of RIC and are (adapted from Ovize *et al*.[103]):

- Induction of a pharmacological cardioprotective effect by exogenous administration of the mediator at the time of reperfusion;
- Abolition of the effect by specific receptor blockade or by inhibition of the mediator's production;
- Increased production or maintenance of extracellular concentrations of the mediator(s) as a direct effect of RIC and
- Absence of cardioprotection in animals, tissues or cells with genetic disruption of the mediator's production or its receptor(s).

These criteria form the basis of subsequent chapters, and the limited number of studies that have investigated whether SDF-1α-CXCR4 meets any of these criteria are discussed therein. The first of these criteria is to investigate whether a pharmacological cardioprotective effect could be induced by exogenous administration of the mediator (SDF-1α) at the time of reperfusion.

## 5.2 Research aims and objectives

The objective of this chapter was to investigate whether exogenous administration of SDF-1α at the time of reperfusion mediates a pharmacological cardioprotective effect.

Aim 1: Investigate whether exogenous administration of SDF-1α at the time of reperfusion mediates a pharmacological cardioprotective effect

### 5.2.1 Background

The evidence for exogenous SDF-1α being cardioprotective in the context of myocardial IRI is considered in detail in section 1.4.2. As discussed, in data from our laboratory from a model of simulated IRI applied to *ex vivo* rat papillary muscle, SDF-1α administered prior to hypoxia significantly increased recovery of contractile function (Figure 5-1).[31]

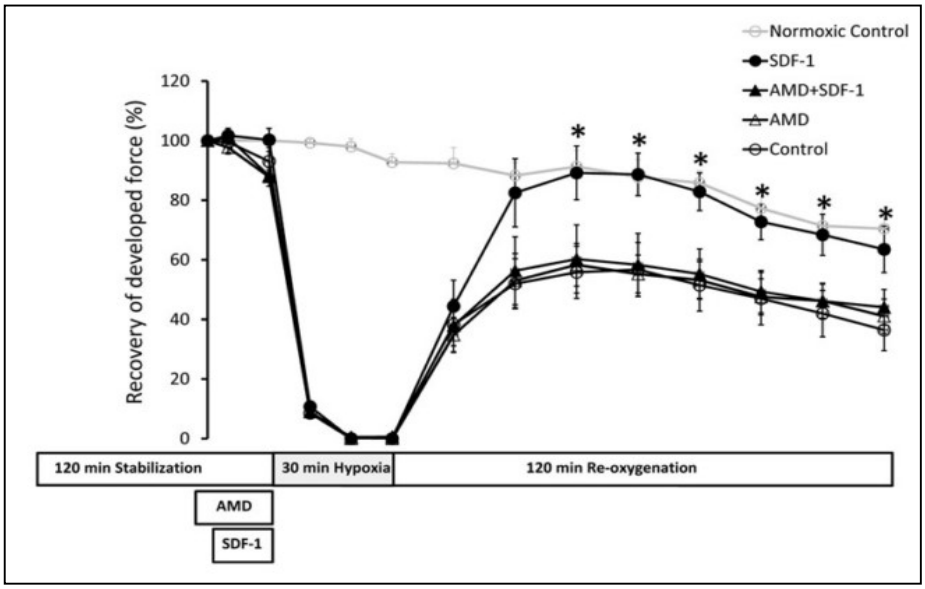


**Figure 5-1: The effect of SDF-1α in the recovery of developed force in isolated rat heart papillary muscle after simulated ischaemia reperfusion injury**

SDF-1α prior to ischaemia improves contractile recovery of rat heart papillary muscle that is isolated and subject to 30 min hypoxia and 2 h reoxygenation, compared to untreated (control) muscle. Before hypoxia, the rat papillary muscle was perfused with (1) SDF-1α for 10 min; or (2) AMD3100 for 5 min then AMD3100 plus SDF-1α for 10 min; or (3) AMD3100 alone for 15 min. Statistical significance was assessed using two-way ANOVA and Fisher's protected least significant difference test for multiple comparisons, n=6, *P<0.05. Figure from [31].

Similarly, SDF-1α has been shown to mimic the cardioprotection conferred by hypoxic preconditioning in a model of simulated IRI using isolated human atrial trabeculae muscle (Figure 5-2).[151]

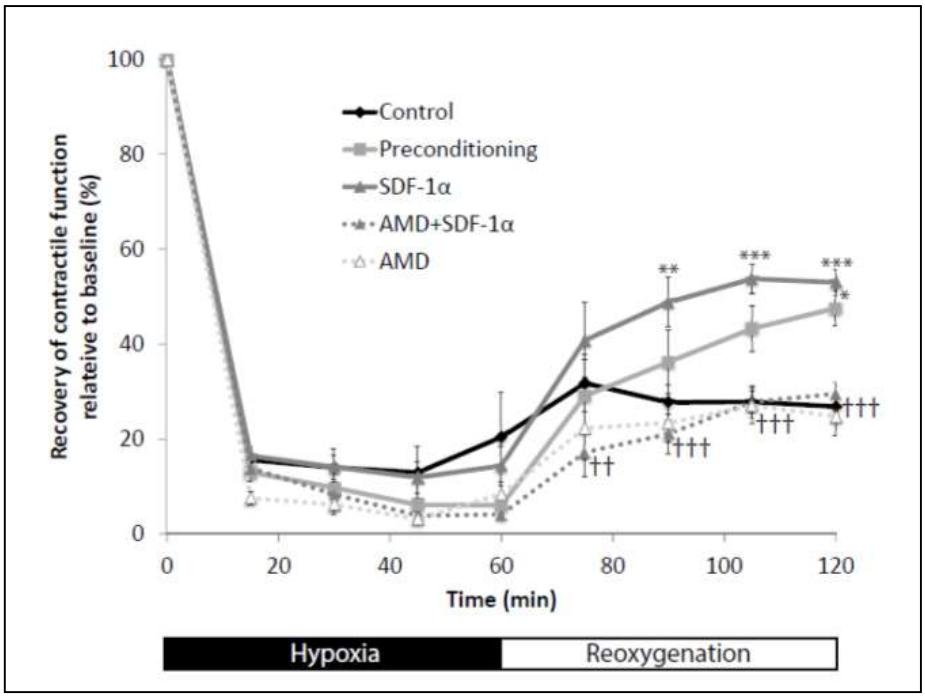


**Figure 5-2: The effect of SDF-1α in the recovery of developed force in human right atrial trabeculae after simulated ischaemia-reperfusion injury**

Recovery of contractile function during 60 min hypoxia and 1 h reoxygenation of isolated human atrial trabeculae is improved by pre-treatment with exogenous SDF-1α to a level similar to that conferred by hypoxic preconditioning. Statistical significance was assessed using two-way ANOVA and Fisher's protected least significant difference test for multiple comparisons, n=11 atrial trabeculae in the control and SDF-1α pre-treatment groups, 10 in the hypoxic preconditioning and AMD3100 + SDF-1α pre-treatment groups and 5 in the AMD3100 pre-treatment group, *SDF-1α vs. control, †AMD + SDF-1α vs. SDF-1α. Figure from [151].

Other laboratories have reported similar findings in a variety of settings. Huang *et al.* demonstrated better functional recovery after administering SDF-1α prior to the onset of ischaemia in an isolated mouse heart model of simulated IRI.[149] Jang *et al.* used a similar Langendorff model in rats and demonstrated a significant benefit on IS after the infusion of SDF-1α around the time of reperfusion.[150] In the only *in vivo* model investigating the potential acute efficacy of SDF-1α to date, Hu *et al*. demonstrated significantly reduced IS after infusing SDF-1α into the LV cavity of C57BL/6 mice prior to myocardial IRI.[46] Saxena *et al.* also administered intra-cardiac SDF-1α, albeit in a mouse model of permanent LAD ligation, and found better long-term recovery of function and less adverse remodelling.[20]

However, despite the promising results of Hu *et al.*, the direct translational potential of their approach is limited by both the necessity to administer SDF-1α before the onset of ischaemia, which is impossible to predict in MI, and the impracticality of infusing SDF-1α into the LV cavity. Furthermore, the paradigm for RIC defined in this thesis requires demonstrating an effect at the time of reperfusion. Therefore, the aim of this section was to investigate whether exogenous SDF-1α, administered peripherally during ischaemia and prior to reperfusion, can reduce the injury conferred by myocardial IRI.

### 5.2.2 Methods

$CXCR4^{flox/flox}$ $Cre^{+/+}$ mice that were neither injected with tamoxifen nor vehicle (phenotypically wild type) were used in this experiment. First, male mice were treated with either 0.9% saline (control) or 80 μg/kg SDF-1α (100 μl of 20 μg/ml stock for a 25 g animal, for example) by tail vein injection 10 min prior to blood sampling and analysis for SDF-1α as described in section 2.4.4. This served to demonstrate the efficacy of tail vein injection as well as ensuring that the administered dose of SDF-1α, chosen based on the studies described in section 5.2.1, resulted in plasma concentrations at the time of reperfusion at least as high as those described as being protective after RIC in the literature. For example, Jiang *et al.* demonstrated serum SDF-1α after RIC of approximately 7000 pg/ml,[29] and Kamota *et al.* measured peak levels in unfractionated plasma of approximately 3000 pg/ml.[30]

To test the protective utility of SDF-1α mice underwent 5 min of stabilisation, 40 min of (index) LAD ischaemia and 2 h of reperfusion, as described above. 80 μg/kg rhSDF-1α was administered by tail vein injection 10 min prior to reperfusion. Importantly, both male and female mice were used in this and subsequent experiments in mice.

Sample size was calculated using a two-sided test for the comparison of two means. Based on the results described in section 4.4.3, the following assumptions were made: a 20% estimate of effect size (which is more conservative than the benefit seen by Hu *et al.* which exceeded 30%[46]), a control IS of 40%, an SD of 10%, a significance

level of 5% (α=0.05) and 80% power (β=0.2). This required a minimum sample size of four animals per group.

### 5.2.3 Results

The surgical complications encountered in this experiment were similar to those described in section 4.4.3, although it is reassuring that the proportion of operator-dependent exclusions was reduced and there were no operator-independent exclusions. A summary is given in Figure 5-3.

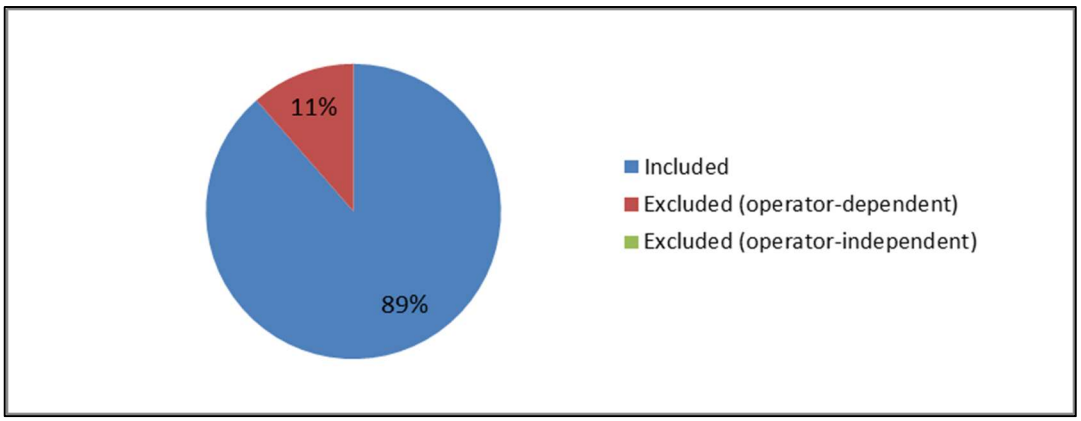


**Figure 5-3: Experimental success during investigation of whether SDF-1α is cardioprotective when given before reperfusion**

35 animals were used during the course of the experiment. 31 were included in the analysis (89%). All exclusions were defined as operator-dependent, and included three cases of accidental anaesthetic overdose and one case of missed tail vein injection.

This study confirmed that treatment with 80 μg/kg SDF-1α prior to reperfusion elevates the serum level of SDF-1α to 32,000 pg/ml (32 ng/ml), giving an approximate percentage recovery of 3% (Figure 5-4).

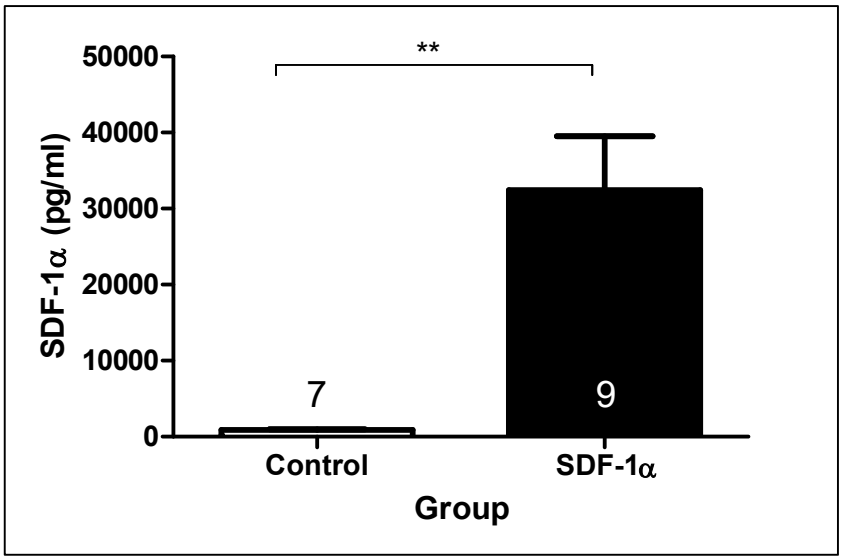


**Figure 5-4: Effect of tail vein injection of SDF-1α on concentration in platelet-free plasma in mice**

80 μg/kg rhSDF-1α or saline vehicle was administered by tail vein injection 10 min prior to blood sampling and analysis of PFP with ELISA. Statistical significance was assessed using an unpaired t-test, n=7-9, **P<0.01.

IS was measured as a proportion of AAR in C57BL/6 mice following *in vivo* IRI with injection of SDF-1α into the tail vein. Interim analysis revealed mean AAR of 65±5% and mean IS/AAR of 47±2% (n=3). This experiment was terminated prematurely (without a control group) as tail vein injection proved technically more difficult than in the characterisation experiment, possibly due to sympathetic activation during myocardial ischaemia. Therefore, RV administration was chosen to mimic peripheral administration as closely as possible. Furthermore, the apparent lack of cardioprotection (mean IS was similar to that described in section 4.4) in the present experiment may have been consequent upon an inadequate dose, which was subsequently increased to 200 μg/kg.

RV injection was well tolerated with no excess mortality. In the subsequent experiment, six animals were included per group and analysis of their respective areas at risk, to ensure surgical consistency, revealed no significant differences (control + vehicle 56±2% vs. control + SDF-1α 58±4%, n=6, P=NS, Figure 5-5).

Furthermore, the areas at risk in this experiment were very similar to those described in the characterisation experiment (section 4.4.3).

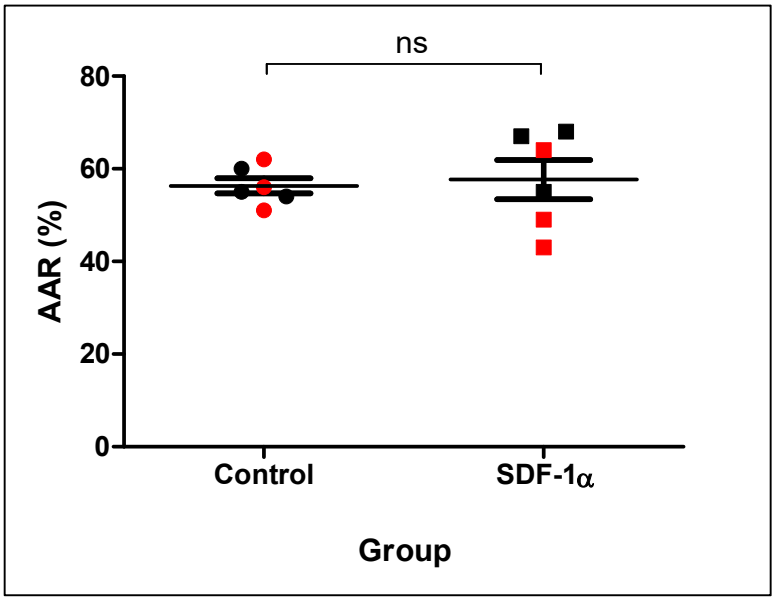


**Figure 5-5: Comparison of area at risk between control and SDF-1α groups**

C57BL/6 mice were anaesthetised and treated with either 200 µg/kg SDF-1α or 0.9% saline (control) by RV puncture prior to 40 min ischaemia and 2 h reperfusion *in vivo*. Analysis of their respective AAR revealed no statistically significant differences. Black points indicate male mice and red points indicate female mice. Statistical significance was assessed using an unpaired t-test, n=6, P=NS. Data presented as mean ± SEM.

Analysis of IS demonstrated that SDF-1α significantly reduced IS as a proportion of AAR (19±4%) compared to saline vehicle control (57±5%, n=6, P<0.001, Figure 5-6). The control group excluded a cardioprotective effect of RV puncture. In fact, the mean control IS in this experiment was greater than that described in section 4.4.3 (57±5% vs. 43±2%), suggesting a possible injurious effect of RV puncture *per se*, despite being ostensibly well tolerated. Representative transverse heart sections are shown in Figure 5-6.

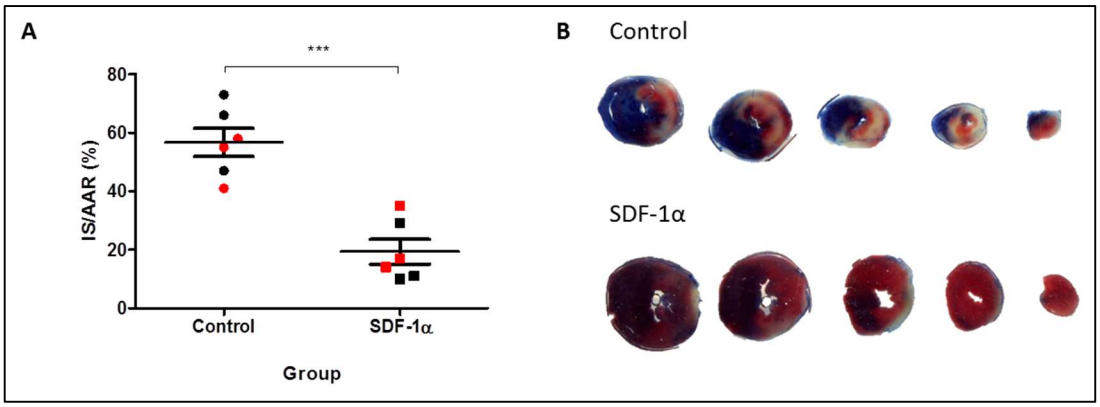


**Figure 5-6: Infarct size following the administration of SDF-1α prior to reperfusion *in vivo***

C57BL/6 mice were anaesthetised and treated with either 200 µg/kg SDF-1α or 0.9% saline (vehicle control) by RV punture 40 min prior to ischaemia and 2 h after reperfusion *in vivo.* IS as a proportion of AAR was analysed using Evans Blue and TTC staining. (A) SDF-1α administered by RV puncture 10 min prior to reperfusion significantly reduced IS compared to control + vehicle. Black points indicate male mice and red points indicate female mice. Statistical significance was assessed using an unpaired t-test, n=6, ***P<0.001. Data presented as mean ± SEM; (B) Representative scanned transverse heart sections demonstrating Evans Blue area (blue), area at risk (pink) and infarct (white).

### 5.2.4 Discussion

This study demonstrated that SDF-1α, delivered prior to reperfusion, is acutely cardioprotective in a mouse *in vivo* model of myocardial IRI. Importantly, it is the first time SDF-1α has been shown to protect when administered during ischaemia, thereby improving its translational potential.

SDF-1α was administered prior to reperfusion for several reasons: (1) as discussed in 0, SDF-1α has an estimated plasma half-life of 25.8±4.6 min, due to proteolysis by DPP4 and other peptidases.[53] In the present study, percentage recovery of injected SDF-1α from plasma using an ELISA specific for the active form was only 3%. Therefore, if SDF-1α was administered prior to ischaemia (to correlate with the application of RIC) almost complete degradation would be expected by the time of reperfusion. This is important because, as discussed in section 1.4.4, SDF-1α is posited to confer cardioprotection by activating the protective RISK pathway at the time of reperfusion. This degradation could be prevented by the co-administration of a DPP4 inhibitor. However, this would confound the present result due to preservation of GLP-1, which is also postulated to be cardioprotective in myocardial

IRI (reviewed by Clarke *et al.*[346]); (2) studies have suggested that SDF-1α takes up to 1 h to reach peak levels after the application of RIC.[29, 30] If correct, this further supports the hypothesis that if SDF-1α mediates remote ischaemic *pre*-conditioning it does so via an effect at the time of reperfusion. This is discussed in detail in Chapter 7; and (3) although not directly related to the present hypothesis, administering a pharmacological conditioning mimetic prior to reperfusion is more clinically relevant than administration prior to ischaemia, which is impossible to predict in humans. Hu *et al.* infused SDF-1α into the LV cavity followed by 10 min washout before the induction of ischaemia.[46] Therefore, the SDF-1α would have reached, and potentially affected, effector cells in the heart prior to ischaemia. This is not feasible in human patients suffering MI who, by definition, do not present until after the onset of ischaemia. The present study therefore confirms an effect specifically on reperfusion injury.

The initial absence of benefit from SDF-1α could either be due to inadequate delivery via the tail vein or an insufficient dose. The *in vivo* studies described above administered SDF-1α in concentrations of 12-175 μg/kg.[20, 46] In the absence of protection with the initial dose of 80 μg/kg, the dose was successfully increased to 200 μg/kg. Although Jang *et al.* have demonstrated dose-dependent cardioprotection with SDF-1α using an *ex vivo* Langendorff model of myocardial IRI,[150] it is not possible to comment on possible dose-dependent cardioprotection in the present study as the tested doses were administered via different routes. Nonetheless, control mice treated with saline vehicle via RV puncture remained significantly more injured than SDF-1α-treated groups.

Hu *et al.* identified CXCR4 on cardiomyocytes and cardiac fibroblasts, and induced SDF-1α release from *in vitro* cardiomyocytes using hypoxia.[46] This engendered the hypothesis that exogenous SDF-1α is cardioprotective by augmenting endogenous autocrine/paracrine signalling. The present experiment does not specifically implicate CXCR4 as the mediator of protection conferred by SDF-1α. Instead, SDF-1α could exert its effects via CXCR7, an alternative chemokine receptor for SDF-1α that is discussed in more detail in section 6.3.4, or via another mechanism entirely. It

would be possible to confirm this by addition of AMD3100, in a similar manner to the experiment described in Chapter 6. However, this was beyond the scope of this thesis, which specifically aimed to investigate a putative mechanism of RIC. Nor does the present finding identify the organ or cell type upon which SDF-1α is acting, which is discussed further in Chapter 8.

Finally, the specific intracellular mechanism of SDF-1α that affects cardioprotection is unknown and remains controversial. As discussed in 0, several mechanisms by which SDF-1α exerts acute cardioprotection have been proposed. For example, Huang *et al.* identified activation of STAT3 without concomitant phosphorylation of Akt or Erk1/2 and no loss of protection with LY294002.[149] Importantly, however, the inhibitors were given prior to ischaemia and not prior to reperfusion (the time-point at which the RISK kinases are defined to act), and hence it may be that Akt is still integral to mitigating reperfusion injury specifically. Others have implicated a role for Akt and Erk1/2 when SDF-1α is administered around the time of reperfusion.[150] The intracellular mechanism of SDF-1α-mediated cardioprotection is not specifically investigated in this thesis but is an important target for subsequent clarification.

## 5.3 Summary

This chapter provides the first description of cardioprotection as a result of the administration of exogenous SDF-1α prior to reperfusion in a murine model of myocardial IRI. The use of SDF-1α during ischaemia builds upon previous *in vivo* studies that reduced IS using SDF-1α prior to the onset of ischaemia, thereby improving its therapeutic relevance. The present study does not indicate a target cell-type or potential mechanism of action of SDF-1α, but does satisfy the first criteria necessary to define a molecule as a mediator of RIC.

# Chapter 6 Does the SDF-1α receptor blocker, AMD3100 abrogate the cardioprotective effect of remote ischaemic conditioning?

## 6.1 Introduction

The second condition that must be satisfied to define a molecule as an endogenous mediator of cardioprotection, according to The Working Group of Cellular Biology of the Heart of the European Society of Cardiology,[103] is abolition of the effect by specific receptor blockade.

AMD3100 (Plerixafor) is a specific inhibitor of CXCR4 that retains its specificity independent of the cell type carrying the receptor, although it should be noted that allosteric agonism of CXCR7 has recently been reported.[32, 347] No selectivity data comparing different CXC receptors has been published but AMD3100 is known to have a $K_i$ of 100-650 nM for CXCR4.[348, 349] Numerous studies have demonstrated a loss of effect of SDF-1α when given with or after AMD3100 in a variety of settings and models including in the *in vivo* model of myocardial IRI employed by Hu *et al*.[46] It was therefore essential to the present study to examine the effect of AMD3100 on cardioprotection conferred by RIC *in vivo*.

## 6.2 Research aims and objectives

The main objective of this chapter was to investigate whether the SDF-1α receptor blocker AMD3100 abrogates the cardioprotective effect of RIC. The research aims for this objective were:

1. Investigate whether the SDF-1α receptor blocker AMD3100 abrogates the cardioprotective effect of RIC;
2. Identify CXCR4 on rat and human cardiomyocytes.

## 6.3 Aim 1: Investigate whether the SDF-1α receptor blocker AMD3100 abrogates the cardioprotective effect of remote ischaemic conditioning

Rat cardiomyocytes used in this section were isolated and donated by Dr O. Ziff, Hatter Cardiovascular Institute (UCL, UK).

### 6.3.1 Background

As discussed in Chapter 1 and section 5.2.1, numerous studies have abrogated beneficial effects of SDF-1α with AMD3100, thereby implicating CXCR4 in the mechanism. This has also been shown in the context of RIC, albeit in an isolated cardiac papillary muscle model.[31] Davidson *et al.* demonstrated that RIC applied *in vivo* to a rat, prior to isolation of papillary muscle and simulated IRI, significantly improved functional recovery (Figure 6-1).[31] This effect was blocked by AMD3100. Likewise, AMD3100 abrogated the benefit conferred by the addition of SDF-1α in the same model, as discussed in section 5.2.1 (Figure 5-1).

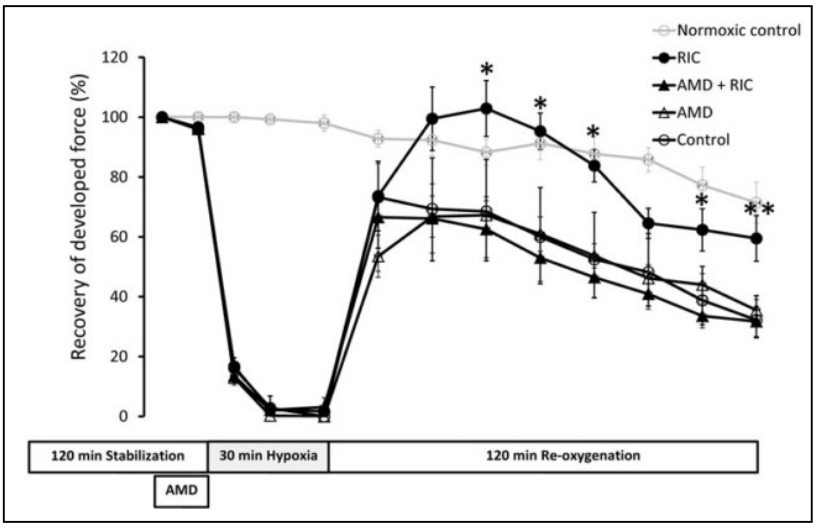


**Figure 6-1: The effect of AMD3100 on the improvement of developed force after remote ischaemic conditioning in isolated rat heart papillary muscle**

*In vivo* RIC (three cycles of 5 min hind limb ischaemia and 5 min reperfusion) prior to isolation of rat heart papillary muscle and simulated IRI (30 min hypoxia and 2h reoxygenation) improved contractile recovery. Before hypoxia, the rat papillary muscle was perfused with AMD3100 for 15 min. Control papillary muscle was untreated. The functional recovery of muscle treated with RIC was significantly improved, an effect that was abrogated by AMD3100. Statistical significance was assessed using two-way ANOVA and Fisher's protected least significant difference test for multiple comparisons, n=6, *P<0.05, **P<0.01. Figure taken from [31].

Similarly, in the model of simulated IRI using isolated human atrial trabeculae, AMD3100 abrogated the beneficial effect of SDF-1α in terms of recovery of contractile function.[151] Therefore, the aim of this section was to investigate whether

AMD3100, administered peripherally prior to IRI, can abrogate the beneficial effect of RIC on myocardial IRI *in vivo*.

### 6.3.2 Methods

Rats were randomly assigned to control plus vehicle, control plus AMD3100, RIC plus vehicle or RIC plus AMD3100 groups. 10 µg/kg (250 µl of 10µg/ml stock for a 250 g animal, for example) AMD3100 (Tocris Bioscience, C of Bris, UK) was administered to a rat by intravenous tail vein injection 5 min prior to the first cycle of cuff inflation (Figure 6-2). This dose was chosen based on previous experience in our laboratory.[31]

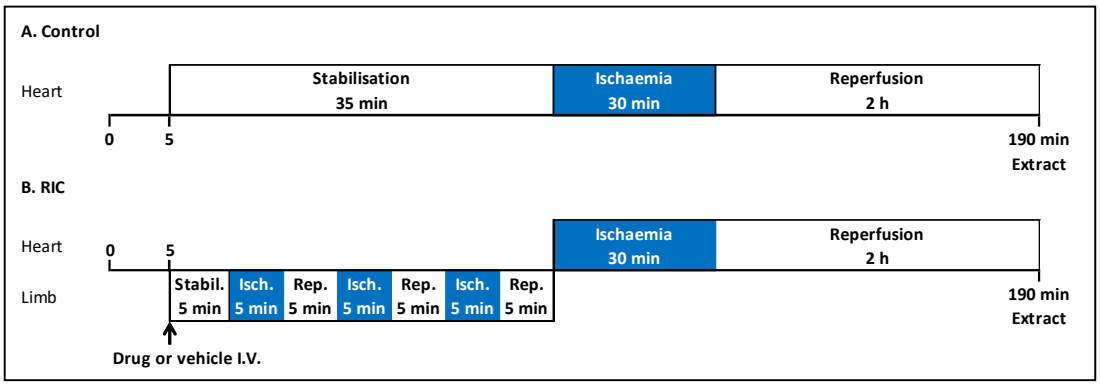


**Figure 6-2: Remote ischaemic conditioning and ischaemia-reperfusion injury protocols, and AMD3100 administration**

(A) Control: 35 min stabilisation, 30 min ischaemia and 2 h reperfusion; (B) RIC: 5 min stabilisation, three cycles of 5 min hind limb ischaemia and 5 min reperfusion, 30 min ischaemia and 2 h reperfusion. AMD3100 or vehicle was administered by tail vein injection at the beginning of the stabilisation period. Figure not to scale.

Sample size was not calculated *a priori* for any experiments in rats, in which six animals were used per group in line with convention.

### 6.3.3 Results

The surgical complications encountered in this experiment were similar to those described in section 4.3, although it is reassuring that the number of operator-dependent exclusions and total number of included animals were improved in comparison. None were excluded due to missed tail vein injection, although it was

occasionally necessary to attempt tail vein injection up to three times. A summary is given in Figure 6-3.

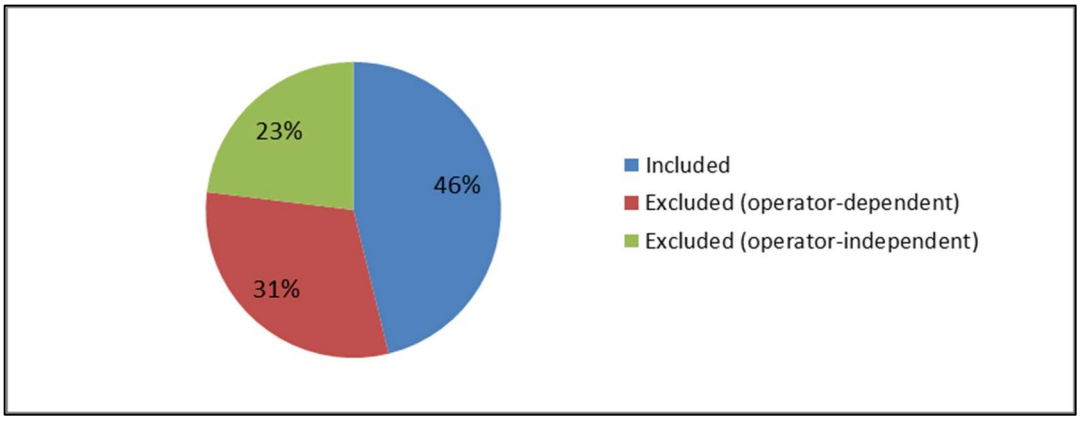


**Figure 6-3: Experimental success during investigation of whether AMD3100 abrogates the cardioprotective effect of remote ischaemic conditioning**

52 animals were used during the course of the experiment. 24 were included in the analysis (46%). Excluded animals were defined as operator-dependent (57% of exclusions) or operator-independent (43% of exclusions). Surgically-induced haemorrhage was eliminated by the refinements described in section 4.3 and the subsequent predominant reason for operator-dependent exclusions was inadequate staining with Evans blue. Reasons for operator-independent exclusions were similar to those described in section 4.3.

This experiment measured IS as a proportion of AAR in Sprague Dawley rats following *in vivo* IRI. Six animals were included per group and analysis of their respective areas at risk, to ensure surgical consistency, revealed no significant differences (control + vehicle 55±2% vs. control + AMD 55±4% vs. RIC + vehicle 61±4% vs. RIC + AMD 53±5%, n=6, P=NS, Figure 6-4).

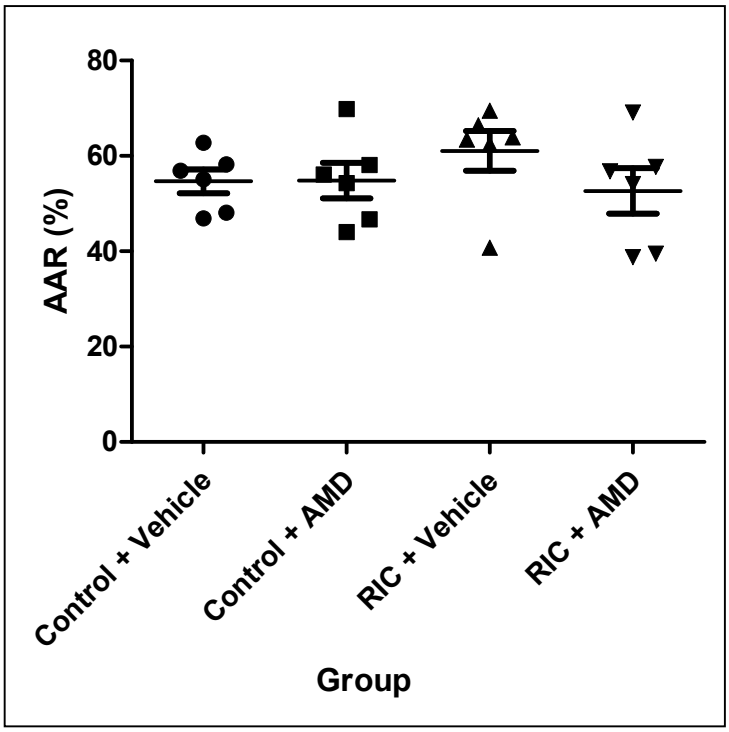


**Figure 6-4: Comparison of area at risk in rat hearts between control and remote ischaemic conditioning groups, treated with or without AMD3100**

Sprague Dawley rats were anaesthetised and treated with RIC (three cycles of 5 min hind limb ischaemia and 5 min reperfusion) or acted as sham controls. Rats were treated in vivo with or without 10 μg/kg AMD3100 (AMD) or 0.9% saline (vehicle control) 35 mins prior to 30 min of ischaemia and 2 h of reperfusion. Data presented as mean ± SEM. Statistical significance was assessed using one-way ANOVA and Tukey's multiple comparison test, n=6, P=NS. Analysis of their respective areas at risk (AAR), to ensure surgical consistency, revealed no statistically significant differences. Data presented as mean ± SEM.

Subsequent analysis of IS as a proportion of AAR repeated the finding in section 4.3 that RIC significantly reduced IS as a proportion of AAR (31±3%, n=6) compared to either control (57±3%, n=6, P<0.001 vs. RIC + vehicle) or the administration of AMD3100 alone (62±2%, n=6, P<0.001 vs. RIC + vehicle, Figure 6-5). In support of the hypothesis, pre-treatment with AMD3100 abrogated the beneficial effect of RIC (56±4%, n=6, P<0.01 vs. RIC + vehicle, Figure 6-5). Representative transverse heart sections are shown in Figure 6-5.

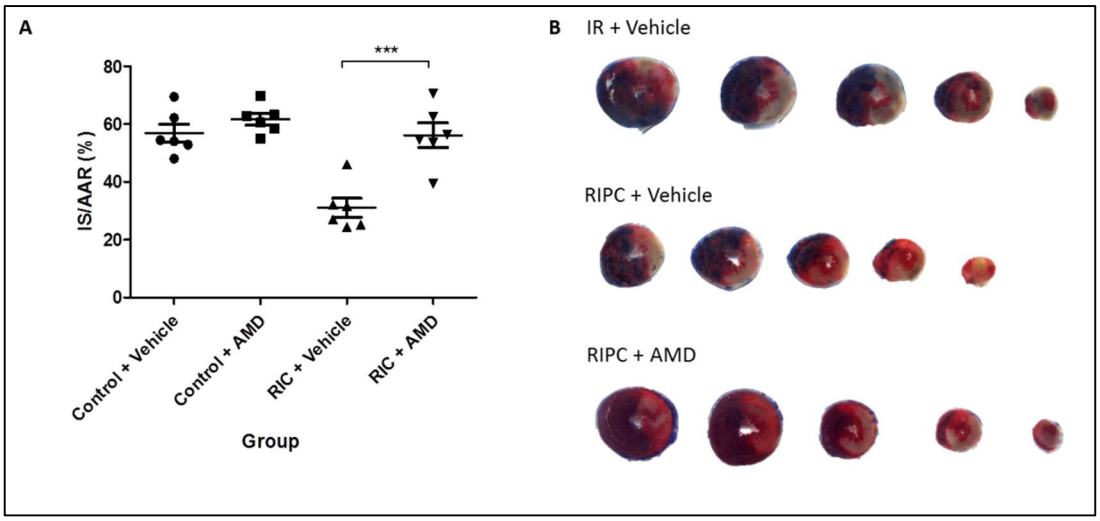


**Figure 6-5: Infarct size following myocardial ischaemia-reperfusion injury (control) with remote ischaemic conditioning *in vivo*, with or without AMD3100**

Sprague Dawley rats were anaesthetised and treated with RIC (three cycles of 5 min hind limb ischaemia and 5 min reperfusion) or sham, with or without AMD3100 or 0.9% saline control, prior to 30 min ischaemia and 2 h reperfusion *in vivo.* IS as a proportion of AAR was analysed using Evans Blue and TTC staining. (A) RIC + vehicle significantly reduced IS compared to control + vehicle, which was abrogated by the addition of AMD3100. AMD3100 alone (control + AMD) did not alter IS. Statistical significance was assessed using one-way ANOVA and Tukey's multiple comparison test, n=6, ***P<0.001. Data presented as mean ± SEM; (B) Representative scanned transverse heart sections demonstrating Evans Blue area (blue), area at risk (pink) and infarct (white).

As discussed, parametric tests cannot correctly be applied to non-Gaussian data; however, statistical tests of normality are precluded by small sample sizes, and non-parametric statistical tests have significantly lower power. Therefore, the control data from both this experiment and the characterisation experiment described in section 4.3 were retrospectively combined to test the assumption made in section 2.10 that animal data in this thesis is normally distributed. The D'Agostino-Pearson omnibus test confirmed a Gaussian distribution (P=0.9969), which will continue to be assumed throughout this thesis.

### 6.3.4 Discussion

This experiment investigated the effect of pre-treatment with AMD3100 on the efficacy of RIC in a rat *in vivo* model of myocardial IRI. Rats were used for this experiment in view of the difficulty with SDF-1α administration described in section

5.2.3. Here, the larger size of rats compared to mice facilitated tail vein injection. While it would be preferable to investigate all aspects of this project in the same species, visual inspection of the funnel plot in Chapter 3 revealed no difference in the efficacy of RIC between rats and mice. Furthermore, if SDF-1α is central to the mechanism of RIC, it is known to be highly conserved between species.[28, 38]

AMD3100 was given prior to RIC to facilitate CXCR4 antagonism prior to possible SDF-1α up-regulation during RIC. Of note, AMD3100 was expected to continue blocking CXCR4 at the time of reperfusion, evidenced by binding assays showing it to be selective, tight-binding and slowly reversible (taking up to 48 h in one study).[348] As expected, pre-treatment with AMD3100 abrogated the beneficial effect of RIC in this model. Although this strongly implicates SDF-1α in the mechanism of RIC, it does not necessarily prove it as other potential ligands for CXCR4 have been identified, including MIF and ubiquitin.[350] [351]

MIF, like SDF-1α, is a chemokine that plays a role in monocyte recruitment and has attracted attention in the context of IRI.[350] It is known to be immobilised on the endothelial surface and mediate the arrest of rolling macrophages in inflammation via CXCR2.[350] MIF has also been implicated in cardioprotection from myocardial IRI, via AMP-activated protein kinase signalling, inhibition of apoptosis and the reduction of oxidative stress,[352] effects that are enhanced by post-translational S-nitrosation of MIF.[353] These findings have begun to be translated to clinical studies, with the majority of studies to date noting a significant increase in MIF after a cardiac insult, including MI, PPCI, cardiac surgery and cardiopulmonary resuscitation (reviewed by Rassaf *et al.*).[352] In clinical studies, high levels of MIF have been associated with improved outcome after cardiac surgery.[354] There is, however, no published pre-clinical or clinical data on MIF-mediated RIC to date, although the RIPHeart group examined MIF levels at several time points before and after RIC and IRI and found no significant differences (personal communication).

Ubiquitin is a small intracellular protein that is involved in post-translational modification (so-called ubiquination). However, they have also been reported to be

extracellular and to agonise CXCR4, but not CXCR7.[351] Saini *et al.* report that unlike SDF-1α, ubiquitin binds independently of the CXCR4 N-terminal receptor domain.[351] However, they found it to cause a similar G protein-coupled up-regulation of intracellular Akt and Erk phosphorylation, albeit much more transiently than by SDF-1α. The impact of ubiquitin, if any, on IRI has not been investigated.

Other limitations of this experiment include that AMD3100 is a partial agonist of CXCR7, the role of which was not investigated here. However, as AMD3100 is a partial agonist of CXCR7, any effect on CXCR7 in the context of myocardial IRI should be evident in the group treated with AMD3100 alone. This group was statistically indistinct from the group pre-treated with saline vehicle and it is therefore unlikely that CXCR7 is important in the context of this experiment.

Finally, it should be considered that AMD3100 might have other 'off-target' effects. Although AMD3100 is thought to be highly specific, without interaction with either CXC or CC receptor subtypes (apart from CXCR7, as described),[32] it is impossible to definitively exclude alternative actions. However, an alternative approach is to confirm the role of CXCR4 by using CXCR4 null mice, which is addressed in Chapter 8.

## 6.4 Identify CXCR4 on rat and human cardiomyocytes

### 6.4.1 Background

The experiments described in sections 5.2.1 demonstrate a protective effect of SDF-1α in *ex vivo* isolated rat papillary muscle and isolated human atrial trabeculae subjected to simulated IRI.[31, 151] Moreover, AMD3100 has also been found to abrogate the protective utility of exogenous SDF-1α in both of these models.[31, 151] In the absence of other organs and tissues, these findings engender the hypothesis that SDF-1α protects the myocardium from (simulated) IRI via its action(s) on one or more cardiac cell types.

As discussed in 0, CXCR4 is reported to be expressed by a range of cardiac cell types. Its expression by cardiomyocytes, which account for 25-35% of all cells in the heart,[355]

is well documented but it has also been identified in vascular smooth muscle cells,[47] endothelial cells,[44] and fibroblasts.[46] In the context of acute cardioprotection, only cardiomyocytes and fibroblasts have been investigated to date. Hu *et al.* isolated ventricular cardiomyocytes and cardiac fibroblasts from adult male C57BL/6 mice and found both cell types to express CXCR4 and SDF-1α.[46] Hypoxia and reoxygenation resulted in significantly increased SDF-1α release from cardiomyocytes but not from cardiac fibroblasts. They next administered exogenous SDF-1α to isolated cardiomyocytes and found increased phosphorylation of both Erk1/2 and Akt, less lactate dehydrogenase release and less apoptosis, thereby implicating cardiomyocyte-expressed CXCR4 in the mechanism of protection.

Aside from the limited literature on SDF-1α-CXCR4 in the context of acute cardioprotection, cardiomyocytes are also implicated in the wider field of SDF-1α-CXCR4 in chronic cardioprotection. Most notably, Dong *et al.* described loss of the beneficial effect of MSC infusion after permanent ligation of the LAD in cardiomyocyte-specific CXCR4 null mice.[75]

To support the hypothesis that SDF-1α protects the myocardium from IRI via its action on cardiomyocytes, it is necessary to demonstrate the expression of CXCR4 by cardiomyocytes. The aim of this section was therefore to confirm that CXCR4 is present in rat and human cardiomyocytes, to support the preliminary data discussed above and the finding reported in section 6.3.

### 6.4.2 Methods

Isolated cardiomyocytes obtained from male Sprague Dawley rats weighing 200-250 g were prepared and stained for immunofluorescence as described in section 2.6. The primary antibody was rabbit monoclonal anti-CXCR4 (ab124824), which was used at a dilution of 1:100. Alexa Fluor 488 anti-rabbit secondary antibody was diluted 1:400. Control samples were incubated in Alexa Fluor 488 in the absence of primary antibody, to exclude non-specific staining with secondary antibody.

In a separate series of experiments, isolated human atrial trabeculae were obtained and processed as described in section 2.6, and labelled as above. To investigate the spatial distribution of CXCR4, immunofluorescent co-staining of CXCR4 and cardiomyocytes was performed using mouse 1:10 anti-cardiac troponin T (ab8295) and anti-mouse Alexa Fluor 555 secondary antibody. A sample incubated in secondary antibody alone was included as a control.

### 6.4.3 Results

Immunofluorescent staining of isolated rat cardiomyocytes appeared to demonstrate the presence of CXCR4 (Figure 6-6). However, control samples that were stained with secondary antibody alone demonstrated similar fluorescence intensity. It is therefore unlikely that the signal in these images represents the true distribution of CXCR4 but instead may represent non-specific binding of the secondary antibody.

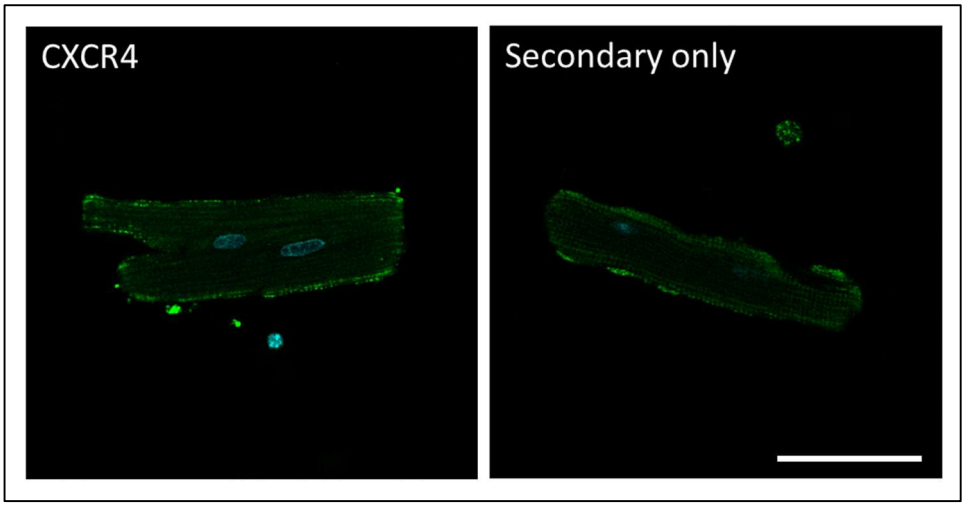


**Figure 6-6: Immunofluorescent staining of isolated rat cardiomyocytes**

Immunofluorescent staining for CXCR4 using a monoclonal antibody (ab124824) and Alexa Fluor 488 anti-rabbit secondary antibody (green) in an isolated rat cardiomyocyte. Equal intensity was found using primary and secondary antibodies (left panel) compared to secondary alone (right panel). Representative images, 50 µm scale bar.

Similar immunofluorescent staining in isolated human atrial trabeculae suggested the presence of CXCR4 on cardiomyocytes and endothelial cells (Figure 6-7). Importantly,

this staining appeared to be specific due to its absence in secondary-only control samples.

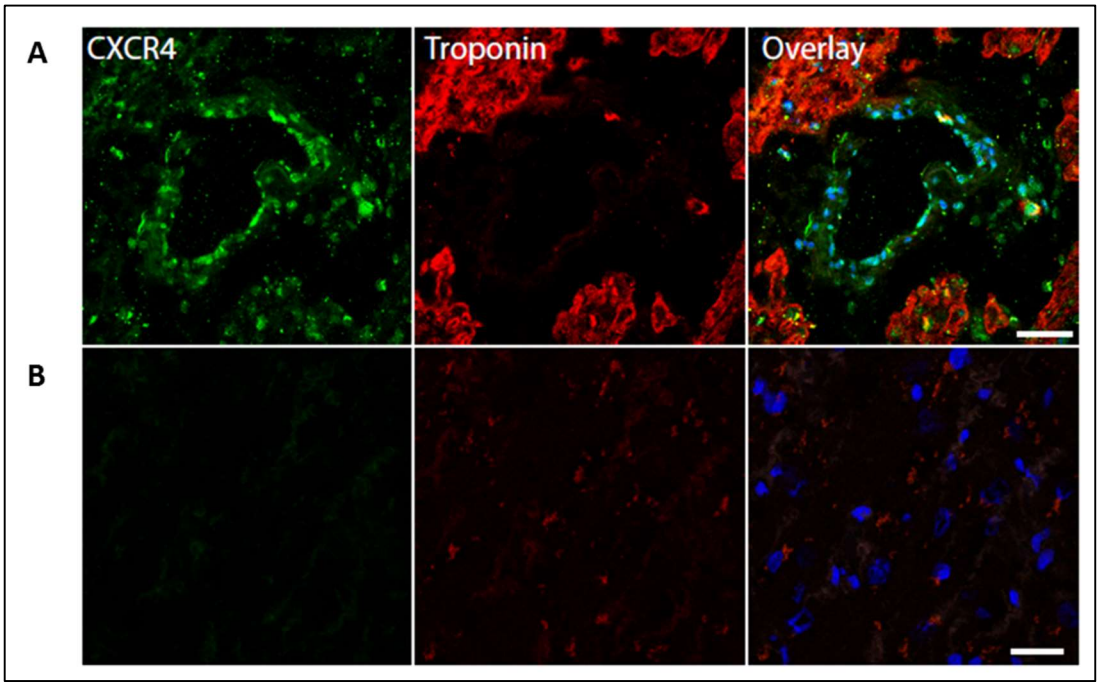


**Figure 6-7: Immunofluorescent staining of isolated human atrial trabeculae**

Row (A) Immunofluorescent staining demonstrates the distribution of CXCR4 (ab124824, green) in relation to troponin (ab8295, red). Hoechst nuclear stain shown in blue; Row (B) Immunofluorescent staining using secondary antibody in the absence of primary antibody. Representative images from n=2 independent experiments, 50 µm scale bar.

### 6.4.4 Discussion

The isolated rat cardiomyocyte immunohistochemistry demonstrated non-specific fluorescence suggestive of non-specific binding of the fluorescent secondary antibody, therefore precluding any conclusions about the presence and distribution of CXCR4. This was possibly a result of over-fixation of the sample but was not investigated any further in rats. The distribution of CXCR4 on mouse cardiomyocytes is discussed in more detail in section 8.3. In contrast, the secondary antibody-only staining of isolated human atrial trabeculae sections demonstrated minimal fluorescence, suggesting that the observed signal represents the true distribution of CXCR4.

Of course, SDF-1α (and AMD3100) may be exerting effects on several other cell types in the heart, including vascular smooth muscle cells, endothelial cells and fibroblasts. Whilst cardiomyocyte CXCR4 is the most described and investigated, it does not preclude a (central) role for other cell types that express CXCR4. For example, endothelial cells are of particular interest due to their abundance in the heart.[355, 356] Although these were not specifically investigated here, they should be considered when attempting to resolve the mechanism for SDF-1α-mediated cardioprotection.

Finally, it is important to acknowledge that, in contrast to the *ex vivo* experiments described, the *in vivo* experiments presented in this thesis do not necessarily implicate an action of SDF-1α (or AMD3100) in the heart. The study of simulated IRI in isolated rat papillary muscle by Davidson *et al.* administered AMD3100 *in vivo*, prior to RIC and surgical removal of the heart for placement on a Langendorff apparatus.[31] Consequently, SDF-1α (and AMD3100) could be exerting an effect in the limb or elsewhere and exerting cardioprotection via either a secondary messenger or neural pathway. It has been demonstrated that transient limb ischaemia liberates a protective dialysable factor(s) with a molecular weight below 15 kDa.[28] The role of SDF-1α in signal transduction in RIC could be elucidated by subjecting an animal to RIC *in vivo*, with and without pre-treatment with AMD3100, and isolating plasma dialysate which could subsequently be exposed to a naïve heart on a Langendorff apparatus (which itself could be pre-treated with AMD3100 or vehicle). This plasma dialysate model has been well described and is valuable for distinguishing processes occurring in the limb from those in the heart. This was not specifically investigated here but is an interesting avenue for future enquiry.

Furthermore, CXCR4 is also present on circulating cells that are sequestered by the heart following IRI. For example, Xu *et al.* reported an influx of platelets to the area at risk in early reperfusion in a murine model of myocardial IRI.[357] They demonstrated an important role for platelet activation in the pathophysiology of myocardial IRI, which is interesting when considering that platelets constitutively express CXCR4 and release SDF-1α from their α-granules when activated.[358, 359] The potential role of platelets in relation to RIC is explored in section 7.6 but, suffice to say that, the

apparent presence of cardiomyocyte CXCR4 described in the present experiment does not confirm cardiomyocytes to be the target of SDF-1α or AMD3100 in the studies described in Chapter 5 and section 6.3, respectively. However, it is possible to investigate the importance of cardiomyocytes by using cardiomyocyte-specific CXCR4 null mice. Both this and the demonstration of cardiomyocyte CXCR4 in mice is described in detail in Chapter 8.

## 6.5 Summary

This chapter describes the use of AMD3100, a highly specific inhibitor of CXCR4, to abolish the beneficial effect of RIC in a rat *in vivo* model of myocardial IRI. This is the second condition that must be satisfied to define a molecule as a mediator of cardioprotection and, when considered alongside the finding in Chapter 5 that exogenous SDF-1α is cardioprotective when administered prior to reperfusion, remains supportive of the hypothesis that SDF-1α is central to the mechanism of RIC. Furthermore, immunofluorescent staining of isolated human atrial trabeculae indicated the presence of CXCR4 on cardiomyocytes, which is likewise consistent with the paradigm defined in Chapter 5. As discussed, the present findings do not confirm the importance of cardiomyocyte CXCR4 (or indeed any cardiac cell type) in the mechanism of RIC, which will be considered in detail in Chapter 8.

# Chapter 7 Does remote ischaemic conditioning increase the production of SDF-1α?

## 7.1 Introduction

The third condition, according to The Working Group of Cellular Biology of the Heart of the European Society of Cardiology,[103] that must be satisfied to define a molecule as an endogenous mediator of cardioprotection is increased production or maintenance of extracellular concentrations of the mediator(s) as a direct effect of RIC.

The current humoral paradigm for RIC asserts that a factor, between 3.5 kDa and 15 kDa in size,[27, 28] is released from the remote organ or tissue that is subject to cyclical, non-lethal ischaemia and reperfusion, and is carried by the blood to exert a protective effect on cardiac cells following lethal IRI. Investigation of SDF-1α as the potential mediator of RIC is complicated by its relatively short half-life due to cleavage and inactivation by DPP4.[52, 201] No convenient method exists to specifically quantify full-length SDF-1α in plasma, as all known antibodies recognize both the intact and cleaved forms. This chapter aims to investigate the acute role of SDF-1α in RIC but to do this it was first necessary to develop and characterise a novel recombinant antibody for use in an ELISA for full-length SDF-1α.

## 7.2 Research aims and objectives

The main objective of this chapter was to investigate the acute role of SDF-1α in RIC. The research aims for this objective were:

1. Validate and characterise an ELISA to the active (full-length) form of SDF-1α;
2. Investigate whether the ligands of CXCR4 are increased in the blood of rats and humans subjected to RIC;
3. Investigate the contribution of DPP4 to SDF-1α dynamics after RIC;
4. Investigate the role of platelets in SDF-1α dynamics after RIC.

## 7.3 Aim 1: Validate and characterise an ELISA to the active (full-length) form of SDF-1α

### 7.3.1 Background

SDF-1α is described by the primary sequence KPVSLSYRC PCRFFESHVA RANVKHLKIL NTPNCALQIV ARLKNNNRQV CIDPKLKWIQ EYLEKALNK and is cleaved by DPP4 at its proline residue (position 2) and by MMP-2/9 position 4,[51] although DPP4 is responsible for the majority of SDF-1α cleavage and is the focus here.[52] Currently, no method exists to specifically quantify full-length SDF-1α in plasma as all known antibodies recognize both intact SDF-1α and SDF-1α after cleavage (Figure 7-1).

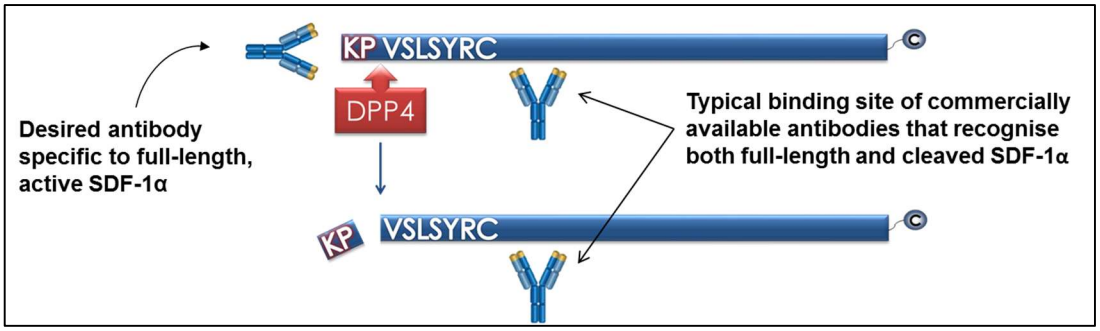


**Figure 7-1: Representation of binding sites of commercially available antibodies to SDF-1α**

Dipeptidyl peptidase-4 (DPP4) is an extracellular peptidase that cleaves SDF-1α at its N-terminus. Commercially available antibodies recognise both intact and cleaved forms of SDF-1α, whereas the aim of this section was to characterise an antibody to the N-terminus, which is specific to the intact from.

Most commonly, polyclonal antibodies are made by inoculating the antigen of interest into a mammal. This results in the production of specific IgG immunoglobulins by B lymphocytes of different lineages, each of which recognise a different epitope. It was hypothesised here that the reason for the lack of an antibody specific to full-length SDF-1α was its short *in vivo* half-life and its very high interspecies homology. To overcome these hurdles, an *in vitro* screening method was utilised in order to obtain a specific recombinant antibody for a single epitope. This approach has the additional advantages of being automated, rapid, animal-free and flexible, insofar as a number of antibody formats can be generated.[360, 361]

A custom human IgG1 bivalent mini-antibody against the N-terminus of SDF-1α was identified by screening the HuCAL® (Human Combinatorial Antibody Library) phage-display library containing several billion, distinct, fully human antibodies.[360, 361] In this method a random cDNA library encoding each distinct human antibody is inserted into a bacteriophage coat protein gene, causing the phage to display a variable peptide (antibody) on its outside while containing the gene encoding that specific antibody inside the same phage. The library was screened using positive selection for binding to the peptide KPVSLSYR-Ttds-C derived from full-length SDF-1α and negative selection for binding to the peptide VSLSYR-Ttds-C derived from cleaved SDF-1α (AbD Serotec, Oxon, UK). This approach has the advantage of defining the antibody's antigenicity.

The HuCAL® antibodies are initially produced as human IgG1 monovalent or bivalent mini-antibodies, which have greater sensitivity due to having more binding sites (Figure 7-2). AbD Serotec (Oxon, UK) are able to convert these into full-length IgG1 if the Fc domain is required. However, this was not necessary since the HuCAL® antibodies are supplied with two embedded epitope tags, a FLAG octapeptide tag and a polyhistidine (His6) tag, facilitating the use of anti-FLAG and anti-His6 secondary antibodies, as well as anti-human Fab secondary antibodies.

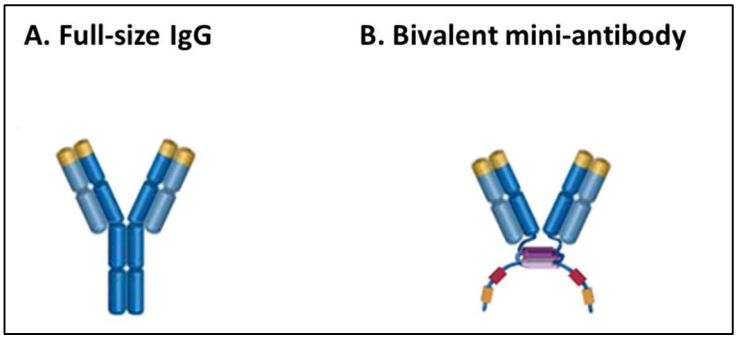


**Figure 7-2: HuCAL® antibody format**

(A) Representative image of full size IgG; (B) Bivalent mini-antibody structure used in this thesis. Each Fab fragment consists of the first two domains of the antibody heavy chain (VH and CH1) plus the complete light chain (from either the κ or λ family) and contains two epitope tags. Figure adapted from [362].

Fourteen candidate antibodies, labelled A-N, were provided by AbD Serotec after their initial screening, which determined that they detected full-length but not cleaved SDF-1α. These screening reactions had been performed using SDF protein conjugated to human transferrin (TRF). Therefore, the first aim of this chapter was to validate and characterise the binding of these custom antibodies to unbound, active, full-length SDF-1α using an ELISA format. The terms 'full-length', 'intact' and 'active' are used interchangeably in this section, as are the terms 'cleaved' and 'inactive'.

### 7.3.2 Methods

The initial step was to validate these antibodies in a direct ELISA using the standard protocol provided by AbD Serotec, which is as follows: 100 µl of full-length and cleaved SDF-1α-TRF at 5 µg/ml, as well as full-length rhSDF-1α (Miltenyi Biotec, CA, USA), in Hispec buffer (AbD Serotec, Oxon, UK) were incubated on a black, flat bottom, MaxiSorp, 96-well ELISA plate (Thermo Fisher Scientific, MA, USA) at 4$^{o}$C overnight. Wells were washed three times for 5 min with 0.05% PBS-T before blocking with 300 µl of 5% non-fat dry milk in PBS-T for 1 h at RT. After three further 5 min washes with PBS-T, 100 µl of primary anti-Fab antibody (HuCAL® A-N) at 2 µg/ml in Hispec buffer was added per well and incubated for 1 h at RT. After five 5 min washes with PBS-T, 100 µl of alkaline phosphatase conjugated polyclonal goat anti-human Fab secondary antibody (STAR126A, AbD Serotec, Oxon, UK) diluted in Hispec at a concentration of 1:5000 was added to each well and incubated for a further 1 h at RT. Following incubation, wells were washed a further three 5 min with PBS-T.

Detection was performed using AttoPhos® AP Fluorescent Substrate System (AttoPhos, Roche, Sussex, UK). This provides a highly sensitive fluorescent substrate for the alkaline phosphatase contained within the anti-human Fab secondary antibody described above. Specifically, the substrate (2'-[2-benzothiazoyl]-6'-hydroxybenzothiazole phosphate (BBTP)) is cleaved by alkaline phosphatase to produce inorganic phosphate and 2'-[2-benzothiazoyl]-6'-hydroxybenzothiazole (BBT), which has enhanced fluorescence compared to the substrate.[363] 100 µl of AttoPhos® substrate diluted to 1:10 with distilled water was added to each well. In each experiment, separate wells were prepared containing Hispec buffer (zero

control or blank) and AttoPhos® Calibration Solution (500±50 ng/ml BBT in 2.4 M dienthanolamine buffer), to which AttoPhos® Substrate Solution was added.

Fluorescence was recorded using a FLUOstar Omega microplate reader. An excitation wavelength of 440±10 nm and an emission wavelength of 550±10 nm were selected, as per AttoPhos® recommendations. Sample measurements were calibrated using the AttoPhos® Calibration Solution well, and blank-corrected using the zero control well. All analyses, including samples and standards, were performed in duplicate and readings were averaged to minimise intra-assay variability.

### 7.3.3 Results

Initial results are shown in Figure 7-3, Panel A. This demonstrated greater signal than noise for full-length SDF-1α-TRF (green bars) and rhSDF-1α (red bars) for five of the candidate antibodies: C, G, H, M and N. The protocol described above was subsequently optimised in a series of steps in order to maximise the sensitivity of the assay. Variations tested were: concentration (1:10 vs. 1:2 dilutions in distilled water) and duration of exposure (0, 1 and 2 h) to AttoPhos® Substrate Solution; number of excitation flashes emitted by the FLUOstar Omega microplate reader per well (10 vs. 50); fluorescence emission filter (550±10 nm vs. 560±40 nm); and well orbital averaging versus central measurement. The 560±40 nm filter was chosen for comparison to encompass the peak emission wavelength cited in the AttoPhos® literature.

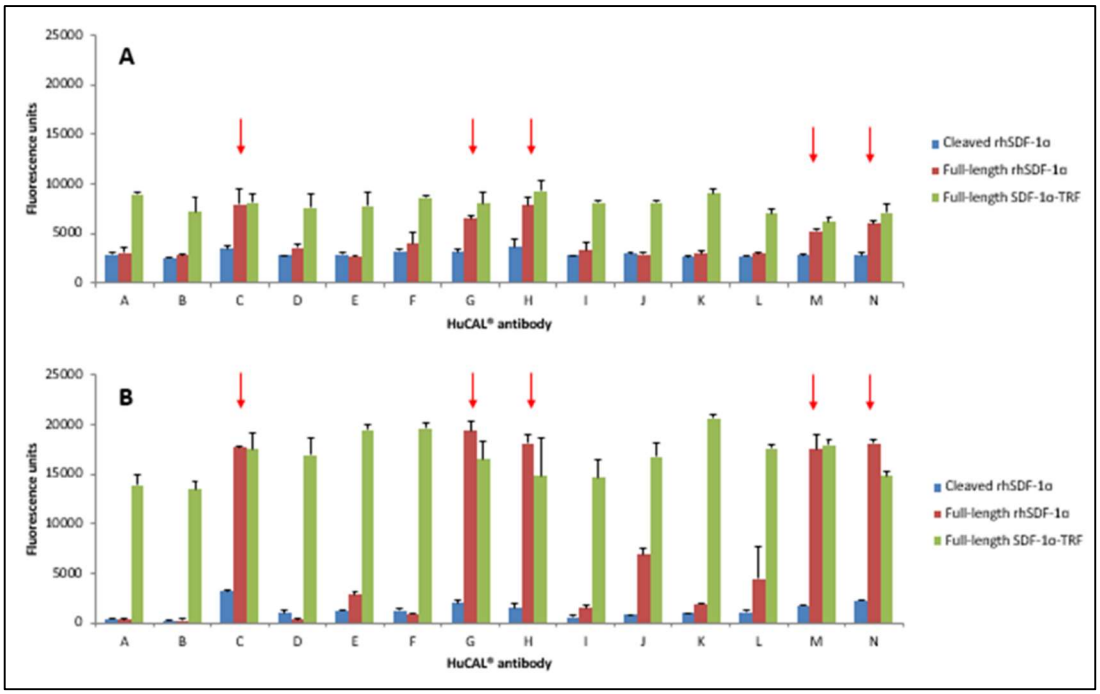


**Figure 7-3: Validation of HuCAL® antibodies against full-length and cleaved SDF-1α**

HuCAL® antibodies A-N were tested against full-length and cleaved SDF-1α-TRF, and full-length rhSDF-1α. (A) Initial results using standard protocols. HuCAL® antibodies C, G, H, M and N (arrowed) detected full-length forms of SDF-1α (red and green bars) but not cleaved forms (blue bars); (B) Following optimisation of the ELISA protocol, there was improved signal:noise. Again, HuCAL® antibodies C, G, H, M and N demonstrated a favourable profile (arrowed). The remaining HuCAL® antibodies were excluded from further characterisation.

The results of this optimisation are displayed in Figure 7-3, Panel B, and were: orbital averaging with 50 flashes per well immediately after addition of 1:10 AttoPhos® Substrate Solution, using a 560±40 nm filter. Again, HuCAL® antibodies C, G, H, M and N displayed a favourable profile. The remaining HuCAL® antibodies were excluded from further characterisation. In control experiments, GLP-1, another incretin that is proteolysed by DPP4, and cleaved rhSDF-1α were also tested (data not shown) and found not to have any signal above background. Henceforth, only rhSDF-1α unbound to transferrin was used for characterisation.

The five candidate HuCAL® antibodies were then tested for their ability to detect full-length rhSDF-1α in human plasma. As a negative control, *cleaved* rhSDF-1α was prepared by incubating 20 µg full-length rhSDF-1α (2.4 nmol) with 0.1 µg recombinant human DPP4 (R&D Systems, Oxon, UK) in 25 mM Tris buffer, pH 8.0,

which cleaves 2.5 nmol SDF-1α per min per µg of DPP4, at 37°C for 60 min. Human plasma was collected on ice in citrated tubes (BD, Oxon, UK), then centrifuged at 1,600 x g for 20 min then 10,000 x g for 30 min to remove platelets. Full-length and cleaved rhSDF-1α were diluted in human plasma spiked with 10 µM Sitagliptin per well to inhibit DPP4 and prevent proteolysis of full-length rhSDF-1α by endogenous DPP4. Unfortunately, the direct ELISA configuration described was unable to detect signal above noise for any tested quantity of full-length rhSDF-1α in plasma, indicating a need to further increase sensitivity (data not shown).

To increase sensitivity, the ELISA was changed to a 'sandwich' configuration (Figure 7-4), and several combinations of capture antibody, blocking agent, detection antibody, secondary antibody and detection reagent were tested (see Table 7-1).

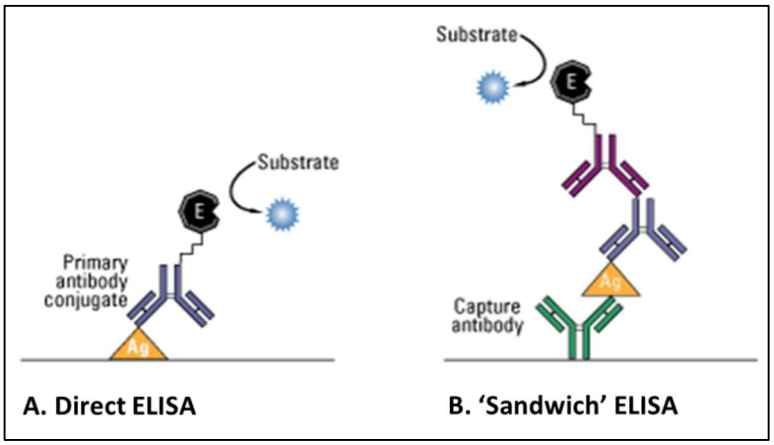


**Figure 7-4: Comparison of direct and 'sandwich' ELISA configurations**

(A) Direct ELISA configuration, whereby the antigen (Ag) is adsorbed onto the plate prior to addition of the primary antibody; (B) A 'sandwich' ELISA configuration, whereby a capture antibody is adsorbed to the plate surface prior to addition of the sample. In both cases, detection may be direct (via an enzyme (E)-conjugated primary antibody) or indirect (via a conjugated secondary antibody). Figure adapted from [364].

| Capture antibody | Blocking agent | Detection antibody | Secondary | Reagent |
|---|---|---|---|---|
| MAB350 | 5% milk | **HuCAL® C** | STAR126A | Attophos |
| AF310NA | 5% milk | **HuCAL® C** | STAR126A | Attophos |
| **HuCAL® G** | 2% BSA/PBS-T | AF310NA | ab97102 | Attophos |
| AF310NA | 2% BSA/PBS-T | **HuCAL® G** | STAR126A | Attophos |
| AF310NA | 5% BSA/PBS-T | **HuCAL® A-N** | STAR126B | Streptavidin-HRP |
| MAB350 | 5% BSA/PBS-T | **HuCAL® A-N** | STAR126B | Streptavidin-HRP |
| AF310NA | 5% BSA/PBS-T | **HuCAL® C,G,H,M,N** | STAR126B | Streptavidin-HRP |
| **HuCAL® C,G,H,M,N** | 5% BSA/PBS-T | BAF310 | - | Streptavidin-HRP |
| **HuCAL® C** | 5% BSA/PBS-T | BAF310 | - | Streptavidin-HRP |

**Table 7-1: Sandwich ELISA configurations tested during ELISA characterisation**

The working configuration is highlighted in grey. MAB350 (R&D Systems, Oxon, UK) is a monoclonal mouse IgG against mouse and human SDF-1α. STAR126A (AbD Serotec, Oxon, UK) is a polyclonal goat anti-human IgG F(ab')2:Alk.Phos. AF310NA (R&D Systems, Oxon, UK) is a polyclonal goat IgG against total human SDF-1α. Ab97102 is a polyclonal rabbit anti-goat IgG H&L (Alkaline Phosphatase). STAR126B (AbD Serotec, Oxon, UK) is a polyclonal goat anti-human IgG F(ab')2:Biotin. BAF310 (R&D Systems, Oxon, UK) is a polyclonal goat IgG against total human and mouse SDF-1α.

The principle problem with the sandwich ELISA, and reasons for testing several configurations, was cross-reactivity between components of the ELISA, resulting in signal even in the absence of full-length SDF-1α. Examples of two ELISA configurations that exhibit this substrate-independent signal are shown in Figure 7-5 (compare Panel A in the presence of SDF-1α to Panel B in the absence of SDF-1α for AF310NA, and Panel C with Panel D for MAB350).

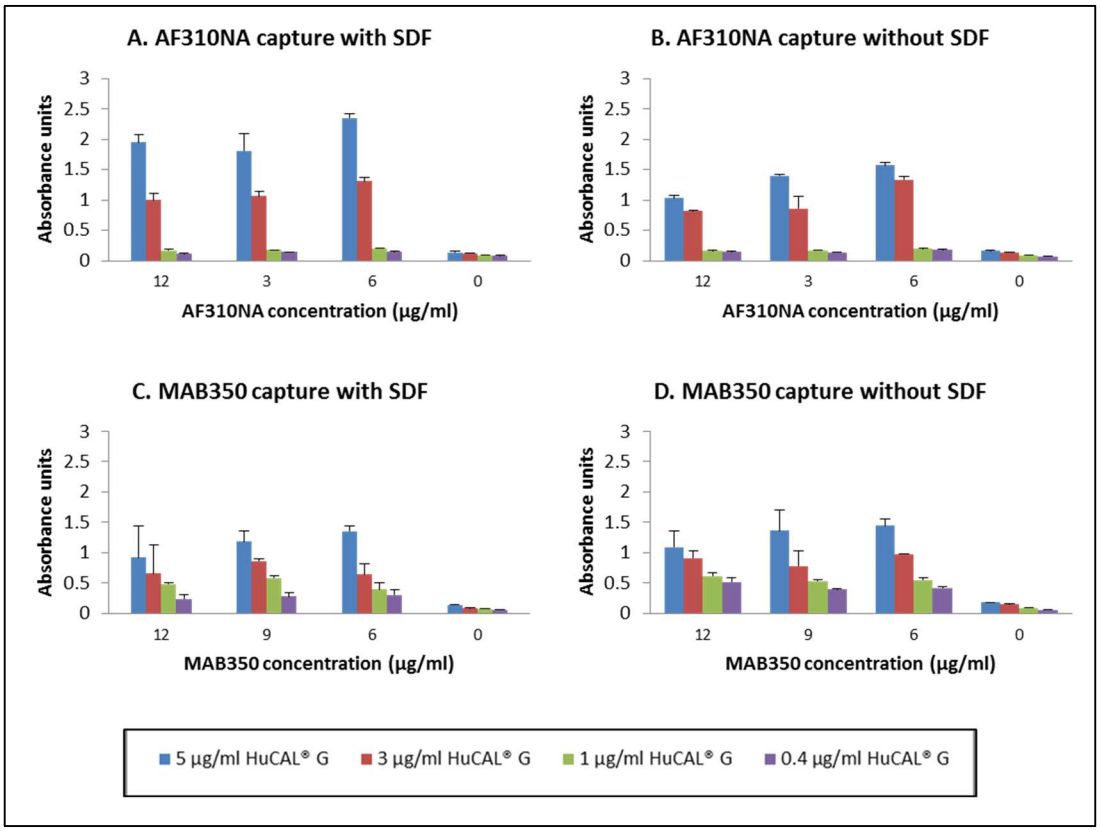


**Figure 7-5: Effect of cross-reactivity when HuCAL® antibody used for detection**

Panels A and C demonstrate an apparently appropriate diminution of signal with lower concentrations of capture (AF310NA and MAB350) and detection (HuCAL® G) antibody. However, when the antigen (full-length rhSDF-1α) was absent from the assay similar results were seen (Panels B and D).

The successful configuration, highlighted in grey in Table 7-1, utilised the HuCAL® Fab fragment as the capture, rather than the detection, antibody. The capture HuCAL® antibody was diluted in 0.2M anhydrous sodium carbonate-sodium bicarbonate buffer to improve binding conditions and incubated in MaxiSorp, 96-well ELISA plates at 4$^{o}$C overnight. A biotinylated polyclonal goat IgG against human and mouse SDF-

1α (BAF310), diluted in Hispec buffer, was used as the detection antibody. The biotin tag permitted a streptavidin protein detection step, owing to the high affinity of streptavidin for biotin. Substrate Solution, composed of a 1:1 mix of hydrogen peroxide and tetramethylbenzidine, was added because in the presence of HRP, tetramethylbenzidine donates hydrogen ions for the reduction of hydrogen peroxide to water, forming tetramethylbenzidine diimine. The latter causes the solution to turn blue and the colour intensity develops in proportion to the amount of streptavidin-HRP, and therefore the amount of full-length rhSDF-1α. After stop solution was added, the optical density of each well was immediately measured as described in section 2.8. Prior to reading, 5 sec of double orbital shaking at 500 rpm were applied, to ensure the solution was thoroughly mixed.

Following these adjustments, antibodies C, H and N were found to have an appropriate full-length rhSDF-1α concentration-signal curve in the absence of plasma (Figure 7-6). Antibodies G and M were excluded from further characterisation as they failed to show any signal above background (indicated by the 0 pg/ml rhSDF-1α column).

HuCAL® antibodies C, G and M were subsequently tested against full-length rhSDF-1α at physiological concentrations in plasma (estimated as 2000 pg/ml, see Table 7-2), to ensure the assay would have utility for experimental samples. In addition, to permit comparison with commercially available assays MAB350, a monoclonal mouse IgG against mouse and human SDF-1α, was tested as the detection antibody using the same assay protocol. This antibody was selected based on the capture antibody used in a commercially available ELISA for total SDF-1α (Quantikine® ELISA for Human CXCL12, R&D Systems, Oxon, UK). Similarly, MAB350 was tested with estimated physiological concentrations of SDF-1α in plasma. Figure 7-7 demonstrates that HuCAL® antibody C and MAB350 continued to generate highly sensitive and quantity-dependent SDF-1α concentration-signal curves, and were therefore selected for use in the final configuration of the assay. HuCAL® antibody C was subsequently designated HCI.SDF1α, and this name is used henceforth.

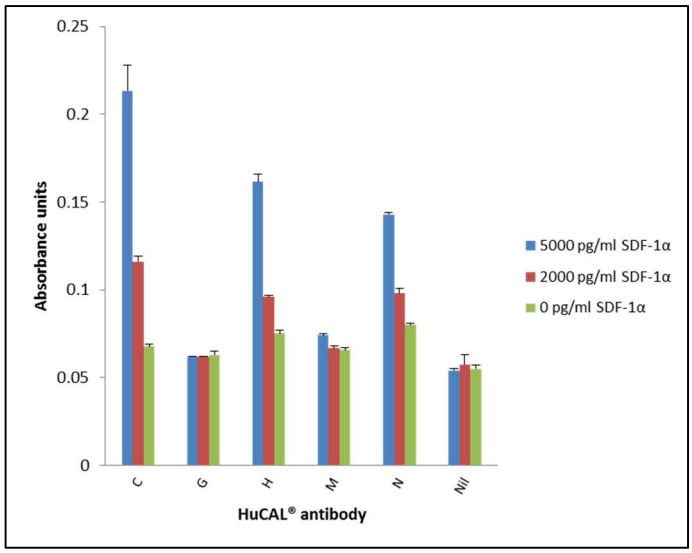


**Figure 7-6: Concentration-signal curves with HuCAL® capture antibody and a streptavidin amplification step**

HuCAL® C, G, H, M and N antibodies were used in the capture step together with a biotinylated detection antibody (BAF310) and streptavidin amplification. This reduced false positive signal and generated an appropriate concentration curve for HuCAL® antibodies C, H and N. HuCAL® antibodies G and M were excluded from further characterisation.

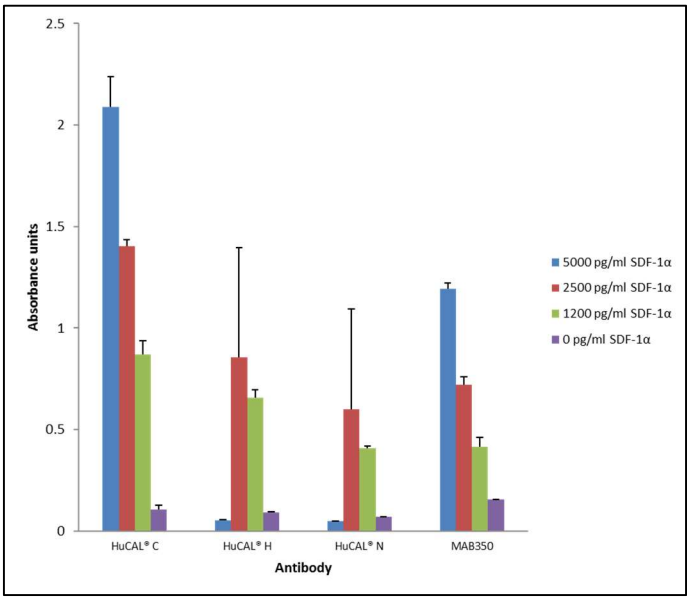


9

**Figure 7-7: HuCAL® C, H and N antibodies and MAB350 against rhSDF-1α were tested in plasma**

At physiological concentrations of SDF-1α, HuCAL® antibody C and MAB350 continued to generate appropriate concentration-response curves. HuCAL® antibodies H and N did not and were excluded from further characterisation.

Following selection of the optimal primary antibodies, it was necessary to optimise the concentrations of both detection and capture antibody to maximise signal:noise. The approach to this was twofold. Firstly, varying concentrations of capture and detection antibody were tested against a fixed concentration of rhSDF-1α (5000 pg/ml) to estimate the optimum combination of tested antibody concentrations (Figure 7-8, Panels A and C). Concentrations tried were based on a technical guide to ELISA available from Thermo Fisher Scientific (MA, USA).[365] Secondly, a low and a high concentration of capture and detection antibody were tested in the absence of SDF-1α in order to estimate their relative contribution to assay noise (Figure 7-8, Panels B and D). This process was applied to both HCI.SDF1α (Figure 7-8, Panels A and B) and MAB350 (Figure 7-8, Panels C and D). In both assays, higher concentrations of BAF310 made a larger contribution to assay noise than higher concentrations of capture antibody and, with this in mind, the working antibody concentrations were chosen as 5 µg/ml HCI.SDF1α and 0.4 µg/ml BAF310 (arrowed in Figure 7-8, Panel A), and 9 µg/ml MAB310 and 0.4 µg/ml BAF310 (arrowed in Figure 7-8, Panel C).

Further modifications to the protocol included testing different ELISA plates, based on which flat bottom clear polystyrene microplates (R&D Systems, Oxon, UK) were selected (data not shown). The effect of shaking the plate during incubation steps and diluting the sample to improve analyte recovery were also investigated, neither of which increased assay signal (data not shown).

Sample SDF-1α values were interpolated from a standard curve generated using known concentrations of full-length rhSDF-1α (R&D Systems, Oxon, UK). The effect of different standard diluents on the interpolated SDF-1α value was investigated and found to have a significant effect, due to variable target analyte recovery (Figure 7-9, Panel A). Full-length rhSDF-1α standards in plasma and in Hispec buffer were compared and demonstrated over-estimation of the quantity of SDF-1α with Hispec buffer (blue line), particularly at the lowest concentrations of SDF-1α, compared to plasma (green line, Figure 7-9, Panel B). The effect of using Hispec buffer to dilute standards, therefore, was underestimation of SDF-1α in experimental plasma samples interpolated from this curve. This was corrected by using BUF037A, a

commercially available diluent with mammalian serum proteins, designed to mimic the recovery profile of human plasma (AbD Serotec, Oxon, UK). The standard profile of BUF037A is shown in Figure 7-9 (Panel B, red line). Averaged samples were baseline corrected using duplicate BUF037A wells without SDF-1α to account for any SDF-1α in the mammalian serum proteins included with this diluent. A sensitivity analysis was performed by multiple serial dilutions of standard samples in BUF037A, and a limit of detection (LOD) of 300 pg/ml was ascertained (Figure 7-9, Panel C). Limit of quantification (LOQ) was not calculated for this assay but was expected to be satisfactory as the typical concentration range of SDF-1α in biological samples is well above the LOD (see Table 7-2).

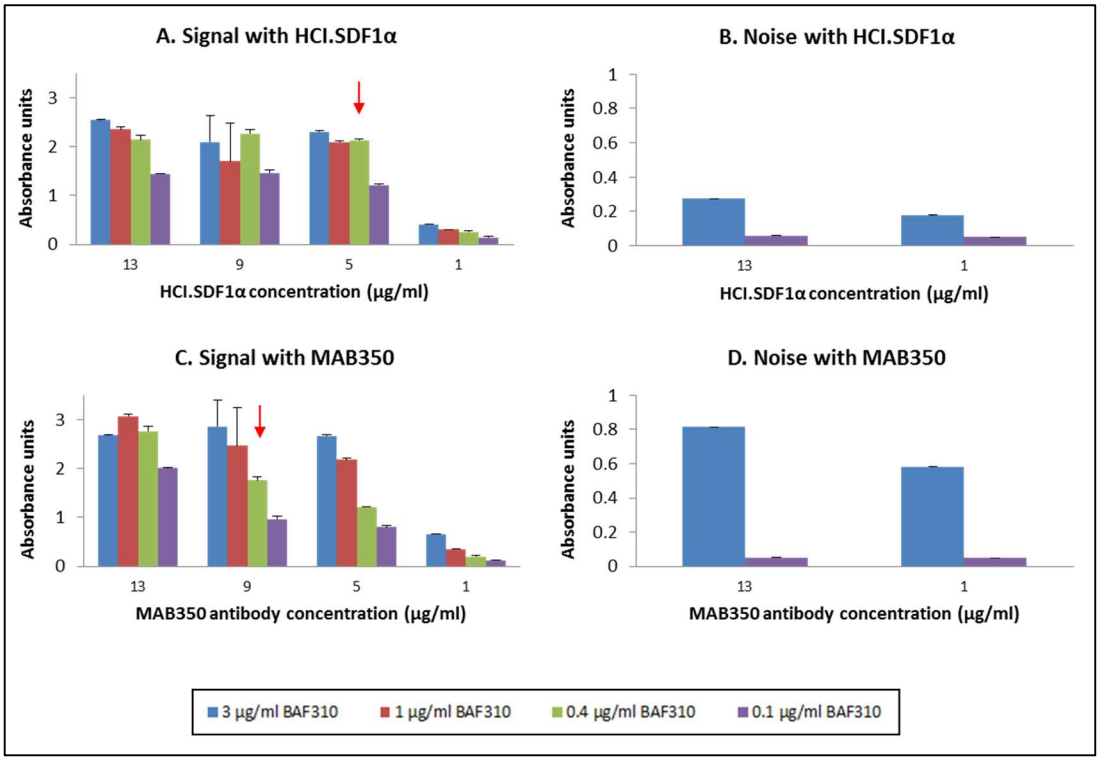


**Figure 7-8: Optimising signal:noise for HCI.SDF1α and MAB350 ELISA**

Concentrations of capture and detection antibody were optimised for both assays. (A) Signal produced by 5000 pg/ml full-length rhSDF-1α at variable concentrations of both HCI.SDF1α (capture) and BAF310 (detection) antibodies; (B) Assay noise at variable concentrations of both antibodies when no SDF-1α was added. The working antibody concentrations were chosen as 5 µg/ml HCI.SDF1α and 0.4 µg/ml BAF310 (arrowed in Panel A); (C) Signal produced by 5000 pg/ml full-length rhSDF-1α at variable concentrations of both MAB310 (capture) and BAF310 (detection) antibodies; (D) Assay noise at variable concentrations of both antibodies when no SDF-1α was added. The working antibody concentrations were chosen as 9 µg/ml MAB310 and 0.4 µg/ml BAF310 (arrowed in Panel C).

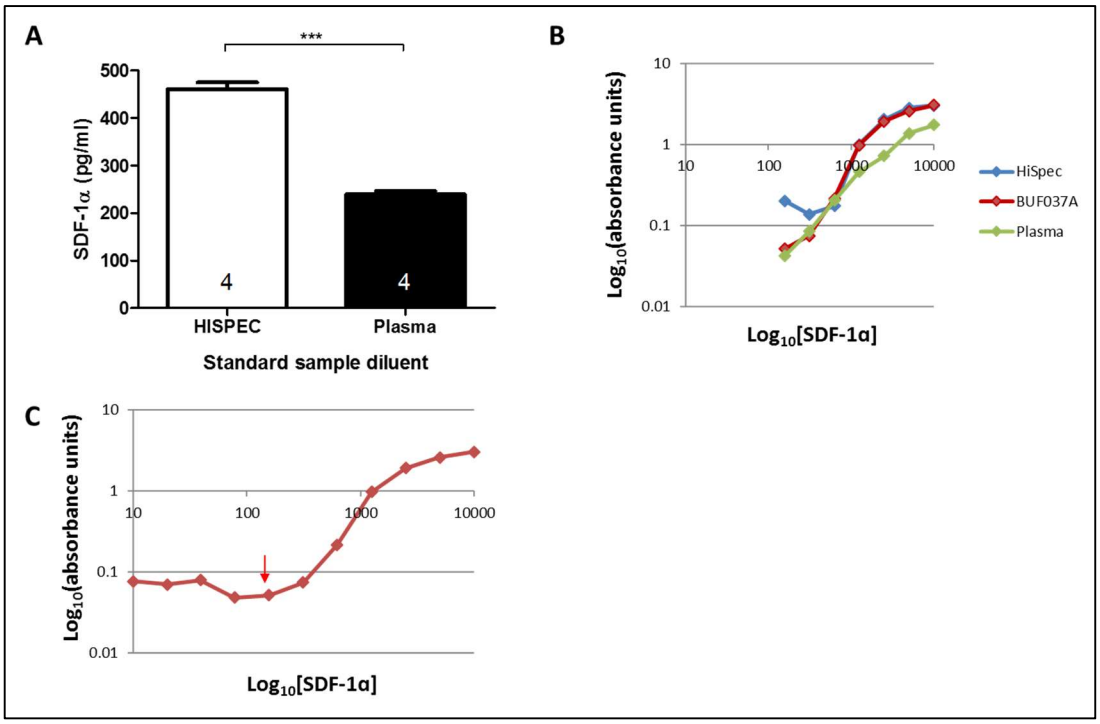


**Figure 7-9: Optimising the standard sample diluent for SDF-1α value interpolation**

(A) Effect of the standard sample diluent on the interpolated value for full-length SDF-1α samples. The same raw sample data, from a full-length SDF-1α assay, was used for each regression analysis using a standard curve in either Hispec or plasma. Statistical significance was assessed using an unpaired t-test, n=4, P<0.001; (B) Difference in Hispec and plasma standard curves at lower values of full-length SDF-1α, which represents the concentration range of interest in this chapter. BUF037A mimicked plasma at lower concentrations of SDF-1α and prevented underestimation of sample values; (C) Sensitivity assay using BUF037A, which indicated a LOD of 300 pg/ml (arrowed).

To ascertain the effect of freezing on target analyte recovery, rat plasma samples spiked with 2500 pg/ml full-length rhSDF-1α were subjected to repeated freeze-thaw cycles (Figure 7-10). There was an unexpected difference between the absolute value of SDF-1α as measured by HCI.SDF1α and MAB350, which may be a consequence of sample processing by proteases in the rat plasma or may be statistical chance in view of the small sample size. Nonetheless, there was no evidence of SDF-1α degradation as measured with either HCI.SDF1α or MAB350, albeit with a sample size of one.

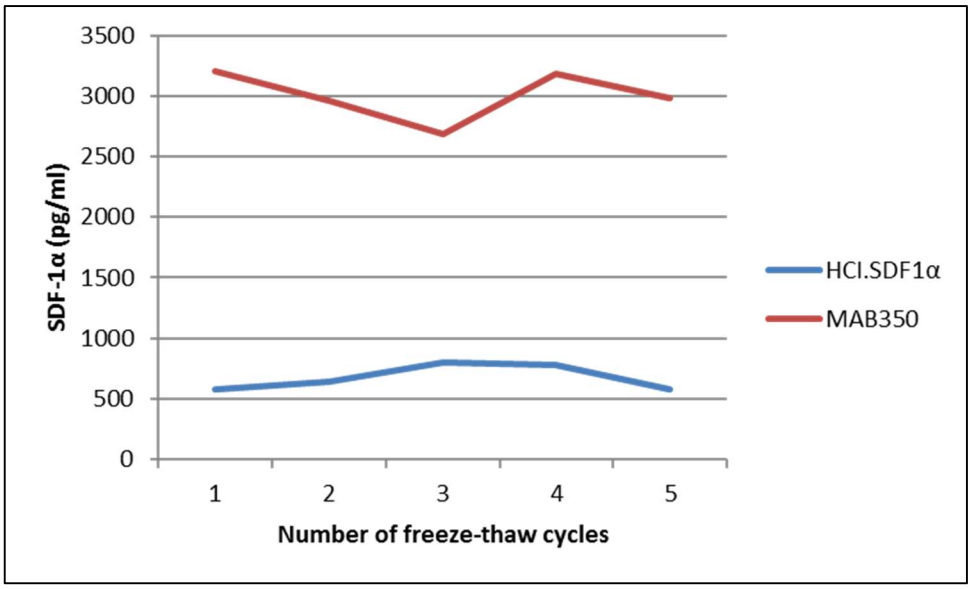


**Figure 7-10: Effect of freeze-thaw cycles on SDF-1α recovery**

Rat plasma was spiked with 2500 pg/ml full-length rhSDF-1α and divided into 500 µl aliquots. Each aliquot was frozen and thawed a different number of times to ascertain whether this would degrade the sample (n=1).

Finally, the percentage intra- and inter-assay coefficients of variation were calculated as [mean of SD x 100 / mean] and [SD of mean x 100 / mean], respectively. For HCI.SDF1α these values were 2.7% and 7.1%, and for MAB350 they were 3.4% and 4.5%. All values were below the recommended maximum threshold of 10%.

Once this ELISA for full-length SDF-1α was validated and characterised, it was necessary to compare the specificity against existing commercial antibodies. By assaying different proportions of intact and cleaved SDF-1α it was possible to demonstrate that HCI.SDF1α is specific for full-length SDF-1α, whereas commercial assays report a combination of intact and cleaved SDF-1α (Figure 7-11), making the results with the commercial antibody difficult to interpret in terms of SDF-1α activity.

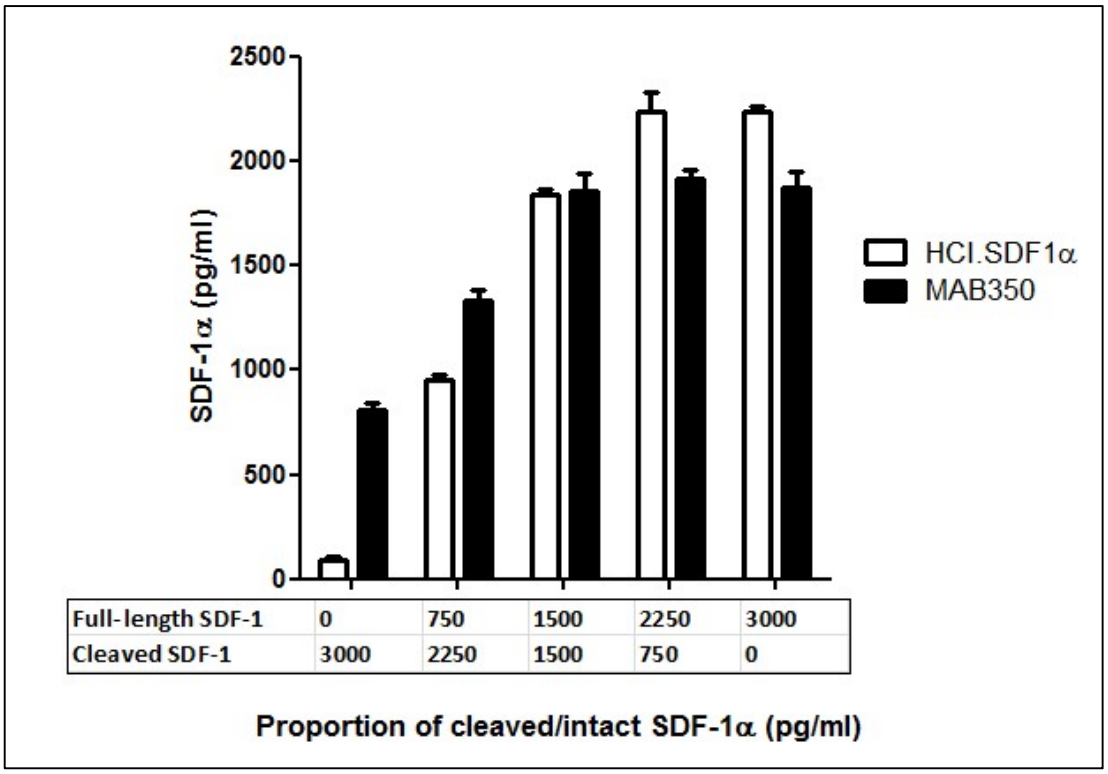


**Figure 7-11: Specificity of HCI.SDF1α and MAB350 for full-length and cleaved rhSDF-1α**

HCI.SDF1α is specific for active SDF-1α, with very low signal in the absence of intact SDF-1α, whereas there is substantial residual signal in the absence of intact SDF-1α in the case of MAB350.

### 7.3.4 Discussion

This section reports the successful characterisation and validation of a novel antibody (HCI.SDF1α), specific for the N-terminus of SDF-1α, and the development and optimisation of an immunoassay using this antibody that is specific for intact, active SDF-1α. HCI.SDF1α was identified as having specific and robust binding to full-length SDF-1α without any binding to cleaved SDF-1α or to GLP-1, an unrelated protein that is also cleaved by DPP4. It should be acknowledged that this approach does not preclude cross-reaction with other proteins, although a Basic Local Alignment Search Tool (BLAST) search for the sequence of interest in a human protein database revealed only protocadherin Fat 1 precursor as a potential match.[366] Fat 1 is a 50 kDa protein that is expressed in epithelial and endothelial smooth muscle cells and, although its precise role remains poorly defined, it may have a role in promoting vascular remodelling after arterial injury.[367] Western blotting would be an

appropriate method to exclude this as an important target of HCI.SDF1α in the samples used in this study. Although this was not done, it is unlikely to be present in plasma samples as, unlike SDF-1α, it is not secreted by cells.[368] Furthermore, it should be noted that all isoforms of SDF-1α share the same N-terminal sequence. However, SDF-1α is the most prevalent and HCI.SDF1α is described in these terms to be consistent with the literature and commercially available antibodies.[40] The relative quantities of each isoform in samples relevant to this study could be assessed by Western blotting, but was not pursued here because of time limitations.

Cleavage reduces the affinity of SDF-1α for CXCR4, rendering it inactive. This is evidenced by the significant reduction in bio-reactivity in response to cleavage by DPP4.[52, 201] Furthermore, studies using bioengineered SDF-1 that is resistant to cleavage by DPP4 have demonstrated improved stem cell homing, angiogenesis and EF.[51, 369]

Baerts *et al.* described a significant reduction in immunoreactivity after they measured DPP4-cleaved rhSDF-1α using several different commercial ELISA kits (including R&D Systems, Raybiotech and Peprotech).[151] They also determined that DPP4 was predominant in mediating cleavage of SDF-1α. However, despite currently available commercial antibodies having different affinities towards intact and DPP4-truncated SDF-1α,[52, 53] this section describes incomplete loss of signal in an ELISA using MAB350 following complete cleavage of SDF-1α with DPP4. This may potentially be explained by the fact that binding of MAB350 to an internal sequence in SDF-1α would leave a decreased number of SDF-1α binding sites available to the polyclonal detection antibody used in this sandwich ELISA format, despite loss of the N-terminus. As loss of the N-terminal $Lys^1$ confers a complete loss of bio-reactivity, this observation confounds interpretation of both basic and clinical studies of SDF-1α that have used commercially available ELISA assays. Accurate measurement is crucial given the growing interest in SDF-1α as a potential biomarker [370-375] and therapy for ischaemic cardiomyopathy.[93, 100, 200, 369, 376]

ELISAs depend on the assembly of a large immune complex, and failure of any of its component parts can result in a failure of signal. A number of these problems were encountered, and remedied, in this study. The most problematic of these were low signal:noise in plasma samples and poorly representative standard curves, and these are discussed in turn. However, extensive refinement and incremental improvements to the assay have resulted in a robust and reliable assay for full-length SDF-1α.

There were a number of possible reasons for initial poor signal:noise in plasma, related to either low signal or excessive background noise. Here, the biggest benefit was gained by switching from direct detection to a sandwich ELISA. Full-length SDF-1α is expected to be present at low levels in the plasma and by immobilising SDF-1α using a specific antibody, rather than the spectrum of proteins present in plasma using a non-specific plate, the sensitivity of the assay was increased. This was augmented by optimising each individual component of the assay to ensure none was present at a limiting concentration. The optimisation of the capture and detection antibodies, for example, is demonstrated in Figure 7-8. Another important consideration was selecting pairs of antibodies that work in combination. This was challenging, as indicated by Figure 7-5, primarily due to cross-reactivity between antibodies. Specifically, initial attempts with a secondary antibody to the biotin tag in the HuCAL® antibodies cross-reacted with the biotin tag in the polyclonal goat IgG capture antibody (AF310NA; R&D Systems, Oxon, UK). Other cross-reactions were less easy to define and were solved by testing a number of combinations (see Table 7-1).

Secondly, optimising the standard diluent posed significant difficulty. Initially, a general ELISA diluent (Hispec, AbD Serotec, Oxon, UK) was used, as per the protocol provided by AbD Serotec (Oxon, UK). However, this led to relative over-estimation of the quantity of SDF-1α in standard samples resulting in under-estimation of sample values, particularly at the lowest concentrations of SDF-1α. As the concentration of full-length SDF-1α in actual samples was expected to be low it was important to address this issue. Initial attempts used a human or rat plasma standard diluent, which were successful but not sustainable. Furthermore, this approach complicated

analysis due to the SDF-1α naturally present in plasma. The issue was resolved by identifying a commercially available diluent that includes goat serum proteins that mimic the constitution and target analyte recovery profile of plasma samples without interfering with the assay (BUF037A, AbD Serotec, Oxon, UK). Once baseline SDF-1α was corrected for, this diluent had a good dynamic range and linearity-of-dilution.

## 7.4 Aim 2: Investigate whether levels of CXCR4 ligands are increased in the blood of rats and humans subjected to remote ischaemic conditioning

### 7.4.1 Background

Several studies have correlated increased SDF-1α following RIC, as measured with commercially available ELISA kits (R&D Systems, Oxon, UK), with a range of protective phenomena. Jiang *et al.* demonstrated increased serum and myocardial SDF-1α after a remote IPostC protocol consisting of clamping the infra-renal abdominal aorta for four cycles of 5 min ischaemia and 5 min reperfusion. SDF-1α levels peaked at 1 h, with an 80±5% increase ($P<0.001$) compared to control (sham surgery) animals. The authors associated this with improved retention of intravenously administered MSCs in a murine model of MI.[29] In a similar experiment, Kamota *et al.* conferred RIC using repetitive occlusion of the abdominal aorta in mice prior to IRI of the LAD territory.[30] Using a standard ELISA, they measured 4-fold levels of SDF-1α after 1 h in unfractionated plasma samples. Finally, Davidson *et al*. confirmed that circulating SDF-1α levels were altered in rats subjected to three cycles of 5 min hind limb ischaemia and reperfusion, increasing by 50% in PFP samples to a peak of 890±70 pg/ml.[31]

However, all of these studies used the monoclonal mouse IgG, MAB350. As discussed in section 7.3, MAB350 reports a combination of intact and cleaved SDF-1α and any effect of RIC on full-length SDF-1α has not been documented. Furthermore, published results using commercially available assays for SDF-1α are also highly variable (see Table 7-2). Examination of the methods used in these studies revealed variable protocols, particularly with reference to sample type, and the effect of sample collection and preparation is considered in this section.

| Reference | Species | SDF-1α (pg/ml) |
|---|---|---|
| **Serum** | | |
| [377] | Human | 1264±251* |
| [67] | Human | 2500** |
| [65] | Mouse | 1700** |
| **Plasma** | | |
| [378] | Human | 2447 |
| [379] | Human | 2565 (1322-4174) |
| [373] | Human | 1508 (1102-2016) |
| [375] | Human | 1894 (742–17,633) |
| [30] | Mouse | 800** |
| [374] | Human | 3400** |
| [380] | Human | 1869 |
| [381] | Human | 2000 |
| [370] | Human | 2420 (2070-2810) |
| [65] | Mouse | 1700** |
| [382] | Mouse | 1879±1417 |
| [383] | Rat | 1200±100 |
| [31] | Rat | 590 ± 50 |
| **Sample type not stated** | | |
| [384] | Human | 2166±489 |

**Table 7-2: Control SDF-1α levels from published studies**

All studies used an SDF-1α Quantikine ELISA Kit (R&D Systems, Oxon, UK) or equivalent reagents. Value given is mean±SD or median (interquartile range) SDF-1α from the control group. *Study methods do not match stated sample type. **Value estimated from study figure.

Unfractionated plasma describes the fraction of whole blood that holds blood cells in suspension. It is obtained after collection in citrated or heparinised tubes (to prevent clotting) and centrifugation (to remove red and white blood cells). Unfractionated plasma contains platelets as well as proteins, clotting factors, and several other dissolved substances. PFP is the residual supernatant after further centrifugation to aggregate platelets. Finally, serum describes the blood fraction obtained after

activation of clotting cascades and removal of the clot by centrifugation. It contains neither blood cells nor clotting factors.

Therefore, the aim of this section was to investigate whether levels of active SDF-1α are increased in the blood of rats and humans subjected to RIC. As discussed in section 6.3.4, the inhibition of RIC by AMD3100 strongly implicates CXCR4, but not necessarily SDF-1α. The most attractive alternative ligand for CXCR4 in the context of cardioprotection is MIF, and its kinetics in response to RIC are also examined in this section. Finally, this section aims to ascertain the effect of sample preparation on SDF-1α measurement.

### 7.4.2 Methods

Sprague Dawley rats were used for all animal experiments in this section due to their greater blood volume compared to mice, and were randomly assigned to control or RIC groups. RIC was conducted using three cycles of 5 min cuff inflation and 5 min deflation. Samples were collected either immediately after RIC or 1 h later (Figure 7-12).

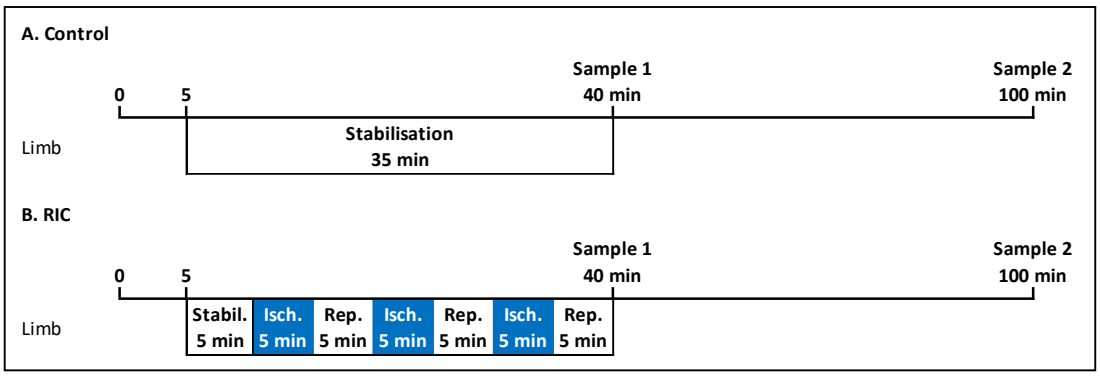


**Figure 7-12: Remote ischaemic conditioning and blood sampling protocol**

(A) Control: 35 min stabilisation; (B) RIC: 5 min stabilisation, three cycles of 5 min hind limb ischaemia and 5 min reperfusion. Animals were exsanguinated by cardiac puncture either immediately after RIC (sample 1) or 60 min thereafter (sample 2). Figure not to scale.

Samples were prepared and assayed as described in Chapter 2. Rat samples were assayed for MIF using a custom sandwich ELISA protocol provided by Professor Bernhagen (Aachen, Germany). This was the same as the SDF-1α assay described in

section 2.8, with the following differences: clear, flat bottom, 96-well MaxiSorp ELISA plates (Thermo Fisher Scientific, MA, USA) were coated with 7.5 µg/ml anti-MIF monoclonal antibody (MAb XIV.14.3, courtesy of Professor Bernhagen) in PBS overnight at RT. Wells were blocked with a buffer containing 1% BSA and 5% sucrose in PBS for 1 h at RT. 100 µl of sample diluted 1:10 in Tris-buffered saline (TBS, consisting of 0.05 M Tris and 0.15 M sodium chloride at pH 7.6) with 0.1% BSA and 0.05% Tween® 20 was added to each well. Standard samples were prepared using purified rat MIF (BioTrend, Köln, Germany) starting at 200 ng/ml with twofold dilution steps (range 4-200 ng/ml) in TBS with 0.1% BSA and 0.05% Tween® 20. Biotinylated polyclonal goat anti-human and mouse MIF secondary antibody (BAF289, R&D Systems, Oxon, UK) diluted in TBS with 0.1% BSA and 0.05% Tween® 20 to 200 ng/ml was added to each well for a further 1 h at RT. All analyses, including samples and standards, were performed in duplicate and readings were averaged to minimise intra-assay variability.

No exclusion criteria were defined beyond those described in section 4.3.2. To ensure the correct curve fit was used in the SDF-1α assay, standard curves of values from fourteen assays were plotted using both linear and non-linear methods. Next, standards were treated as unknown values and interpolated from each standard curve. The resultant values were compared with the expected values using the Pearson product-moment correlation coefficient (r) and the curve fit yielding the best correlation was used. Consequently, full-length SDF-1α values were interpolated from linear regression of the HCI.SDF1α standard curve ($r=0.9996$, $P<0.001$), whereas the commercially available MAB350 standard curve was evaluated with nonlinear regression using log(agonist) versus response ($r=0.9993$, $P<0.001$).

Sample size for rat experiments was calculated using a two-sided test for the comparison of two means. Based on the most conservative increase in SDF-1α, reported by Davidson *et al.* from our laboratory,[31] the following assumptions were made: a 50% estimate of effect size, a control value of 600 pg/ml, an SD of 150 pg/ml,

a significance level of 5% (α=0.05) and 80% power (β=0.2). This required a minimum sample size of four animals per group.

Six healthy male subjects volunteered to participate in the human arm of the study. None were taking any regular medication and no heparin was administered. Each volunteer was subjected to RIC as described in section 2.9 and samples were again collected either immediately after RIC or 1 h later. Experiments were all conducted at the same time of day. Platelet count and waist circumference was measured in all participants. The samples were assayed for full-length SDF-1α, as described above, and for MIF using the R&D ELISA (R&D Systems, Oxon, UK) according to the manufacturers' instructions.

### 7.4.3 Results

The surgical complications encountered in this experiment were negligible compared to *in vivo* myocardial ischaemia-reperfusion experiments as, apart from intubation and exsanguination, no invasive surgical procedures were applied. 48 animals were included in the analysis, with only two exclusions due to anaesthetic-related cardio-respiratory arrest and ventilation complications.

This experiment measured intact and cleaved SDF-1α after RIC in Sprague Dawley rats subjected to a standard RIC protocol. The main difficulty during this study was successfully aspirating blood for analysis. This was initially done by transecting a major vessel and allowing the animal to exsanguinate into its chest cavity, before aspirating blood into a syringe. However, this method activated clotting, which was a potential source of confounding. To test this, PFP prepared by the differential centrifugation protocol described in section 7.4.2 was compared to serum. To prepare serum, blood was collected into tubes with DPP4 inhibitor as before but without citrate. Blood was allowed to clot at RT for 20 min before centrifuging at 1,600 g for 10 min. This removes red and white blood cells, clotting factors, and causes the activation of platelets.[385] SDF-1α measured with both HCl.SDF1α and MAB350 were significantly higher in serum than in PFP samples (HCl.SDF1α PFP 1200±200 pg/ml vs. serum 5000±200 pg/ml, n=3-7, P<0.001; MAB350 PFP 490±30

pg/ml vs. serum 4400±300 pg/ml, n=3-7, P<0.001, Figure 7-13). For completeness, separate samples were taken from the same animals for the measurement of unfractionated plasma. Blood was taken into citrated tubes containing DPP4 inhibitor and immediately centrifuged at 1,600 g for 20 min, without subsequent centrifugation at 10,000 g. Likewise, SDF-1α measured with either antibody was significantly higher in serum than in unfractionated plasma samples (HCI.SDF1α unfractionated plasma 1100±200 pg/ml vs. serum 5000±200 pg/ml, n=3-4, P<0.001; MAB350 unfractionated plasma 1200±100 pg/ml vs. serum 4400±300 pg/ml, n=3-4, P<0.001, Figure 7-13). In order to limit the number of animals used, samples for unfractionated plasma and serum were collected from the same animals using separate RV punctures whenever possible.

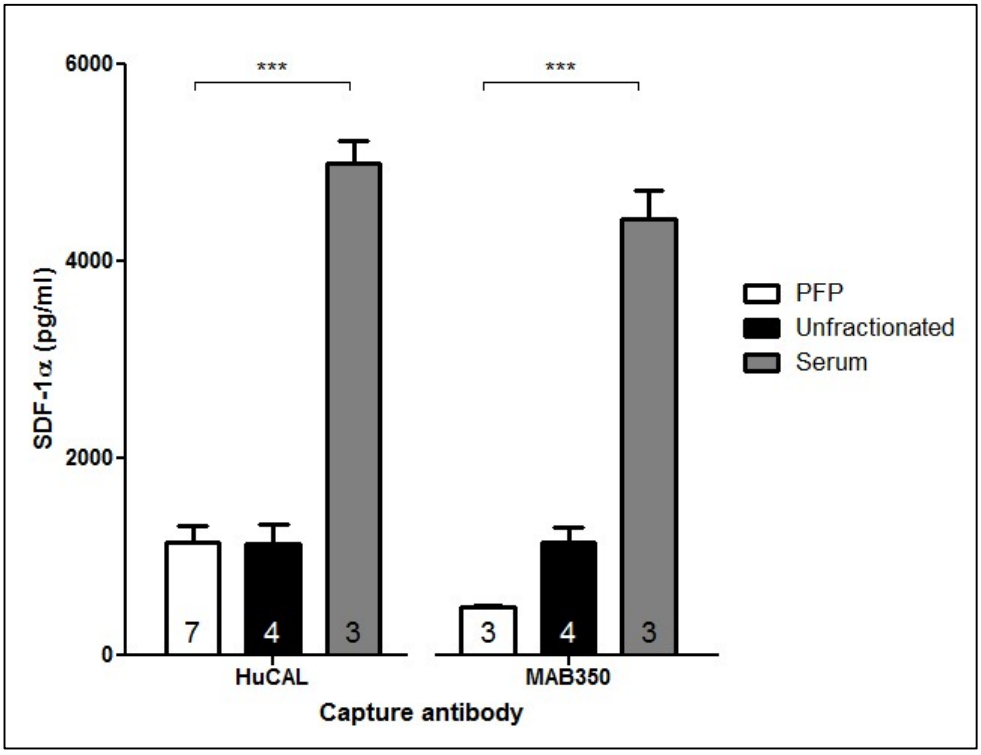


**Figure 7-13: Effect of sample preparation on SDF-1α concentration in rat blood**

Sprague Dawley rats were anaesthetised and exsanguinated via RV puncture for analysis of SDF-1α in different blood fractions. Serum samples had significantly more SDF-1α using either HCI.SDF1α or MAB350 assays than PFP or unfractionated plasma samples. Statistical significance was assessed using one-way ANOVA and Tukey's multiple comparison test for each assay, n=3-7, ***P<0.001.

In view of the high concentration of SDF-1α in serum samples and the potential confounding effect of platelets in unfractionated plasma, PFP samples were used in all subsequent experiments. Additionally, blood was collected via cardiac puncture, and further incremental improvements were made by reducing needle length and increasing needle gauge to reduce activation of clotting.

An ELISA of PFP samples using MAB350 replicated the published finding of significantly higher SDF-1α after RIC,[29-31] and this difference was still present 1 h after the RIC protocol (0 min control 490±20 pg/ml vs. RIC 760±60 pg/ml, n=3, P<0.05; 60 min control 500±100 pg/ml vs. RIC 740±20 pg/ml, n=4, P<0.05, Figure 7-14). However, when measured using HCl.SDF1α, levels of full-length SDF-1α unexpectedly decreased immediately after RIC (700±100 pg/ml vs. 1200±200 pg/ml, n=7-9, P<0.05, Figure 7-14) and normalised by 1 h (900±100 pg/ml vs. 950±90 pg/ml, n=4, P=NS, Figure 7-14). Samples were taken at 0 and 60 min after RIC to reflect reports in the literature that total SDF-1α significantly increased only after 60 min.[29, 30]

These findings suggest increased cleavage of SDF-1α after RIC, at least in the circulation, which is discussed further in section 7.5. However, it is known that endothelial sulphated glycoasaminoglycans, including heparan sulfate (HS), sequester SDF-1α from the circulation,[386, 387] promoting its oligomerization and competitively inhibit its interaction with CXCR4.[388] It was therefore necessary to test for any change in the quantity of sequestered SDF-1α in response to RIC.

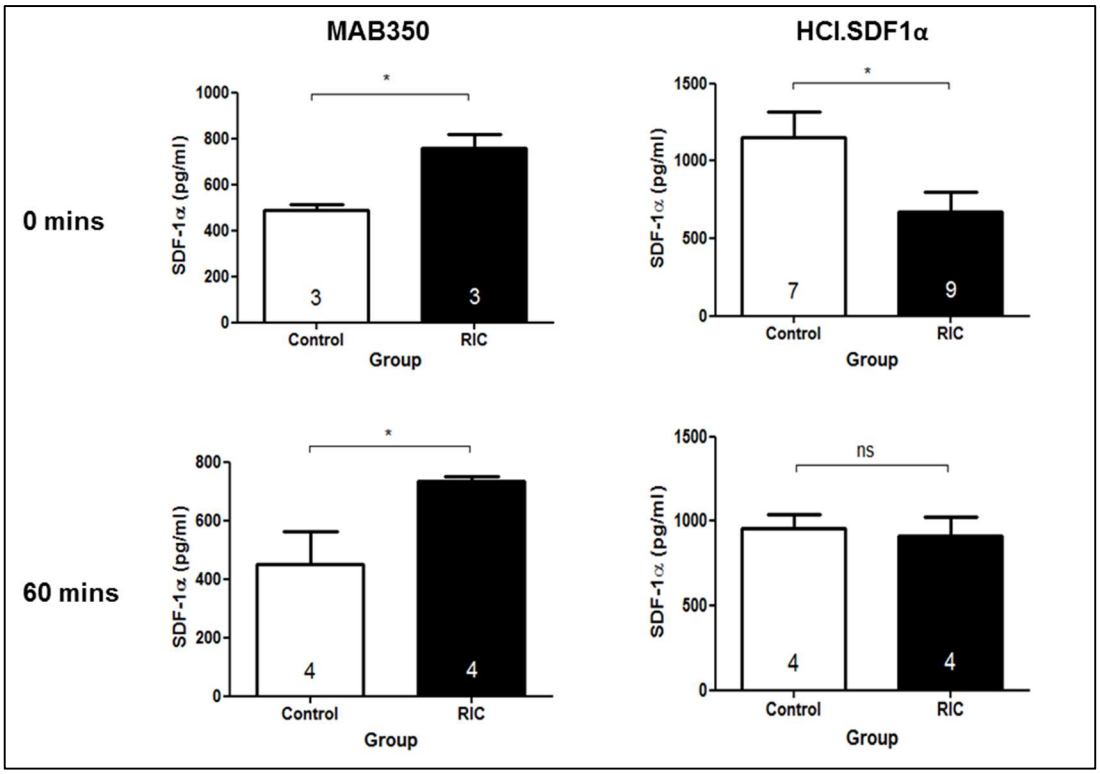


**Figure 7-14: Rat PFP SDF-1α measured using HCl.SDF1α and MAB350 immediately and 1 h after remote ischaemic conditioning**

Sprague Dawley rats were anaesthetised and treated with either RIC (three cycles of 5 min hind limb ischaemia and 5 min reperfusion) or sham procedure. Blood was taken by RV puncture at either 0 min or 60 min and processed to obtain PFP. ELISA using MAB350 detected an increase in plasma SDF-1α levels whereas HCl.SDF1α, which is more specific for full-length SDF-1α, measured a decrease immediately after RIC that returned to baseline by 1 h. Statistical significance was assessed with unpaired t-tests, n=3-9, *P<0.05.

To investigate the significance of the association between SDF-1α and cell surface HS rats were pre-treated with either intraperitoneal heparin oligosaccharides (heparin sodium 500 IU combined with usual anaesthetic), which competitively displaces sequestered pools of SDF-1α and increase circulating levels,[386] or saline vehicle control. As expected, heparin treatment significantly increased SDF-1α in control animals from 490±20 pg/ml to 1100±100 pg/ml (n=4, P<0.01, Figure 7-15) when assayed using MAB350. However, it did not significantly increase PFP full-length SDF-1α (no heparin 1200±200 pg/ml vs. heparin 1400±200 pg/ml, n=3-7, P=NS, Figure 7-15).

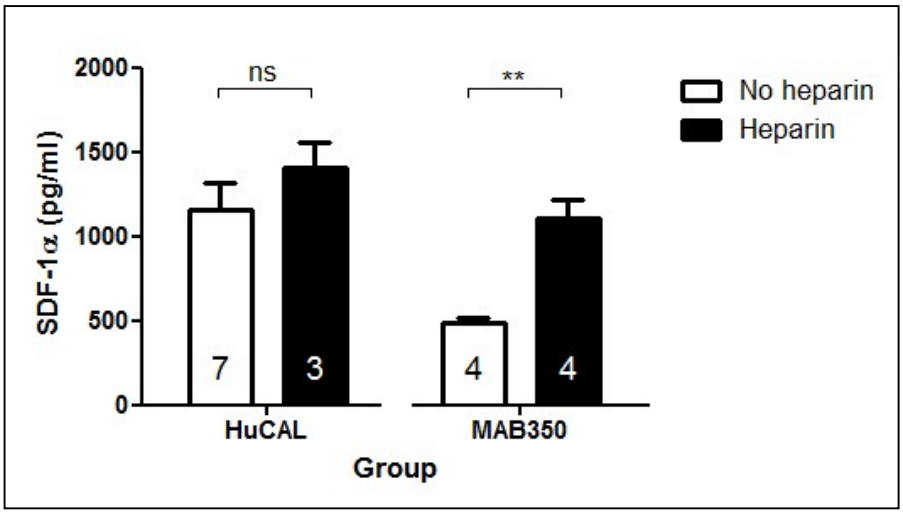


**Figure 7-15: Rat platelet-free plasma SDF-1α measured using HCI.SDF1α and MAB350 after pre-treatment with intraperitoneal heparin**

Sprague Dawley rats were anaesthetised with either intraperitoneal pentobarbitone alone or in combination with 500 IU heparin. Blood was taken by RV puncture and processed to obtain PFP. Animals that were pre-treated with heparin had significantly more full-length SDF-1α than un-heparinised controls. Statistical significance was assessed using unpaired t-tests, n=3-7, **P<0.01.

Next, the RIC experiments were repeated to determine whether a significant elevation in active SDF-1α levels after RIC could be unmasked by the addition of heparin. Rats were randomly allocated to either the control or RIC arm of the study. Blood was taken both immediately and 1 h after RIC, and SDF-1α was measured using HCI.SDF1α. Interestingly, rather than reveal an increase in active SDF-1α, pre-treatment of animals with heparin prior to RIC increased overall levels of PFP SDF-1α and abolished the significant reduction in SDF-1α seen immediately after RIC in Figure 7-14 (0 min control 1400±200 pg/ml vs. RIC 1230±50 pg/ml, n=4, P=NS; 60 min control 1500±400 pg/ml vs. RIC 1200±300 pg/ml, n=4, P=NS, Figure 7-16).

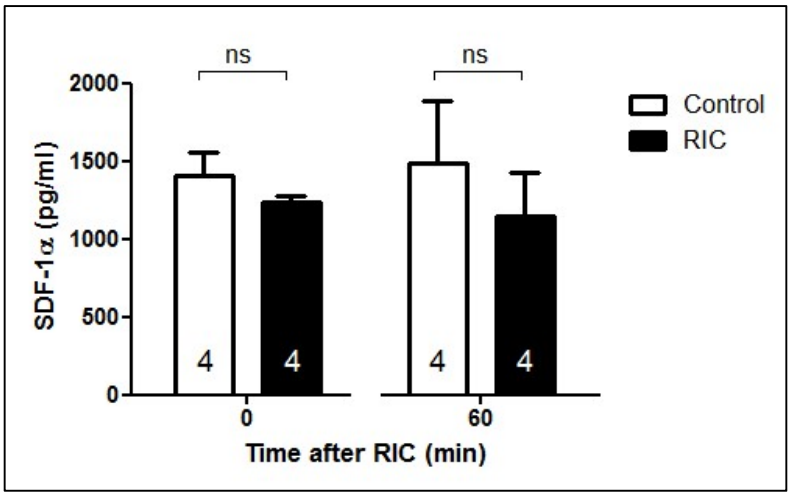


**Figure 7-16: Rat SDF-1α measured in platelet-free plasma using HCI.SDF1α immediately and 1 h after remote ischaemic conditioning in animals pre-treated with heparin**

Sprague Dawley rats were anaesthetised with intraperitoneal pentobarbitone in combination with 500 IU heparin prior to RIC (three cycles of 5 min hind limb ischaemia and 5 min reperfusion) or sham procedure. Blood was taken by RV puncture at 0 min and 60 min and processed to obtain PFP. In rats pre-treatment with heparin, RIC did not significantly increase active SDF-1α at either 0 or 60 min. Statistical significance was assessed using unpaired t-tests, n=4, P=NS.

In the absence of a detectable increase in active SDF-1α, it may be another ligand of CXCR4 that increases in response to RIC. To test this MIF was assayed in the same samples as above. There was no detectable change in MIF concentration after RIC in PFP (Panel A: 0 min control 24±6 ng/ml vs. RIC 18±7 ng/ml, n=4, P=NS; 60 min control 24±8 ng/ml vs. RIC 45±27 ng/ml, n=4, P=NS, Figure 7-17) or serum samples (Panel B: 0 min control 300 ng/ml vs. RIC 290±11 ng/ml, n=1-3, P=NS; 60 min control 290±25 ng/ml vs. 340±20 ng/ml, n=3-4, P=NS, Figure 7-17).

To confirm the surprising finding that RIC resulted in a reduction of full-length SDF-1α, the RIC protocol was repeated on the upper limb of six healthy human volunteers. Despite significant inter-individual variability and exclusion of a haemolysed sample (because haemolysis is known to interfere with the assay), a small but significant decrease in active SDF-1α was observed (pre-RIC 380.0±154.9 pg/ml vs. 0 min 337.5±148.3 pg/ml vs. 60 min 329.8±148.7 pg/ml, n=5, $P<0.05$, Figure 7-18). There was no correlation with waist circumference, which has previously been associated with SDF-1α, albeit using commercially available antibodies (Pearson's r -0.04,

P=NS),[389] nor was any association with platelet count observed (Pearson's r -0.41, P=NS).

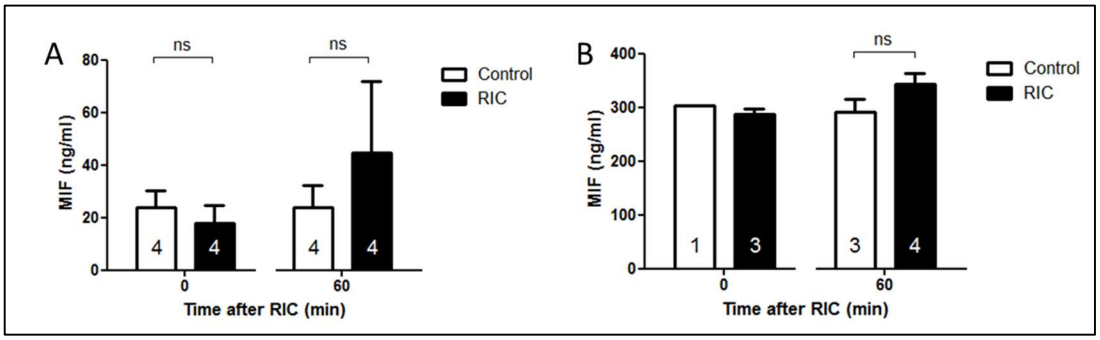


**Figure 7-17: MIF measured in rat platelet-free plasma (Panel A) and serum (Panel B) immediately and 1 h after remote ischaemic conditioning**

Sprague Dawley rats were anaesthetised and subjected to RIC (three cycles of 5 min hind limb ischaemia and 5 min reperfusion) or sham procedure. Blood was taken by RV puncture at 0 min and 60 min and processed to obtain PFP. RIC did not significantly increase MIF at either 0 or 60 min in either blood fraction. Statistical significance was assessed using unpaired t-tests, n=1-4, P=NS.

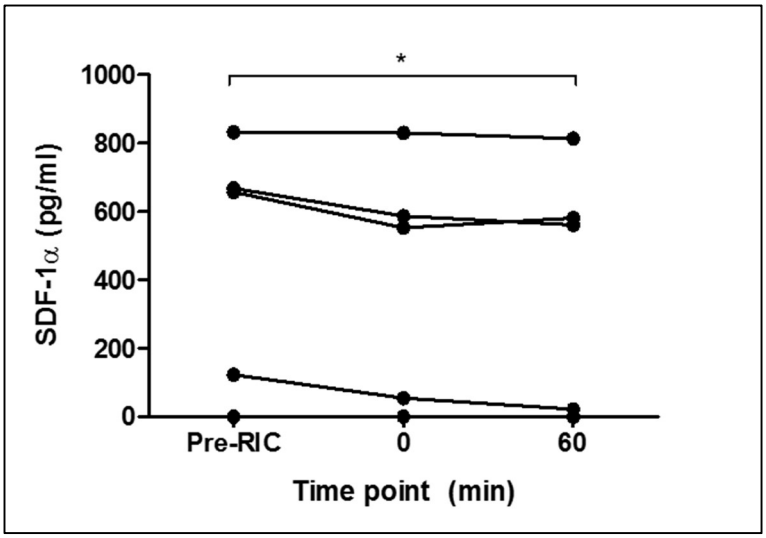


**Figure 7-18: PFP SDF-1α measured in healthy male volunteers using HCl.SDF1α at baseline, and immediately and 1 h after remote ischaemic conditioning**

RIC consisting of three cycles of 5 min right upper limb ischaemia and 5 min reperfusion was applied by inflation of a manual sphygmomanometer to a pressure of 200 mmHg. Blood samples were collected into citrated tubes at baseline and after the final 5 min of reperfusion. Samples were immediately prepared to obtain PFP. Despite marked baseline variation, there was a decrease in plasma full-length SDF-1α levels after RIC. Statistical significance was assessed using one-way ANOVA and Tukey's multiple comparison test, n=5, *P<0.05.

The same samples were assayed for MIF with a commercial ELISA as MIF was undetectable in human samples when using the same custom ELISA used in rats. A haemolysed sample was excluded from the human volunteer baseline group. The remaining samples indicated there was no significant difference either immediately or 1 h after RIC (baseline 16±1 ng/ml vs. 0 min 15±3 ng/ml vs. 60 min 18±4 ng/ml, n=5-6, P=NS, Figure 7-19).

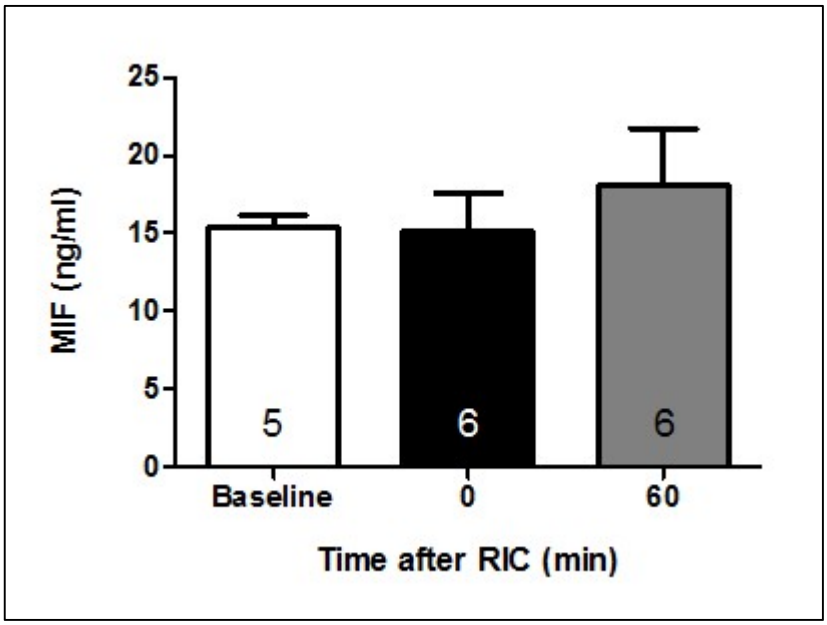


**Figure 7-19: Platelet-free plasma MIF measured in healthy male volunteers at baseline, and immediately and 1 h after remote ischaemic conditioning**

RIC consisting of three cycles of 5 min right upper limb ischaemia and 5 min reperfusion was applied by inflation of a manual sphygmomanometer to a pressure of 200 mmHg. Blood samples were collected into citrated tubes at baseline and after the final 5 min of reperfusion. Samples were immediately prepared to obtain PFP. MIF in the PFP of healthy human volunteers was unaffected by RIC. Statistical significance was assessed using one-way ANOVA and Tukey's multiple comparison test, n=5-6, P=NS.

### 7.4.4 Discussion

The main finding reported in this section is that, surprisingly, full-length SDF-1α significantly decreased immediately after RIC, in both rats and humans. In rats, this had returned to baseline by 60 min. Combined with the observation here and in the literature that SDF-1α levels appear to increase when measured with commercial assays, this suggests that there is, in fact, an increase in cleaved, inactive SDF-1α.

It is unclear how increased cleavage can relate to acute cardioprotection given the existing paradigm that anticipates increased production or maintenance of extracellular concentrations of SDF-1α as a direct effect of RIC.[103] There are several hypotheses for this finding in the context of this thesis, that include: (1) RIC-mediated increases in SDF-1α expression are limited to a specific circulating cell type such as platelets or inflammatory cells; (2) RIC-mediated increases in SDF-1α expression are predominantly sequestered by endothelial sulphated proteoglycans; (3) an alternative ligand for CXCR4 is responsible for the cardioprotection conferred by RIC; (4) SDF-1α is important in either the trigger or effector phases of RIC, but is not the humoral factor; and (5) cardioprotection in response to RIC is related to altered receptor dynamics, rather than up-regulation of SDF-1α. These hypotheses will be discussed in turn.

Firstly, regarding the hypothesis that RIC-mediated increases in SDF-1α expression are limited to a specific circulating cell type, platelets are of particular interest. Activated platelets are known to express SDF-1α and adhere to injured endothelium via inflammatory cell adhesion molecules in MI.[358, 390] Furthermore, platelets are removed during the preparation of PFP and any such up-regulation may not be detectable in the ELISA described here. With this in mind, it was further hypothesised that platelets may be central to SDF-1α dynamics after RIC, and this is examined further in section 7.6. The potential role of inflammatory cells is discussed in section 8.4.4.

Secondly, RIC-mediated increases in SDF-1α expression may be predominantly sequestered by endothelial sulphated proteoglycans.[386, 387] Any change in SDF-1α conferred by RIC may be undetectable by ELISA if SDF-1α is absent from the circulation. Exogenous heparin can be useful in this regard as it is known to liberate HS-bound SDF-1α and increase circulating levels.[386] Interestingly, it has been reported that heparin is cardioprotective in the context of IRI,[242-246] although it is not known whether this is related to altered SDF-1α dynamics. This seems unlikely given that glycosaminoglycans (including heparin) promote dimerisation of SDF-1α, which abrogates the cardioprotection conferred by SDF-1α in an isolated rat heart model of

IRI by impairing the ability of SDF-1α to bind to CXCR4.[388] However, this finding may further contribute to elevated circulating SDF-1α after heparin administration. It is notable that studies that demonstrate increased SDF-1α after RIC use variable protocols, however only one (Davidson *et al*.[31]) specifically documents the use of intraperitoneal heparin sodium prior to RIC.

In the present study, only circulating SDF-1α measured using MAB350 was significantly increased after the administration of heparin, suggesting it was the cleaved fraction. It is unclear then exactly what form (full-length or cleaved) of SDF-1α binds to cell-surface HS, but to investigate this further was beyond the scope of this project. Importantly, pre-treatment with exogenous heparin did not unmask any change after RIC but instead abrogated the significant reduction in SDF-1α seen immediately after RIC in experiments performed without heparin. This may relate to the finding by Ziarek *et al.* that HS- and heparin-induced SDF-1α dimerisation also inhibits its proteolytic degradation by DPP4 by shielding DPP4 from its binding sites,[388] rather than altered activity *per se*,[391] although this hypothesis was not specifically tested here.

Thirdly, an alternative ligand for CXCR4 may be responsible for RIC-induced cardioprotection. This justifies both the failure of the present study to demonstrate increased SDF-1α in the plasma of rats subjected to RIC and the finding that the CXCR4 receptor antagonist AMD3100 abrogates the cardioprotective effect of RIC. To this end, MIF was assayed after RIC in rat PFP and serum without any detectable increase. MIF values were generally higher in serum samples, although the inclusion of only one sample in the 0 min control group precluded statistical comparison. Like SDF-1α, this may relate to its expression by platelets although, unlike SDF-1α, its release from activated platelets is delayed for up to 2 h.[392, 393] Furthermore, it is not clear whether MAb XIV.14.3 measures intact or cleaved MIF. Nonetheless, there was no indication from these experiments that this is an important consideration and it was not investigated further. In addition to MIF, ubiquitin is a recognised ligand for CXCR4. As discussed in section 6.3.4, it has not yet been investigated in cardioprotection and this was not specifically addressed here.

Fourthly, it is possible that SDF-1α increases locally to the limb stimulus or remotely in the effector organ, perhaps via a neural or humoral intermediary.[181] To be certain it would be necessary to demonstrate increased extracellular concentrations of active SDF-1α at these locations. This was not possible during the course of this project, but could be investigated using immunofluorescence with standard anti-CXCR4 antibodies or by exploiting a molecule called Ac-TZ14011-FITC, which is a validated, fluorescent CXCR4-binding peptide.[394]

Fifthly, it may be the case that, rather than fluctuations in SDF-1α concentration that are important for acute cardioprotection, it is alterations in CXCR4 expression that are central to the mechanism of RIC. This is discussed in more detail in Chapter 8.

To confirm the unanticipated finding that full-length SDF-1α is degraded by RIC, the study was repeated in healthy human volunteers. A similar decrease in SDF-1α levels after RIC was seen, despite there being significant variability in baseline SDF-1α measurements. Previously, variability in circulating SDF-1α has been associated with waist circumference,[389] time of day and acute stress.[327] In this study, there was no association between waist circumference and baseline SDF-1α, all experiments were performed at the same time of day to account for SDF-1α circadian rhythm, and no major differences in stress levels of the subjects were apparent, although this was not specifically controlled for. Platelet count was measured in each subject but no significant correlation was found.

The experiments in this section measured SDF-1α in different blood fractions, including unfractionated plasma, PFP and serum. SDF-1α levels were found to be dramatically increased in serum, compared to platelet-free and unfractionated plasma samples. As discussed, SDF-1α is known to be contained in platelet α-granules and be expressed upon platelet activation and degranulation,[358] as occurs during the preparation of serum samples. The present finding therefore emphasises the importance of correct sample preparation when measuring SDF-1α. Interestingly, the methods described in published studies investigating SDF-1α are highly variable and often include the analysis of serum samples, for example the study by Jiang *et al.*

described above, which complicates interpretation of the existing literature and suggests that some published results may be anomalous. [29, 65, 67, 377]

Overall, it seems likely that the apparent increased cleavage of SDF-1α in response to RIC does not relate to acute cardioprotection. Instead, this finding may relate to the gradient-guided homing, reparative properties of the SDF-1α-CXCR4 axis in response to tissue ischaemia. The precise mechanism is not clear, and is beyond the scope of this project, but it is intriguing to consider a possible role of SDF-1α in relation to recent large randomised control trials of DPP4 inhibitors, which are described in more detail in section 7.5.1. Specifically, SAVOR-TIMI 53 compared Saxagliptin and placebo in 16,492 patients with a history of, or at risk for, cardiovascular events.[395] It unexpectedly reported an increased risk of hospitalisation for heart failure (hazard ratio 1.27, 95% CI 1.07-1.51, P=0.007), which a subsequent sub-study found to be highest in patients with elevated natriuretic peptides, previous heart failure or chronic kidney disease.[396] Combined with mixed results from observational studies, the relationship between DPP4 inhibitors and heart failure is controversial. A recent systematic review and meta-analysis concluded that, despite an abundance of low-quality evidence, DPP4 inhibitors 'may increase the risk of hospital admission for heart failure in those patients with existing cardiovascular diseases or multiple risk factors for vascular diseases, compared with no use'.[397] Although SDF-1α has not been investigated in this context, it may be speculated that increased cleavage of SDF-1α after tissue injury (MI, for example) is part of a reparative mechanism that, if interrupted by DPP4 inhibitors, results in worse outcomes. It is anticipated that resolving the role of SDF-1α and DPP4 in response to ischaemia would yield important and timely information in this area of clinical uncertainty.

## 7.5 Aim 3: Investigate the contribution of DPP4 to SDF-1α dynamics after remote ischaemic conditioning

### 7.5.1 Background

DPP4 is an extracellular peptidase that cleaves SDF-1α at its position 2 proline residue. It is present on many of the same cell types as CXCR4, including B and T

lymphocytes, endothelial cells and $CD34^+$ haematopoietic progenitor cells, as well as being present in plasma.[17, 398] Several studies have attempted to interfere with SDF-1α proteolysis by DPP4. For example, bioengineered SDF-1 that is resistant to cleavage by DPP4 and MMP-2 has been associated with improved stem cell homing, angiogenesis and EF.[51, 369] With regard to DPP4 inhibitors, Christopherson *et al.* first showed that DPP4 inhibition increased stem cell homing to bone marrow,[399] following which Zaruba *et al.* combined DPP4 inhibition with G-CSF-mediated stem cell mobilisation in a murine model of MI.[200] They found increased $CXCR4^+$ EPC homing (an effect that was abrogated by administration of AMD3100), reduced cardiac remodelling and apoptosis, and improved EF and survival. This approach was recently tested in a phase III clinical trial using Sitagliptin (Safety and efficacy of SITAgliptin plus Granulocyte-colony-stimulating factor in patients suffering from Acute Myocardial Infarction, SITAGRAMI).[400] They randomised 174 patients to either G-CSF and Sitagliptin or placebo after PPCI for MI in a multi-centre, double-blind design. The primary endpoint of improved combined global LV and RV EF as assessed by magnetic resonance imaging at 6 months was not met and while there was a trend towards reduced major adverse cardiac events, it was not significant. This may be explained by the inclusion of only 21% of patients with LV EF below 50%, thereby obfuscating any potential benefit of this therapy.

Similarly, three large multicentre clinical trials have recently failed to demonstrate a benefit of DPP4 inhibitors on cardiovascular outcomes in patients with type 2 diabetes at high risk for cardiovascular events. SAVOR-TIMI 53, described above, found no significant difference in the primary endpoint of cardiovascular death, MI or stroke between Saxagliptin and placebo.[395] Similarly, EXAMINE compared Alogliptin with placebo in 5380 patients with type 2 diabetes and recent acute coronary syndrome over median follow-up of 18 months and found no significant difference in the primary endpoint of cardiovascular death, non-fatal MI or non-fatal stroke.[401] In a post-hoc analysis, there was no evidence of excess admissions for heart failure.[402] Most recently, TECOS compared Sitagliptin to placebo in 14,671 patients with type 2 diabetes and cardiovascular disease, and found no difference with respect to the composite primary outcome of cardiovascular death, nonfatal MI,

nonfatal stroke, or hospitalization for unstable angina.[403] In a subgroup analysis, there was no difference in the rate of hospitalisation for heart failure.

However, none of the aforementioned studies elucidated the contribution, if any, of DPP4 inhibitors in the acute phase of MI. In the context of RIC, Davidson *et al.* found no increase in *plasma* DPP4 activity after RIC in rats.[31] However, it is not known if the expression or activity of membrane-bound DPP4 changes following RIC and whether this impacts on SDF-1α dynamics. It was therefore hypothesised that the increased cleavage of SDF-1α described in section 7.4 was consequent upon increased membrane-bound DPP4 activity in response to RIC.

### 7.5.2 Methods

To confirm the absence of increased circulating DPP4 activity as the cause of SDF-1α cleavage, rats were randomly assigned to control or RIC groups. Soluble DPP4 activity was measured using the DPPIV-Glo™ Protease Assay (Promega, Essex, UK) according to the manufacturer's instructions. Briefly, plasma samples were added to an equal volume of DPPIV-Glo™ reagent, mixed using a plate shaker and incubated at RT for 2 h. Luminescence was measured on a 96 well microplate reader (FLUOstar Omega, BMG Labtech, Germany). All samples were measured in duplicate. As a significant increase in circulating DPP4 activity after RIC has not been reported in the literature, a pragmatic decision was made to test a minimum of four animals per group. Assuming a control value and SD of 1.2 LU and 0.3 LU, respectively, based on the report by Davidson *et al.*,[31] a significance level of 5% ($\alpha$=0.05) and 80% power ($\beta$=0.2), this sample size would detect an effect size of 50%

Endothelium membrane-bound DPP4 activity was investigated using human umbilical vein endothelial cells (HUVECs). 5 x $10^4$ cells were seeded per well of a 96-well flat-bottomed plate in 200 µl of the endothelial cell growth medium EGM-2 supplemented with 2% foetal bovine serum (Lonza, Berks, UK) until confluence was achieved. To apply oxidative stress, medium was removed and replaced with PBS containing 1 mM $H_2O_2$ at RT. After 5 min this was removed and replaced with 200 µl EGM-2 medium for 150 min, after which the supernatant was removed and replaced

with 50 µl EGM-2 medium and 50µl DPPIV-Glo™ reagent. All groups were performed in triplicate.

### 7.5.3 Results

Circulating plasma DPP4 activity was not significantly altered when assayed immediately after RIC, and activity actually decreased by 1 h post RIC (0 min control 440±30 LU vs. RIC 360±60 LU, n=4, P=NS; 60 min control 440±10 LU vs. RIC 380±20 LU, n=4, P<0.05, Figure 7-20). No surgical complications were encountered in this experiment.

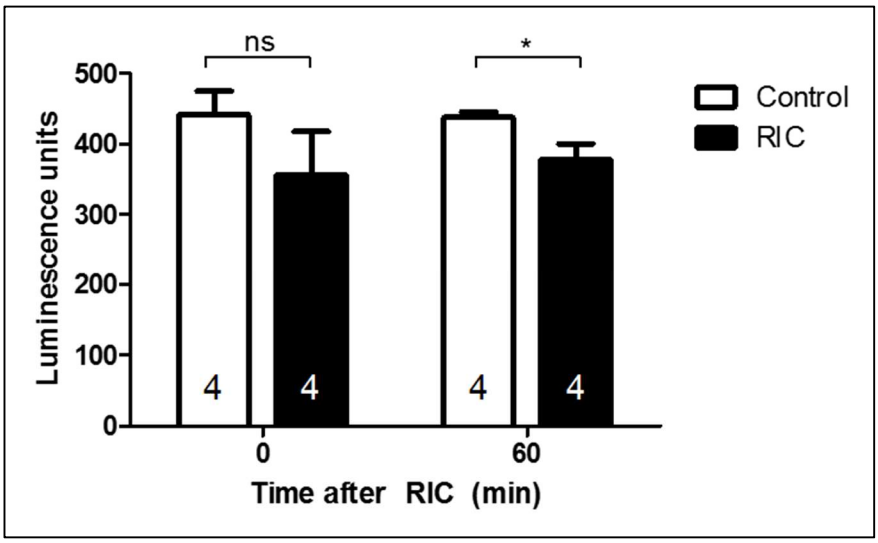


**Figure 7-20: Dipeptidyl peptidase 4 activity measured in rats immediately and 1 h after remote ischaemic conditioning**

Sprague Dawley rats were anaesthetised and treated with either RIC (three cycles of 5 min hind limb ischaemia and 5 min reperfusion) or sham procedure prior to exsanguination via RV puncture for analysis of DPP4 activity at 0 min and 60 min. Levels of circulating DPP4 were unchanged immediately after RIC but significantly decreased by 1 h. Statistical significance was assessed using unpaired t-tests, n=4, *P<0.05.

To investigate the possibility that the activity of membrane-bound DPP4 on endothelial cells could be specifically altered, cultured HUVECs were stimulated with transient (5 min) $H_2O_2$ to simulate the oxidative stress conferred by IPC.[404] This resulted in a significant increase in DPP4 activity in stressed cells (140±7 vs. 120±4, n=4, P<0.05, Figure 7-21).

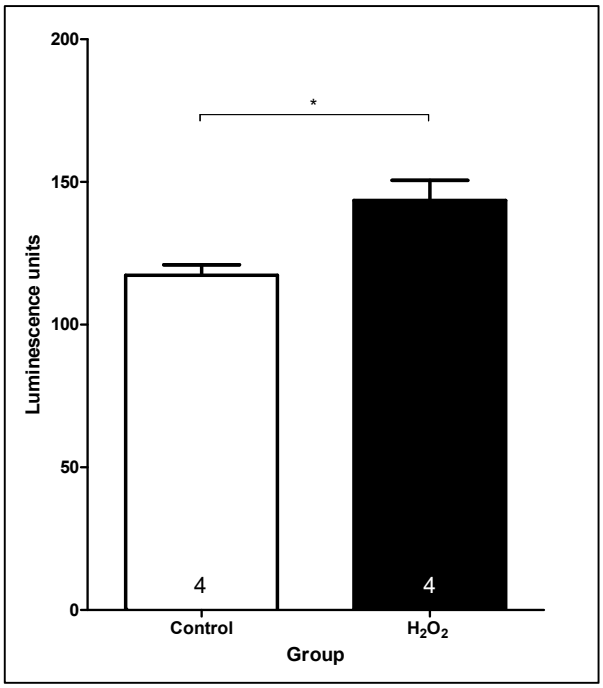


**Figure 7-21: Effect of heparin on DPP4 activity HUVECs stimulated with to $H_2O_2$**

To simulate RIC in primary endothelial cells, HUVECs were briefly (5 min) exposed to 100 μM $H_2O_2$. There was a significant increase in DPP4 activity in stressed cells. Statistical significance was assessed using an unpaired t-test, n=4, *P<0.05.

### 7.5.4 Discussion

The finding of increased cleavage of SDF-1α immediately after RIC could not be explained by increased circulating DPP4, which is consistent with the finding of Davidson *et al.*[31] However, DPP4 is known to be predominantly active on endothelium,[391] and this experiment provides the first description of the activity of membrane-bound DPP4 being increased in response to oxidative stress, which was used to mimic RIC in HUVECs.

This experiment provides some justification for the unexpected finding of increased SDF-1α cleavage in response to RIC. However, it is unclear if this mechanism relates to acute cardioprotection. In the context of the hypothesis that SDF-1α mediates RIC it might instead be expected that acute DPP4 *inhibition*, to increase the half-life of SDF-1α by preventing its degradation, would be advantageous. Only a relatively small number of pre-clinical studies have investigated whether DPP4 inhibitors confer acute cardioprotection after IRI in non-diabetic animals.[405-409] For example, Chinda *et*

*al.* found that Vildagliptin significantly reduced IS in an *in vivo* rat model of IRI.[406] This was associated with reduced mitochondrial ROS, mitochondrial swelling, and increased markers of cardiomyocyte apoptosis, including Bcl-2 and pro-caspase 3. Ye *et al.* reported a similar result with Sitagliptin, via cAMP dependent PKA activation,[408] and Sauve *et al.* demonstrated smaller IS following IRI in isolated hearts from DPP4 null mice.[407] The involvement of SDF-1α in these studies was not tested.

No study to date has examined whether pre-treatment with a DPP4 inhibitor can augment RIC-induced cardioprotection. This was not addressed here in view of the absence of a detectable increase in full-length SDF-1α after RIC. Furthermore, as discussed in section 7.4, it is not clear whether DPP4 inhibition would compromise the beneficial effects of the SDF-1α-CXCR4 axis with respect to ventricular remodelling.

## 7.6 Aim 4: Investigate the role of platelets in SDF-1α dynamics after remote ischaemic conditioning

### 7.6.1 Background

As discussed, a possible reason for the unexpected absence of an increase in PFP SDF-1α after RIC might relate to the role of platelets in SDF-1α kinetics. As presented in Figure 7-13, serum samples, that contain activated platelets, have significantly more SDF-1α than PFP samples. This leads to the hypothesis that RIC might activate platelets, by hypoxia for example,[410] triggering the release and expression of SDF-1α.

It is well established that platelets contain SDF-1α within α-granules and express CXCR4 on their surface.[358] Furthermore, Chatterjee *et al.* have shown that stimulating platelets using protease-activated receptor (PAR)-1-activating peptide, ADP (via P2Y12 receptors) or glycoprotein VI-targeting collagen-related peptide induces SDF-1α release and surface expression.[358] As platelets are activated in the preparation of serum samples as part of a general activation of clotting pathways, this is the likely mechanism of SDF-1α release described in Figure 7-13.

Interestingly, it has been hypothesised that RIC activates platelets, albeit without specific reference to SDF-1α. Oberkofler *et al.* applied RIC to the femoral vascular bundle prior to hepatic IRI in mice.[411] As well as hepatic protection, RIC caused platelet activation as evidenced by a 40% reduction in platelet numbers and an associated increase in serum P-selectin, which is ubiquitous in α-granules.[412] Furthermore, RIC was abolished when platelet activation was inhibited using a platelet-activating factor (PAF) receptor antagonist.

Taken together, these findings engender the hypothesis that RIC is mediated by platelet activation and the release of proteins contained within α-granules, including SDF-1α. This is consistent with the finding of diminished full-length SDF-1α in PFP samples described in section 7.3.4 if it is hypothesised that SDF-1α interacts with platelet-expressed CXCR4 and is then removed along with platelets during centrifugation. In this case, an increase in SDF-1α might only be detectable in serum samples or directly on platelets. This is supported by the use of serum by Jiang *et al.* in their report of increased SDF-1α following RIC,[29] and its investigation is the next aim of this chapter.

### 7.6.2 Methods

For rat experiments, animals were randomly assigned to control or RIC groups. Anaesthetised rats were subjected to RIC consisting of three cycles of 5 min cuff inflation and 5 min deflation. Blood was taken via ventricular puncture immediately and 1 h after the RIC protocol (Figure 7-12). Blood was centrifuged to obtain serum, which was subsequently assayed for levels of intact SDF-1α.

Sample size was calculated using a two-sided test for the comparison of two means. Based on the increase in SDF-1α after RIC in serum reported by Jiang *et al.*, the following assumptions were made: an 80% estimate of effect size, a control value of 3.5 ng/ml, an SD of 1 ng/ml, a significance level of 5% ($\alpha$=0.05) and 80% power ($\beta$=0.2). This required a minimum sample size of two animals per group.

The methods used for human experiments were based on those described in section 2.9, with details specific to this experiment described here. Three healthy male volunteers participated in the study after giving informed consent. None were taking any regular medication and no heparin was administered. Experiments were all conducted at the same time of day.

Samples were taken at baseline and immediately after RIC. No 1 h sample was taken in this experiment as SDF-1α is known to be released within minutes of platelet activation.[392] Whole blood was either immediately fixed in 1% PFA or diluted with PBS containing 0.1% BSA and treated with 10 μM ADP for 20 min at RT, then 1% PFA added for 10 min at RT to a final dilution of 1:20. Blood samples taken after RIC were prepared in the same way and both groups were subsequently prepared and analysed as described in section 2.9.

### 7.6.3 Results

The aim of this section was to investigate the hypothesis that RIC activates platelets, triggering the release and expression of SDF-1α. The surgical complications encountered in this experiment were negligible. 24 animals were included in the analysis, with no exclusions.

In the first experiment, serum samples were measured to determine whether there was any difference in SDF-1α between control and RIC groups. Any such difference would suggest that RIC potentiates SDF-1α release and expression by platelets that are activated in the preparation of serum. However, despite finding high levels of SDF-1α, no difference was observed between the control and RIC group either immediately or 1 h after RIC (0 min control 4300±300 pg/ml vs. RIC 4300±300 pg/ml, n=5-6, P=NS; 60 min control 5000±200 pg/ml vs. RIC 4900±300 pg/ml, n=4, P=NS, Figure 7-22).

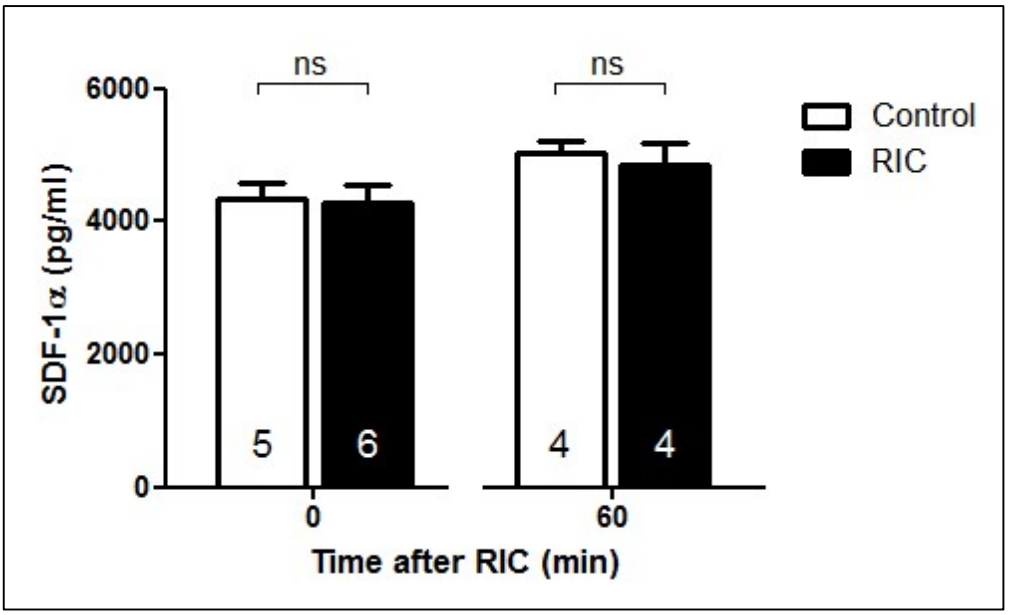


**Figure 7-22: Full-length SDF-1α measured in rat serum immediately and 1 h after remote ischaemic conditioning**

Sprague Dawley rats were anaesthetised and treated with either RIC (three cycles of 5 min hind limb ischaemia and 5 min reperfusion) or sham procedure. Blood was taken by RV puncture at either 0 min or 60 min and processed to obtain serum. Serum samples were prepared by allowing whole blood to clot for 10 min prior to removing the clot by centrifugation and analysis for full-length SDF-1α. Samples prepared in this way had high levels of SDF-1α but there were no significant differences between control and RIC groups at either time point. Statistical significance was assessed using unpaired t-tests, n=4-6, P=NS.

This finding remains consistent with the hypothesis that RIC stimulates the release of SDF-1α from α-granules because the massive SDF-1α release from activated serum samples might obscure any change conferred by RIC. Therefore, the presence of an interaction between SDF-1α and platelet-expressed CXCR4 was investigated, instead, using unfractionated plasma samples that are expected to retain a platelet population. These were incubated with 5 μg/ml of AMD3100, a competitive antagonist of CXCR4, for 1 h prior to measuring full-length SDF-1α. This demonstrated a significant increase in detectable SDF-1α versus Hispec buffer control (AMD3100 640±60 pg/ml vs. control 460±70 pg/ml, n=3, $P<0.01$, Figure 7-23), suggesting a reversible association of SDF-1α with CXCR4 on platelets.

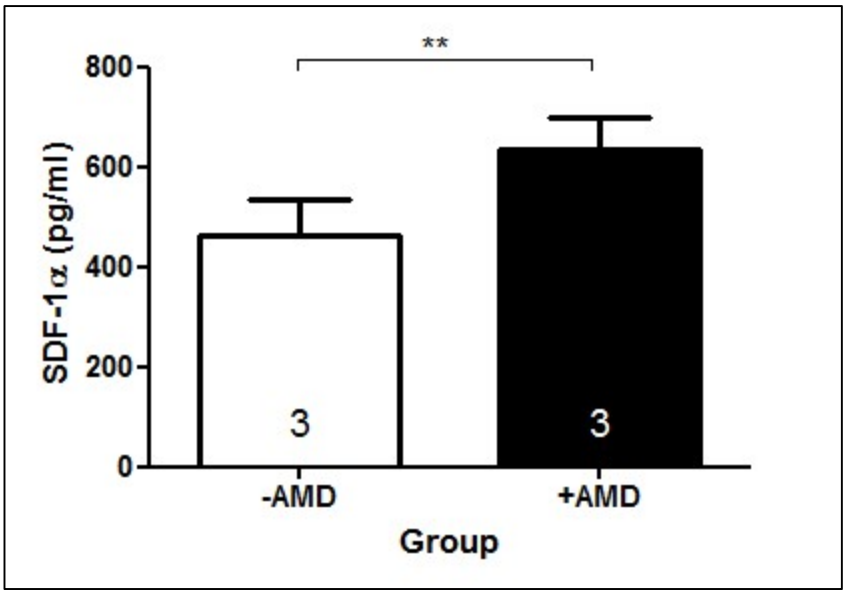


**Figure 7-23: SDF-1α levels in rat unfractionated plasma samples after incubation with AMD3100**

Unfractionated plasma samples obtained from Sprague Dawley rats via RV puncture were incubated with 5 µg/ml AMD3100 (AMD) for 1 h prior to measurement of full-length SDF-1α. There was significantly more SDF-1α in the AMD3100 group. Statistical significance was assessed using a paired t-test, n=3, **P<0.01.

To ascertain whether there was any difference in platelet-expression of SDF-1α between control and RIC groups, healthy male volunteers were subjected to RIC and whole blood samples were fixed and analysed by flow cytometry using HCl.SDF1α. As a positive control, whole blood was fixed and treated with 10 µM ADP, which has been shown to cause α-degranulation and the increased expression of SDF-1α.[358] There was a marked, albeit not statistically significant, increase in the numbers of platelets expressing SDF-1α in the ADP group (control 12±4% vs. RIC 8±2%, n=3, P=NS, Figure 7-24) but no increased expression in the RIC group (control 12±4% vs. ADP 25±8%, n=3, P=NS, Figure 7-24), indicating that platelet-derived SDF-1α is an unlikely mediator of RIC.

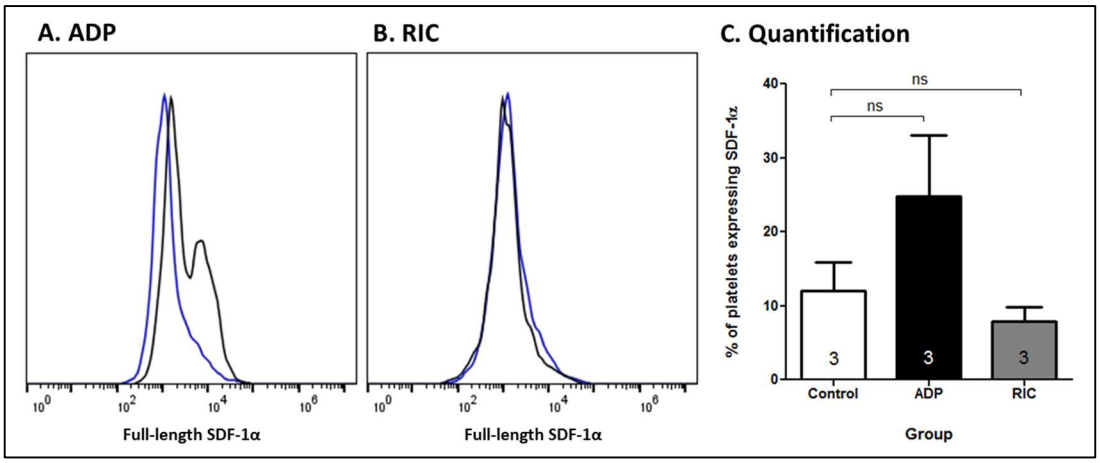


**Figure 7-24: Effect of ADP and remote ischaemic conditioning on platelet surface expression of SDF-1α in humans**

RIC consisting of three cycles of 5 min right upper limb ischaemia and 5 min reperfusion was applied by inflation of a manual sphygmomanometer to a pressure of 200 mmHg. Human whole blood samples were fixed and a positive control group immediately treated with 10 µM ADP prior to flow cytometry analysis of full-length SDF-1α expression. (A) Representative image demonstrating an obvious rightward shift in fluorescence in the ADP group (black line) versus control (blue line) that was absent in the RIC group (Panel B); (C) This was not significant when assessed using one-way ANOVA and Tukey's multiple comparison test, n=3, P=NS.

### 7.6.4 Discussion

In view of the absence of a detectable increase in SDF-1α in PFP, described in section 7.3.4, this section aimed to ascertain what role, if any, platelets contribute to putative SDF-1α-mediated cardioprotection, predicated on the observation that platelets contain large amounts of SDF-1α that they release after activation. Unsurprisingly, no difference in SDF-1α was detected between control and RIC groups when serum samples were assayed because extensive degranulation during serum preparation results in large increases in SDF-1α levels, which is likely to obscure subtler changes in SDF-1α *in vivo*. This is interesting when considering that three of the studies in Table 7-2 report SDF-1α levels measured in serum samples and might, therefore, be anomalous.

It remained possible that there was a difference in platelet-expression of SDF-1α after RIC. To confirm an interaction between SDF-1α and platelet-expressed CXCR4, AMD3100 was incubated with unfractionated plasma samples and found to increase

SDF-1α. To investigate the role of platelet-expressed SDF-1α in RIC, flow cytometry was used to measure platelet surface SDF-1α and similarly found no increase in response to RIC. Although this study did not directly measure platelet activation, degranulation and consequent SDF-1α expression is an established surrogate.[413] Therefore, in contrast to the study by Oberkofler *et al.*, RIC appears not to activate platelets in the present study.[411] Note that although the samples incubated with ADP were not significantly different from control samples, there was a clear trend and there was considered to be sufficient evidence to avoid further venepuncture of healthy volunteers and to terminate the study.

These findings are supported by those of Cohen *et al.* who found that platelet-depletion using anti-thrombocyte serum did not abrogate the cardioprotective effect of IPC in open-chest rats subjected to 30 min ischaemia and 2 h reperfusion.[414] Although this has not been tested in the context of RIC, the present results would predict a similar outcome. In the context of the study by Oberkofler *et al.* it remains possible that platelets play a role in cardioprotection, although this would appear not to be mediated by SDF-1α.[411] The present study did not investigate the potential importance of other proteins contained within α-granules as this is beyond the scope of this project. Furthermore, it should be noted that MIF is expressed by platelets, although it does not co-localise with SDF-1α, has distinct activating stimuli and has delayed secretion kinetics.[392, 393] Nonetheless, the role of platelet-expressed MIF in RIC is an attractive hypothesis for future investigation.

## 7.7 Summary

This chapter reports the successful characterisation and validation of an ELISA for the specific and robust detection of full-length SDF-1α using the novel antibody HCI.SDF1α. At the same time, frequently used commercial assays were found to report a combination of full-length and cleaved SDF-1α. These assays were used in combination to investigate the dynamics of SDF-1α after RIC, and unexpectedly demonstrated increased cleavage. The proposed mechanism relates to the increased activity of endothelial cell membrane-bound DPP4 in response to oxidative stress but is unlikely to be significant in the mechanism of remote preconditioning.

Therefore, the third condition necessary to define a molecule as a mediator of cardioprotection, the increased production or maintenance of extracellular concentrations of the mediator(s) as a direct effect of RIC, has not been met. This is a difficult criterion to satisfy given the plethora of ways SDF-1α could contribute to RIC. The most likely outstanding hypotheses are that SDF-1α is important in either the trigger or effector phases of RIC, but is not the humoral factor, or that cardioprotection in response to RIC is related to altered CXCR4 dynamics rather than up-regulation of SDF-1α. These are addressed in Chapter 6 and Chapter 8, respectively.

# Chapter 8 Is remote ischaemic conditioning still effective in cardiomyocyte-specific CXCR4 null mice?

## 8.1 Introduction

The final condition, according to The Working Group of Cellular Biology of the Heart of the European Society of Cardiology,[103] that must be satisfied to define a molecule as an endogenous mediator of cardioprotection is the absence of cardioprotection in animals, tissues or cells with genetic disruption of the mediator's production or its receptor(s).

As described in section 1.2, CXCR4 is critical in embryogenesis and transgenic mice with global CXCR4 deficiency suffer various lethal developmental abnormalities including VSD.[57, 415, 416] Therefore, to investigate the effect of genetic disruption of CXCR4 it is necessary to use a cell-specific CXCR4 knockout model.

As discussed in section 6.4.4, cardiomyocytes are the best described cardiac cell-type in the context of SDF-1α-CXCR4-mediated effects. Hu *et al.* demonstrated increased SDF-1α release from cardiomyocytes, but not cardiac fibroblasts, subjected to hypoxia and reoxygenation.[46] Furthermore, isolated cardiomyocytes treated with exogenous SDF-1α responded by up-regulating the protective kinases Akt and Erk1/2. Similarly, Dong *et al.* demonstrated loss of benefit from infused MSCs after permanent LAD ligation in mice lacking cardiomyocyte CXCR4.[75] Therefore, cardiomyocyte-specific CXCR4 deletion was selected to investigate the role of SDF-1α in RIC in a murine model of myocardial IRI.

Interestingly, congenital cardiomyocyte-specific CXCR4 deletion is not fatal *in utero*. Given the defective cardiogenesis apparent in mice with global CXCR4 deficiency, it is surprising that Agarwal *et al.* found $CXCR4^{flox/flox}$ mice that were crossed with MLC2v-$Cre^{+/-}$, resulting in congenital cardiomyocyte-specific recombination and CXCR4 deletion, were viable, had normal cardiac function and no evidence of VSD.[207]

Nonetheless, in order to ensure the absence of developmental effects, and in view of our laboratories experience with conditional knockout strains, the tamoxifen-

inducible MYH6-MerCreMer mouse was used in the present study, as described in section 2.3.

## 8.2 Research aims and objectives

The main objective of this chapter was to investigate whether RIC remains effective in cardiomyocyte CXCR4 null mice. The research aims for this objective were:

1. Confirm cardiomyocyte-specific deletion of CXCR4 after tamoxifen administration;
2. Investigate whether RIC is effective in cardiomyocyte CXCR4 null mice.

## 8.3 Aim 1: Confirm cardiomyocyte-specific deletion of CXCR4 after tamoxifen administration

### 8.3.1 Background

To investigate the hypothesis that RIC is not effective in cardiomyocyte-specific CXCR4 null mice subjected to *in vivo* myocardial IRI, it was first necessary to test the efficacy of CXCR4 ablation by Cre recombinase in mice treated with tamoxifen.

In general, the MYH6-MerCreMer system is expected to result in approximately 70-90% reduction of gene expression after 5-7 days of tamoxifen treatment.[209, 211] The time-course of CXCR4 protein reduction depends on the efficacy of gene ablation and turnover rate of CXCR4. $CXCR4^{flox/flox}$ MYH6-MerCreMer mice that have been induced by tamoxifen injection have previously been used 3 weeks after the completion of 5 days dosing with tamoxifen.[75] This interval also allows any transient tamoxifen-induced dilated cardiomyopathy to normalise prior to experimentation,[417] although the inclusion of tamoxifen-injected MYH6-$MerCreMer^{+/+}$ control mice also mitigates any confounding effect of this possibility.

Using this protocol, Agarwal *et al.* confirmed CXCR4 deletion from genomic DNA using PCR of homogenate obtained from hearts, but not tails, of injected mice 1 week after completion of tamoxifen dosing.[207] They subjected these mice to permanent LAD ligation 3 weeks after completion of dosing and were able to demonstrate reduction

of CXCR4 protein expression by immunofluorescence in cardiomyocytes, but not endothelial cells, 48 h later. This was quantified as a 90% reduction by Western blot analysis.

The aim of this section was to confirm cardiomyocyte-specific deletion of CXCR4 after induction of MYH6-MerCreMer with tamoxifen. Several methods were attempted due to technical issues with reagents, which are described below.

### 8.3.2 Methods

This study first generated a colony of inducible cardiomyocyte-specific CXCR4$^{flox/flox}$ mice, as described in section 2.3. Male CXCR4$^{flox/flox}$ MYH6-MerCreMer$^{+/-}$ and CXCR4$^{flox/flox}$ MYH6-MerCreMer$^{+/+}$ mice between 4 to 10 weeks old were injected IP with 20 mg/kg/day of tamoxifen continuously for 5 days. For brevity, the consequent phenotypes will henceforth be labelled CM-CXCR4$^{KO}$ and CM-CXCR4$^{WT}$, respectively. Experiments were performed 3 weeks after completion of tamoxifen dosing.

Ventricular samples or isolated cardiomyocytes were extracted and prepared for either Western blot or immunofluorescence as described in sections 2.5 and 2.6, respectively. The anti-CXCR4 primary antibody was either ab2074 or ab124824, both at a dilution of 1:100. The secondary antibody was anti-rabbit Alexa Fluor 488, diluted 1:400. Control samples for immunofluorescence were incubated in Alexa Fluor 488 in the absence of primary antibody, to exclude non-specific staining with secondary antibody. A positive control sample was taken from the spleen, which is abundant with CXCR4-expressing lymphohaematopoietic progenitor cells, and stained alongside ventricular samples.

RNA extraction, cDNA synthesis and QPCR was performed as described in section 2.7. To avoid amplification of non-specific DNA products (including primer dimers) it was necessary to use the lowest concentration of primers possible without compromising the sensitivity of the assay. Therefore, primer concentrations between 0.25 µl and 2.5 µl for both CXCR4 and the positive control genes GAPDH and HPRT were tested. It was then necessary to validate the PRC reaction by demonstrating Ct values that

were proportional to the quantity of template cDNA, for which a concentration range of 0.6-2.5 µl cDNA per reaction was tested.

### 8.3.3 Results

Western blot analysis of ventricular lysates from CM-CXCR4$^{WT}$ and CM-CXCR4$^{KO}$ mice, using ab2074 anti-CXCR4 primary antibody, did not successfully demonstrate loss of CXCR4 protein in the latter group (Figure 8-1). In fact, the Western blot suggested non-specific binding to proteins of a range of sizes, as indicated by the number of bands visible outside the expected size of 48 kDa. Despite optimisation of the protocol, including testing of different antibodies, adjustment of antibody concentrations, blocking buffer constitution, gel type for SDS-PAGE, washing protocol, quantity of protein loaded and sample preparation, this remained consistent.

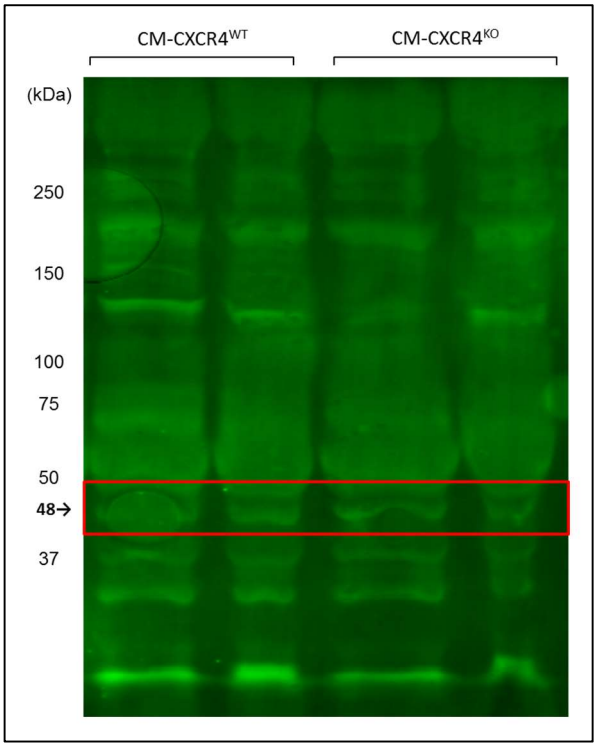


**Figure 8-1: Western blot analysis of ventricular lysates from CM-CXCR4$^{WT}$ and CM-CXCR4$^{KO}$ mice using the monoclonal anti-CXCR4 antibody, ab2074**

Western blot analysis demonstrated several non-specific bands and no evidence of CXCR4 deletion at the expected size of 48 kDa (red box).

Next, immunofluorescent staining of isolated cardiomyocytes was performed in a wild type C57BL/6 mouse, with a view to applying the technique to cells from experimental animals. However, initial characterisation using ab2074 anti-CXCR4 primary antibody demonstrated apparently non-specific binding (Figure 8-2).

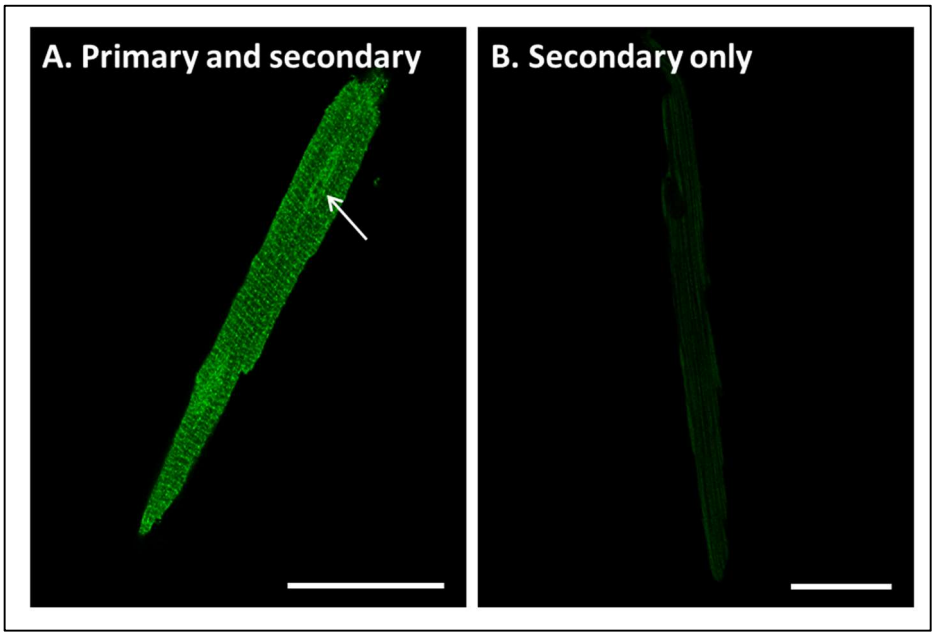


**Figure 8-2: Representative image showing immunofluorescent staining of isolated WT mouse cardiomyocytes with anti-CXCR4 (ab2074, green)**

(A) High signal intensity in cells treated with primary antibody; however, there is significant non-specific nuclear staining (arrowed); (B) Low signal intensity in cells stained with secondary antibody-only. 50 µm scale bar.

Although ab2074 was well-described and used successfully for both published Western blots and immunohistochemistry,[356, 418] it was unfortunately withdrawn from sale by Abcam for unspecified reasons. Further experiments were conducted using the recombinant rabbit monoclonal anti-CXCR4 antibody ab124824. Subsequent immunofluorescent staining of sections from CM-CXCR4$^{WT}$ and CM-CXCR4$^{KO}$ mice showed no differences in signal intensity, although it is noteworthy that the greatest signal in both groups was apparently endothelial (Figure 8-3).

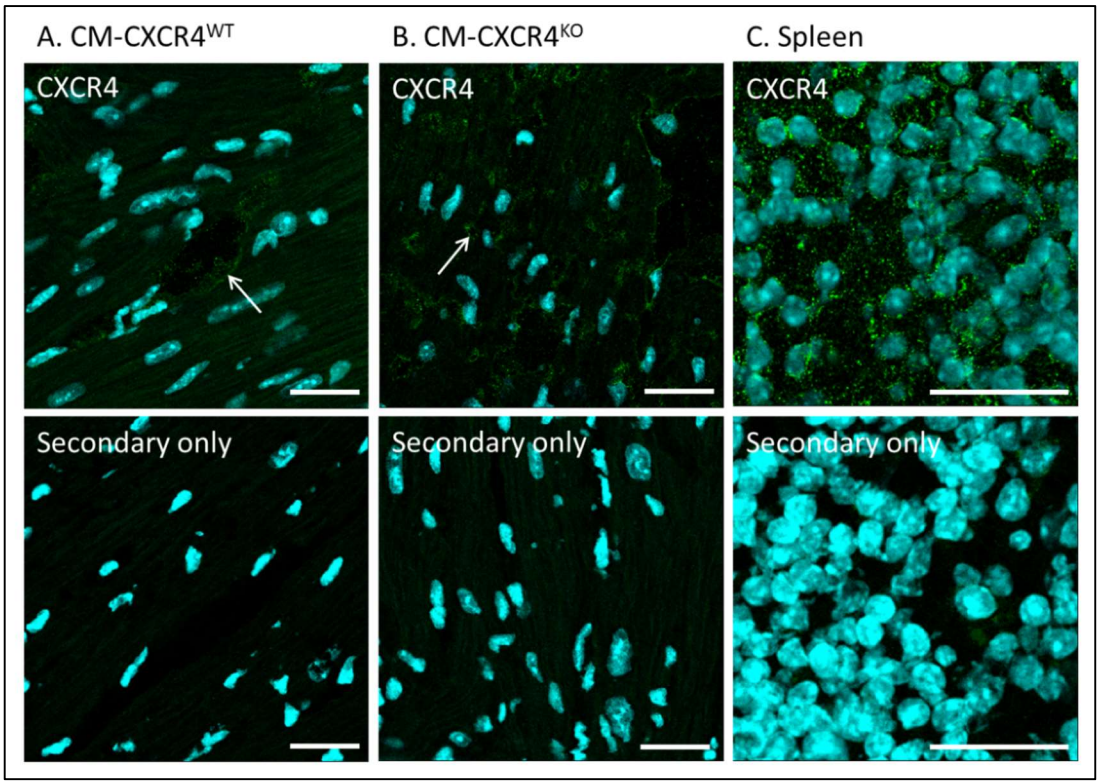


**Figure 8-3: Representative images demonstrating immunofluorescent staining of ventricular sections from CM-CXCR4$^{WT}$ and CM-CXCR4$^{KO}$ mice with anti-CXCR4 (ab124824, green). Arrows indicate positive staining**

Greater signal intensity was observed after incubation with primary antibody compared to secondary antibody alone in all samples; however, no difference between CM-CXCR4$^{WT}$ and CM-CXCR4$^{KO}$ sections was observed (Panels A and B). Staining in both groups was predominantly endothelial (arrowed); (C) Positive CXCR4 immunofluorescence of B cells in mouse spleen. 25 µm scale bar.

The final immunological approach to demonstrating CXCR4 loss in CM-CXCR4$^{KO}$ mice was Western blotting of isolated cardiomyocytes using ab124824. The use of isolated cells in combination with ab124824 reduced the non-specific binding present in Figure 8-1. Four animals were included per group and CXCR4 signal intensity was normalised to α-tubulin loading control. A CM-CXCR4$^{WT}$ sample that failed to run correctly was excluded. Despite optimisation, the band obtained was weak, even in CM-CXCR4$^{WT}$ samples, and subsequent analysis revealing reduced CXCR4 in the CM-CXCR4$^{KO}$ group failed to reach statistical significance (CM-CXCR4$^{WT}$ 0.29±0.16 AU vs. CM-CXCR4$^{KO}$ 0.12±0.01 AU, n=3-4, P=NS, Figure 8-4).

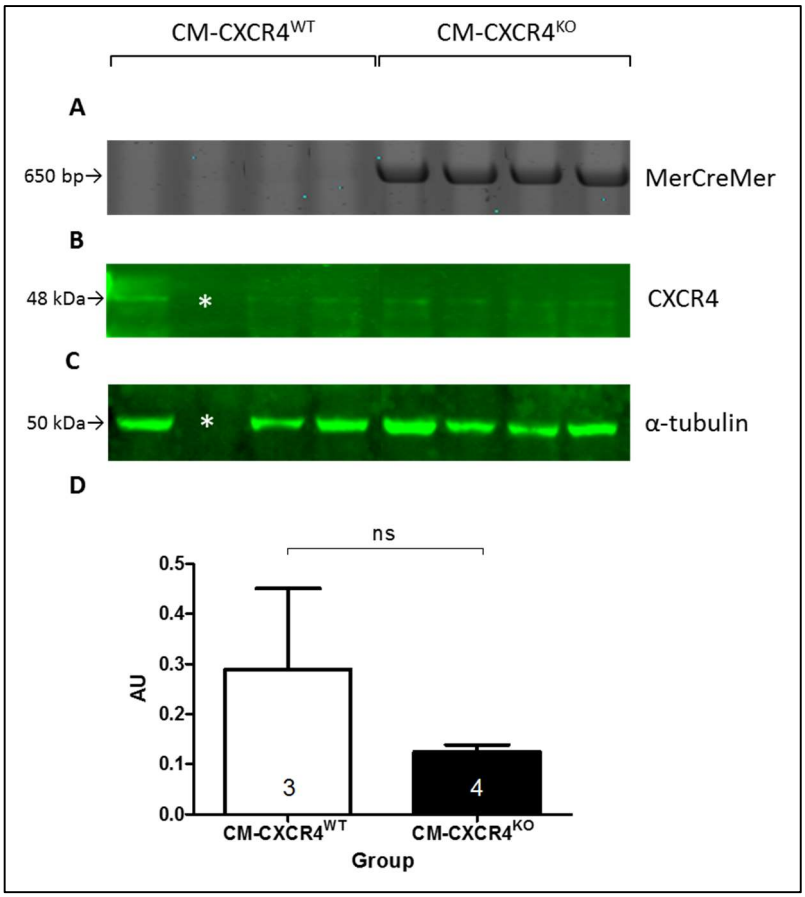


**Figure 8-4: PCR and Western blot analysis of isolated cardiomyocytes from CM-CXCR4$^{WT}$ and CM-CXCR4$^{KO}$ mice using the monoclonal anti-CXCR4 antibody, ab124824**

(A) PCR confirmed MYH6-MerCreMer status, with no band present in MYH6-MerCreMer$^{+/+}$ mice and a 650 bp band in MYH6-MerCreMer$^{+/-}$ mice; (B) Western blot analysis using the monoclonal anti-CXCR4 antibody ab124824 demonstrated a specific band at 48 kDa; (C) α-tubulin loading control; (D) Densitometry showed no significant difference between CM-CXCR4$^{WT}$ and CM-CXCR4$^{KO}$ mice. Statistical significance was assessed using an unpaired t-test, n=3-4, P=NS. *Sample failed to run correctly.

In view of the problems with antibodies, quantitative reverse transcriptase QPCR, which is a sensitive tool for even subtle changes in gene expression,[419] was used instead to quantify CXCR4 expression. First it was necessary to optimise primer concentration. Primer concentrations between 0.25 µl and 2.5 µl for CXCR4, GAPDH and HPRT were tested (Figure 8-5). Based on the optimal signal:noise ratio, 1 µl of each primer was used per reaction for all subsequent experiments.

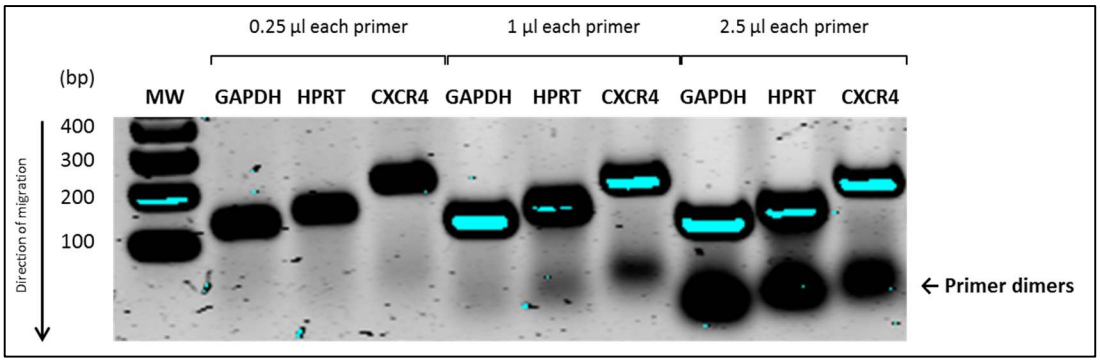


**Figure 8-5: Evaluation of primer concentration in QPCR reaction using WT mouse cDNA**

0.25, 1 and 2.5 µl per reaction of each primer (forward and reverse) were tested for GAPDH, HPRT and CXCR4. Signal:noise was best when 1 µl of each primer was used.

QPCR was then validated by performing reactions with 2.5, 1.3 and 0.6 µl cDNA. Using $2^{-\Delta\Delta Ct}$ analysis, no difference in expression was detectable between 2.5 µl and 1.3 µl samples. However, the expression fold change between samples containing 1.3 µl and 0.6 µl was 0.53. Therefore, the QPCR protocol was able to accurately differentiate 0.6 µl from 1.3 µl of template cDNA and the latter volume was therefore used for all subsequent reactions.

When cDNA isolated from CM-CXCR4$^{WT}$ and CM-CXCR4$^{KO}$ mice was analysed in this way, residual CXCR4 gene expression in CM-CXCR4$^{KO}$ mice was 38±35%. In the absence of gene expression, the receptor is expected to be eliminated from 3 weeks after the completion of 5 days dosing with tamoxifen, as discussed in section 8.3.1.

### 8.3.4 Discussion

This experiment investigated the efficacy of cardiomyocyte-specific CXCR4 deletion in a tamoxifen-inducible MerCreMer system and, overall, demonstrated residual CXCR4 gene expression in CM-CXCR4$^{KO}$ mice of 38±35%.

Initial analysis of myocardial protein was obfuscated by a non-specific commercially available anti-CXCR4 antibody (ab2074). In isolated mouse cardiomyocytes, while staining with primary plus secondary antibodies exceeded that with secondary antibody alone, there was artefactual perinuclear staining. Furthermore, although

staining in the T-tubules was convincing, Segret *et al.* used confocal and electron microscopy to show that CXCR4 is localised on the plasma membrane of cardiomyocytes, not in the T-tubules.[45]

Subsequent immunofluorescence experiments compared CM-CXCR4$^{WT}$ and CM-CXCR4$^{KO}$ samples to define any confounding non-specific staining. Ventricular sections were used to facilitate assessment of the cellular distribution of CXCR4 staining. Using an alternative antibody (ab124824) there was no difference between CM-CXCR4$^{WT}$ and CM-CXCR4$^{KO}$ samples, although fluorescence with primary plus secondary antibodies again exceeded that observed with secondary antibody alone. The lack of difference may have represented failure of inducible recombination or may signify non-specific binding. Given this absence of a difference between genotypes, it is worth considering that the positive CXCR4 immunofluorescence observed in isolated human trabeculae samples in section 6.4 may, in fact, be artefactual.

These issues relate to the more general limitations of immunolabelling. The monoclonal antibodies used outght to be highly specific, but they are vulnerable to loss of their epitope as a result of protein post-translational modification or altered tertiary structure of the target protein.[420] This can be exacerbated by cross-linking of amino acids as a result of formalin fixation resulting in further conformational change. Potential solutions include the use of heat-induced antigen retrieval or, as in the present experiments, fixation with HistoChoice®, which is designed to preserve antigenic sites.[421] A further limitation is non-specific binding as a result of hydrophobic and ionic interactions.[420] BSA was used to limit non-specific binding; an alternative approach would be the addition of goat serum as a blocking agent, which was not tried here.

Another potential reason for the present finding is failure of antibodies to permeate into the fixed ventricular samples, and groups using similar protocols to stain for CXCR4 have previously included a permeablisation step with 0.1% Triton X-100.[422] In addition to permeablisation, it may also be possible to enhance the signal using, for

example, tyramide signal amplification, although these techniques were not applied in this case.[423]

Aside from technical limitations, the relative paucity of cardiomyocyte-specific CXCR4 in either group may relate to a finding by Zhang *et al.* that CXCR4 is only up-regulated in cardiomyocytes after an insult.[68] In particular, they demonstrated up-regulation of cardiomyocyte-specific CXCR4 in the infarct zone of mice subjected to permanent LAD ligation after 24 h, although they did not include a baseline sample. Furthermore, they did not report the specific Abcam antibody they used, which may have been the obsolete ab2074. Finally, Segret *et al.* have reported the presence of CXCR4 on cardiomyocytes at baseline.[45] However, if cardiomyocyte-specific CXCR4 is only up-regulated after MI it may not be relevant in the context of RIC-induced cardioprotection, unless it is speculated that RIC remotely up-regulates CXCR4 in the effector organ.

It is also interesting to reflect on the relatively greater fluorescent signal on the endothelium in both CM-CXCR4$^{WT}$ and CM-CXCR4$^{KO}$ samples. Although this might be artefactual, the possible presence and importance of CXCR4 on endothelial cells warrants further investigation. This will be discussed in section 8.4.4.

To overcome the problems with antibodies described above, QPCR was employed to demonstrate deletion of CXCR4. Despite large statistical error, this technique successfully demonstrated loss of CXCR4 in disrupted and homogenised ventricular samples. However, it should be acknowledged that this will reflect total mRNA, which may not necessarily correlate precisely with protein content and does not distinguish between intracellular and extracellular receptors. The observed residual expression is likely to reflect incomplete deletion and CXCR4 on other cardiac cell types, including vascular smooth muscle, endothelial cells and cardiac fibroblasts. To consolidate this result, it would be necessary to perform QPCR for CXCR4 cDNA in isolated cardiomyocytes, which was not attempted in thisstudy. Furthermore, it would be desirable to include positive and negative control samples, which could be achieved

using adenovirus-mediated CXCR4 over-expression and congenital cardiomyocyte CXCR4 deletion, both of which have been described in the literature.[88, 207]

As discussed, MerCreMer systems are imperfect, resulting in absence of expression in approximately 70-90% of cardiomyocytes after treatment with tamoxifen.[209, 211] The cDNA for Cre recombinase is derived from the genome of a P1 bacteriophage that, as a non-eukaryote, is thought to result in suboptimal Cre expression when expressed in mammals.[424] This has subsequently been remedied by developing iCre, or *improved* Cre, which has been optimised for codon usage for mammals and to reduce the chance of epigenetic silencing in mammals.[424] This could be applied to future experiments of this type to mitigate the potential confounding effect of inefficient recombination. Interestingly, the best recombination with iCre has been reported in immature animals.[425] In adult mice, however, reasonable recombination has been reported in tissues including the heart from qualitative evaluation in ROSA-lacZ reporter mice. In these mice, Cre expression drives recombination and removal of a *loxP*-flanked stop sequence resulting in the expression of a lacZ transgene, which encodes β-galactosidase.[426] This can be stained blue with X-gal.

## 8.4 Aim 2: Investigate whether remote ischaemic conditioning is effective in cardiomyocyte CXCR4 null mice

### 8.4.1 Background

Once the reduction of CXCR4 expression in CM-CXCR4$^{KO}$ mice after tamoxifen administration was confirmed, it was possible to test the hypothesis that cardioprotection by RIC would be abolished in these mice.

In view of the complexity of this experimental model, several control groups are potentially necessary to address a number of possible confounding factors. These include tamoxifen toxicity, Cre recombinase toxicity and the effect of *loxP* site insertion. These have been reviewed by Davis *et al*. and are outlined in Table 8-1 with reference to the current study.[211]

| Group (genotype and treatment) | Group | Reason for inclusion |
|---|---|---|
| $CXCR4^{flox/flox}$ $MCM^{+/-}$ + tamoxifen | Control | Knockout control group |
| $CXCR4^{flox/flox}$ $MCM^{+/-}$ + vehicle | RIC | Wild type experimental group |
| $CXCR4^{flox/flox}$ $MCM^{+/-}$ + tamoxifen | RIC | Knockout experimental group |
| $CXCR4^{flox/flox}$ $MCM^{+/+}$ + tamoxifen | Control | Wild type control for tamoxifen |
| $CXCR4^{+/+}$ $MCM^{+/-}$ + tamoxifen | Control | Wild type control for Cre recombinase |
| $CXCR4^{flox/flox}$ $MCM^{+/+}$ + vehicle | Control | Wild type control for *LoxP* insertion |

**Table 8-1: Potential control groups required for experiments using the tamoxifen-inducible MYH6-MerCreMer system**

Experiments using this system have several potential confounding factors that require careful consideration. These have been reviewed by Davis *et al*.[211] MCM, MerCreMer.

Despite this, it is not practicable, or necessary, in view of a considerable literature,[211] to include an exhaustive list of control groups. In view of the transient but severe dilated cardiomyopathy that has been observed after tamoxifen administration,[417] the tamoxifen-injected $CXCR4^{flox/flox}$ MYH6-$MerCreMer^{+/+}$ (CM-$CXCR4^{WT}$) group is particularly important to control for tamoxifen administration. *LoxP* sites do not alter gene expression and are therefore not expected to affect IS or the ability to confer cardioprotection. Furthermore, all mice used in the experiments reported in Chapter 4 and Chapter 5 had a $CXCR4^{flox/flox}$ $Cre^{+/+}$ genotype and were neither excessively protected nor resistant to cardioprotection using RIC, hypothermia or exogenous SDF-1α. Despite the animals not being injected with vehicle, it suggests that controlling for the presence of *LoxP* sites is unnecessary. Regarding Cre recombinase, MerCreMer proteins can interact with oestrogen receptor signalling.[427] As a result of the expression of several oestrogen receptor subtypes in the myocardium,[428]

activated MerCreMer has been reported to have detrimental effects on cardiac function, myocardial $Ca^{2+}$ handling and energy production.[417] However, it has been used extensively in relation to SDF-1α-CXCR4 without unduly confounding the results and is therefore used here without a specific control group.[75, 207] All control group animals were littermates of experimental animals to reduce other confounding factors, including environmental factors and genetic drift.[211]

The aim of this section was to investigate whether the efficacy of RIC observed in Chapter 4 can be abrogated by cardiomyocyte-specific deletion of CXCR4 expression.

### 8.4.2 Methods

4-10 week old male and female mice were injected IP with 20 mg/kg/day of tamoxifen continuously for 5 days. To test the hypothesis that RIC would confer cardioprotection upon wild type but not CXCR4 knockout mice compared to control, experimental groups were defined *a priori* as follows:

1. Tamoxifen-injected $CXCR4^{flox/flox}$ MYH6-$MerCreMer^{+/-}$ ($CM\text{-}CXCR4^{KO}$) control;
2. Tamoxifen-injected $CXCR4^{flox/flox}$ MYH6-$MerCreMer^{+/-}$ ($CM\text{-}CXCR4^{KO}$) RIC;
3. Tamoxifen-injected $CXCR4^{flox/flox}$ MYH6-$MerCreMer^{+/+}$ ($CM\text{-}CXCR4^{WT}$) control;
4. Tamoxifen-injected $CXCR4^{flox/flox}$ MYH6-$MerCreMer^{+/+}$ ($CM\text{-}CXCR4^{WT}$) RIC.

A vehicle-injected $CXCR4^{flox/flox}$ MYH6-$MerCreMer^{+/-}$ (wild type) RIC group was not included as this was accounted for by tamoxifen-injected $CXCR4^{flox/flox}$ MYH6-$MerCreMer^{+/+}$ ($CM\text{-}CXCR4^{WT}$) mice and could be added if tamoxifen was unexpectedly suspected of conferring cardioprotection. Control groups for Cre recombinase expression and *LoxP* insertion were not included for the reasons outlined above. All mice were subjected to myocardial IRI aged 8-16 weeks, with subsequent analysis of IS/AAR.

Sample size was calculated using a two-sided test for the comparison of two means. Based on the results described in section 4.4.3, the following assumptions were made: a 20% estimate of effect size, a control IS of 40%, an SD of 10%, a significance

level of 5% (α=0.05) and 80% power (β=0.2). This required a minimum sample size of four animals per group.

### 8.4.3 Results

The surgical complications encountered in this experiment were similar to those described in section 4.4, although the total proportion of included animals increased. A summary is given in Figure 8-6.

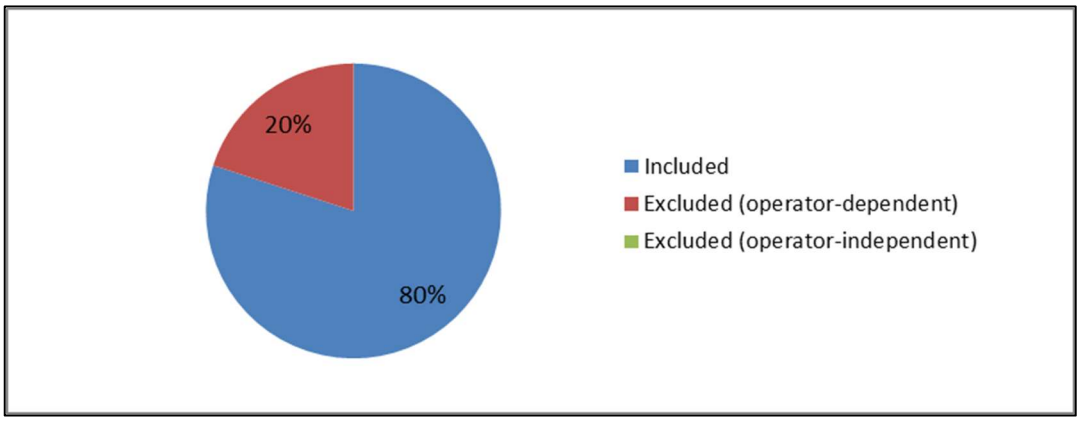


**Figure 8-6: Experimental success during investigation of whether cardiomyocyte-specific CXCR4 deletion abrogates the cardioprotective effect of remote ischaemic conditioning**

15 animals were used during the course of the experiment and 12 were included in the analysis (80%). All excluded animals were operator-dependent, and included anaesthetic and staining complications.

This experiment measured IS as a proportion of AAR in transgenic mice following *in vivo* myocardial IRI. It became apparent that CM-CXCR4$^{KO}$ control mice had surprisingly small IS, therefore confounding any attempt to demonstrate the abrogation of RIC in these animals. Consequently, they were instead compared to CM-CXCR4$^{WT}$ control mice to ascertain whether Cre-induced recombination or tamoxifen administration triggered the observed protection. Six animals were included per group and analysis of their respective areas at risk, to ensure surgical consistency, revealed no significant differences (CM-CXCR4$^{WT}$ 53±4% vs. CM-CXCR4$^{KO}$ 62±5%, n=6, P=NS, Figure 8-7).

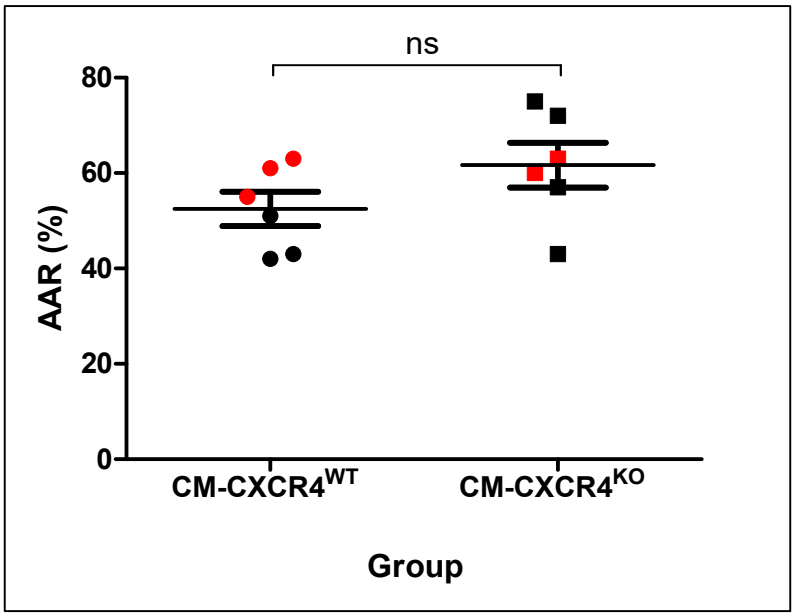


**Figure 8-7: Comparison of area at risk between CM-CXCR4$^{WT}$ and CM-CXCR4$^{KO}$ groups**

C57BL/6 CM-CXCR4$^{WT}$ and CM-CXCR4$^{KO}$ mice were anaesthetised and subjected to 40 min ischaemia and 2 h reperfusion *in vivo*. Analysis of their respective areas at risk, to ensure surgical consistency, revealed no statistically significant differences. Black points indicate male mice and red points indicate female mice. Statistical significance was assessed using an unpaired t-test, n=6, P=NS. Data presented as mean ± SEM.

Analysis of IS demonstrated that CM-CXCR4$^{KO}$ had a marked reduction in IS as a proportion of AAR (12±3%, n=6) compared to CM-CXCR4$^{WT}$ mice (36±4%, n=6, P<0.001, Figure 8-8). Representative transverse heart sections are shown in Figure 8-8.

To test the hypothesis that baseline differences in cardiac function may have altered the susceptibility of CM-CXCR4$^{KO}$ mice to myocardial injury, baseline echocardiographic parameters were compared between CM-CXCR4$^{WT}$ and CM-CXCR4$^{KO}$ mice. As expected, CM-CXCR4$^{WT}$ values were comparable to those described in Chapter 4 and no differences with CM-CXCR4$^{KO}$ mice were identified (Figure 8-9).

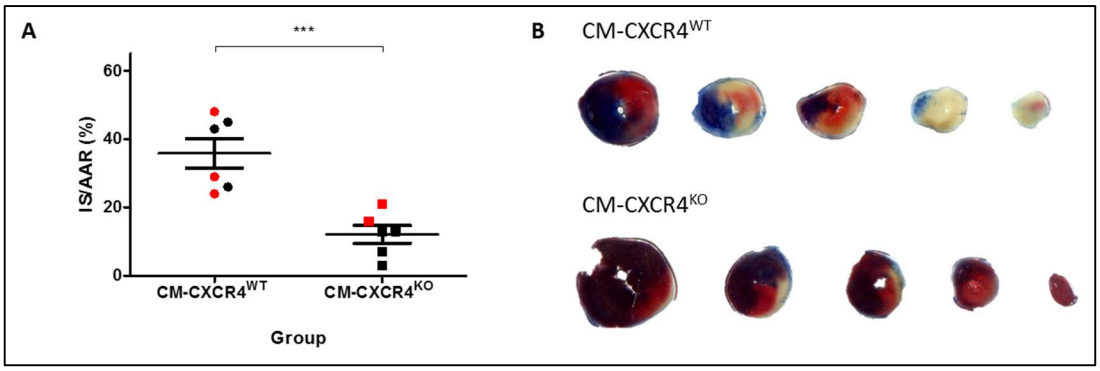


**Figure 8-8: Infarct size following myocardial ischaemia-reperfusion injury in CM-CXCR4$^{WT}$ and CM-CXCR4$^{KO}$ groups**

CM-CXCR4$^{WT}$ and CM-CXCR4$^{KO}$ mice were anaesthetised and subjected to 40 min ischaemia and 2 h reperfusion *in vivo.* IS as a proportion of AAR was analysed using Evans Blue and TTC staining. (A) IS was significantly smaller in CM-CXCR4$^{KO}$ mice compared to CM-CXCR4$^{WT}$ mice. Black points indicate male mice and red points indicate female mice. Statistical significance was assessed using an unpaired t-test, n=6, ***P<0.001. Data presented as mean ± SEM; (B) Representative scanned transverse heart sections demonstrating Evans Blue area (blue), area at risk (pink) and infarct (white).

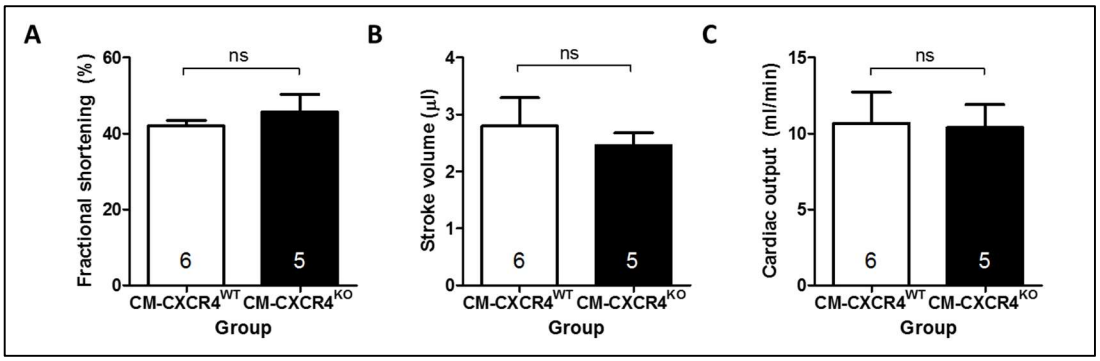


**Figure 8-9: Baseline echocardiographic parameters in CM-CXCR4$^{WT}$ and CM-CXCR4$^{KO}$ mice**

CM-CXCR4$^{WT}$ and CM-CXCR4$^{KO}$ were anaesthetised and transthoracic 2D echocardiography was performed at baseline. There were no statistically significant differences between CM-CXCR4$^{WT}$ and CM-CXCR4$^{KO}$ groups with respect to fractional shortening, stroke volume or cardiac output. Statistical significance was assessed using unpaired t-tests, n=5-6, P=NS.

In addition, there was no evidence of cardiac hypertrophy as a result of cardiomyocyte-specific CXCR4 deletion, with no differences in interventricular septum (IVSd), LV internal diameter (LVIDd) and posterior wall (LVPWd) dimensions evident in diastole between groups (Figure 8-10).

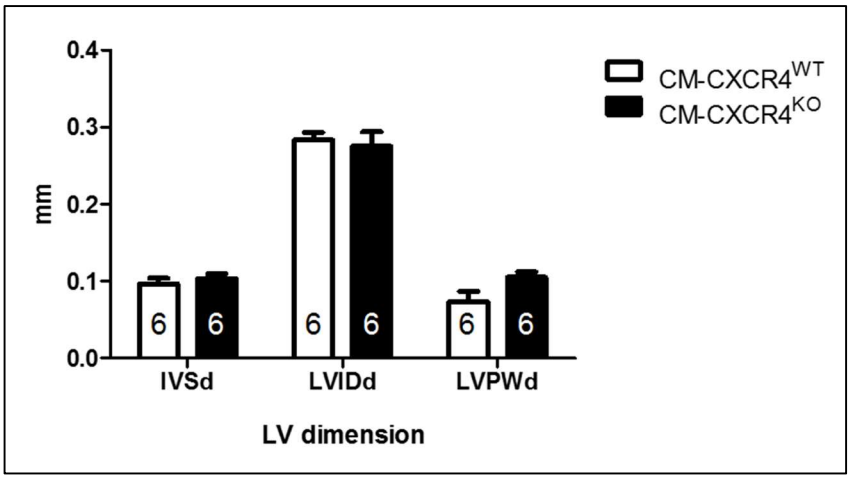


**Figure 8-10: Left ventricular dimensions in CM-CXCR4$^{WT}$ and CM-CXCR4$^{KO}$ mice**

CM-CXCR4$^{WT}$ and CM-CXCR4$^{KO}$ were anaesthetised and transthoracic 2D echocardiography was performed at baseline. Echocardiography did not reveal any difference in IVSd, LVIDd or LPWDd between groups. Statistical significance was assessed using two-way ANOVA with Bonferroni correction for multiple comparisons, n=6, P=NS.

### 8.4.4 Discussion

This experiment unexpectedly demonstrated that cardiomyocyte-specific CXCR4 deletion, 3 weeks after completion of tamoxifen dosing, significantly abrogated the acute injury associated with myocardial IRI. This precluded investigation of the original hypothesis that the beneficial effect of RIC would be abrogated by cardiomyocyte-specific CXCR4 deletion, which was protective *per se*. It remains possible that another cardiac cell-type is important in this regard. This could be investigated using similar inducible or congenital transgenic models of CXCR4 deletion. For example, 4-hydroxytamoxifen-inducible endothelial-specific platelet-derived growth factor subunit B (PDGFB)-iCreER$^{T2}$ mice that have been reported in the literature.[425] These could be crossed with CXCR4$^{flox/flox}$ transgenic mice to generate a tamoxifen-inducible endothelium-specific CXCR4$^{flox/flox}$ bitransgenic strain. It is important for this to be inducible as mutations involving the vasculature can be lethal *in utero*.[425] An alternative approach would be to demonstrate the absence of cardioprotection in animals, tissues or cells with genetic disruption of the production of SDF-1α. However, this is complicated by the fact that animals lacking SDF-1α die in utero. Another possibility could instead be to use a neutralising antibody.[57]

The finding of cardioprotection in CM-CXCR4$^{KO}$ mice is surprising in view of the literature demonstrating a cardioprotective role for CXCR4, albeit generally in models of ventricular remodelling. However, many of these studies artificially recruit the SDF-1α-CXCR4 axis, by various means, without necessarily implicating it in the intrinsic response to injury, about which less is known. For example, Agarwal *et al.* subjected mice with either inducible or congenital absence of cardiomyocyte-specific CXCR4 to permanent LAD ligation.[207] At 21 days they found no difference in measures of cardiac function or adverse ventricular remodelling compared to CM-CXCR4$^{WT}$ mice, suggesting that CXCR4 has no endogenous role in these processes. Using a similar model, the same group administered MSCs following MI and observed improved progenitor cell recruitment, less apoptotic cell death and better echocardiographic parameters, all of which were abrogated in CM-CXCR4$^{KO}$ mice.[75] They attribute these results to the asynchronous time courses of SDF-1α and CXCR4 expression after MI.[75] Specifically, SDF-1α is reportedly up-regulated 1 h after MI,[76] while cardiomyocyte-specific CXCR4 is not increased until 36-48 h later.[68]

In the context of asynchronous time courses of SDF-1α and CXCR4, it is unsurprising that some studies have reported beneficial effects of artificially over-expressing CXCR4 with viral vectors at the time of peak SDF-1α expression. For example, Larocca *et al.* subjected mice over-expressing cardiac CXCR4 to aortic banding (pressure overload) and demonstrated advantageous effects on ventricular remodelling, capillary density, cardiac function and haemodynamics.[429] Similarly, Cai *et al.* over-expressed CXCR4 in isolated adult rat ventricular cardiomyocytes that were subsequently protected from hypoxia-reoxygenation injury, which they attributed to increased mitochondrial STAT3.[84]

However, in a study with results that most closely reflect the present experiment and as discussed in 0, Chen *et al.* used adenovirus-mediated over-expression of CXCR4 injected into the rat heart 1 week prior to myocardial IRI and found significantly increased scar size, worse fractional shortening, increased cardiomyocyte apoptosis and more LV hypertrophy at 24 h, which were associated with significantly higher inflammatory cell infiltrate at 24 h in CXCR4-overexpressed hearts.[88] However, CXCR4

expression was driven by a cytomegalovirus promoter and, despite injection into the heart, CXCR4 is likely to have been constitutively over-expressed, including on inflammatory cells. It is therefore not clear that the effect they observed was driven by cardiomyocyte-specific CXCR4.

Nonetheless, inflammatory cell infiltration is of interest in the context of the present results. The use of anti-inflammatories in myocardial IRI is controversial, especially given the acuity of the present experiments (reviewed by Baxter[430]). However, some pathways may remain relevant here. For example, Montecucco *et al.* investigated FK866, which inhibits nicotinamide adenine dinucleotide (NAD)-driven inflammation.[431] They subjected male C57BL/6 mice treated with FK866 to *in vivo* myocardial IRI and found reduced IS, neutrophil infiltration and ROS production. Interestingly, these benefits were not replicated in a Langendorff model, suggesting a requirement for circulating leukocytes. Furthermore, FK866-treated mice had reduced circulating SDF-1α, which is also known to be diminished in CM-CXCR4$^{KO}$ mice.[207] This therefore engenders the hypothesis that the cardioprotection observed in CM-CXCR4$^{KO}$ mice is related to a dampened inflammatory response. Interestingly, it is known that approximately 5% of all cells in the heart are resident leukocytes and it would be useful to explore whether this number is reduced in CM-CXCR4$^{KO}$ mice.[355] However, it is important to note that Montecucco *et al.* observed effects at 8 h, but not at 1 h, after reperfusion.[431] Although a 2 h time point to reflect the model used in this thesis was not tested, an anti-inflammatory mechanism may be too slow to explain the present results.

To complement studies of CXCR4 over-expression, Liehn *et al.* investigated the intrinsic functions of CXCR4 using an *in vivo* model of permanent LAD ligation in global CXCR4 heterozygous mice (that displayed significantly lower CXCR4 expression).[432] They unsurprisingly reported impaired basal coronary flow and defective neovascularisation after MI in CXCR4$^{+/-}$ mice, given the role of the SDF-1α-CXCR4 axis in angiogenesis. Interestingly, however, they reported smaller IS in heterozygous mice compared to wild types at 4 weeks, which they also attributed to an attenuated inflammatory response. Furthermore, they found phosphatidylserine-rich lipid

deposits in CXCR4$^{+/-}$ mouse hearts, which protect cardiomyocytes from hypoxic stress *in vitro*, although the exact mechanisms are unclear. Such deposits are likely to represent an adaptive response to congenitally decreased coronary flow in CXCR4$^{+/-}$ mice and it is doubtful whether they could accumulate in the time course from tamoxifen administration in the present experiment.

Finally, it is notable that the loss-of-function and gain-of-function studies described generally report a normal cardiac phenotype at baseline.[75, 432] However, Wang *et al.* showed that cardiomyocyte-specific CXCR4 deletion results in unopposed β2 adrenergic receptor-induced hypertrophy and worsened fractional shortening in response to isoproterenol administration.[433] This was reportedly associated with up-regulation of the apoptotic markers p53 and Bax, and was rescued by adenovirus-mediated re-expression of CXCR4. Liehn *et al.* also described marked reduction in baseline cardiac perfusion in global CXCR4 heterozygous mice.[432] Conversely, Cai *et al.* found reduced baseline contractility using *in vitro* adult rat ventricular cardiomyocytes when CXCR4 was over-expressed.[84] Similarly, Pyo *et al.* found a negative inotropic effect of SDF-1 on murine papillary muscles and cardiomyocytes during calcium stimulation, an effect that was exacerbated by adenovirus-mediated over-expression of CXCR4 but attenuated by AMD3100.[434] They attributed this to CXCR4-mediated modulation of L-type calcium channel activity. These studies are interesting because they suggest an intrinsic defect associated with CXCR4 that is unrelated to inflammatory cells. Therefore, a further hypothesis for the results described in this chapter might be that altered cardiac dimensions and function at baseline in CM-CXCR4$^{KO}$ mice may impact upon their susceptibility to infarction. However, the studies discussed above are challenged by data from our laboratory that shows better functional recovery of muscle treated with SDF-1 relative to control muscle.[31, 151] Furthermore, no differences in baseline functional or dimensional parameters were identified between CM-CXCR4$^{WT}$ and CM-CXCR4$^{KO}$ mice in this section, making this mechanism unlikely.

## 8.5 Summary

This chapter describes the development and investigation of a cardiomyocyte-specific CXCR4 null transgenic mouse strain. This was used for the first time to examine its role in acute myocardial IRI. Surprisingly, the application of myocardial IRI in these mice caused significantly smaller IS than in littermate controls.

This finding is difficult to reconcile with the findings in Chapter 5 and Chapter 6. However, it seems likely given the pleiotropic and opposing effects of the SDF-1α-CXCR4 axis in different aspects of myocardial IRI, including acute cardioprotection, modulation of cardiomyocyte contractility and longer-scale processes such as angiogenesis and pro-inflammatory responses, that the timing of CXCR4 activation is key. For example, it could be hypothesised that SDF-1α has injurious effects during ischaemia but is beneficial in reperfusion and to prevent adverse ventricular remodelling. Future work should focus on ascertaining the importance of timing and the role of different cell types with respect to SDF-1α-CXCR4 in myocardial IRI.

The final condition that must be satisfied to define a molecule as a mediator of cardioprotection is the absence of protection in animals with genetic disruption of the mediator's receptor. The present finding precludes resolution of this condition because genetic disruption of the mediator's receptor is protective *per se*. Instead, future studies might focus on genetic disruption of SDF-1α production or antibody neutralisation as a means to defining its potential role in RIC.

# Chapter 9 Overall conclusions

Reperfusion injury makes an important contribution to myocardial injury after a lethal ischaemic insult in animal models. RIC has emerged as a powerful protective phenomenon in the pre-clinical setting, which has heralded a hunt for the mechanism. This is thought to include a humoral factor(s) carried from the preconditioned organ or tissue to the heart, where endogenous pro-survival signalling pathways are activated.

Current knowledge on the functions of SDF-1α broadly delineates dual effects on ischaemic myocardium: direct protection via intracellular pro-survival signal transduction pathways and stem cell mobilisation and gradient-guided homing to mitigate adverse ventricular remodelling, possibly via a paracrine mechanism.

The aim of this project was to investigate the hypothesis that SDF-1α plays a central role in the mechanism of cardioprotection against acute myocardial IRI conferred by RIC. This thesis defined a paradigm for evidencing this role that included induction of pharmacological cardioprotection by exogenous administration of SDF-1α at the time of reperfusion, abolition of cardioprotection by specific antagonism of CXCR4, increased production of SDF-1α as a direct effect of RIC and absence of cardioprotection in CXCR4 deficient mice. Each of these facets has been discussed in detail in the previous chapters.

This thesis provides the first description of cardioprotection against myocardial IRI as a result of the administration of exogenous SDF-1α prior to reperfusion, which has important therapeutic implications. Moreover, AMD3100, a highly specific inhibitor of CXCR4, abolishes the beneficial effect of RIC *in vivo*. Next, a novel ELISA specific for active SDF-1α was developed to circumvent the confounding effects of SDF-1α cleavage. This was exploited to ascertain the dynamics of circulating SDF-1α and unexpectedly demonstrated increased cleavage and inactivation of SDF-1α immediately after RIC, in both rats and humans, which may be attributable to up-regulation of endothelial DPP4 in response to oxidative stress. Finally, this thesis established a transgenic mouse model of inducible, cardiomyocyte-specific CXCR4

deletion that was unexpectedly found to exhibit protection against myocardial IRI. The mechanism behind this protection was not established and, furthermore, it prohibited the use of these mice in experiments to validate the role of CXCR4 signalling in RIC.

Overall, it appears that SDF-1α has potential utility in cardioprotection against myocardial IRI. Whether it plays an intrinsic role in RIC is less clear, with only two of four criteria met, but modulation of the SDF-1α-CXCR4 axis with other approaches, including exogenous SDF-1α, appears to be a viable therapeutic target.

With respect to RIC, further work should characterise the most effective protocol and continue pursuing the mechanism in pre-clinical models to maximise the chance of successful clinical translation. Despite recent setbacks in large clinical outcome studies, it remains a clinically feasible, non-invasive, inexpensive therapeutic intervention with the potential to avert a legacy of ischaemic cardiomyopathy in patients suffering STEMI.

In regard to SDF-1α, further studies aimed at clarifying the target cell type, precise timing and intra-cellular mechanism of SDF-1α in IRI are required. In particular, cell-specific inducible or congenital transgenic models of CXCR4 deletion are of particular interest. Furthermore, exogenous SDF-1α should be tested in animal models that reflect the complex risk factor, comorbidity and treatment profile of humans with cardiovascular disease to determine its potential clinical value. Nonetheless, SDF-1α remains of considerable interest, and unravelling its pleiotropic effects in cardioprotection is paramount for maximising its potential in cardiac patients.

# Chapter 10 References


1. Mortality GBD and Causes of Death C. Global, regional, and national age-sex specific all-cause and cause-specific mortality for 240 causes of death, 1990-2013: a systematic analysis for the Global Burden of Disease Study 2013. *Lancet*. 2015;385:117-71.
2. Gibson CM. NRMI and current treatment patterns for ST-elevation myocardial infarction. *Am Heart J*. 2004;148:S29-33.
3. Keeley EC, Boura JA and Grines CL. Primary angioplasty versus intravenous thrombolytic therapy for acute myocardial infarction: a quantitative review of 23 randomised trials. *Lancet*. 2003;361:13-20.
4. Pedersen F, Butrymovich V, Kelbaek H, Wachtell K, Helqvist S, Kastrup J, Holmvang L, Clemmensen P, Engstrom T, Grande P, Saunamaki K and Jorgensen E. Short- and long-term cause of death in patients treated with primary PCI for STEMI. *J Am Coll Cardiol*. 2014;64:2101-8.
5. Braunwald E and Kloner RA. Myocardial reperfusion: a double-edged sword? *J Clin Invest*. 1985;76:1713-9.
6. Yellon DM and Hausenloy DJ. Myocardial reperfusion injury. *N Engl J Med*. 2007;357:1121-35.
7. Monassier JP. Reperfusion injury in acute myocardial infarction: from bench to cath lab. Part II: Clinical issues and therapeutic options. *Arch Cardiovasc Dis*. 2008;101:565-75.
8. Zweier JL. Measurement of superoxide-derived free radicals in the reperfused heart. Evidence for a free radical mechanism of reperfusion injury. *J Biol Chem*. 1988;263:1353-7.
9. Piper HM, Garcia-Dorado D and Ovize M. A fresh look at reperfusion injury. *Cardiovasc Res*. 1998;38:291-300.
10. Lemasters JJ, Bond JM, Chacon E, Harper IS, Kaplan SH, Ohata H, Trollinger DR, Herman B and Cascio WE. The pH paradox in ischemia-reperfusion injury to cardiac myocytes. *EXS*. 1996;76:99-114.
11. Vinten-Johansen J. Involvement of neutrophils in the pathogenesis of lethal myocardial reperfusion injury. *Cardiovasc Res*. 2004;61:481-97.
12. Jonassen AK, Sack MN, Mjos OD and Yellon DM. Myocardial protection by insulin at reperfusion requires early administration and is mediated via Akt and p70s6 kinase cell-survival signaling. *Circ Res*. 2001;89:1191-8.
13. Apstein CS and Opie LH. A challenge to the metabolic approach to myocardial ischaemia. *Eur Heart J*. 2005;26:956-9.
14. Hausenloy DJ and Yellon DM. Myocardial ischemia-reperfusion injury: a neglected therapeutic target. *J Clin Invest*. 2013;123:92-100.
15. Bromage DI, Davidson SM and Yellon DM. Stromal derived factor 1alpha: A chemokine that delivers a two-pronged defence of the myocardium. *Pharmacology & therapeutics*. 2014.
16. Penn MS, Pastore J, Miller T and Aras R. SDF-1 in myocardial repair. *Gene Ther*. 2012;19:583-7.
17. Zaruba MM and Franz WM. Role of the SDF-1-CXCR4 axis in stem cell-based therapies for ischemic cardiomyopathy. *Expert Opin Biol Ther*. 2010;10:321-35.

18. Ghadge SK, Muhlstedt S, Ozcelik C and Bader M. SDF-1alpha as a therapeutic stem cell homing factor in myocardial infarction. *Pharmacol Ther*. 2011;129:97-108.
19. Takahashi M. Role of the SDF-1/CXCR4 system in myocardial infarction. *Circ J*. 2010;74:418-23.
20. Saxena A, Fish JE, White MD, Yu S, Smyth JW, Shaw RM, DiMaio JM and Srivastava D. Stromal cell-derived factor-1alpha is cardioprotective after myocardial infarction. *Circulation*. 2008;117:2224-31.
21. Tang J, Wang J, Song H, Huang Y, Yang J, Kong X, Guo L, Zheng F and Zhang L. Adenovirus-mediated stromal cell-derived factor-1 alpha gene transfer improves cardiac structure and function after experimental myocardial infarction through angiogenic and antifibrotic actions. *Mol Biol Rep*. 2010;37:1957-69.
22. Misao Y, Takemura G, Arai M, Ohno T, Onogi H, Takahashi T, Minatoguchi S, Fujiwara T and Fujiwara H. Importance of recruitment of bone marrow-derived CXCR4+ cells in post-infarct cardiac repair mediated by G-CSF. *Cardiovasc Res*. 2006;71:455-65.
23. Sasaki T, Fukazawa R, Ogawa S, Kanno S, Nitta T, Ochi M and Shimizu K. Stromal cell-derived factor-1alpha improves infarcted heart function through angiogenesis in mice. *Pediatr Int*. 2007;49:966-71.
24. Hausenloy DJ and Yellon DM. New directions for protecting the heart against ischaemia-reperfusion injury: targeting the Reperfusion Injury Salvage Kinase (RISK)-pathway. *Cardiovasc Res*. 2004;61:448-60.
25. Hausenloy DJ and Yellon DM. Preconditioning and postconditioning: united at reperfusion. *Pharmacol Ther*. 2007;116:173-91.
26. Hausenloy DJ and Yellon DM. Reperfusion injury salvage kinase signalling: taking a RISK for cardioprotection. *Heart Fail Rev*. 2007;12:217-34.
27. Serejo FC, Rodrigues LF, Jr., da Silva Tavares KC, de Carvalho AC and Nascimento JH. Cardioprotective properties of humoral factors released from rat hearts subject to ischemic preconditioning. *J Cardiovasc Pharmacol*. 2007;49:214-20.
28. Shimizu M, Tropak M, Diaz RJ, Suto F, Surendra H, Kuzmin E, Li J, Gross G, Wilson GJ, Callahan J and Redington AN. Transient limb ischaemia remotely preconditions through a humoral mechanism acting directly on the myocardium: evidence suggesting cross-species protection. *Clin Sci (Lond)*. 2009;117:191-200.
29. Jiang Q, Song P, Wang E, Li J, Hu S and Zhang H. Remote ischemic postconditioning enhances cell retention in the myocardium after intravenous administration of bone marrow mesenchymal stromal cells. *J Mol Cell Cardiol*. 2013;56:1-7.
30. Kamota T, Li TS, Morikage N, Murakami M, Ohshima M, Kubo M, Kobayashi T, Mikamo A, Ikeda Y, Matsuzaki M and Hamano K. Ischemic pre-conditioning enhances the mobilization and recruitment of bone marrow stem cells to protect against ischemia/reperfusion injury in the late phase. *J Am Coll Cardiol*. 2009;53:1814-22.
31. Davidson SM, Selvaraj P, He D, Boi-Doku C, Yellon RL, Vicencio JM and Yellon DM. Remote ischaemic preconditioning involves signalling through the SDF-1alpha/CXCR4 signalling axis. *Basic Res Cardiol*. 2013;108:377.
32. De Clercq E. The bicyclam AMD3100 story. *Nat Rev Drug Discov*. 2003;2:581-7.
33. Ceradini DJ, Kulkarni AR, Callaghan MJ, Tepper OM, Bastidas N, Kleinman ME, Capla JM, Galiano RD, Levine JP and Gurtner GC. Progenitor cell trafficking is

regulated by hypoxic gradients through HIF-1 induction of SDF-1. *Nat Med*. 2004;10:858-64.
34. Gerard C and Rollins BJ. Chemokines and disease. *Nat Immunol*. 2001;2:108-15.
35. Matsumori A, Furukawa Y, Hashimoto T, Yoshida A, Ono K, Shioi T, Okada M, Iwasaki A, Nishio R, Matsushima K and Sasayama S. Plasma levels of the monocyte chemotactic and activating factor/monocyte chemoattractant protein-1 are elevated in patients with acute myocardial infarction. *J Mol Cell Cardiol*. 1997;29:419-23.
36. Riesenberg K, Levy R, Katz A, Galkop S and Schlaeffer F. Neutrophil superoxide release and interleukin 8 in acute myocardial infarction: distinction between complicated and uncomplicated states. *Eur J Clin Invest*. 1997;27:398-404.
37. Rollins BJ. Chemokines. *Blood*. 1997;90:909-28.
38. Shirozu M, Nakano T, Inazawa J, Tashiro K, Tada H, Shinohara T and Honjo T. Structure and chromosomal localization of the human stromal cell-derived factor 1 (SDF1) gene. *Genomics*. 1995;28:495-500.
39. Janowski M. Functional diversity of SDF-1 splicing variants. *Cell Adh Migr*. 2009;3:243-9.
40. Davis DA, Singer KE, De La Luz Sierra M, Narazaki M, Yang F, Fales HM, Yarchoan R and Tosato G. Identification of carboxypeptidase N as an enzyme responsible for C-terminal cleavage of stromal cell-derived factor-1alpha in the circulation. *Blood*. 2005;105:4561-8.
41. Kucia M, Reca R, Miekus K, Wanzeck J, Wojakowski W, Janowska-Wieczorek A, Ratajczak J and Ratajczak MZ. Trafficking of normal stem cells and metastasis of cancer stem cells involve similar mechanisms: pivotal role of the SDF-1-CXCR4 axis. *Stem Cells*. 2005;23:879-94.
42. Nagasawa T, Nakajima T, Tachibana K, Iizasa H, Bleul CC, Yoshie O, Matsushima K, Yoshida N, Springer TA and Kishimoto T. Molecular cloning and characterization of a murine pre-B-cell growth-stimulating factor/stromal cell-derived factor 1 receptor, a murine homolog of the human immunodeficiency virus 1 entry coreceptor fusin. *Proc Natl Acad Sci U S A*. 1996;93:14726-9.
43. Ratajczak MZ, Zuba-Surma E, Kucia M, Reca R, Wojakowski W and Ratajczak J. The pleiotropic effects of the SDF-1-CXCR4 axis in organogenesis, regeneration and tumorigenesis. *Leukemia*. 2006;20:1915-24.
44. Chatterjee M and Gawaz M. Platelet-derived CXCL12 (SDF-1alpha): basic mechanisms and clinical implications. *J Thromb Haemost*. 2013;11:1954-67.
45. Segret A, Rucker-Martin C, Pavoine C, Flavigny J, Deroubaix E, Chatel MA, Lombet A and Renaud JF. Structural localization and expression of CXCL12 and CXCR4 in rat heart and isolated cardiac myocytes. *J Histochem Cytochem*. 2007;55:141-50.
46. Hu X, Dai S, Wu WJ, Tan W, Zhu X, Mu J, Guo Y, Bolli R and Rokosh G. Stromal cell derived factor-1 alpha confers protection against myocardial ischemia/reperfusion injury: role of the cardiac stromal cell derived factor-1 alpha CXCR4 axis. *Circulation*. 2007;116:654-63.
47. Damas JK, Eiken HG, Oie E, Bjerkeli V, Yndestad A, Ueland T, Tonnessen T, Geiran OR, Aass H, Simonsen S, Christensen G, Froland SS, Attramadal H, Gullestad L and Aukrust P. Myocardial expression of CC- and CXC-chemokines and their receptors in human end-stage heart failure. *Cardiovasc Res*. 2000;47:778-87.

48. Aiuti A, Webb IJ, Bleul C, Springer T and Gutierrez-Ramos JC. The chemokine SDF-1 is a chemoattractant for human CD34+ hematopoietic progenitor cells and provides a new mechanism to explain the mobilization of CD34+ progenitors to peripheral blood. *J Exp Med*. 1997;185:111-20.
49. Kondo K, Shintani S, Shibata R, Murakami H, Murakami R, Imaizumi M, Kitagawa Y and Murohara T. Implantation of adipose-derived regenerative cells enhances ischemia-induced angiogenesis. *Arterioscler Thromb Vasc Biol*. 2009;29:61-6.
50. Ashburner M, Ball CA, Blake JA, Botstein D, Butler H, Cherry JM, Davis AP, Dolinski K, Dwight SS, Eppig JT, Harris MA, Hill DP, Issel-Tarver L, Kasarskis A, Lewis S, Matese JC, Richardson JE, Ringwald M, Rubin GM and Sherlock G. Gene ontology: tool for the unification of biology. The Gene Ontology Consortium. *Nat Genet*. 2000;25:25-9.
51. Segers VF, Tokunou T, Higgins LJ, MacGillivray C, Gannon J and Lee RT. Local delivery of protease-resistant stromal cell derived factor-1 for stem cell recruitment after myocardial infarction. *Circulation*. 2007;116:1683-92.
52. Baerts L, Waumans Y, Brandt I, Jungraithmayr W, Van der Veken P, Vanderheyden M and De Meester I. Circulating Stromal Cell-Derived Factor 1alpha Levels in Heart Failure: A Matter of Proper Sampling. *PLoS One*. 2015;10:e0141408.
53. Misra P, Lebeche D, Ly H, Schwarzkopf M, Diaz G, Hajjar RJ, Schecter AD and Frangioni JV. Quantitation of CXCR4 expression in myocardial infarction using 99mTc-labeled SDF-1alpha. *J Nucl Med*. 2008;49:963-9.
54. Kucia M, Jankowski K, Reca R, Wysoczynski M, Bandura L, Allendorf DJ, Zhang J, Ratajczak J and Ratajczak MZ. CXCR4-SDF-1 signalling, locomotion, chemotaxis and adhesion. *J Mol Histol*. 2004;35:233-45.
55. Wong D and Korz W. Translating an Antagonist of Chemokine Receptor CXCR4: from bench to bedside. *Clin Cancer Res*. 2008;14:7975-80.
56. McGrath KE, Koniski AD, Maltby KM, McGann JK and Palis J. Embryonic expression and function of the chemokine SDF-1 and its receptor, CXCR4. *Dev Biol*. 1999;213:442-56.
57. Zou YR, Kottmann AH, Kuroda M, Taniuchi I and Littman DR. Function of the chemokine receptor CXCR4 in haematopoiesis and in cerebellar development. *Nature*. 1998;393:595-9.
58. Hernandez PA, Gorlin RJ, Lukens JN, Taniuchi S, Bohinjec J, Francois F, Klotman ME and Diaz GA. Mutations in the chemokine receptor gene CXCR4 are associated with WHIM syndrome, a combined immunodeficiency disease. *Nat Genet*. 2003;34:70-4.
59. Hoffmann F, Muller W, Schutz D, Penfold ME, Wong YH, Schulz S and Stumm R. Rapid uptake and degradation of CXCL12 depend on CXCR7 carboxyl-terminal serine/threonine residues. *J Biol Chem*. 2012;287:28362-77.
60. Berahovich RD, Zabel BA, Lewen S, Walters MJ, Ebsworth K, Wang Y, Jaen JC and Schall TJ. Endothelial Expression of CXCR7 and the Regulation of Systemic CXCL12 Levels. *Immunology*. 2013.
61. Sanchez-Martin L, Sanchez-Mateos P and Cabanas C. CXCR7 impact on CXCL12 biology and disease. *Trends Mol Med*. 2013;19:12-22.
62. Liu H, Liu S, Li Y, Wang X, Xue W, Ge G and Luo X. The role of SDF-1-CXCR4/CXCR7 axis in the therapeutic effects of hypoxia-preconditioned

mesenchymal stem cells for renal ischemia/reperfusion injury. *PLoS One*. 2012;7:e34608.
63. Pillarisetti K and Gupta SK. Cloning and relative expression analysis of rat stromal cell derived factor-1 (SDF-1)1: SDF-1 alpha mRNA is selectively induced in rat model of myocardial infarction. *Inflammation*. 2001;25:293-300.
64. Askari AT and Penn MS. Stromal cell-derived factor-1 mediates stem cell homing and tissue regeneration. *Discov Med*. 2003;3:46-7.
65. Abbott JD, Huang Y, Liu D, Hickey R, Krause DS and Giordano FJ. Stromal cell-derived factor-1alpha plays a critical role in stem cell recruitment to the heart after myocardial infarction but is not sufficient to induce homing in the absence of injury. *Circulation*. 2004;110:3300-5.
66. Yamani MH, Ratliff NB, Cook DJ, Tuzcu EM, Yu Y, Hobbs R, Rincon G, Bott-Silverman C, Young JB, Smedira N and Starling RC. Peritransplant ischemic injury is associated with up-regulation of stromal cell-derived factor-1. *J Am Coll Cardiol*. 2005;46:1029-35.
67. Leone AM, Rutella S, Bonanno G, Contemi AM, de Ritis DG, Giannico MB, Rebuzzi AG, Leone G and Crea F. Endogenous G-CSF and CD34+ cell mobilization after acute myocardial infarction. *Int J Cardiol*. 2006;111:202-8.
68. Unzek S, Zhang M, Mal N, Mills WR, Laurita KR and Penn MS. SDF-1 recruits cardiac stem cell-like cells that depolarize in vivo. *Cell Transplant*. 2007;16:879-86.
69. Jujo K, Hamada H, Iwakura A, Thorne T, Sekiguchi H, Clarke T, Ito A, Misener S, Tanaka T, Klyachko E, Kobayashi K, Tongers J, Roncalli J, Tsurumi Y, Hagiwara N and Losordo DW. CXCR4 blockade augments bone marrow progenitor cell recruitment to the neovasculature and reduces mortality after myocardial infarction. *Proc Natl Acad Sci U S A*. 2010;107:11008-13.
70. Kucia M, Dawn B, Hunt G, Guo Y, Wysoczynski M, Majka M, Ratajczak J, Rezzoug F, Ildstad ST, Bolli R and Ratajczak MZ. Cells expressing early cardiac markers reside in the bone marrow and are mobilized into the peripheral blood after myocardial infarction. *Circ Res*. 2004;95:1191-9.
71. Lapidot T and Petit I. Current understanding of stem cell mobilization: the roles of chemokines, proteolytic enzymes, adhesion molecules, cytokines, and stromal cells. *Exp Hematol*. 2002;30:973-81.
72. Cottler-Fox MH, Lapidot T, Petit I, Kollet O, DiPersio JF, Link D and Devine S. Stem cell mobilization. *Hematology Am Soc Hematol Educ Program*. 2003:419-37.
73. Levesque JP, Hendy J, Takamatsu Y, Simmons PJ and Bendall LJ. Disruption of the CXCR4/CXCL12 chemotactic interaction during hematopoietic stem cell mobilization induced by GCSF or cyclophosphamide. *J Clin Invest*. 2003;111:187-96.
74. Liles WC, Broxmeyer HE, Rodger E, Wood B, Hubel K, Cooper S, Hangoc G, Bridger GJ, Henson GW, Calandra G and Dale DC. Mobilization of hematopoietic progenitor cells in healthy volunteers by AMD3100, a CXCR4 antagonist. *Blood*. 2003;102:2728-30.
75. Dong F, Harvey J, Finan A, Weber K, Agarwal U and Penn MS. Myocardial CXCR4 expression is required for mesenchymal stem cell mediated repair following acute myocardial infarction. *Circulation*. 2012;126:314-24.
76. Askari AT, Unzek S, Popovic ZB, Goldman CK, Forudi F, Kiedrowski M, Rovner A, Ellis SG, Thomas JD, DiCorleto PE, Topol EJ and Penn MS. Effect of stromal-cell-

derived factor 1 on stem-cell homing and tissue regeneration in ischaemic cardiomyopathy. *Lancet*. 2003;362:697-703.
77. Leone AM, Rutella S, Bonanno G, Abbate A, Rebuzzi AG, Giovannini S, Lombardi M, Galiuto L, Liuzzo G, Andreotti F, Lanza GA, Contemi AM, Leone G and Crea F. Mobilization of bone marrow-derived stem cells after myocardial infarction and left ventricular function. *Eur Heart J*. 2005;26:1196-204.
78. Gao H, Priebe W, Glod J and Banerjee D. Activation of signal transducers and activators of transcription 3 and focal adhesion kinase by stromal cell-derived factor 1 is required for migration of human mesenchymal stem cells in response to tumor cell-conditioned medium. *Stem cells*. 2009;27:857-65.
79. Haider H, Jiang S, Idris NM and Ashraf M. IGF-1-overexpressing mesenchymal stem cells accelerate bone marrow stem cell mobilization via paracrine activation of SDF-1alpha/CXCR4 signaling to promote myocardial repair. *Circ Res*. 2008;103:1300-8.
80. Zhao T, Zhang D, Millard RW, Ashraf M and Wang Y. Stem cell homing and angiomyogenesis in transplanted hearts are enhanced by combined intramyocardial SDF-1alpha delivery and endogenous cytokine signaling. *Am J Physiol Heart Circ Physiol*. 2009;296:H976-86.
81. Elmadbouh I, Haider H, Jiang S, Idris NM, Lu G and Ashraf M. Ex vivo delivered stromal cell-derived factor-1alpha promotes stem cell homing and induces angiomyogenesis in the infarcted myocardium. *J Mol Cell Cardiol*. 2007;42:792-803.
82. Deglurkar I, Mal N, Mills WR, Popovic ZB, McCarthy P, Blackstone EH, Laurita KR and Penn MS. Mechanical and electrical effects of cell-based gene therapy for ischemic cardiomyopathy are independent. *Hum Gene Ther*. 2006;17:1144-51.
83. Sundararaman S, Miller TJ, Pastore JM, Kiedrowski M, Aras R and Penn MS. Plasmid-based transient human stromal cell-derived factor-1 gene transfer improves cardiac function in chronic heart failure. *Gene Ther*. 2011;18:867-73.
84. Cai WF, Kang K, Huang W, Liang JL, Feng YL, Liu GS, Chang DH, Wen ZL, Paul C, Xu M, Millard RW and Wang Y. CXCR4 attenuates cardiomyocytes mitochondrial dysfunction to resist ischaemia-reperfusion injury. *J Cell Mol Med*. 2015;19:1825-35.
85. Cheng Z, Ou L, Zhou X, Li F, Jia X, Zhang Y, Liu X, Li Y, Ward CA, Melo LG and Kong D. Targeted migration of mesenchymal stem cells modified with CXCR4 gene to infarcted myocardium improves cardiac performance. *Mol Ther*. 2008;16:571-9.
86. Shiba Y, Takahashi M, Hata T, Murayama H, Morimoto H, Ise H, Nagasawa T and Ikeda U. Bone marrow CXCR4 induction by cultivation enhances therapeutic angiogenesis. *Cardiovasc Res*. 2009;81:169-77.
87. Chiang KH, Cheng WL, Shih CM, Lin YW, Tsao NW, Kao YT, Lin CT, Wu SC, Huang CY and Lin FY. Statins, HMG-CoA reductase inhibitors, improve neovascularization by increasing the expression density of CXCR4 in endothelial progenitor cells. *PLoS One*. 2015;10:e0136405.
88. Chen J, Chemaly E, Liang L, Kho C, Lee A, Park J, Altman P, Schecter AD, Hajjar RJ and Tarzami ST. Effects of CXCR4 gene transfer on cardiac function after ischemia-reperfusion injury. *Am J Pathol*. 2010;176:1705-15.
89. Koch KC, Schaefer WM, Liehn EA, Rammos C, Mueller D, Schroeder J, Dimassi T, Stopinski T and Weber C. Effect of catheter-based transendocardial delivery of stromal cell-derived factor 1alpha on left ventricular function and perfusion in a porcine model of myocardial infarction. *Basic Res Cardiol*. 2006;101:69-77.

90. Maekawa Y, Anzai T, Yoshikawa T, Sugano Y, Mahara K, Kohno T, Takahashi T and Ogawa S. Effect of granulocyte-macrophage colony-stimulating factor inducer on left ventricular remodeling after acute myocardial infarction. *J Am Coll Cardiol*. 2004;44:1510-20.
91. Teicher BA and Fricker SP. CXCL12 (SDF-1)/CXCR4 pathway in cancer. *Clin Cancer Res*. 2010;16:2927-31.
92. Burger JA and Peled A. CXCR4 antagonists: targeting the microenvironment in leukemia and other cancers. *Leukemia*. 2009;23:43-52.
93. Chung ES, Miller L, Patel AN, Anderson RD, Mendelsohn FO, Traverse J, Silver KH, Shin J, Ewald G, Farr MJ, Anwaruddin S, Plat F, Fisher SJ, AuWerter AT, Pastore JM, Aras R and Penn MS. Changes in ventricular remodelling and clinical status during the year following a single administration of stromal cell-derived factor-1 non-viral gene therapy in chronic ischaemic heart failure patients: the STOP-HF randomized Phase II trial. *Eur Heart J*. 2015;36:2228-38.
94. Braunersreuther V, Mach F and Steffens S. The specific role of chemokines in atherosclerosis. *Thromb Haemost*. 2007;97:714-21.
95. Kodali R, Hajjou M, Berman AB, Bansal MB, Zhang S, Pan JJ and Schecter AD. Chemokines induce matrix metalloproteinase-2 through activation of epidermal growth factor receptor in arterial smooth muscle cells. *Cardiovasc Res*. 2006;69:706-15.
96. Nemenoff RA, Simpson PA, Furgeson SB, Kaplan-Albuquerque N, Crossno J, Garl PJ, Cooper J and Weiser-Evans MC. Targeted deletion of PTEN in smooth muscle cells results in vascular remodeling and recruitment of progenitor cells through induction of stromal cell-derived factor-1alpha. *Circ Res*. 2008;102:1036-45.
97. Satoh K, Fukumoto Y, Nakano M, Sugimura K, Nawata J, Demachi J, Karibe A, Kagaya Y, Ishii N, Sugamura K and Shimokawa H. Statin ameliorates hypoxia-induced pulmonary hypertension associated with down-regulated stromal cell-derived factor-1. *Cardiovasc Res*. 2009;81:226-34.
98. Tang JM, Wang JN, Zhang L, Zheng F, Yang JY, Kong X, Guo LY, Chen L, Huang YZ, Wan Y and Chen SY. VEGF/SDF-1 promotes cardiac stem cell mobilization and myocardial repair in the infarcted heart. *Cardiovasc Res*. 2011;91:402-11.
99. Theiss HD, David R, Engelmann MG, Barth A, Schotten K, Naebauer M, Reichart B, Steinbeck G and Franz WM. Circulation of CD34+ progenitor cell populations in patients with idiopathic dilated and ischaemic cardiomyopathy (DCM and ICM). *Eur Heart J*. 2007;28:1258-64.
100. Penn MS, Mendelsohn FO, Schaer GL, Sherman W, Farr M, Pastore J, Rouy D, Clemens R, Aras R and Losordo DW. An open-label dose escalation study to evaluate the safety of administration of nonviral stromal cell-derived factor-1 plasmid to treat symptomatic ischemic heart failure. *Circ Res*. 2013;112:816-25.
101. Murry CE, Jennings RB and Reimer KA. Preconditioning with ischemia: a delay of lethal cell injury in ischemic myocardium. *Circulation*. 1986;74:1124-36.
102. Wever KE, Hooijmans CR, Riksen NP, Sterenborg TB, Sena ES, Ritskes-Hoitinga M and Warle MC. Determinants of the Efficacy of Cardiac Ischemic Preconditioning: A Systematic Review and Meta-Analysis of Animal Studies. *PLoS One*. 2015;10:e0142021.
103. Ovize M, Baxter GF, Di Lisa F, Ferdinandy P, Garcia-Dorado D, Hausenloy DJ, Heusch G, Vinten-Johansen J, Yellon DM and Schulz R. Postconditioning and

protection from reperfusion injury: where do we stand? Position paper from the Working Group of Cellular Biology of the Heart of the European Society of Cardiology. *Cardiovasc Res*. 2010;87:406-23.
104. Shanmuganathan S, Hausenloy DJ, Duchen MR and Yellon DM. Mitochondrial permeability transition pore as a target for cardioprotection in the human heart. *Am J Physiol Heart Circ Physiol*. 2005;289:H237-42.
105. Deussen A, Moser G and Schrader J. Contribution of coronary endothelial cells to cardiac adenosine production. *Pflugers Arch*. 1986;406:608-14.
106. Faigle M, Seessle J, Zug S, El Kasmi KC and Eltzschig HK. ATP release from vascular endothelia occurs across Cx43 hemichannels and is attenuated during hypoxia. *PLoS One*. 2008;3:e2801.
107. Dorge H, Schulz R, Belosjorow S, Post H, van de Sand A, Konietzka I, Frede S, Hartung T, Vinten-Johansen J, Youker KA, Entman ML, Erbel R and Heusch G. Coronary microembolization: the role of TNF-alpha in contractile dysfunction. *J Mol Cell Cardiol*. 2002;34:51-62.
108. Schulz R, Aker S, Belosjorow S and Heusch G. TNFalpha in ischemia/reperfusion injury and heart failure. *Basic Res Cardiol*. 2004;99:8-11.
109. Heusch G, Boengler K and Schulz R. Cardioprotection: nitric oxide, protein kinases, and mitochondria. *Circulation*. 2008;118:1915-9.
110. Zhao ZQ, Corvera JS, Halkos ME, Kerendi F, Wang NP, Guyton RA and Vinten-Johansen J. Inhibition of myocardial injury by ischemic postconditioning during reperfusion: comparison with ischemic preconditioning. *Am J Physiol Heart Circ Physiol*. 2003;285:H579-88.
111. Halkos ME, Kerendi F, Corvera JS, Wang NP, Kin H, Payne CS, Sun HY, Guyton RA, Vinten-Johansen J and Zhao ZQ. Myocardial protection with postconditioning is not enhanced by ischemic preconditioning. *Ann Thorac Surg*. 2004;78:961-9; discussion 969.
112. Lacerda L, Somers S, Opie LH and Lecour S. Ischaemic postconditioning protects against reperfusion injury via the SAFE pathway. *Cardiovasc Res*. 2009;84:201-8.
113. Yellon DM and Baxter GF. Reperfusion injury revisited: is there a role for growth factor signaling in limiting lethal reperfusion injury? *Trends Cardiovasc Med*. 1999;9:245-9.
114. Baxter GF, Mocanu MM, Brar BK, Latchman DS and Yellon DM. Cardioprotective effects of transforming growth factor-beta1 during early reoxygenation or reperfusion are mediated by p42/p44 MAPK. *J Cardiovasc Pharmacol*. 2001;38:930-9.
115. Brar BK, Jonassen AK, Stephanou A, Santilli G, Railson J, Knight RA, Yellon DM and Latchman DS. Urocortin protects against ischemic and reperfusion injury via a MAPK-dependent pathway. *J Biol Chem*. 2000;275:8508-14.
116. Tong H, Chen W, Steenbergen C and Murphy E. Ischemic preconditioning activates phosphatidylinositol-3-kinase upstream of protein kinase C. *Circ Res*. 2000;87:309-15.
117. Mocanu MM, Bell RM and Yellon DM. PI3 kinase and not p42/p44 appears to be implicated in the protection conferred by ischemic preconditioning. *J Mol Cell Cardiol*. 2002;34:661-8.

118. Fryer RM, Pratt PF, Hsu AK and Gross GJ. Differential activation of extracellular signal regulated kinase isoforms in preconditioning and opioid-induced cardioprotection. *J Pharmacol Exp Ther*. 2001;296:642-9.
119. Kunuthur SP, Mocanu MM, Hemmings BA, Hausenloy DJ and Yellon DM. The Akt1 isoform is an essential mediator of ischaemic preconditioning. *J Cell Mol Med*. 2012;16:1739-49.
120. Downey JM and Cohen MV. We think we see a pattern emerging here. *Circulation*. 2005;111:120-1.
121. Hausenloy DJ, Tsang A and Yellon DM. The reperfusion injury salvage kinase pathway: a common target for both ischemic preconditioning and postconditioning. *Trends Cardiovasc Med*. 2005;15:69-75.
122. Hausenloy DJ, Mocanu MM and Yellon DM. Activation of the pro-survival kinases (PI3 kinase-Akt and Erk 1/2) at reperfusion is essential for preconditioning-induced protection. *Circulation*. 2003;108:62-62.
123. Tamareille S, Mateus V, Ghaboura N, Jeanneteau J, Croue A, Henrion D, Furber A and Prunier F. RISK and SAFE signaling pathway interactions in remote limb ischemic perconditioning in combination with local ischemic postconditioning. *Basic Res Cardiol*. 2011;106:1329-39.
124. Lecour S, Suleman N, Deuchar GA, Somers S, Lacerda L, Huisamen B and Opie LH. Pharmacological preconditioning with tumor necrosis factor-alpha activates signal transducer and activator of transcription-3 at reperfusion without involving classic prosurvival kinases (Akt and extracellular signal-regulated kinase). *Circulation*. 2005;112:3911-8.
125. Goodman MD, Koch SE, Fuller-Bicer GA and Butler KL. Regulating RISK: a role for JAK-STAT signaling in postconditioning? *Am J Physiol Heart Circ Physiol*. 2008;295:H1649-56.
126. Di Lisa F and Bernardi P. A CaPful of mechanisms regulating the mitochondrial permeability transition. *J Mol Cell Cardiol*. 2009;46:775-80.
127. Griffiths EJ and Halestrap AP. Mitochondrial non-specific pores remain closed during cardiac ischaemia, but open upon reperfusion. *Biochem J*. 1995;307 ( Pt 1):93-8.
128. Di Lisa F, Menabo R, Canton M, Barile M and Bernardi P. Opening of the mitochondrial permeability transition pore causes depletion of mitochondrial and cytosolic NAD+ and is a causative event in the death of myocytes in postischemic reperfusion of the heart. *J Biol Chem*. 2001;276:2571-5.
129. Murata M, Akao M, O'Rourke B and Marban E. Mitochondrial ATP-sensitive potassium channels attenuate matrix Ca(2+) overload during simulated ischemia and reperfusion: possible mechanism of cardioprotection. *Circ Res*. 2001;89:891-8.
130. Kim JS, Jin Y and Lemasters JJ. Reactive oxygen species, but not Ca2+ overloading, trigger pH- and mitochondrial permeability transition-dependent death of adult rat myocytes after ischemia-reperfusion. *Am J Physiol Heart Circ Physiol*. 2006;290:H2024-34.
131. Matsumoto-Ida M, Akao M, Takeda T, Kato M and Kita T. Real-time 2-photon imaging of mitochondrial function in perfused rat hearts subjected to ischemia/reperfusion. *Circulation*. 2006;114:1497-503.

132. Argaud L, Gateau-Roesch O, Raisky O, Loufouat J, Robert D and Ovize M. Postconditioning inhibits mitochondrial permeability transition. *Circulation*. 2005;111:194-7.
133. Hausenloy DJ, Yellon DM, Mani-Babu S and Duchen MR. Preconditioning protects by inhibiting the mitochondrial permeability transition. *Am J Physiol Heart Circ Physiol*. 2004;287:H841-9.
134. Javadov SA, Clarke S, Das M, Griffiths EJ, Lim KH and Halestrap AP. Ischaemic preconditioning inhibits opening of mitochondrial permeability transition pores in the reperfused rat heart. *J Physiol*. 2003;549:513-24.
135. Bopassa JC, Vandroux D, Ovize M and Ferrera R. Controlled reperfusion after hypothermic heart preservation inhibits mitochondrial permeability transition-pore opening and enhances functional recovery. *Am J Physiol Heart Circ Physiol*. 2006;291:H2265-71.
136. Zhao ZQ and Vinten-Johansen J. Postconditioning: reduction of reperfusion-induced injury. *Cardiovasc Res*. 2006;70:200-11.
137. Juhaszova M, Zorov DB, Kim SH, Pepe S, Fu Q, Fishbein KW, Ziman BD, Wang S, Ytrehus K, Antos CL, Olson EN and Sollott SJ. Glycogen synthase kinase-3beta mediates convergence of protection signaling to inhibit the mitochondrial permeability transition pore. *J Clin Invest*. 2004;113:1535-49.
138. Bopassa JC, Ferrera R, Gateau-Roesch O, Couture-Lepetit E and Ovize M. PI 3-kinase regulates the mitochondrial transition pore in controlled reperfusion and postconditioning. *Cardiovasc Res*. 2006;69:178-85.
139. Davidson SM, Hausenloy D, Duchen MR and Yellon DM. Signalling via the reperfusion injury signalling kinase (RISK) pathway links closure of the mitochondrial permeability transition pore to cardioprotection. *Int J Biochem Cell Biol*. 2006;38:414-9.
140. Smith CC, Dixon RA, Wynne AM, Theodorou L, Ong SG, Subrayan S, Davidson SM, Hausenloy DJ and Yellon DM. Leptin-induced cardioprotection involves JAK/STAT signaling that may be linked to the mitochondrial permeability transition pore. *Am J Physiol Heart Circ Physiol*. 2010;299:H1265-70.
141. Griffiths EJ and Halestrap AP. Protection by Cyclosporin A of ischemia/reperfusion-induced damage in isolated rat hearts. *J Mol Cell Cardiol*. 1993;25:1461-9.
142. Baines CP, Kaiser RA, Purcell NH, Blair NS, Osinska H, Hambleton MA, Brunskill EW, Sayen MR, Gottlieb RA, Dorn GW, Robbins J and Molkentin JD. Loss of cyclophilin D reveals a critical role for mitochondrial permeability transition in cell death. *Nature*. 2005;434:658-62.
143. Nakagawa T, Shimizu S, Watanabe T, Yamaguchi O, Otsu K, Yamagata H, Inohara H, Kubo T and Tsujimoto Y. Cyclophilin D-dependent mitochondrial permeability transition regulates some necrotic but not apoptotic cell death. *Nature*. 2005;434:652-8.
144. Piot C, Croisille P, Staat P, Thibault H, Rioufol G, Mewton N, Elbelghiti R, Cung TT, Bonnefoy E, Angoulvant D, Macia C, Raczka F, Sportouch C, Gahide G, Finet G, Andre-Fouet X, Revel D, Kirkorian G, Monassier JP, Derumeaux G and Ovize M. Effect of cyclosporine on reperfusion injury in acute myocardial infarction. *N Engl J Med*. 2008;359:473-81.

145. Cung TT, Morel O, Cayla G, Rioufol G, Garcia-Dorado D, Angoulvant D, Bonnefoy-Cudraz E, Guerin P, Elbaz M, Delarche N, Coste P, Vanzetto G, Metge M, Aupetit JF, Jouve B, Motreff P, Tron C, Labeque JN, Steg PG, Cottin Y, Range G, Clerc J, Claeys MJ, Coussement P, Prunier F, Moulin F, Roth O, Belle L, Dubois P, Barragan P, Gilard M, Piot C, Colin P, De Poli F, Morice MC, Ider O, Dubois-Rande JL, Unterseeh T, Le Breton H, Beard T, Blanchard D, Grollier G, Malquarti V, Staat P, Sudre A, Elmer E, Hansson MJ, Bergerot C, Boussaha I, Jossan C, Derumeaux G, Mewton N and Ovize M. Cyclosporine before PCI in Patients with Acute Myocardial Infarction. *N Engl J Med*. 2015;373:1021-31.
146. Lim WY, Messow CM and Berry C. Cyclosporin variably and inconsistently reduces infarct size in experimental models of reperfused myocardial infarction: a systematic review and meta-analysis. *Br J Pharmacol*. 2012;165:2034-43.
147. Hausenloy DJ and Yellon DM. Remote ischaemic preconditioning: underlying mechanisms and clinical application. *Cardiovasc Res*. 2008;79:377-86.
148. Tang YL, Zhu W, Cheng M, Chen L, Zhang J, Sun T, Kishore R, Phillips MI, Losordo DW and Qin G. Hypoxic preconditioning enhances the benefit of cardiac progenitor cell therapy for treatment of myocardial infarction by inducing CXCR4 expression. *Circ Res*. 2009;104:1209-16.
149. Huang C, Gu H, Zhang W, Manukyan MC, Shou W and Wang M. SDF-1/CXCR4 mediates acute protection of cardiac function through myocardial STAT3 signaling following global ischemia/reperfusion injury. *Am J Physiol Heart Circ Physiol*. 2011;301:H1496-505.
150. Jang YH, Kim JH, Ban C, Ahn K, Cheong JH, Kim HH, Kim JS, Park YH, Kim J, Chun KJ, Lee GH, Kim M, Kim C and Xu Z. Stromal cell derived factor-1 (SDF-1) targeting reperfusion reduces myocardial infarction in isolated rat hearts. *Cardiovasc Ther*. 2012;30:264-72.
151. Malik A, Bromage DI, He Z, Candilio L, Hamarneh A, Taferner S, Davidson SM and Yellon DM. Exogenous SDF-1alpha Protects Human Myocardium from Hypoxia-Reoxygenation Injury via CXCR4. *Cardiovasc Drugs Ther*. 2015.
152. Busillo JM and Benovic JL. Regulation of CXCR4 signaling. *Biochim Biophys Acta*. 2007;1768:952-63.
153. Vila-Coro AJ, Rodriguez-Frade JM, Martin De Ana A, Moreno-Ortiz MC, Martinez AC and Mellado M. The chemokine SDF-1alpha triggers CXCR4 receptor dimerization and activates the JAK/STAT pathway. *FASEB J*. 1999;13:1699-710.
154. Tong H, Rockman HA, Koch WJ, Steenbergen C and Murphy E. G protein-coupled receptor internalization signaling is required for cardioprotection in ischemic preconditioning. *Circ Res*. 2004;94:1133-41.
155. Lin L, Han MM, Wang F, Xu LL, Yu HX and Yang PY. CXCR7 stimulates MAPK signaling to regulate hepatocellular carcinoma progression. *Cell Death Dis*. 2014;5:e1488.
156. Kim KS, Abraham D, Williams B, Violin JD, Mao L and Rockman HA. beta-Arrestin-biased AT1R stimulation promotes cell survival during acute cardiac injury. *Am J Physiol Heart Circ Physiol*. 2012;303:H1001-10.
157. Staat P, Rioufol G, Piot C, Cottin Y, Cung TT, L'Huillier I, Aupetit JF, Bonnefoy E, Finet G, Andre-Fouet X and Ovize M. Postconditioning the human heart. *Circulation*. 2005;112:2143-8.

158. Thibault H, Piot C, Staat P, Bontemps L, Sportouch C, Rioufol G, Cung TT, Bonnefoy E, Angoulvant D, Aupetit JF, Finet G, Andre-Fouet X, Macia JC, Raczka F, Rossi R, Itti R, Kirkorian G, Derumeaux G and Ovize M. Long-term benefit of postconditioning. *Circulation*. 2008;117:1037-44.
159. Lonborg J, Kelbaek H, Vejlstrup N, Jorgensen E, Helqvist S, Saunamaki K, Clemmensen P, Holmvang L, Treiman M, Jensen JS and Engstrom T. Cardioprotective effects of ischemic postconditioning in patients treated with primary percutaneous coronary intervention, evaluated by magnetic resonance. *Circ Cardiovasc Interv*. 2010;3:34-41.
160. Sorensson P, Saleh N, Bouvier F, Bohm F, Settergren M, Caidahl K, Tornvall P, Arheden H, Ryden L and Pernow J. Effect of postconditioning on infarct size in patients with ST elevation myocardial infarction. *Heart*. 2010;96:1710-5.
161. Tarantini G, Favaretto E, Marra MP, Frigo AC, Napodano M, Cacciavillani L, Giovagnoni A, Renda P, De Biasio V, Plebani M, Mion M, Zaninotto M, Isabella G, Bilato C and Iliceto S. Postconditioning during coronary angioplasty in acute myocardial infarction: the POST-AMI trial. *Int J Cardiol*. 2012;162:33-8.
162. Freixa X, Bellera N, Ortiz-Perez JT, Jimenez M, Pare C, Bosch X, De Caralt TM, Betriu A and Masotti M. Ischaemic postconditioning revisited: lack of effects on infarct size following primary percutaneous coronary intervention. *Eur Heart J*. 2012;33:103-12.
163. Przyklenk K, Bauer B, Ovize M, Kloner RA and Whittaker P. Regional ischemic 'preconditioning' protects remote virgin myocardium from subsequent sustained coronary occlusion. *Circulation*. 1993;87:893-9.
164. Mcclanahan TB, Nao BS, Wolke LJ, Martin BJ, Mertz TE and Gallagher KP. Brief Renal Occlusion and Reperfusion Reduces Myocardial Infarct Size in Rabbits. *Faseb Journal*. 1993;7:A118-A118.
165. Birnbaum Y, Hale SL and Kloner RA. Ischemic preconditioning at a distance: reduction of myocardial infarct size by partial reduction of blood supply combined with rapid stimulation of the gastrocnemius muscle in the rabbit. *Circulation*. 1997;96:1641-6.
166. Andreka G, Vertesaljai M, Szantho G, Font G, Piroth Z, Fontos G, Juhasz ED, Szekely L, Szelid Z, Turner MS, Ashrafian H, Frenneaux MP and Andreka P. Remote ischaemic postconditioning protects the heart during acute myocardial infarction in pigs. *Heart*. 2007;93:749-52.
167. Kharbanda RK, Mortensen UM, White PA, Kristiansen SB, Schmidt MR, Hoschtitzky JA, Vogel M, Sorensen K, Redington AN and MacAllister R. Transient limb ischemia induces remote ischemic preconditioning in vivo. *Circulation*. 2002;106:2881-2883.
168. Gunaydin B, Cakici I, Soncul H, Kalaycioglu S, Cevik C, Sancak B, Kanzik I and Karadenizli Y. Does remote organ ischaemia trigger cardiac preconditioning during coronary artery surgery? *Pharmacol Res*. 2000;41:493-6.
169. Hausenloy DJ, Mwamure PK, Venugopal V, Harris J, Barnard M, Grundy E, Ashley E, Vichare S, Di Salvo C, Kolvekar S, Hayward M, Keogh B, MacAllister RJ and Yellon DM. Effect of remote ischaemic preconditioning on myocardial injury in patients undergoing coronary artery bypass graft surgery: a randomised controlled trial. *Lancet*. 2007;370:575-9.

170. Venugopal V, Hausenloy DJ, Ludman A, Di Salvo C, Kolvekar S, Yap J, Lawrence D, Bognolo J and Yellon DM. Remote ischaemic preconditioning reduces myocardial injury in patients undergoing cardiac surgery with cold-blood cardioplegia: a randomised controlled trial. *Heart*. 2009;95:1567-71.
171. Thielmann M, Kottenberg E, Boengler K, Raffelsieper C, Neuhaeuser M, Peters J, Jakob H and Heusch G. Remote ischemic preconditioning reduces myocardial injury after coronary artery bypass surgery with crystalloid cardioplegic arrest. *Basic Res Cardiol*. 2010;105:657-64.
172. Hoole SP, Heck PM, Sharples L, Khan SN, Duehmke R, Densem CG, Clarke SC, Shapiro LM, Schofield PM, O'Sullivan M and Dutka DP. Cardiac Remote Ischemic Preconditioning in Coronary Stenting (CRISP Stent) Study: a prospective, randomized control trial. *Circulation*. 2009;119:820-7.
173. Botker HE, Kharbanda R, Schmidt MR, Bottcher M, Kaltoft AK, Terkelsen CJ, Munk K, Andersen NH, Hansen TM, Trautner S, Lassen JF, Christiansen EH, Krusell LR, Kristensen SD, Thuesen L, Nielsen SS, Rehling M, Sorensen HT, Redington AN and Nielsen TT. Remote ischaemic conditioning before hospital admission, as a complement to angioplasty, and effect on myocardial salvage in patients with acute myocardial infarction: a randomised trial. *Lancet*. 2010;375:727-34.
174. Schmidt MR, Smerup M, Konstantinov IE, Shimizu M, Li J, Cheung M, White PA, Kristiansen SB, Sorensen K, Dzavik V, Redington AN and Kharbanda RK. Intermittent peripheral tissue ischemia during coronary ischemia reduces myocardial infarction through a $K_{ATP}$-dependent mechanism: first demonstration of remote ischemic perconditioning. *Am J Physiol Heart Circ Physiol*. 2007;292:H1883-90.
175. Kerendi F, Kin H, Halkos ME, Jiang R, Zatta AJ, Zhao ZQ, Guyton RA and Vinten-Johansen J. Remote postconditioning. Brief renal ischemia and reperfusion applied before coronary artery reperfusion reduces myocardial infarct size via endogenous activation of adenosine receptors. *Basic Res Cardiol*. 2005;100:404-12.
176. Rentoukas I, Giannopoulos G, Kaoukis A, Kossyvakis C, Raisakis K, Driva M, Panagopoulou V, Tsarouchas K, Vavetsi S, Pyrgakis V and Deftereos S. Cardioprotective role of remote ischemic periconditioning in primary percutaneous coronary intervention: enhancement by opioid action. *JACC Cardiovasc Interv*. 2010;3:49-55.
177. Eitel I, Stiermaier T, Rommel KP, Fuernau G, Sandri M, Mangner N, Linke A, Erbs S, Lurz P, Boudriot E, Mende M, Desch S, Schuler G and Thiele H. Cardioprotection by combined intrahospital remote ischaemic perconditioning and postconditioning in ST-elevation myocardial infarction: the randomized LIPSIA CONDITIONING trial. *Eur Heart J*. 2015;36:3049-57.
178. Hausenloy DJ, Candilio L, Evans R, Ariti C, Jenkins DP, Kolvekar S, Knight R, Kunst G, Laing C, Nicholas J, Pepper J, Robertson S, Xenou M, Clayton T, Yellon DM and Investigators ET. Remote Ischemic Preconditioning and Outcomes of Cardiac Surgery. *N Engl J Med*. 2015;373:1408-17.
179. Meybohm P, Bein B, Brosteanu O, Cremer J, Gruenewald M, Stoppe C, Coburn M, Schaelte G, Boning A, Niemann B, Roesner J, Kletzin F, Strouhal U, Reyher C, Laufenberg-Feldmann R, Ferner M, Brandes IF, Bauer M, Stehr SN, Kortgen A, Wittmann M, Baumgarten G, Meyer-Treschan T, Kienbaum P, Heringlake M, Schon J, Sander M, Treskatsch S, Smul T, Wolwender E, Schilling T, Fuernau G, Hasenclever D,

Zacharowski K and Collaborators RIS. A Multicenter Trial of Remote Ischemic Preconditioning for Heart Surgery. *N Engl J Med*. 2015;373:1397-407.
180. Hausenloy DJ, Kharbanda R, Rahbek Schmidt M, Moller UK, Ravkilde J, Okkels Jensen L, Engstrom T, Garcia Ruiz JM, Radovanovic N, Christensen EF, Sorensen HT, Ramlall M, Bulluck H, Evans R, Nicholas J, Knight R, Clayton T, Yellon DM and Botker HE. Effect of remote ischaemic conditioning on clinical outcomes in patients presenting with an ST-segment elevation myocardial infarction undergoing primary percutaneous coronary intervention. *Eur Heart J*. 2015;36:1846-8.
181. Lim SY, Yellon DM and Hausenloy DJ. The neural and humoral pathways in remote limb ischemic preconditioning. *Basic Res Cardiol*. 2010;105:651-5.
182. Dickson EW, Lorbar M, Porcaro WA, Fenton RA, Reinhardt CP, Gysembergh A and Przyklenk K. Rabbit heart can be "preconditioned" via transfer of coronary effluent. *Am J Physiol*. 1999;277:H2451-7.
183. Leung CH, Wang L, Nielsen JM, Tropak MB, Fu YY, Kato H, Callahan J, Redington AN and Caldarone CA. Remote Cardioprotection by Transfer of Coronary Effluent from Ischemic Preconditioned Rabbit Heart Preserves Mitochondrial Integrity and Function via Adenosine Receptor Activation. *Cardiovascular drugs and therapy / sponsored by the International Society of Cardiovascular Pharmacotherapy*. 2013.
184. Weinbrenner C, Schulze F, Sarvary L and Strasser RH. Remote preconditioning by infrarenal aortic occlusion is operative via delta1-opioid receptors and free radicals in vivo in the rat heart. *Cardiovasc Res*. 2004;61:591-9.
185. Wolfrum S, Schneider K, Heidbreder M, Nienstedt J, Dominiak P and Dendorfer A. Remote preconditioning protects the heart by activating myocardial PKCepsilon-isoform. *Cardiovasc Res*. 2002;55:583-9.
186. Breivik L, Helgeland E, Aarnes EK, Mrdalj J and Jonassen AK. Remote postconditioning by humoral factors in effluent from ischemic preconditioned rat hearts is mediated via PI3K/Akt-dependent cell-survival signaling at reperfusion. *Basic Res Cardiol*. 2011;106:135-45.
187. Cai ZP, Parajuli N, Zheng X and Becker L. Remote ischemic preconditioning confers late protection against myocardial ischemia-reperfusion injury in mice by upregulating interleukin-10. *Basic Res Cardiol*. 2012;107:277.
188. Hausenloy DJ, Iliodromitis EK, Andreadou I, Papalois A, Gritsopoulos G, Anastasiou-Nana M, Kremastinos DT and Yellon DM. Investigating the signal transduction pathways underlying remote ischemic conditioning in the porcine heart. *Cardiovasc Drugs Ther*. 2012;26:87-93.
189. Rassaf T, Totzeck M, Hendgen-Cotta UB, Shiva S, Heusch G and Kelm M. Circulating nitrite contributes to cardioprotection by remote ischemic preconditioning. *Circ Res*. 2014;114:1601-10.
190. Kalakech H, Tamareille S, Pons S, Godin-Ribuot D, Carmeliet P, Furber A, Martin V, Berdeaux A, Ghaleb B and Prunier F. Role of hypoxia inducible factor-1alpha in remote limb ischemic preconditioning. *J Mol Cell Cardiol*. 2013;65:98-104.
191. Cai Z, Luo W, Zhan H and Semenza GL. Hypoxia-inducible factor 1 is required for remote ischemic preconditioning of the heart. *Proc Natl Acad Sci U S A*. 2013;110:17462-7.
192. Contractor H, Stottrup NB, Cunnington C, Manlhiot C, Diesch J, Ormerod JO, Jensen R, Botker HE, Redington A, Schmidt MR, Ashrafian H and Kharbanda RK.

Aldehyde dehydrogenase-2 inhibition blocks remote preconditioning in experimental and human models. *Basic Res Cardiol*. 2013;108:343.
193. Slagsvold KH, Rognmo O, Hoydal M, Wisloff U and Wahba A. Remote ischemic preconditioning preserves mitochondrial function and influences myocardial microRNA expression in atrial myocardium during coronary bypass surgery. *Circ Res*. 2014;114:851-9.
194. Mastitskaya S, Marina N, Gourine A, Gilbey MP, Spyer KM, Teschemacher AG, Kasparov S, Trapp S, Ackland GL and Gourine AV. Cardioprotection evoked by remote ischaemic preconditioning is critically dependent on the activity of vagal pre-ganglionic neurones. *Cardiovasc Res*. 2012;95:487-94.
195. Gourine A and Gourine AV. Neural mechanisms of cardioprotection. *Physiology (Bethesda)*. 2014;29:133-40.
196. Mastitskaya S, Basalay M, Hosford PS, Ramage AG, Gourine A and Gourine AV. Identifying the Source of a Humoral Factor of Remote (Pre)Conditioning Cardioprotection. *PLoS One*. 2016;11:e0150108.
197. Konstantinov IE, Li J, Cheung MM, Shimizu M, Stokoe J, Kharbanda RK and Redington AN. Remote ischemic preconditioning of the recipient reduces myocardial ischemia-reperfusion injury of the denervated donor heart via a Katp channel-dependent mechanism. *Transplantation*. 2005;79:1691-5.
198. Valenzuela-Fernandez A, Planchenault T, Baleux F, Staropoli I, Le-Barillec K, Leduc D, Delaunay T, Lazarini F, Virelizier JL, Chignard M, Pidard D and Arenzana-Seisdedos F. Leukocyte elastase negatively regulates Stromal cell-derived factor-1 (SDF-1)/CXCR4 binding and functions by amino-terminal processing of SDF-1 and CXCR4. *J Biol Chem*. 2002;277:15677-89.
199. Ravassa S, Zudaire A and Diez J. GLP-1 and cardioprotection: from bench to bedside. *Cardiovasc Res*. 2012;94:316-23.
200. Zaruba MM, Theiss HD, Vallaster M, Mehl U, Brunner S, David R, Fischer R, Krieg L, Hirsch E, Huber B, Nathan P, Israel L, Imhof A, Herbach N, Assmann G, Wanke R, Mueller-Hoecker J, Steinbeck G and Franz WM. Synergy between CD26/DPP-IV inhibition and G-CSF improves cardiac function after acute myocardial infarction. *Cell Stem Cell*. 2009;4:313-23.
201. Crump MP, Gong JH, Loetscher P, Rajarathnam K, Amara A, Arenzana-Seisdedos F, Virelizier JL, Baggiolini M, Sykes BD and Clark-Lewis I. Solution structure and basis for functional activity of stromal cell-derived factor-1; dissociation of CXCR4 activation from binding and inhibition of HIV-1. *EMBO J*. 1997;16:6996-7007.
202. Flecknell P. Laboratory Animal Anaesthesia, 3rd Edition. *Laboratory Animal Anaesthesia, 3rd Edition*. 2009:1-300.
203. Liu YH, Yang XP, Nass O, Sabbah HN, Peterson E and Carretero OA. Chronic heart failure induced by coronary artery ligation in Lewis inbred rats. *Am J Physiol*. 1997;272:H722-7.
204. Mortensen RM. Double knockouts. Production of mutant cell lines in cardiovascular research. *Hypertension*. 1993;22:646-51.
205. Alberts B. *Molecular biology of the cell.* 4th ed. New York: Garland Science; 2002.
206. Nie Y, Waite J, Brewer F, Sunshine MJ, Littman DR and Zou YR. The role of CXCR4 in maintaining peripheral B cell compartments and humoral immunity. *J Exp Med*. 2004;200:1145-56.

207. Agarwal U, Ghalayini W, Dong F, Weber K, Zou YR, Rabbany SY, Rafii S and Penn MS. Role of cardiac myocyte CXCR4 expression in development and left ventricular remodeling after acute myocardial infarction. *Circ Res*. 2010;107:667-76.
208. Agah R, Frenkel PA, French BA, Michael LH, Overbeek PA and Schneider MD. Gene recombination in postmitotic cells. Targeted expression of Cre recombinase provokes cardiac-restricted, site-specific rearrangement in adult ventricular muscle in vivo. *The Journal of clinical investigation*. 1997;100:169-79.
209. Sohal DS, Nghiem M, Crackower MA, Witt SA, Kimball TR, Tymitz KM, Penninger JM and Molkentin JD. Temporally regulated and tissue-specific gene manipulations in the adult and embryonic heart using a tamoxifen-inducible Cre protein. *Circ Res*. 2001;89:20-5.
210. Metzger D, Clifford J, Chiba H and Chambon P. Conditional Site-Specific Recombination in Mammalian-Cells Using a Ligand-Dependent Chimeric Cre Recombinase. *Proceedings of the National Academy of Sciences of the United States of America*. 1995;92:6991-6995.
211. Davis J, Maillet M, Miano JM and Molkentin JD. Lost in transgenesis: a user's guide for genetically manipulating the mouse in cardiac research. *Circ Res*. 2012;111:761-77.
212. Korbie DJ and Mattick JS. Touchdown PCR for increased specificity and sensitivity in PCR amplification. *Nat Protoc*. 2008;3:1452-6.
213. Andersson KB, Winer LH, Mork HK, Molkentin JD and Jaisser F. Tamoxifen administration routes and dosage for inducible Cre-mediated gene disruption in mouse hearts. *Transgenic Res*. 2010;19:715-25.
214. Champy MF, Selloum M, Zeitler V, Caradec C, Jung B, Rousseau S, Pouilly L, Sorg T and Auwerx J. Genetic background determines metabolic phenotypes in the mouse. *Mamm Genome*. 2008;19:318-31.
215. Flecknell PA. *Laboratory animal anaesthesia : an introduction for research workers and technicians*. London ; San Diego: Academic Press; 1987.
216. Fisher SG and Marber MS. An in vivo model of ischaemia-reperfusion injury and ischaemic preconditioning in the mouse heart. *J Pharmacol Toxicol Methods*. 2002;48:161-9.
217. Yellon DM and Downey JM. Preconditioning the myocardium: from cellular physiology to clinical cardiology. *Physiol Rev*. 2003;83:1113-51.
218. Lim SY, Davidson SM, Hausenloy DJ and Yellon DM. Preconditioning and postconditioning: the essential role of the mitochondrial permeability transition pore. *Cardiovasc Res*. 2007;75:530-5.
219. Speechly-Dick ME, Mocanu MM and Yellon DM. Protein kinase C. Its role in ischemic preconditioning in the rat. *Circ Res*. 1994;75:586-90.
220. Flatt PR, Bailey CJ and Green BD. Dipeptidyl peptidase IV (DPP IV) and related molecules in type 2 diabetes. *Frontiers in Bioscience*. 2008;13:3648-3660.
221. Dwenger A. Radioimmunoassay: an overview. *J Clin Chem Clin Biochem*. 1984;22:883-94.
222. Fishbein MC, Meerbaum S, Rit J, Lando U, Kanmatsuse K, Mercier JC, Corday E and Ganz W. Early phase acute myocardial infarct size quantification: validation of the triphenyl tetrazolium chloride tissue enzyme staining technique. *Am Heart J*. 1981;101:593-600.

223. Gao XM, Dart AM, Dewar E, Jennings G and Du XJ. Serial echocardiographic assessment of left ventricular dimensions and function after myocardial infarction in mice. *Cardiovasc Res*. 2000;45:330-8.
224. Pollick C, Hale SL and Kloner RA. Echocardiographic and cardiac Doppler assessment of mice. *J Am Soc Echocardiogr*. 1995;8:602-10.
225. Tournoux F, Petersen B, Thibault H, Zou L, Raher MJ, Kurtz B, Halpern EF, Chaput M, Chao W, Picard MH and Scherrer-Crosbie M. Validation of noninvasive measurements of cardiac output in mice using echocardiography. *J Am Soc Echocardiogr*. 2011;24:465-70.
226. Carerj S, Micari A, Trono A, Giordano G, Cerrito M, Zito C, Luzza F, Coglitore S, Arrigo F and Oreto G. Anatomical M-mode: an old-new technique. *Echocardiography*. 2003;20:357-61.
227. Dyson A, Rudiger A and Singer M. Temporal changes in tissue cardiorespiratory function during faecal peritonitis. *Intensive Care Med*. 2011;37:1192-200.
228. Hartley CJ, Michael LH and Entman ML. Noninvasive measurement of ascending aortic blood velocity in mice. *Am J Physiol*. 1995;268:H499-505.
229. Hall AR, Burke N, Dongworth RK, Kalkhoran SB, Dyson A, Vicencio JM, Dorn Ii GW, Yellon DM and Hausenloy DJ. Hearts deficient in both Mfn1 and Mfn2 are protected against acute myocardial infarction. *Cell Death Dis*. 2016;7:e2238.
230. Taylor S, Wakem M, Dijkman G, Alsarraj M and Nguyen M. A practical approach to RT-qPCR-Publishing data that conform to the MIQE guidelines. *Methods*. 2010;50:S1-5.
231. Aboumrad E, Madec AM and Thivolet C. The CXCR4/CXCL12 (SDF-1) signalling pathway protects non-obese diabetic mouse from autoimmune diabetes. *Clin Exp Immunol*. 2007;148:432-9.
232. Higuchi R, Fockler C, Dollinger G and Watson R. Kinetic PCR analysis: real-time monitoring of DNA amplification reactions. *Biotechnology (N Y)*. 1993;11:1026-30.
233. Livak KJ and Schmittgen TD. Analysis of relative gene expression data using real-time quantitative PCR and the 2(-Delta Delta C(T)) Method. *Methods*. 2001;25:402-8.
234. Alugupalli KR, Michelson AD, Barnard MR and Leong JM. Serial determinations of platelet counts in mice by flow cytometry. *Thromb Haemost*. 2001;86:668-71.
235. Inc. GS. Statistics Guide. 2007;2016.
236. Pickard JM, Botker HE, Crimi G, Davidson B, Davidson SM, Dutka D, Ferdinandy P, Ganske R, Garcia-Dorado D, Giricz Z, Gourine AV, Heusch G, Kharbanda R, Kleinbongard P, MacAllister R, McIntyre C, Meybohm P, Prunier F, Redington A, Robertson NJ, Suleiman MS, Vanezis A, Walsh S, Yellon DM and Hausenloy DJ. Remote ischemic conditioning: from experimental observation to clinical application: report from the 8th Biennial Hatter Cardiovascular Institute Workshop. *Basic Res Cardiol*. 2015;110:453.
237. Lecour S, Botker HE, Condorelli G, Davidson SM, Garcia-Dorado D, Engel FB, Ferdinandy P, Heusch G, Madonna R, Ovize M, Ruiz-Meana M, Schulz R, Sluijter JP, Van Laake LW, Yellon DM and Hausenloy DJ. ESC working group cellular biology of the heart: position paper: improving the preclinical assessment of novel cardioprotective therapies. *Cardiovasc Res*. 2014;104:399-411.

238. Przyklenk K. Ischaemic conditioning: pitfalls on the path to clinical translation. *Br J Pharmacol*. 2015;172:1961-73.
239. Hausenloy DJ, Erik Botker H, Condorelli G, Ferdinandy P, Garcia-Dorado D, Heusch G, Lecour S, van Laake LW, Madonna R, Ruiz-Meana M, Schulz R, Sluijter JP, Yellon DM and Ovize M. Translating cardioprotection for patient benefit: position paper from the Working Group of Cellular Biology of the Heart of the European Society of Cardiology. *Cardiovasc Res*. 2013;98:7-27.
240. Whittington HJ, Harding I, Stephenson CI, Bell R, Hausenloy DJ, Mocanu MM and Yellon DM. Cardioprotection in the aging, diabetic heart: the loss of protective Akt signalling. *Cardiovasc Res*. 2013;99:694-704.
241. Kato R and Foex P. Myocardial protection by anesthetic agents against ischemia-reperfusion injury: an update for anesthesiologists. *Can J Anaesth*. 2002;49:777-91.
242. Black SC, Gralinski MR, Friedrichs GS, Kilgore KS, Driscoll EM and Lucchesi BR. Cardioprotective effects of heparin or N-acetylheparin in an in vivo model of myocardial ischaemic and reperfusion injury. *Cardiovasc Res*. 1995;29:629-36.
243. Gralinski MR, Driscoll EM, Friedrichs GS, DeNardis MR and Lucchesi BR. Reduction of Myocardial Necrosis After Glycosaminoglycan Administration: Effects of a Single Intravenous Administration of Heparin or N-Acetylheparin 2 Hours Before Regional Ischemia and Reperfusion. *J Cardiovasc Pharmacol Ther*. 1996;1:219-228.
244. Barry WH and Kennedy TP. Heparins with reduced anti-coagulant activity reduce myocardial reperfusion injury. *Recent Pat Cardiovasc Drug Discov*. 2011;6:148-57.
245. Kouretas PC, Kim YD, Cahill PA, Myers AK, To LN, Wang YN, Sitzmann JV and Hannan RL. Nonanticoagulant heparin prevents coronary endothelial dysfunction after brief ischemia-reperfusion injury in the dog. *Circulation*. 1999;99:1062-8.
246. Kouretas PC, Myers AK, Kim YD, Cahill PA, Myers JL, Wang YN, Sitzmann JV, Wallace RB and Hannan RL. Heparin and nonanticoagulant heparin preserve regional myocardial contractility after ischemia-reperfusion injury: role of nitric oxide. *J Thorac Cardiovasc Surg*. 1998;115:440-8; discussion 448-9.
247. Zweier JL, Chae JK and Talukder MAH. Sodium Nitrite Administered Immediately before Reperfusion Reduces in vivo Myocardial Infarction and Improves Postischemic Cardiac Function: Significance of Critical Dose Response and Safety Margin of Nitrite in Cardioprotection. *Faseb Journal*. 2012;26.
248. Kottenberg E, Musiolik J, Thielmann M, Jakob H, Peters J and Heusch G. Interference of propofol with signal transducer and activator of transcription 5 activation and cardioprotection by remote ischemic preconditioning during coronary artery bypass grafting. *J Thorac Cardiovasc Surg*. 2014;147:376-82.
249. Garratt KN, Whittaker P and Przyklenk K. Remote Ischemic Conditioning and the Long Road to Clinical Translation: Lessons Learned From ERICCA and RIPHeart. *Circ Res*. 2016;118:1052-4.
250. van Hout GP, Jansen Of Lorkeers SJ, Wever KE, Sena ES, Kouwenberg LH, van Solinge WW, Macleod MR, Doevendans PA, Pasterkamp G, Chamuleau SA and Hoefer IE. Translational failure of anti-inflammatory compounds for myocardial infarction: a meta-analysis of large animal models. *Cardiovasc Res*. 2016;109:240-8.
251. Liberati A, Altman DG, Tetzlaff J, Mulrow C, Gotzsche PC, Ioannidis JP, Clarke M, Devereaux PJ, Kleijnen J and Moher D. The PRISMA statement for reporting

systematic reviews and meta-analyses of studies that evaluate healthcare interventions: explanation and elaboration. *BMJ*. 2009;339:b2700.
252. Flores-Mir C, Major MP and Major PW. Search and selection methodology of systematic reviews in orthodontics (2000-2004). *Am J Orthod Dentofacial Orthop*. 2006;130:214-7.
253. Major MP, Major PW and Flores-Mir C. An evaluation of search and selection methods used in dental systematic reviews published in English. *J Am Dent Assoc*. 2006;137:1252-7.
254. Major MP, Major PW and Flores-Mir C. Benchmarking of reported search and selection methods of systematic reviews by dental speciality. *Evid Based Dent*. 2007;8:66-70.
255. O'Connor D, Green S and Higgins JPT. Chapter 5: Defining the review question and developing criteria for including studies. *Cochrane handbook for systematic reviews of interventions version 510*. 2011.
256. Bell RM, Mocanu MM and Yellon DM. Retrograde heart perfusion: the Langendorff technique of isolated heart perfusion. *J Mol Cell Cardiol*. 2011;50:940-50.
257. Rochitte CE and Azevedo CF. The myocardial area at risk. *Heart*. 2012;98:348-50.
258. Ytrehus K, Liu Y, Tsuchida A, Miura T, Liu GS, Yang XM, Herbert D, Cohen MV and Downey JM. Rat and rabbit heart infarction: effects of anesthesia, perfusate, risk zone, and method of infarct sizing. *Am J Physiol*. 1994;267:H2383-90.
259. Marber MS, Latchman DS, Walker JM and Yellon DM. Cardiac stress protein elevation 24 hours after brief ischemia or heat stress is associated with resistance to myocardial infarction. *Circulation*. 1993;88:1264-72.
260. Kuzuya T, Hoshida S, Yamashita N, Fuji H, Oe H, Hori M, Kamada T and Tada M. Delayed effects of sublethal ischemia on the acquisition of tolerance to ischemia. *Circ Res*. 1993;72:1293-9.
261. Szekeres L, Papp JG, Szilvassy Z, Udvary E and Vegh A. Moderate stress by cardiac pacing may induce both short term and long term cardioprotection. *Cardiovasc Res*. 1993;27:593-6.
262. Consumers and Communication Group resources for authors. 2013;2015.
263. McGrath JC, Drummond GB, McLachlan EM, Kilkenny C and Wainwright CL. Guidelines for reporting experiments involving animals: the ARRIVE guidelines. *Br J Pharmacol*. 2010;160:1573-6.
264. Kilkenny C, Browne W, Cuthill IC, Emerson M, Altman DG and Group NCRRGW. Animal research: reporting in vivo experiments: the ARRIVE guidelines. *Br J Pharmacol*. 2010;160:1577-9.
265. Macleod MR, O'Collins T, Howells DW and Donnan GA. Pooling of animal experimental data reveals influence of study design and publication bias. *Stroke*. 2004;35:1203-8.
266. Alburquerque-Bejar JJ, Barba I, Inserte J, Miro-Casas E, Ruiz-Meana M, Poncelas M, Vilardosa U, Valls-Lacalle L, Rodriguez-Sinovas A and Garcia-Dorado D. Combination therapy with remote ischaemic conditioning and insulin or exenatide enhances infarct size limitation in pigs. *Cardiovasc Res*. 2015;107:246-54.

267. Basalay M, Barsukevich V, Mrochek A, Gourine AV and Gourine A. Right vs left vagus and cardioprotection conferred by remote ischaemic pre- and perconditioning. *European Heart Journal*. 2013;34:666-667.
268. Basalay M, Barsukevich V, Mastitskaya S, Mrochek A, Pernow J, Sjoquist PO, Ackland GL, Gourine AV and Gourine A. Remote ischaemic pre- and delayed postconditioning - similar degree of cardioprotection but distinct mechanisms. *Exp Physiol*. 2012;97:908-17.
269. Cellier L, Tamareille S, Kalakech H, Guillou S, Lenaers G, Prunier F and Mirebeau-Prunier D. Remote Ischemic Conditioning Influences Mitochondrial Dynamics. *Shock*. 2016;45:192-7.
270. Grall S, Prunier-Mirebeau D, Tamareille S, Mateus V, Lamon D, Furber A and Prunier F. Endoplasmic reticulum stress pathway involvement in local and remote myocardial ischemic conditioning. *Shock*. 2013;39:433-9.
271. Heinen NM, Putz VE, Gorgens JI, Huhn R, Gruber Y, Barthuber C, Preckel B, Pannen BH and Bauer I. Cardioprotection by remote ischemic preconditioning exhibits a signaling pattern different from local ischemic preconditioning. *Shock*. 2011;36:45-53.
272. Hibert P, Prunier-Mirebeau D, Beseme O, Chwastyniak M, Tamareille S, Lamon D, Furber A, Pinet F and Prunier F. Apolipoprotein a-I is a potential mediator of remote ischemic preconditioning. *PLoS One*. 2013;8:e77211.
273. Jeanneteau J, Hibert P, Martinez MC, Tual-Chalot S, Tamareille S, Furber A, Andriantsitohaina R and Prunier F. Microparticle release in remote ischemic conditioning mechanism. *Am J Physiol Heart Circ Physiol*. 2012;303:H871-7.
274. Kalakech H, Hibert P, Prunier-Mirebeau D, Tamareille S, Letournel F, Macchi L, Pinet F, Furber A and Prunier F. RISK and SAFE signaling pathway involvement in apolipoprotein A-I-induced cardioprotection. *PLoS One*. 2014;9:e107950.
275. Kiss A, Tratsiakovich Y, Gonon AT, Fedotovskaya O, Lanner JT, Andersson DC, Yang J and Pernow J. The role of arginase and rho kinase in cardioprotection from remote ischemic perconditioning in non-diabetic and diabetic rat in vivo. *PLoS One*. 2014;9:e104731.
276. Li CM, Zhang XH, Ma XJ and Luo M. Limb ischemic postconditioning protects myocardium from ischemia-reperfusion injury. *Scand Cardiovasc J*. 2006;40:312-7.
277. Lu Y, Dong CS, Yu JM and Li H. Morphine reduces the threshold of remote ischemic preconditioning against myocardial ischemia and reperfusion injury in rats: the role of opioid receptors. *J Cardiothorac Vasc Anesth*. 2012;26:403-6.
278. Gourine A, Gourine A, Mastitskaya S and Ackland G. "Remote preconditioning reflex" - a neural pathway of cardioprotection during myocardial ischaemia and reperfusion induced by remote ischaemic preconditioning. *European Heart Journal*. 2010;31:319-319.
279. Sachdeva J, Dai W, Gerczuk PZ and Kloner RA. Combined remote perconditioning and postconditioning failed to attenuate infarct size and contractile dysfunction in a rat model of coronary artery occlusion. *J Cardiovasc Pharmacol Ther*. 2014;19:567-73.
280. Schmidt MR, Stottrup NB, Contractor H, Hyldebrandt JA, Johannsen M, Pedersen CM, Birkler R, Ashrafian H, Sorensen KE, Kharbanda RK, Redington AN and Botker HE. Remote ischemic preconditioning with--but not without--metabolic

support protects the neonatal porcine heart against ischemia-reperfusion injury. *Int J Cardiol*. 2014;170:388-93.
281. Shahid M, Tauseef M, Sharma KK and Fahim M. Brief femoral artery ischaemia provides protection against myocardial ischaemia-reperfusion injury in rats: the possible mechanisms. *Exp Physiol*. 2008;93:954-68.
282. Wei M, Xin P, Li S, Tao J, Li Y, Li J, Liu M, Li J, Zhu W and Redington AN. Repeated remote ischemic postconditioning protects against adverse left ventricular remodeling and improves survival in a rat model of myocardial infarction. *Circ Res*. 2011;108:1220-5.
283. Weinbrenner C, Nelles M, Herzog N, Sarvary L and Strasser RH. Remote preconditioning by infrarenal occlusion of the aorta protects the heart from infarction: a newly identified non-neuronal but PKC-dependent pathway. *Cardiovasc Res*. 2002;55:590-601.
284. Wong GT, Lu Y, Mei B, Xia Z and Irwin MG. Cardioprotection from remote preconditioning involves spinal opioid receptor activation. *Life Sci*. 2012;91:860-5.
285. Xin P, Zhu W, Li J, Ma S, Wang L, Liu M, Wei M and Redington AN. Combined local ischemic postconditioning and remote perconditioning recapitulate cardioprotective effects of local ischemic preconditioning. *Am J Physiol Heart Circ Physiol*. 2010;298:H1819-31.
286. Xu YC, Li RP, Xue FS, Cui XL, Wang SY, Liu GP, Yang GZ, Sun C and Liao X. kappa-Opioid receptors are involved in enhanced cardioprotection by combined fentanyl and limb remote ischemic postconditioning. *J Anesth*. 2015;29:535-43.
287. Yu Y, Jia XJ, Zong QF, Zhang GJ, Ye HW, Hu J, Gao Q and Guan SD. Remote ischemic postconditioning protects the heart by upregulating ALDH2 expression levels through the PI3K/Akt signaling pathway. *Mol Med Rep*. 2014;10:536-42.
288. Zhang JQ, Wang Q, Xue FS, Li RP, Cheng Y, Cui XL, Liao X and Meng FM. Ischemic preconditioning produces more powerful anti-inflammatory and cardioprotective effects than limb remote ischemic postconditioning in rats with myocardial ischemia-reperfusion injury. *Chin Med J (Engl)*. 2013;126:3949-55.
289. Zhang SZ, Wang NF, Xu J, Gao Q, Lin GH, Bruce IC and Xia Q. Kappa-opioid receptors mediate cardioprotection by remote preconditioning. *Anesthesiology*. 2006;105:550-6.
290. Zhu SB, Liu Y, Zhu Y, Yin GL, Wang RP, Zhang Y, Zhu J and Jiang W. Remote preconditioning, perconditioning, and postconditioning: a comparative study of their cardio-protective properties in rat models. *Clinics (Sao Paulo)*. 2013;68:263-8.
291. Hood WB, Jr., McCarthy B and Lown B. Myocardial infarction following coronary ligation in dogs. Hemodynamic effects of isoproterenol and acetylstrophanthidin. *Circ Res*. 1967;21:191-9.
292. Klocke R, Tian W, Kuhlmann MT and Nikol S. Surgical animal models of heart failure related to coronary heart disease. *Cardiovasc Res*. 2007;74:29-38.
293. Hodgin JB and Maeda N. Minireview: estrogen and mouse models of atherosclerosis. *Endocrinology*. 2002;143:4495-501.
294. Murphy E and Steenbergen C. Gender-based differences in mechanisms of protection in myocardial ischemia-reperfusion injury. *Cardiovasc Res*. 2007;75:478-86.
295. Black SC and Rodger IW. Methods for studying experimental myocardial ischemic and reperfusion injury. *J Pharmacol Toxicol Methods*. 1996;35:179-90.

296. Redfors B, Shao Y and Omerovic E. Influence of anesthetic agent, depth of anesthesia and body temperature on cardiovascular functional parameters in the rat. *Lab Anim*. 2014;48:6-14.
297. Kottenberg E, Thielmann M, Bergmann L, Heine T, Jakob H, Heusch G and Peters J. Protection by remote ischemic preconditioning during coronary artery bypass graft surgery with isoflurane but not propofol - a clinical trial. *Acta Anaesthesiol Scand*. 2012;56:30-8.
298. Heusch G and Gersh BJ. ERICCA and RIPHeart: two nails in the coffin for cardioprotection by remote ischemic conditioning? Probably not! *Eur Heart J*. 2016;37:200-2.
299. Reimer KA, Lowe JE, Rasmussen MM and Jennings RB. The wavefront phenomenon of ischemic cell death. 1. Myocardial infarct size vs duration of coronary occlusion in dogs. *Circulation*. 1977;56:786-94.
300. Tsutsumi YM, Patel HH, Lai NC, Takahashi T, Head BP and Roth DM. Isoflurane produces sustained cardiac protection after ischemia-reperfusion injury in mice. *Anesthesiology*. 2006;104:495-502.
301. Kleinbongard P, Neuhauser M, Thielmann M, Kottenberg E, Peters J, Jakob H and Heusch G. Confounders of Cardioprotection by Remote Ischemic Preconditioning in Patients Undergoing Coronary Artery Bypass Grafting. *Cardiology*. 2016;133:128-33.
302. Johnsen J, Pryds K, Salman R, Lofgren B, Kristiansen SB and Botker HE. The remote ischemic preconditioning algorithm: effect of number of cycles, cycle duration and effector organ mass on efficacy of protection. *Basic Res Cardiol*. 2016;111:10.
303. van der Worp HB and Macleod MR. Preclinical studies of human disease: time to take methodological quality seriously. *J Mol Cell Cardiol*. 2011;51:449-50.
304. Sena ES, van der Worp HB, Bath PM, Howells DW and Macleod MR. Publication bias in reports of animal stroke studies leads to major overstatement of efficacy. *PLoS Biol*. 2010;8:e1000344.
305. van der Worp HB, Howells DW, Sena ES, Porritt MJ, Rewell S, O'Collins V and Macleod MR. Can animal models of disease reliably inform human studies? *PLoS Med*. 2010;7:e1000245.
306. Vesterinen HM, Sena ES, Egan KJ, Hirst TC, Churolov L, Currie GL, Antonic A, Howells DW and Macleod MR. Meta-analysis of data from animal studies: a practical guide. *J Neurosci Methods*. 2014;221:92-102.
307. Hooijmans CR, IntHout J, Ritskes-Hoitinga M and Rovers MM. Meta-analyses of animal studies: an introduction of a valuable instrument to further improve healthcare. *ILAR J*. 2014;55:418-26.
308. Holm S. A Simple Sequentially Rejective Multiple Test Procedure. *Scandinavian Journal of Statistics*. 1979;6:65-70.
309. Samanta A and Dawn B. Remote Ischemic Preconditioning for Cardiac Surgery: Reflections on Evidence of Efficacy. *Circ Res*. 2016;118:1055-8.
310. Zaugg M and Lucchinetti E. Remote Ischemic Preconditioning in Cardiac Surgery--Ineffective and Risky? *N Engl J Med*. 2015;373:1470-2.
311. Mewton N, Bergerot C and Ovize M. Cyclosporine before PCI in Acute Myocardial Infarction. *N Engl J Med*. 2016;374:90.

312. Stub D, Smith K, Bernard S, Nehme Z, Stephenson M, Bray JE, Cameron P, Barger B, Ellims AH, Taylor AJ, Meredith IT and Kaye DM. Air Versus Oxygen in ST-Segment-Elevation Myocardial Infarction. *Circulation*. 2015;131:2143-50.
313. Yellon DM and Baxter GF. A "second window of protection" or delayed preconditioning phenomenon: future horizons for myocardial protection? *J Mol Cell Cardiol*. 1995;27:1023-34.
314. Society BCI. BCIS Audit Returns Adult Interventional Procedures. 2014;2016.
315. Chen J, Hsieh AF, Dharmarajan K, Masoudi FA and Krumholz HM. National trends in heart failure hospitalization after acute myocardial infarction for Medicare beneficiaries: 1998-2010. *Circulation*. 2013;128:2577-84.
316. Sobel BE, Bresnahan GF, Shell WE and Yoder RD. Estimation of infarct size in man and its relation to prognosis. *Circulation*. 1972;46:640-8.
317. Graham MM, Faris PD, Ghali WA, Galbraith PD, Norris CM, Badry JT, Mitchell LB, Curtis MJ, Knudtson ML and Investigators A. Validation of three myocardial jeopardy scores in a population-based cardiac catheterization cohort. *Am Heart J*. 2001;142:254-61.
318. Bulluck H, White SK, Frohlich GM, Casson SG, O'Meara C, Newton A, Nicholas J, Weale P, Wan SM, Sirker A, Moon JC, Yellon DM, Groves A, Menezes L and Hausenloy DJ. Quantifying the Area at Risk in Reperfused ST-Segment-Elevation Myocardial Infarction Patients Using Hybrid Cardiac Positron Emission Tomography-Magnetic Resonance Imaging. *Circ Cardiovasc Imaging*. 2016;9:e003900.
319. Price AN, Cheung KK, Lim SY, Yellon DM, Hausenloy DJ and Lythgoe MF. Rapid assessment of myocardial infarct size in rodents using multi-slice inversion recovery late gadolinium enhancement CMR at 9.4T. *J Cardiovasc Magn Reson*. 2011;13:44.
320. Hood WB, Jr., McCarthy B and Lown B. Myocardial infarction following coronary ligation in dogs. Hemodynamic effects of isoproterenol and acetylstrophanthidin. *Circulation research*. 1967;21:191-9.
321. Pfeffer MA, Pfeffer JM, Fishbein MC, Fletcher PJ, Spadaro J, Kloner RA and Braunwald E. Myocardial infarct size and ventricular function in rats. *Circ Res*. 1979;44:503-12.
322. Liu Y and Downey JM. Ischemic preconditioning protects against infarction in rat heart. *Am J Physiol*. 1992;263:H1107-12.
323. Linden M, Sirsjo A, Lindbom L, Nilsson G and Gidlof A. Laser-Doppler perfusion imaging of microvascular blood flow in rabbit tenuissimus muscle. *Am J Physiol*. 1995;269:H1496-500.
324. Bonheur JA, Albadawi H, Patton GM and Watkins MT. A noninvasive murine model of hind limb ischemia-reperfusion injury. *J Surg Res*. 2004;116:55-63.
325. Dyson A, Stidwill R, Taylor V and Singer M. Tissue oxygen monitoring in rodent models of shock. *Am J Physiol Heart Circ Physiol*. 2007;293:H526-33.
326. Durgan DJ, Pulinilkunnil T, Villegas-Montoya C, Garvey ME, Frangogiannis NG, Michael LH, Chow CW, Dyck JR and Young ME. Short communication: ischemia/reperfusion tolerance is time-of-day-dependent: mediation by the cardiomyocyte circadian clock. *Circ Res*. 2010;106:546-50.
327. Mendez-Ferrer S, Lucas D, Battista M and Frenette PS. Haematopoietic stem cell release is regulated by circadian oscillations. *Nature*. 2008;452:442-7.

328. Michael LH, Entman ML, Hartley CJ, Youker KA, Zhu J, Hall SR, Hawkins HK, Berens K and Ballantyne CM. Myocardial ischemia and reperfusion: a murine model. *Am J Physiol*. 1995;269:H2147-54.
329. Guo Y, Wu WJ, Qiu Y, Tang XL, Yang Z and Bolli R. Demonstration of an early and a late phase of ischemic preconditioning in mice. *Am J Physiol*. 1998;275:H1375-87.
330. Dongworth RK, Mukherjee UA, Hall AR, Astin R, Ong SB, Yao Z, Dyson A, Szabadkai G, Davidson SM, Yellon DM and Hausenloy DJ. DJ-1 protects against cell death following acute cardiac ischemia-reperfusion injury. *Cell Death Dis*. 2014;5:e1082.
331. Hamamoto H, Sakamoto H, Leshnower BG, Parish LM, Kanemoto S, Hinmon R, Plappert T, Miyamoto S, St John-Sutton MG, Gorman JH, 3rd and Gorman RC. Very mild hypothermia during ischemia and reperfusion improves postinfarction ventricular remodeling. *Ann Thorac Surg*. 2009;87:172-7.
332. Dae MW, Gao DW, Sessler DI, Chair K and Stillson CA. Effect of endovascular cooling on myocardial temperature, infarct size, and cardiac output in human-sized pigs. *Am J Physiol Heart Circ Physiol*. 2002;282:H1584-91.
333. Kanemoto S, Matsubara M, Noma M, Leshnower BG, Parish LM, Jackson BM, Hinmon R, Hamamoto H, Gorman JH, 3rd and Gorman RC. Mild hypothermia to limit myocardial ischemia-reperfusion injury: importance of timing. *Ann Thorac Surg*. 2009;87:157-63.
334. Miki T, Liu GS, Cohen MV and Downey JM. Mild hypothermia reduces infarct size in the beating rabbit heart: a practical intervention for acute myocardial infarction? *Basic Res Cardiol*. 1998;93:372-83.
335. Otake H, Shite J, Paredes OL, Shinke T, Yoshikawa R, Tanino Y, Watanabe S, Ozawa T, Matsumoto D, Ogasawara D and Yokoyama M. Catheter-based transcoronary myocardial hypothermia attenuates arrhythmia and myocardial necrosis in pigs with acute myocardial infarction. *J Am Coll Cardiol*. 2007;49:250-60.
336. Hale SL, Dave RH and Kloner RA. Regional hypothermia reduces myocardial necrosis even when instituted after the onset of ischemia. *Basic Res Cardiol*. 1997;92:351-7.
337. Hale SL and Kloner RA. Myocardial temperature in acute myocardial infarction: protection with mild regional hypothermia. *Am J Physiol*. 1997;273:H220-7.
338. Chien GL, Wolff RA, Davis RF and van Winkle DM. "Normothermic range" temperature affects myocardial infarct size. *Cardiovasc Res*. 1994;28:1014-7.
339. Hale SL, Dae MW and Kloner RA. Hypothermia during reperfusion limits 'no-reflow' injury in a rabbit model of acute myocardial infarction. *Cardiovasc Res*. 2003;59:715-22.
340. Ning XH, Chi EY, Buroker NE, Chen SH, Xu CS, Tien YT, Hyyti OM, Ge M and Portman MA. Moderate hypothermia (30 degrees C) maintains myocardial integrity and modifies response of cell survival proteins after reperfusion. *Am J Physiol Heart Circ Physiol*. 2007;293:H2119-28.
341. Shao ZH, Chang WT, Chan KC, Wojcik KR, Hsu CW, Li CQ, Li J, Anderson T, Qin Y, Becker LB, Hamann KJ and Vanden Hoek TL. Hypothermia-induced cardioprotection using extended ischemia and early reperfusion cooling. *Am J Physiol Heart Circ Physiol*. 2007;292:H1995-2003.

342. van den Doel MA, Gho BC, Duval SY, Schoemaker RG, Duncker DJ and Verdouw PD. Hypothermia extends the cardioprotection by ischaemic preconditioning to coronary artery occlusions of longer duration. *Cardiovasc Res*. 1998;37:76-81.
343. Villablanca PA, Rao G, Briceno DF, Lombardo M, Ramakrishna H, Bortnick A, Garcia M, Menegus M, Sims D, Makkiya M and Mookadam F. Therapeutic hypothermia in ST elevation myocardial infarction: a systematic review and meta-analysis of randomised control trials. *Heart*. 2016;102:712-9.
344. Christia P, Bujak M, Gonzalez-Quesada C, Chen W, Dobaczewski M, Reddy A and Frangogiannis NG. Systematic characterization of myocardial inflammation, repair, and remodeling in a mouse model of reperfused myocardial infarction. *J Histochem Cytochem*. 2013;61:555-70.
345. Lujan HL, Janbaih H, Feng HZ, Jin JP and DiCarlo SE. Myocardial ischemia, reperfusion, and infarction in chronically instrumented, intact, conscious, and unrestrained mice. *Am J Physiol Regul Integr Comp Physiol*. 2012;302:R1384-400.
346. Clarke SJ, McCormick LM and Dutka DP. Optimising cardioprotection during myocardial ischaemia: targeting potential intracellular pathways with glucagon-like peptide-1. *Cardiovasc Diabetol*. 2014;13:12.
347. Kalatskaya I, Berchiche YA, Gravel S, Limberg BJ, Rosenbaum JS and Heveker N. AMD3100 is a CXCR7 ligand with allosteric agonist properties. *Mol Pharmacol*. 2009;75:1240-7.
348. Fricker SP, Anastassov V, Cox J, Darkes MC, Grujic O, Idzan SR, Labrecque J, Lau G, Mosi RM, Nelson KL, Qin L, Santucci Z and Wong RS. Characterization of the molecular pharmacology of AMD3100: a specific antagonist of the G-protein coupled chemokine receptor, CXCR4. *Biochem Pharmacol*. 2006;72:588-96.
349. Zhang WB, Navenot JM, Haribabu B, Tamamura H, Hiramatu K, Omagari A, Pei G, Manfredi JP, Fujii N, Broach JR and Peiper SC. A point mutation that confers constitutive activity to CXCR4 reveals that T140 is an inverse agonist and that AMD3100 and ALX40-4C are weak partial agonists. *J Biol Chem*. 2002;277:24515-21.
350. Tillmann S, Bernhagen J and Noels H. Arrest Functions of the MIF Ligand/Receptor Axes in Atherogenesis. *Front Immunol*. 2013;4:115.
351. Saini V, Staren DM, Ziarek JJ, Nashaat ZN, Campbell EM, Volkman BF, Marchese A and Majetschak M. The CXC chemokine receptor 4 ligands ubiquitin and stromal cell-derived factor-1alpha function through distinct receptor interactions. *J Biol Chem*. 2011;286:33466-77.
352. Rassaf T, Weber C and Bernhagen J. Macrophage migration inhibitory factor in myocardial ischaemia/reperfusion injury. *Cardiovasc Res*. 2014;102:321-8.
353. Pohl J, Hendgen-Cotta UB, Rammos C, Luedike P, Mull E, Stoppe C, Julicher K, Lue H, Merx MW, Kelm M, Bernhagen J and Rassaf T. Targeted intracellular accumulation of macrophage migration inhibitory factor in the reperfused heart mediates cardioprotection. *Thromb Haemost*. 2016;115:200-12.
354. Stoppe C, Rex S, Goetzenich A, Kraemer S, Emontzpohl C, Soppert J, Averdunk L, Sun Y, Rossaint R, Lue H, Huang C, Song Y, Pantouris G, Lolis E, Leng L, Schulte W, Bucala R, Weber C and Bernhagen J. Interaction of MIF Family Proteins in Myocardial Ischemia/Reperfusion Damage and Their Influence on Clinical Outcome of Cardiac Surgery Patients. *Antioxid Redox Signal*. 2015;23:865-79.

355. Pinto AR, Ilinykh A, Ivey MJ, Kuwabara JT, D'Antoni ML, Debuque R, Chandran A, Wang L, Arora K, Rosenthal NA and Tallquist MD. Revisiting Cardiac Cellular Composition. *Circ Res*. 2016;118:400-9.
356. Noels H, Zhou B, Tilstam PV, Theelen W, Li X, Pawig L, Schmitz C, Akhtar S, Simsekyilmaz S, Shagdarsuren E, Schober A, Adams RH, Bernhagen J, Liehn EA, Doring Y and Weber C. Deficiency of endothelial CXCR4 reduces reendothelialization and enhances neointimal hyperplasia after vascular injury in atherosclerosis-prone mice. *Arterioscler Thromb Vasc Biol*. 2014;34:1209-20.
357. Xu Y, Huo Y, Toufektsian MC, Ramos SI, Ma Y, Tejani AD, French BA and Yang Z. Activated platelets contribute importantly to myocardial reperfusion injury. *Am J Physiol Heart Circ Physiol*. 2006;290:H692-9.
358. Chatterjee M, Huang Z, Zhang W, Jiang L, Hultenby K, Zhu L, Hu H, Nilsson GP and Li N. Distinct platelet packaging, release, and surface expression of proangiogenic and antiangiogenic factors on different platelet stimuli. *Blood*. 2011;117:3907-11.
359. Chatterjee M, Rath D and Gawaz M. Role of chemokine receptors CXCR4 and CXCR7 for platelet function. *Biochem Soc Trans*. 2015;43:720-6.
360. Rothe C, Urlinger S, Lohning C, Prassler J, Stark Y, Jager U, Hubner B, Bardroff M, Pradel I, Boss M, Bittlingmaier R, Bataa T, Frisch C, Brocks B, Honegger A and Urban M. The human combinatorial antibody library HuCAL GOLD combines diversification of all six CDRs according to the natural immune system with a novel display method for efficient selection of high-affinity antibodies. *J Mol Biol*. 2008;376:1182-200.
361. Krebs B, Rauchenberger R, Reiffert S, Rothe C, Tesar M, Thomassen E, Cao M, Dreier T, Fischer D, Hoss A, Inge L, Knappik A, Marget M, Pack P, Meng XQ, Schier R, Sohlemann P, Winter J, Wolle J and Kretzschmar T. High-throughput generation and engineering of recombinant human antibodies. *J Immunol Methods*. 2001;254:67-84.
362. Bio-Rad. HuCAL Services. 2016.
363. Promega. AttoPhos® AP Fluorescent Substrate System. 2009.
364. Abnova. ELISA Pairs Kits. 2016.
365. Scientific T. ELISA technical guide and protocols. 2014.
366. Boratyn GM, Camacho C, Cooper PS, Coulouris G, Fong A, Ma N, Madden TL, Matten WT, McGinnis SD, Merezhuk Y, Raytselis Y, Sayers EW, Tao T, Ye J and Zaretskaya I. BLAST: a more efficient report with usability improvements. *Nucleic Acids Res*. 2013;41:W29-33.
367. Hou R, Liu L, Anees S, Hiroyasu S and Sibinga NE. The Fat1 cadherin integrates vascular smooth muscle cell growth and migration signals. *J Cell Biol*. 2006;173:417-29.
368. Magg T, Schreiner D, Solis GP, Bade EG and Hofer HW. Processing of the human protocadherin Fat1 and translocation of its cytoplasmic domain to the nucleus. *Exp Cell Res*. 2005;307:100-8.
369. Kanki S, Segers VF, Wu W, Kakkar R, Gannon J, Sys SU, Sandrasagra A and Lee RT. Stromal cell-derived factor-1 retention and cardioprotection for ischemic myocardium. *Circ Heart Fail*. 2011;4:509-18.
370. Mehta NN, Matthews GJ, Krishnamoorthy P, Shah R, McLaughlin C, Patel P, Budoff M, Chen J, Wolman M, Go A, He J, Kanetsky PA, Master SR, Rader DJ, Raj D, Gadegbeku CA, Schreiber M, Fischer MJ, Townsend RR, Kusek J, Feldman HI, Foulkes AS and Reilly MP. Higher plasma CXCL12 levels predict incident myocardial infarction

and death in chronic kidney disease: findings from the Chronic Renal Insufficiency Cohort study. *Eur Heart J*. 2014;35:2115-22.
371. Liu K, Yang S, Hou M, Chen T, Liu J and Yu B. Increase of circulating stromal cell-derived factor-1 in heart failure patients. *Herz*. 2015;40 Suppl 1:70-5.
372. Fortunato O, Spinetti G, Specchia C, Cangiano E, Valgimigli M and Madeddu P. Migratory activity of circulating progenitor cells and serum SDF-1alpha predict adverse events in patients with myocardial infarction. *Cardiovasc Res*. 2013;100:192-200.
373. Tong G, Wang N, Zhou Y, Leng J, Gao W, Tong X, Shen Y, Yang J, Ye X, Zhou L and Gao Y. Role of stromal cell-derived factor-1 in patients with non-ST elevation acute coronary syndrome. *Int Heart J*. 2014;55:219-27.
374. Damas JK, Waehre T, Yndestad A, Ueland T, Muller F, Eiken HG, Holm AM, Halvorsen B, Froland SS, Gullestad L and Aukrust P. Stromal cell-derived factor-1alpha in unstable angina: potential antiinflammatory and matrix-stabilizing effects. *Circulation*. 2002;106:36-42.
375. Subramanian S, Liu C, Aviv A, Ho JE, Courchesne P, Muntendam P, Larson MG, Cheng S, Wang TJ, Mehta NN and Levy D. Stromal cell-derived factor 1 as a biomarker of heart failure and mortality risk. *Arterioscler Thromb Vasc Biol*. 2014;34:2100-5.
376. Theiss HD, Gross L, Vallaster M, David R, Brunner S, Brenner C, Nathan P, Assmann G, Mueller-Hoecker J, Vogeser M, Steinbeck G and Franz WM. Antidiabetic gliptins in combination with G-CSF enhances myocardial function and survival after acute myocardial infarction. *Int J Cardiol*. 2013;168:3359-69.
377. Chang LT, Yuen CM, Sun CK, Wu CJ, Sheu JJ, Chua S, Yeh KH, Yang CH, Youssef AA and Yip HK. Role of stromal cell-derived factor-1alpha, level and value of circulating interleukin-10 and endothelial progenitor cells in patients with acute myocardial infarction undergoing primary coronary angioplasty. *Circ J*. 2009;73:1097-104.
378. Cecyn KZ, Schimieguel DM, Kimura EY, Yamamoto M and Oliveira JS. Plasma levels of FL and SDF-1 and expression of FLT-3 and CXCR4 on CD34+ cells assessed pre and post hematopoietic stem cell mobilization in patients with hematologic malignancies and in healthy donors. *Transfus Apher Sci*. 2009;40:159-67.
379. Xiao Q, Ye S, Oberhollenzer F, Mayr A, Jahangiri M, Willeit J, Kiechl S and Xu Q. SDF1 gene variation is associated with circulating SDF1alpha level and endothelial progenitor cell number: the Bruneck Study. *PLoS One*. 2008;3:e4061.
380. Lee BC, Hsu HC, Tseng WY, Su MY, Chen SY, Wu YW, Chien KL and Chen MF. Effect of cardiac rehabilitation on angiogenic cytokines in postinfarction patients. *Heart*. 2009;95:1012-8.
381. Wang Y, Johnsen HE, Mortensen S, Bindslev L, Ripa RS, Haack-Sorensen M, Jorgensen E, Fang W and Kastrup J. Changes in circulating mesenchymal stem cells, stem cell homing factor, and vascular growth factors in patients with acute ST elevation myocardial infarction treated with primary percutaneous coronary intervention. *Heart*. 2006;92:768-74.
382. Liu K, Yang S, Hou M, Chen T, Liu J and Yu B. Increase of circulating stromal cell-derived factor-1 in heart failure patients. *Herz*. 2014.
383. Luyt CE, Meddahi-Pelle A, Ho-Tin-Noe B, Colliec-Jouault S, Guezennec J, Louedec L, Prats H, Jacob MP, Osborne-Pellegrin M, Letourneur D and Michel JB. Low-

molecular-weight fucoidan promotes therapeutic revascularization in a rat model of critical hindlimb ischemia. *J Pharmacol Exp Ther*. 2003;305:24-30.
384. Valgimigli M, Rigolin GM, Fucili A, Porta MD, Soukhomovskaia O, Malagutti P, Bugli AM, Bragotti LZ, Francolini G, Mauro E, Castoldi G and Ferrari R. CD34+ and endothelial progenitor cells in patients with various degrees of congestive heart failure. *Circulation*. 2004;110:1209-12.
385. George ML, Eccles SA, Tutton MG, Abulafi AM and Swift RI. Correlation of plasma and serum vascular endothelial growth factor levels with platelet count in colorectal cancer: clinical evidence of platelet scavenging? *Clin Cancer Res*. 2000;6:3147-52.
386. Sweeney EA, Lortat-Jacob H, Priestley GV, Nakamoto B and Papayannopoulou T. Sulfated polysaccharides increase plasma levels of SDF-1 in monkeys and mice: involvement in mobilization of stem/progenitor cells. *Blood*. 2002;99:44-51.
387. Pablos JL, Santiago B, Galindo M, Torres C, Brehmer MT, Blanco FJ and Garcia-Lazaro FJ. Synoviocyte-derived CXCL12 is displayed on endothelium and induces angiogenesis in rheumatoid arthritis. *J Immunol*. 2003;170:2147-52.
388. Ziarek JJ, Veldkamp CT, Zhang F, Murray NJ, Kartz GA, Liang X, Su J, Baker JE, Linhardt RJ and Volkman BF. Heparin oligosaccharides inhibit chemokine (CXC motif) ligand 12 (CXCL12) cardioprotection by binding orthogonal to the dimerization interface, promoting oligomerization, and competing with the chemokine (CXC motif) receptor 4 (CXCR4) N terminus. *J Biol Chem*. 2013;288:737-46.
389. Jung C, Fischer N, Fritzenwanger M, Pernow J, Brehm BR and Figulla HR. Association of waist circumference, traditional cardiovascular risk factors, and stromal-derived factor-1 in adolescents. *Pediatr Diabetes*. 2009;10:329-35.
390. Soeki T, Tamura Y, Shinohara H, Sakabe K, Onose Y and Fukuda N. Increased soluble platelet/endothelial cell adhesion molecule-1 in the early stages of acute coronary syndromes. *Int J Cardiol*. 2003;90:261-8.
391. Sadir R, Imberty A, Baleux F and Lortat-Jacob H. Heparan sulfate/heparin oligosaccharides protect stromal cell-derived factor-1 (SDF-1)/CXCL12 against proteolysis induced by CD26/dipeptidyl peptidase IV. *J Biol Chem*. 2004;279:43854-60.
392. Wirtz TH, Tillmann S, Strussmann T, Kraemer S, Heemskerk JW, Grottke O, Gawaz M, von Hundelshausen P and Bernhagen J. Platelet-derived MIF: a novel platelet chemokine with distinct recruitment properties. *Atherosclerosis*. 2015;239:1-10.
393. Strussmann T, Tillmann S, Wirtz T, Bucala R, von Hundelshausen P and Bernhagen J. Platelets are a previously unrecognised source of MIF. *Thromb Haemost*. 2013;110:1004-13.
394. Kuil J, Buckle T, Yuan H, van den Berg NS, Oishi S, Fujii N, Josephson L and van Leeuwen FW. Synthesis and evaluation of a bimodal CXCR4 antagonistic peptide. *Bioconjug Chem*. 2011;22:859-64.
395. Scirica BM, Bhatt DL, Braunwald E, Steg PG, Davidson J, Hirshberg B, Ohman P, Frederich R, Wiviott SD, Hoffman EB, Cavender MA, Udell JA, Desai NR, Mosenzon O, McGuire DK, Ray KK, Leiter LA, Raz I, Committee S-TS and Investigators. Saxagliptin and cardiovascular outcomes in patients with type 2 diabetes mellitus. *N Engl J Med*. 2013;369:1317-26.

396. Scirica BM, Braunwald E, Raz I, Cavender MA, Morrow DA, Jarolim P, Udell JA, Mosenzon O, Im K, Umez-Eronini AA, Pollack PS, Hirshberg B, Frederich R, Lewis BS, McGuire DK, Davidson J, Steg PG, Bhatt DL, Committee S-TS and Investigators*. Heart failure, saxagliptin, and diabetes mellitus: observations from the SAVOR-TIMI 53 randomized trial. *Circulation*. 2014;130:1579-88.
397. Li L, Li S, Deng K, Liu J, Vandvik PO, Zhao P, Zhang L, Shen J, Bala MM, Sohani ZN, Wong E, Busse JW, Ebrahim S, Malaga G, Rios LP, Wang Y, Chen Q, Guyatt GH and Sun X. Dipeptidyl peptidase-4 inhibitors and risk of heart failure in type 2 diabetes: systematic review and meta-analysis of randomised and observational studies. *BMJ*. 2016;352:i610.
398. Christopherson KW, 2nd, Cooper S and Broxmeyer HE. Cell surface peptidase CD26/DPPIV mediates G-CSF mobilization of mouse progenitor cells. *Blood*. 2003;101:4680-6.
399. Christopherson KW, 2nd, Hangoc G, Mantel CR and Broxmeyer HE. Modulation of hematopoietic stem cell homing and engraftment by CD26. *Science*. 2004;305:1000-3.
400. Brenner C, Adrion C, Grabmaier U, Theisen D, von Ziegler F, Leber A, Becker A, Sohn HY, Hoffmann E, Mansmann U, Steinbeck G, Franz WM and Theiss HD. Sitagliptin plus granulocyte colony-stimulating factor in patients suffering from acute myocardial infarction: A double-blind, randomized placebo-controlled trial of efficacy and safety (SITAGRAMI trial). *Int J Cardiol*. 2016;205:23-30.
401. White WB, Cannon CP, Heller SR, Nissen SE, Bergenstal RM, Bakris GL, Perez AT, Fleck PR, Mehta CR, Kupfer S, Wilson C, Cushman WC, Zannad F and Investigators E. Alogliptin after acute coronary syndrome in patients with type 2 diabetes. *N Engl J Med*. 2013;369:1327-35.
402. Zannad F, Cannon CP, Cushman WC, Bakris GL, Menon V, Perez AT, Fleck PR, Mehta CR, Kupfer S, Wilson C, Lam H, White WB and Investigators E. Heart failure and mortality outcomes in patients with type 2 diabetes taking alogliptin versus placebo in EXAMINE: a multicentre, randomised, double-blind trial. *Lancet*. 2015;385:2067-76.
403. Green JB, Bethel MA, Armstrong PW, Buse JB, Engel SS, Garg J, Josse R, Kaufman KD, Koglin J, Korn S, Lachin JM, McGuire DK, Pencina MJ, Standl E, Stein PP, Suryawanshi S, Van de Werf F, Peterson ED, Holman RR and Group TS. Effect of Sitagliptin on Cardiovascular Outcomes in Type 2 Diabetes. *N Engl J Med*. 2015;373:232-42.
404. Zahler S, Kupatt C and Becker BF. Endothelial preconditioning by transient oxidative stress reduces inflammatory responses of cultured endothelial cells to TNF-alpha. *FASEB J*. 2000;14:555-64.
405. Hausenloy DJ, Whittington HJ, Wynne AM, Begum SS, Theodorou L, Riksen N, Mocanu MM and Yellon DM. Dipeptidyl peptidase-4 inhibitors and GLP-1 reduce myocardial infarct size in a glucose-dependent manner. *Cardiovasc Diabetol*. 2013;12:154.
406. Chinda K, Sanit J, Chattipakorn S and Chattipakorn N. Dipeptidyl peptidase-4 inhibitor reduces infarct size and preserves cardiac function via mitochondrial protection in ischaemia-reperfusion rat heart. *Diab Vasc Dis Res*. 2014;11:75-83.
407. Sauve M, Ban K, Momen MA, Zhou YQ, Henkelman RM, Husain M and Drucker DJ. Genetic deletion or pharmacological inhibition of dipeptidyl peptidase-4 improves

cardiovascular outcomes after myocardial infarction in mice. *Diabetes*. 2010;59:1063-73.
408. Ye Y, Keyes KT, Zhang C, Perez-Polo JR, Lin Y and Birnbaum Y. The myocardial infarct size-limiting effect of sitagliptin is PKA-dependent, whereas the protective effect of pioglitazone is partially dependent on PKA. *Am J Physiol Heart Circ Physiol*. 2010;298:H1454-65.
409. Hocher B, Sharkovska Y, Mark M, Klein T and Pfab T. The novel DPP-4 inhibitors linagliptin and BI 14361 reduce infarct size after myocardial ischemia/reperfusion in rats. *Int J Cardiol*. 2013;167:87-93.
410. Ponicke K, Sternitzky R and Mest HJ. Stimulation of aggregation and thromboxane A2 formation of human platelets by hypoxia. *Prostaglandins Leukot Med*. 1987;29:49-59.
411. Oberkofler CE, Limani P, Jang JH, Rickenbacher A, Lehmann K, Raptis DA, Ungethuem U, Tian Y, Grabliauskaite K, Humar R, Graf R, Humar B and Clavien PA. Systemic protection through remote ischemic preconditioning is spread by platelet-dependent signaling in mice. *Hepatology*. 2014;60:1409-17.
412. Starlinger P, Haegele S, Offensperger F, Oehlberger L, Pereyra D, Kral JB, Schrottmaier WC, Badrnya S, Reiberger T, Ferlitsch A, Stift J, Luf F, Brostjan C, Gruenberger T and Assinger A. The Profile of Platelet alpha-Granule Released Molecules Affects Postoperative Liver Regeneration. *Hepatology*. 2015.
413. Michelson AD and Furman MI. Laboratory markers of platelet activation and their clinical significance. *Curr Opin Hematol*. 1999;6:342-8.
414. Cohen MV, Yang XM, White J, Yellon DM, Bell RM and Downey JM. Cangrelor-Mediated Cardioprotection Requires Platelets and Sphingosine Phosphorylation. *Cardiovasc Drugs Ther*. 2016;30:229-32.
415. Nagasawa T, Hirota S, Tachibana K, Takakura N, Nishikawa S, Kitamura Y, Yoshida N, Kikutani H and Kishimoto T. Defects of B-cell lymphopoiesis and bone-marrow myelopoiesis in mice lacking the CXC chemokine PBSF/SDF-1. *Nature*. 1996;382:635-8.
416. Tachibana K, Hirota S, Iizasa H, Yoshida H, Kawabata K, Kataoka Y, Kitamura Y, Matsushima K, Yoshida N, Nishikawa S, Kishimoto T and Nagasawa T. The chemokine receptor CXCR4 is essential for vascularization of the gastrointestinal tract. *Nature*. 1998;393:591-4.
417. Koitabashi N, Bedja D, Zaiman AL, Pinto YM, Zhang M, Gabrielson KL, Takimoto E and Kass DA. Avoidance of transient cardiomyopathy in cardiomyocyte-targeted tamoxifen-induced MerCreMer gene deletion models. *Circ Res*. 2009;105:12-5.
418. Rafii S, Cao Z, Lis R, Siempos, II, Chavez D, Shido K, Rabbany SY and Ding BS. Platelet-derived SDF-1 primes the pulmonary capillary vascular niche to drive lung alveolar regeneration. *Nat Cell Biol*. 2015;17:123-36.
419. Valasek MA and Repa JJ. The power of real-time PCR. *Adv Physiol Educ*. 2005;29:151-9.
420. Buchwalow I, Samoilova V, Boecker W and Tiemann M. Non-specific binding of antibodies in immunohistochemistry: fallacies and facts. *Sci Rep*. 2011;1:28.
421. Vince DG, Tbakhi A, Gaddipati A, Cothren RM, Cornhill JF and Tubbs RR. Quantitative comparison of immunohistochemical staining intensity in tissues fixed in formalin and Histochoice. *Anal Cell Pathol*. 1997;15:119-29.

422. Ivins S, Chappell J, Vernay B, Suntharalingham J, Martineau A, Mohun TJ and Scambler PJ. The CXCL12/CXCR4 Axis Plays a Critical Role in Coronary Artery Development. *Dev Cell*. 2015;33:455-68.
423. Toda Y, Kono K, Abiru H, Kokuryo K, Endo M, Yaegashi H and Fukumoto M. Application of tyramide signal amplification system to immunohistochemistry: a potent method to localize antigens that are not detectable by ordinary method. *Pathol Int*. 1999;49:479-83.
424. Shimshek DR, Kim J, Hubner MR, Spergel DJ, Buchholz F, Casanova E, Stewart AF, Seeburg PH and Sprengel R. Codon-improved Cre recombinase (iCre) expression in the mouse. *Genesis*. 2002;32:19-26.
425. Claxton S, Kostourou V, Jadeja S, Chambon P, Hodivala-Dilke K and Fruttiger M. Efficient, inducible Cre-recombinase activation in vascular endothelium. *Genesis*. 2008;46:74-80.
426. Soriano P. Generalized lacZ expression with the ROSA26 Cre reporter strain. *Nat Genet*. 1999;21:70-1.
427. Nilsson S, Makela S, Treuter E, Tujague M, Thomsen J, Andersson G, Enmark E, Pettersson K, Warner M and Gustafsson JA. Mechanisms of estrogen action. *Physiol Rev*. 2001;81:1535-65.
428. Lizotte E, Grandy SA, Tremblay A, Allen BG and Fiset C. Expression, distribution and regulation of sex steroid hormone receptors in mouse heart. *Cell Physiol Biochem*. 2009;23:75-86.
429. Larocca TJ, Jeong D, Kohlbrenner E, Lee A, Chen J, Hajjar RJ and Tarzami ST. CXCR4 gene transfer prevents pressure overload induced heart failure. *J Mol Cell Cardiol*. 2012;53:223-32.
430. Baxter GF. The neutrophil as a mediator of myocardial ischemia-reperfusion injury: time to move on. *Basic Res Cardiol*. 2002;97:268-75.
431. Montecucco F, Bauer I, Braunersreuther V, Bruzzone S, Akhmedov A, Luscher TF, Speer T, Poggi A, Mannino E, Pelli G, Galan K, Bertolotto M, Lenglet S, Garuti A, Montessuit C, Lerch R, Pellieux C, Vuilleumier N, Dallegri F, Mage J, Sebastian C, Mostoslavsky R, Gayet-Ageron A, Patrone F, Mach F and Nencioni A. Inhibition of nicotinamide phosphoribosyltransferase reduces neutrophil-mediated injury in myocardial infarction. *Antioxid Redox Signal*. 2013;18:630-41.
432. Liehn EA, Tuchscheerer N, Kanzler I, Drechsler M, Fraemohs L, Schuh A, Koenen RR, Zander S, Soehnlein O, Hristov M, Grigorescu G, Urs AO, Leabu M, Bucur I, Merx MW, Zernecke A, Ehling J, Gremse F, Lammers T, Kiessling F, Bernhagen J, Schober A and Weber C. Double-edged role of the CXCL12/CXCR4 axis in experimental myocardial infarction. *J Am Coll Cardiol*. 2011;58:2415-23.
433. Wang ER, Jarrah AA, Benard L, Chen J, Schwarzkopf M, Hadri L and Tarzami ST. Deletion of CXCR4 in cardiomyocytes exacerbates cardiac dysfunction following isoproterenol administration. *Gene Ther*. 2014;21:496-506.
434. Pyo RT, Sui J, Dhume A, Palomeque J, Blaxall BC, Diaz G, Tunstead J, Logothetis DE, Hajjar RJ and Schecter AD. CXCR4 modulates contractility in adult cardiac myocytes. *J Mol Cell Cardiol*. 2006;41:834-44.